THE

LONDON, EDINBURGH, AND DUBLIN

PHILOSOPHICAL MAGAZINE

AND

JOURNAL OF SCIENCE.

[SEVENTH SERIES.]

MARCH 1932.

XLVII. *Symbolic Calculus.* *By* BALTH. VAN DER POL, *D.Sc., and* K. F. NIESSEN, *D.Sc., Natuurkundig Laboratorium der N. V. Philips' Gloeilampenfabrieken, Eindhoven, Holland* *.

INTRODUCTION.

BY symbolic calculus we mean the operational calculus of Heaviside in the form given by Carson † and extended by the first of us to the solution of ordinary differential equations (*a*) with constant coefficients ‡ and (*b*) with variable coefficients §. In the title above we use the name *symbolic* instead of *operational* calculus, since, with a view to the rigour of the method, we consider it advisable to abandon the idea of an operator and an operand in the original sense of Heaviside. Instead we base our considerations on Carson's foundation of the calculus, by means of which a given

* Communicated by the Authors.

† John R. Carson, 'Electric Circuit Theory and the Operational Calculus' (McGraw Hill, New York, 1926).

‡ Balth. van der Pol, Phil. Mag. vii. p. 1153 (1929); viii. p. 861 (1929); referred to as P.

§ We also draw attention to a recent book by G. A. Campbell and R. M. Foster (Bell Telephone System, Monograph B 584) which will be of interest for those who study operational methods.

function $h(x)$ is related symbolically to another function $f(p)$, given by the Laplace transform

$$f(p) = p\int_0^\infty e^{-px}h(x)dx, \quad . \quad . \quad . \quad . \quad (1)$$

where it is assumed that the integral converges.

We will speak of an "original" function $h(x)$ and its "image" $f(p)$. The integral relation (1) between $f(p)$ and $h(x)$ we denote as

$$f(p) \doteqdot h(x).$$

When the image $f(p)$ is known, then the original $h(x)$ is found back by means of the Bromwich-Wagner theorem

$$h(x) = \frac{1}{2\pi i}\int_{c-i\infty}^{c+\infty} \frac{f(p)}{p} e^{px}dp, \quad . \quad . \quad . \quad . \quad (2)$$

which is a consequence of the Mellin-Fourier theorem *.

In (2) the straight path of integration is so chosen that all singularities lie to the left.

The relation (2) between $h(x)$ and $f(p)$ will also be indicated by

$$h(x) \doteqdot f(p),$$

where again the symbol $\doteqdot$ is used, although the process to derive $f(p)$ from $h(x)$ (as in (2)) is entirely different from the process to derive $h(x)$ from $f(p)$ (as in (1)).

Confusion between original and image is impossible, since the image always contains the symbolic parameter p. Therefore it is perfectly immaterial whether we write

$$h(x) \doteqdot f(p) \quad \text{or} \quad f(p) \doteqdot h(x):$$

both mean $h(x)$, transformed symbolically, gives $f(p)$, and $f(p)$, interpreted backwards, gives $h(x)$.

In this respect we remark that Dalzell † uses a slightly different nomenclature. He speaks of $\mathrm{F}(p)$, which is the convert of $h(x)$, and of $h(x)$, which is the revert of $\mathrm{F}(p)$. Moreover, his $\mathrm{F}(p)$ is not quite identical with our $f(p)$ of (1), but he uses $\mathrm{F}(p) = \frac{f(p)}{p}$. He too points out that the new method, on account of its exactness, is to be preferred to the original Heaviside operational calculus.

We would like to keep to our own notations of "original"

* Courant und Hilbert, 'Methoden der Mathematischen Physik,' i. s. 90.

† D. P. Dalzell, Proc. Phys. Soc. London, xlii. p. 75 (1929).

$h(x)$ and "image" $f(p)$, where the parameter p is connected with the variable x in the sense of (1).

For instance, to $h(x)=x$ belongs, according to (1), $f(p)=\frac{1}{p}$. The fact that functions of p represent functions of x may therefore be indicated by means of

$$\frac{1}{p} \doteq x \quad \text{or} \quad x \doteq \frac{1}{p}.$$

If we deal with a function of two variables x, y, it is sometimes useful to represent it as a function of x by means of $f(p)$, but as a function of y by means of a function of another symbolic parameter q,

$$\frac{1}{p} \doteq x, \quad \frac{1}{q} \doteq y.$$

Then we will have a case of simultaneous symbolic calculus.

Now several rules have been derived, partly by Carson, partly by van der Pol, which are of very frequent use in symbolic calculations.

For convenience of the reader we collect these rules in Part I. and repeat some results found in P and again to be used in this paper. Moreover, a new rule and some considerations of a general character will be given in Part I. In Part II. we intend to show again how these rules can be used in a very simple way for the derivation of many new relations.

I.—Theoretical Part.

Fundamental Rules.

1. Carson pointed out that from (1) we may conclude

$$f\left(\frac{p}{s}\right) \doteq h(sx), \qquad \text{if } s=\text{constant} > 0, \quad . \quad \text{(R1)}$$

$$pf(p) \doteq \frac{d}{dx}h(x), \qquad \text{if } h(0)=0, \quad . \quad . \quad . \quad . \quad \text{(R2)}$$

$$\frac{1}{p}f(p) \doteq \int_0^x h(x)dx, \quad . \quad . \quad . \quad . \quad . \quad . \quad . \quad . \quad . \quad \text{(R3)}$$

$$\frac{p}{p+\alpha}f(p+\alpha) \doteq e^{-\alpha x}h(x), \quad . \quad . \quad . \quad . \quad . \quad . \quad . \quad . \quad \text{(R4)}$$

$$e^{-\lambda p} f(p) \doteqdot \begin{cases} 0, & \text{for } x < \lambda \\ h(x-\lambda), & \text{for } x > \lambda \end{cases} \text{ if } \lambda > 0, \quad . \quad (R5)$$

$$e^{+\lambda p} f(p) \doteqdot h(x+\lambda), \quad \text{if } \lambda > 0 \text{ and } h(x) = 0 \text{ for } 0 < x < 1. \quad . \quad . \quad (R6)$$

Van der Pol added to this list

$$\left(-p\frac{d}{dp}\right)^n f(p) \doteqdot \left(x\frac{d}{dx}\right)^n h(x), \quad n > 0, \quad . \quad (R7)$$

$$p\left(-\frac{d}{dp}\right)^n \frac{f(p)}{p} \doteqdot x^n h(x), \quad n > 0, \quad . \quad (R8)$$

$$\int_p^\infty \frac{f(p)}{p} dp \doteqdot \int_0^x \frac{h(x)}{x} dx, \quad . \quad . \quad . \quad . \quad (R9)$$

$$\int_0^p \frac{f(p)}{p} dp \doteqdot \int_x^\infty \frac{h(x)}{x} dx, \quad . \quad . \quad . \quad . \quad (R10)$$

and also the following ordinary equalities :

$$\int_0^\infty \frac{f(p)}{p} dp = \int_0^\infty \frac{h(x)}{x} dx, \quad . \quad . \quad . \quad (R11)$$

$$\operatorname*{Lim}_{p \to \infty} f(p) = \operatorname*{Lim}_{x \to 0} h(x), \quad . \quad . \quad . \quad (R12)$$

$$\operatorname*{Lim}_{p \to 0} f(p) = \operatorname*{Lim}_{x \to \infty} h(x), \quad . \quad . \quad . \quad (R13)$$

provided the integrals and limits exist.

Proofs of these rules were given in P.

2. The rule we now wish to add is

$$\frac{h(x)}{x^n} \doteqdot p\int_p^\infty \int_p^\infty \ldots \int_p^\infty \frac{f(p)}{p} (dp)^n, \quad . \quad (R14)$$

provided the multiple integral converges, *i. e.*, if

$$\operatorname*{Lim}_{x \to 0} h(x) = x^m, \qquad m > n-1.$$

This rule can be proved as follows :—

We have

$$\frac{e^{-px}}{x} = \int_p^\infty e^{-px} dp \; ;$$

$$\therefore \quad p\int_0^\infty e^{-px} \frac{h(x)}{x} dx = p\int_0^\infty h(x) \int_p^\infty e^{-px} dp \, dx$$

$$= p\int_p^\infty \int_0^\infty e^{-px} h(x) dx \, dp = p\int_p^\infty \frac{f(p)}{p} dp.$$

In the same way we have

$$\frac{e^{-px}}{x^2} = \int_p^\infty \int_p^\infty e^{-px} dp\, dp\,;$$

$$\therefore \quad p\int_0^\infty e^{-px}\frac{h(x)}{x^2}dx = p\int_0^\infty h(x)\int_p^\infty \int_p^\infty e^{-px}dp\, dp\, dx$$

$$= p\int_p^\infty \int_p^\infty \frac{f(p)}{p}\, dp\, dp,$$

from which the general rule can easily be established.

Moreover, the rule is also proved by repeated application of (R 2) on (R 9).

3. Another rule mentioned by Carson (*l. c.* p. 41) without proof and which can be based upon Volterra's theorem of a "produit de composition" * is

$$\left.\begin{aligned} \frac{1}{p}\cdot f_1(p)\cdot f_2(p) &\doteqdot \int_0^x h_1(\xi)h_2(x-\xi)d\xi, \\ \text{or} \qquad &\doteqdot \int_0^x h_1(x-\xi)h_2(\xi)d\xi, \end{aligned}\right\} \quad \text{(R 15)}$$

where $h_1(x)$ and $h_2(x)$ are the originals of $f_1(p)$ and $f_2(p)$.

A new and very direct proof of this rule is as follows :—

By (1) we have the ordinary equation

$$\frac{1}{p}f_1(p) = \int_0^\infty e^{-p\lambda}h_1(\lambda)d\lambda.$$

Multiplying with $f_2(p)$ we get

$$\frac{1}{p}f_1(p)f_2(p) = \int_0^\infty e^{-p\lambda}f_2(p)h_1(\lambda)d\lambda. \quad . \quad . \quad (3)$$

We now assume p to belong to a variable x in the sense of (1) ; therefore

$$\frac{1}{p} \doteqdot x\,;$$

then by (R 5)

$$e^{-p\lambda}f_2(p) \doteqdot \begin{cases} 0, & \text{for } \lambda > x, \\ h_2(x-\lambda), & \text{for } \lambda < x. \end{cases} \quad . \quad . \quad (4)$$

We substitute this result in the right-hand side of (3),

* Volterra-Péres, 'Leçons sur la composition et les fonctions permutables' (Paris, 1924).

which thus becomes " the original " of the left-hand side, so that we obtain

$$\frac{1}{p} f_1(p) f_2(p) \doteqdot \int_0^x h_2(x-\lambda) h_1(\lambda) d\lambda.$$

The upper limit of the last integral is written x instead of ∞, because of (4).

4. Of the results obtained in P by application of the rules above we mention here a few, which we will afterwards have to use :

$$\frac{1}{p^n} \doteqdot \frac{x^n}{\Pi(n)}, \quad \ldots\ldots\ldots \quad (\mathrm{F}\,1)$$

$$\frac{p}{p+1} \doteqdot e^{-x}, \quad \ldots\ldots\ldots \quad (\mathrm{F}\,2)$$

$$\frac{p}{p^2+1} \doteqdot \sin x, \quad \ldots\ldots\ldots \quad (\mathrm{F}\,3)$$

$$\frac{p^2}{p^2+1} \doteqdot \cos x, \quad \ldots\ldots\ldots \quad (\mathrm{F}\,4)$$

$$\sqrt[n]{x^2}\mathrm{J}_n(2\sqrt{x}) \doteqdot p^{-n} e^{\frac{1}{p}}, \quad \ldots\ldots\ldots \quad (\mathrm{F}\,5)$$

$$x^n \mathrm{J}_n(x) \doteqdot \frac{2^n \Pi(n-\tfrac{1}{2})}{\sqrt{\pi}} \frac{p}{(p^2+1)^{n+\frac{1}{2}}}, \quad (\mathrm{F}\,6)$$

$$\mathrm{J}_n(x) \doteqdot \frac{p}{\sqrt{p^2+1}} (\sqrt{p^2+1}-p)^n, \quad (\mathrm{F}\,7)$$

$$\mathrm{P}_n(1-x) \doteqdot e^{-p} p^{n+1} \left(\frac{1}{p}\frac{d}{dp}\right)^n \left(\frac{e^p}{p}\right), \quad \ldots \quad (\mathrm{F}\,8)$$

$$\mathrm{L}_n^*(x) \doteqdot \Pi(n)\left(1-\frac{1}{p}\right)^n, \quad \ldots \quad (\mathrm{F}\,9)$$

$$p \doteqdot \delta(x). \quad \ldots\ldots\ldots \quad (\mathrm{F}\,10)$$

$\delta(x)$ is the impulsive function, being ∞ for $x = 0$ and 0 for $x \neq 0$ in such a way that

$$\int_{-\infty}^{+\infty} \delta(x) dx = 1.$$

Considerations of a General Character.

5. It may be instructive to analyze the definition (1) of the symbolic calculus in the following way :

Write

$$h(x) \doteqdot p \int_0^\infty e^{-ps} h(s)\,ds. \quad . \quad . \quad . \quad . \quad (5)$$

Now p is the image of an impulsive function having its maximum at $x=0$, and therefore by means of (R 5) the image pe^{-sp} corresponds to an impulsive function, being infinite at $x=s$ and denoted by $\delta(x-s)$:

$$pe^{-ps} \doteqdot \delta(x-s). \quad . \quad . \quad . \quad . \quad . \quad . \quad (6)$$

Substituted in (5) this gives the confirmation

$$h(x) = \int_0^\infty \delta(x-s)h(s)\,ds = h(x).$$

6. It is possible to give the relation between original and image in another form. We have, according to (R 8) and $h(x) = 1 \doteqdot 1 = f(p)$,

$$x^n \doteqdot p\left(-\frac{d}{dp}\right)^n \left(\frac{1}{p}\right);$$

$$\therefore \quad h(x) \doteqdot ph\left(-\frac{d}{dp}\right)\left(\frac{1}{p}\right), \quad . \quad . \quad . \quad . \quad (7)$$

provided $h(x)$ can be expressed as a finite or infinite sum of positive integral powers of x. In this case we have

$$f(p) = ph\left(-\frac{d}{dp}\right)\left(\frac{1}{p}\right). \quad . \quad . \quad . \quad . \quad . \quad (8)$$

Suppose now, that we found already (*e.g.*, by means of (1)) the image of an original.

For instance, for

$h(x) = \mathrm{J}_0(x)$ we know $f(p) = \dfrac{p}{\sqrt{p^2+1}}$,

$h(x) = \cos x$ „ „ $f(p) = \dfrac{p^2}{p^2+1}$,

$h(x) = \mathrm{J}_n(x)$ „ „ $f(p) = \dfrac{p}{\sqrt{p^2+1}}\,(\sqrt{p^2+1}-p)^n$.

Then equation (8) leads to

$$\mathrm{J}_0\left(\frac{d}{ds}\right)\left(\frac{1}{s}\right) = \frac{1}{\sqrt{s^2+1}}, \quad . \quad . \quad . \quad . \quad . \quad . \quad (9)$$

$$\cos\left(\frac{d}{ds}\right)\left(\frac{1}{s}\right) = \frac{s}{s^2+1}, \quad . \quad . \quad . \quad . \quad . \quad . \quad (10)$$

$$J_n\left(\frac{d}{ds}\right)\left(\frac{1}{s}\right)=\frac{1}{\sqrt{s^2+1}}(s-\sqrt{s^2+1})^n, \quad . \quad (11)$$

etc.,

where we replaced p by s, because in these ordinary analytical relations s may represent any positive variable $s>1$.

7. Further, we draw attention to the fact that the symbolic calculus may provide the solution of several integral (or differential integral) equations.

A simple example may first illustrate the idea.

We know

$$f(p)=\frac{p}{p^2+1}\doteqdot \sin x. \quad . \quad . \quad . \quad . \quad (12)$$

Now

$$\frac{p}{p^2+1}=\frac{1}{p+\frac{1}{p}}.$$

In connexion herewith we apply successively the following application of the rules (R) to (12).

$$pf(p)\doteqdot \frac{d}{dx}\sin x, \text{ since } \sin 0=0,$$

$$\frac{1}{p}f(p)\doteqdot \int_0^x \sin x\,dx\ ;$$

$$\therefore \quad \left(p+\frac{1}{p}\right)f(p)=1\doteqdot \frac{d}{dx}\sin x+\int_0^x \sin x\,dx.$$

But

$$1\doteqdot 1;$$

therefore

$$y=\sin x$$

is a solution of the differential integral equation

$$1=\frac{dy}{dx}+\int_0^x y\,dx.$$

Another example is more complicated. Take

$$f(p)=\frac{p}{\sqrt{p^2+1}}\doteqdot J_0(x).$$

Now

$$f(p) = \frac{1}{\sqrt{1+\frac{1}{p^2}}} = \frac{1}{1+\frac{1}{2}\frac{1}{p^2}-\frac{1}{8}\frac{1}{p^4}+\ldots}.$$

Thus we get

$$y = J_0(x)$$

as a solution of the integral equation

$$1 = y + \frac{1}{2}\int_0^x \int_0^x y(dx)^2 - \frac{1}{8}\int_0^x \ldots \int_0^x y(dx)^4 + \ldots$$

8. We conclude our considerations of definition (1) of the symbolic calculus by the remark that we expect this formulation in the future to be extended in some way, so as to cover still more functions. Two of the reasons we will mention here:

First we have the fact that with the definition (1) it is in general not legitimate to derive from

$$f(p) \doteq h(x) \quad . \quad . \quad . \quad . \quad . \quad . \quad (13)$$

the relation

$$f(-p) \doteq h(-x). \quad . \quad . \quad . \quad . \quad . \quad (14)$$

We would have, according to (1),

$$h(-x) \doteq p\int_0^\infty e^{-pt}h(-t)dt,$$

which would imply the knowledge of h for negative values of the argument. Supposing these known, and changing t in $-\tau$, we still would get

$$h(-x) \doteq (-p)\int_0^{-\infty} e^{-(-p)\tau}h(\tau)d\tau,$$

which, however, is not identical with $f(-p)$, the upper limit being $-\infty$ instead of $+\infty$. There are pairs $h(x)$ and $f(p)$ in (13) for which (14) is valid.

One might further suggest to use instead of (1) the definition

$$f(p) = \int_0^\infty e^{-x}h\left(\frac{x}{p}\right)dx, \quad . \quad . \quad . \quad . \quad (15)$$

which has *some* advantage.

But secondly there remain many other difficulties—for instance, the fact that in practical symbolic calculus the relation

$$x^{-\frac{3}{2}} \doteq \Pi\left(-\frac{3}{2}\right)p^{\frac{3}{2}} \quad . \quad . \quad . \quad . \quad . \quad (16)$$

can often be used without any trouble, although the integral definition (1) with $h(x)=x^{-\frac{3}{2}}$ would diverge.

For x^{-n}, where n is a positive integer, we are faced with the same difficulties which are encountered by Volterra in defining his "composition"*.

However, we will base our further considerations strictly on the definition (1), and apply only the rigid rules which could be derived from it, thus avoiding any uncertainty in the exactness of our results.

It was already shown in P that the present formulation of the symbolic calculus is already of an amazing fertility, and in Part II. of this paper we will come to the same conclusion on account of the great number of known and unknown relations found by the application of our rules.

II.—Practical Part.

In Part I. we dealt with general methods ; here we will treat less general methods. Some *special* methods of procedure will be discussed which make use of *peculiarities* of image functions. There are a great number of those special methods, giving us the opportunity of deriving many known and unknown relations between several functions. Nevertheless we can divide several manipulations into groups.

A few of these types may already be found in P, namely :

I. Obtaining relations from summation of images.

II. Using the theorem (R15) mentioned in P, p. 864, as "produit de composition," and here called product theorem.

Some further examples of these groups will be given below. In addition we present here a number of new groups :

III. The evaluation of integrals by introducing a parameter, which is transformed symbolically.

IV. Finding new relations by using a known integral with a parameter α, for which will be substituted a function of the symbolic parameter p. After transformation of the total function of p and interpretation of p backwards again, we get the new relations.

In this group we may distinguish especially two sub-groups :

* Volterra, *l. c.*

IV. *a*. Where the original formula is so changed that a factor $e^{-\frac{1}{p}}$ appears, and

IV. *b*. Where the manipulation brings a factor

$$\frac{p}{\sqrt{p^2+1}}e^{-\lambda\sqrt{p^2+1}}.$$

Some very simple examples of the kind (III.) and (IV. *a*) can already be found in Heaviside *.

All these groups will appear to be of a very fertile nature. Finally we put together in group

V. All those applications of the symbolic calculus which do not belong to one of the preceding groups.

(i.) *Relations from Summation of Images.*

1. For the Laguerre polynomials $L_n(x)$, we have †

$$L_n(x) \doteqdot n!\left(1-\frac{1}{p}\right)^n; \quad . \quad . \quad . \quad . \quad (F\,9)$$

$$\therefore \sum_{n=0}(-1)^n\frac{L_n(x)}{n!}=1-\left(1-\frac{1}{p}\right)+\left(1-\frac{1}{p}\right)^2-\ldots=\frac{1}{2}\frac{p}{p-\frac{1}{2}}$$

Now,

$$\frac{p}{p-\frac{1}{2}} \doteqdot e^{\frac{1}{2}x},$$

and thus

$$\sum_{n=0}^{\infty}(-1)^n\frac{L_n(x)}{n!}=\tfrac{1}{2}e^{\frac{1}{2}x}. \quad . \quad . \quad . \quad . \quad (17)$$

2. Another example is

$$\sum_{n=0}^{\infty}\frac{L_n(x)}{(n!)^2} \doteqdot \sum_{n=0}^{\infty}\frac{\left(1-\frac{1}{p}\right)^n}{n!}=e^{1-\frac{1}{p}},$$

and thus, by interpretation of the right-hand member,

$$\sum_{n=0}^{\infty}\frac{L_n(x)}{(n!)^2}=eJ_0(2\sqrt{x}). \quad . \quad . \quad . \quad . \quad (18)$$

3. Still another example with Laguerre polynomials :

$$\frac{e^{-\frac{x}{2}}L_n(x)}{n!} \doteqdot \frac{p}{p+\frac{1}{2}}\left(\frac{p-\frac{1}{2}}{p+\frac{1}{2}}\right)^n.$$

* O. Heaviside, 'Electromagnetic Theory,' iii. pp. 237, 238.
† P. p. 892.

resulting from application of (R 4) upon (F 9). And by (R 1):

$$\frac{e^{-x}L_n(2x)}{n!} \doteq \frac{p}{p+1}\left(\frac{p-1}{p+1}\right)^n, \quad . \quad . \quad . \quad (19)$$

$$\therefore \quad e^{-x}\sum_{n=0}^{n=\infty}\frac{(-1)^n L_{2n}(2x)}{(2n)!}$$

$$\doteq \frac{p}{p+1}\left[1-\left(\frac{p-1}{p+1}\right)^2+\ldots\right] = \frac{1}{2}\frac{p^2+p}{p^2+1}.$$

Hence by interpretation of the right-hand side by means of (F 3) and (F 4):

$$e^{-x}\sum_{n=0}^{n=\infty}\frac{(-1)^n L_{2n}(2x)}{(2n!)} = \tfrac{1}{2}(\cos x+\sin x). \quad . \quad (20)$$

4. Some examples with Hermite polynomials are based upon the image of $He_n(\sqrt{x})$, which can be found from the differential equation for the Hermite functions in an analogous way as the image of $J_0(2\sqrt{x})$ from the differential equation for Bessel functions (*cf.* P. p. 877). In that way we get for the image of $He_{2n+1}(\sqrt{x})$:

$$He_{2n+1}(\sqrt{x}) \doteq \frac{(2n+1)!}{n!}\frac{\sqrt{\pi}}{\sqrt{p}}\left(\frac{1}{p}-1\right)^n, \quad . \quad (21)$$

$$\therefore \quad \sum_{n=0}^{n=\infty}\frac{(-1)^n}{(2n+1)!}He_{2n+1}(\sqrt{x}) \doteq \frac{\sqrt{\pi}}{\sqrt{p}}e^{1-\frac{1}{p}} \doteq e\sqrt{\pi}x^{\frac{1}{4}}J_{\frac{1}{2}}(2\sqrt{x}).$$

Put

$$2\sqrt{x}=y,$$

then

$$\sum_{n=0}^{n=\infty}\frac{(-1)^n}{(2n+1)!}He_{2n+1}\left(\frac{y}{2}\right) = e\sqrt{\frac{\pi}{2}}\,y\,J_{\frac{1}{2}}(y) = e\sin y. \quad (22)$$

5. In another example, now for Bessel functions, the process is one of reversed direction. We decompose a p-function into a sum of others. Thus we can prove symbolically why Bessel functions of half-integral order can be written in the form

$$J_{n+\frac{1}{2}}(x) = A(x)\sin x + B(x)\cos x, \quad . \quad . \quad (23)$$

where $A(x)$ and $B(x)$ represent finite polynomials.

We multiply first by $x^{n+\frac{1}{2}}$, and use (F 6) for half-integer indices

$$x^{n+\frac{1}{2}}\mathrm{J}_{n+\frac{1}{2}}(x) \doteqdot \frac{2^{n+\frac{1}{2}}\Pi(n)}{\sqrt{\pi}} \frac{p}{(p^2+1)^{n+1}} \cdot \quad . \quad . \quad . \quad (24)$$

It is seen that only integral powers of p^2+1 occur when the order of the Bessel functions is a half integer. We can write

$$\frac{1}{(p^2+1)^{n+1}} = \sum_{m=0}^{m=n} \frac{\mathrm{A}_{n+1-m}^{n+1}}{(p+i)^{n+1-m}} + \sum_{m=0}^{m=n} \frac{\mathrm{B}_{n+1-m}^{n+1}}{(p-i)^{n+1-m}},$$

where the coefficients A are easily obtained by expanding the left-hand member in ascending powers of $(p+i)$, when we let p approach $-i$ and the coefficients B by expanding the same side in ascending powers of $p-i$, provided we take p close to $+i$. We thus find

$$\mathrm{A}_{n+1-m}^{n+1} = (-1)^{n+m+1}\mathrm{B}_{n+1-m}^{n+1} = \frac{(-1)^m(n+m)\,!}{m\,!\;n\,!\,(-2i)^{n+m+1}}.$$

The typical functions of p we thus get to interpret in the right-hand side of (24) are

$$\frac{p}{(p+i)^k} \doteqdot h_1(x) \quad \text{and} \quad \frac{p}{(p-i)^k} \doteqdot h_2(x).$$

Applying (R 4) we derive for $h_1(x)$ and $h_2(x)$ respectively,

$$e^{ix}h_1(x) \doteqdot \frac{1}{p^{k-1}}, \qquad e^{-ix}h_2(x) \doteqdot \frac{1}{p^{k-1}},$$

$$\therefore \quad h_1(x) = e^{-ix}\frac{x^{k-1}}{\Pi(k-1)}, \qquad h_2(x) = e^{ix}\frac{x^{k-1}}{\Pi(k-1)}.$$

In this way we obtain the ordinary equation

$$x^{n+\frac{1}{2}}\mathrm{J}_{n+\frac{1}{2}}(x)$$
$$= \frac{2^{n+\frac{1}{2}}n\,!}{\sqrt{\pi}} \sum_{m=0}^{m=n} \frac{(-1)^m(n+m)\,!}{m\,!\;n\,!} \frac{e^{-ix}+(-1)^{n+m+1}e^{ix}}{(-2i)^{n+m+1}} \frac{x^{n-m}}{(n-m)\,!}.$$

Dividing again by $x^{n+\frac{1}{2}}$ and introducing cos and sin functions, we have for even $n(n=2\nu)$

$$\mathrm{J}_{2\nu+\frac{1}{2}}(x)$$
$$= \frac{1}{\sqrt{\pi}}\left[\cos x \,.\, \sum_{\mu=0}^{\nu-1}(-1)^{\nu+\mu}\frac{(2\nu+2\mu+1)\,!\,2}{(2\mu+1)\,!\,(2\nu-2\mu-1)\,!}\frac{1}{(2x)^{2\mu+\frac{3}{2}}}\right.$$
$$\left. + \sin x \,.\, \sum_{\mu=0}^{\nu}(-1)^{\nu+\mu}\frac{(2\nu+2\mu)\,!\,2}{(2\mu)\,!\,(2\nu-2\mu)\,!}\frac{1}{(2x)^{2\mu+\frac{1}{2}}}\right], \quad . \quad . \quad . \quad (25)$$

and for n odd $(n=2\nu+1)$

$$J_{2\nu+\frac{3}{2}}(x)$$

$$= \frac{1}{\sqrt{\pi}}\left[\cos x \,.\, \sum_{\mu=0}^{\nu} (-1)^{\nu+\mu+1} \frac{(2\nu+2\mu+1)!\,2}{(2\mu)!\,(2\nu-2\mu+1)!} \frac{1}{(2x)^{2\mu+\frac{1}{2}}}\right.$$

$$\left. + \sin x \,.\, \sum_{\mu=0}^{\nu} (-1)^{\nu+\mu} \frac{(2\nu+2\mu+2)!\,2}{(2\mu+1)!\,(2\nu-2\mu)!} \frac{1}{(2x)^{2\mu+\frac{3}{2}}}\right]. \quad . \quad . \quad . \quad (26)$$

6. In another example we expand the image function into an infinite series. The following image is known :

$$\frac{p}{\sqrt{p^2+1}} e^{-\lambda\sqrt{p^2+1}} \doteqdot \begin{cases} J_0(\sqrt{x^2-\lambda^2}) & \text{for } x > \lambda, \\ 0 & \text{for } x < \lambda, \end{cases}$$

from which, by application of (R 5),

$$\frac{p}{\sqrt{p^2+1}} e^{-\lambda(\sqrt{p^2+1}-p)} \doteqdot J_0(\sqrt{x^2+2\lambda x}) \quad \text{for} \quad x > 0. \quad (27)$$

This last image can be expanded as

$$\frac{p}{\sqrt{p^2+1}}\left[1-\lambda(\sqrt{p^2+1}-p)+\frac{\lambda^2}{2!}(\sqrt{p^2+1}-p)^2-\ldots\right],$$

and since by (F 7)

$$J_n(x) \doteqdot \frac{p^n}{\sqrt{p^2+1}}(\sqrt{p^2+1}-p)^n,$$

we have

$$J_0(\sqrt{x^2+2\lambda x}) = J_0(x) - \lambda J_1(x) + \frac{\lambda^2}{2!} J_2(x) - \ldots,$$

giving for $J_n(x)$:

$$J_n(x) = \left[\frac{d^n}{d\lambda^n} J_0(\sqrt{x^2-2\lambda x})\right]_{\lambda=0}. \quad . \quad . \quad (28)$$

(ii.) *Applications of the "Product Theorem."*

1. From the identity

$$\frac{1}{p} \cdot \frac{\Pi(m)}{p^m} \cdot \frac{\Pi(n)}{p^n} = \frac{\Pi(m)\Pi(n)}{p^{m+n+1}},$$

we conclude with the aid of the product theorem (R 15)

$$\int_0^x \xi^m (x-\xi)^n \, d\xi = \frac{\Pi(m)\Pi(n)}{\Pi(m+n+1)} x^{m+n+1}.$$

Thus we find for the Beta function, defined by

$$B(n+1, m+1) = \int_0^1 \xi^m (1-\xi)^n d\xi,$$

immediately its value, expressed in Gamma functions:

$$B(n+1, m+1) = \frac{\Pi(m)\Pi(n)}{\Pi(m+n+1)}$$

or

$$B(n, m) = \frac{\Gamma(m)\Gamma(n)}{\Gamma(m+n)}. \quad . \quad . \quad . \quad (29)$$

2. As another application of the product theorem we consider the image (F 9) of the Laguerre function $L_n(x)$, now with $\Pi(n)$ instead of $n!$, from which, by means of (R 3), we get

$$\int_0^x L_n(\xi)\, d\xi \doteqdot \frac{\Pi(n)}{p}\left(1-\frac{1}{p}\right)^n. \quad . \quad . \quad . \quad (30)$$

The right-hand side can be written as

$$\frac{\Pi(n)}{\Pi(n-m)\Pi(m)}\frac{1}{p}\cdot\Pi(n-m)\left(1-\frac{1}{p}\right)^{n-m}\cdot\Pi(m)\left(1-\frac{1}{p}\right)^m$$

so that the product theorem leads here to

$$\int_0^x L_n(\xi)\, d\xi = \frac{\Pi(n)}{\Pi(n-m)\Pi(m)}\int_0^x L_{n-m}(\xi) L_m(x-\xi)\, d\xi. \quad (31)$$

3. Another example connects the polynomials of Hermite with those of Laguerre. We used already (21), which we now write in the form

$$He_{2n+1}(\sqrt{x}) \doteqdot \frac{(2n+1)!}{n!}\frac{\sqrt{\pi}}{\sqrt{p}}\left(\frac{1}{p}-1\right)^n$$

$$= (-1)^n \frac{(2n+1)!}{(n!)^2}\frac{1}{p}\cdot\sqrt{p}\cdot\sqrt{\pi}\, n!\left(\frac{p-1}{p}\right)^n.$$

From (F 9) and $\sqrt{p} \doteqdot \frac{1}{\sqrt{\pi x}}$ it follows at once, by the product theorem, that

$$He_{2n+1}(\sqrt{x}) = \frac{(-1)^n(2n+1)!}{(n!)^2}\int_0^x \frac{1}{\sqrt{\xi}} L_n(x-\xi)\, d\xi,$$

or, by introducing new variables,

$$He_{2n+1}(x) = (-1)^n \frac{(2n+1)!}{n!\, n!} 2\int_0^x L_n(x^2-\xi^2)\, d\xi. \quad (32)$$

4. There is also a connexion between Bessel and Laguerre functions. Take

$$x^{n+\frac{1}{2}}\mathrm{J}_{n+\frac{1}{2}}(x) \doteq \frac{2^{n+\frac{1}{2}}\Pi(n)}{\sqrt{\pi}} \frac{p}{(p^2+1)^{n+1}}. \quad . \quad . \quad (33)$$

In order to compare this with the image of a Laguerre function, we first transform (33) so as to get a denominator $(p^2-1)^{n+1}$, *i. e.*, one with real roots. This can be done by means of (R 1) with $s=i$, giving

$$x^{n+\frac{1}{2}}\mathrm{I}_{n+\frac{1}{2}}(x) \doteq \frac{2^{n+\frac{1}{2}}\Pi(n)}{\sqrt{\pi}} \frac{p}{(p^2-1)^{n+1}}, \quad . \quad . \quad (34)$$

where

$$\mathrm{I}_n(y) = \frac{1}{i^n}\mathrm{J}_n(iy). \quad . \quad . \quad . \quad . \quad . \quad (35)$$

We now apply rule (R 4), giving

$$e^{-x}x^{n+\frac{1}{2}}\mathrm{I}_{n+\frac{1}{2}}(x) \doteq \frac{2^{n+\frac{1}{2}}}{\sqrt{\pi}}\Pi(n)\frac{1}{(p+2)^{n+1}p^n},$$

or, applying (R 1) with $s=\frac{1}{2}$,

$$e^{-\frac{x}{2}}x^{n+\frac{1}{2}}\mathrm{I}_{n+\frac{1}{2}}\left(\frac{x}{2}\right) \doteq \frac{\Pi(n)}{\sqrt{\pi}} \frac{1}{(p+1)^{n+1}p^n} = \frac{1}{\sqrt{\pi}}\cdot\frac{1}{p}\cdot\frac{1}{p^{2n}}\cdot\frac{\Pi(n)p^{n+1}}{(p+1)^{n+1}}.$$

The factor $\left(\frac{p}{p+1}\right)^{n+1}$ can be related to Laguerre functions by means of an application of (R 4) to (F 9) giving

$$\frac{e^{-x}\mathrm{L}_n(x)}{\Pi(n)} \doteq \left(\frac{p}{p+1}\right)^{n+1}. \quad . \quad . \quad . \quad . \quad (36)$$

Applying the product theorem, we obtain

$$e^{-\frac{x}{2}}x^{n+\frac{1}{2}}\mathrm{I}_{n+\frac{1}{2}}\left(\frac{x}{2}\right) = \frac{1}{\sqrt{\pi}}\int_0^x \frac{\xi^{2n}}{\Pi(2n)}e^{-(x-\xi)}\mathrm{L}_n(x-\xi)\,d\xi,$$

or

$$e^{\frac{x}{2}}x^{n+\frac{1}{2}}\mathrm{I}_{n+\frac{1}{2}}\left(\frac{x}{2}\right) = \frac{1}{\sqrt{\pi}\,\Pi(2n)}\int_0^x e^{\xi}\xi^{2n}\mathrm{L}_n(x-\xi)\,d\xi. \quad (37)$$

5. A great number of the integrals, derived recently by J. G. Rutgers *, can be obtained very directly by means of

* J. G. Rutgers, Proc. Royal Soc. Amsterdam, xxxiv. p. 239 (1931).

the product theorem. It might be sufficient to show this for only one specimen, taken out of his collection, namely, for

$$\int_0 \mathrm{J}_n(x-\xi)\mathrm{J}_{-n-1}(\xi)(x-\xi)^n\xi^{-n}d\xi = \frac{\cos x}{\sin(n+\frac{1}{2})\pi}. \quad (38)$$

The left-hand side has the form

$$\int_0^x h_1(x-\xi)h_2(\xi)\,d\xi,$$

where

$$h_1(x) = x^n\mathrm{J}_n(x) \doteqdot \frac{2^n\Pi(n-\frac{1}{2})}{\sqrt{\pi}}\frac{p}{(p^2+1)^{n+\frac{1}{2}}} = f_1(p)$$

and

$$h_2(x) = x^{-n}\mathrm{J}_{-n-1}(x) = x.x^{-n-1}\mathrm{J}_{-n-1}(x).$$

By (R 8) and (F 6), we have

$$x.x^{-n-1}\mathrm{J}_{-n-1}(x)$$
$$\doteqdot p\left(-\frac{d}{dp}\right)\left\{\frac{2^{-(n+1)}\Pi(-n-\frac{3}{2})}{\sqrt{\pi}}\frac{1}{(p^2+1)^{-n-\frac{1}{2}}}\right\},$$

hence

$$h_2(x) \doteqdot \frac{2^{-n}\Pi(-n-\frac{1}{2})}{\sqrt{\pi}}\frac{p^2}{(p^2+1)^{-n+\frac{1}{2}}} = f_2(p).$$

Thus the left-hand side of (38) is symbolically represented by

$$\frac{1}{p}.f_1(p).f_2(p) = \frac{\Pi(n-\frac{1}{2})\Pi(-n-\frac{1}{2})}{\pi}\frac{p^2}{p^2+1}$$
$$= \frac{1}{\sin(n+\frac{1}{2})\pi}\frac{p^2}{p^2+1},$$

being just the image of the right-hand side of (38). Thus the relation (38) is proved.

6. A last application of the product theorem can be based upon the known images

$$\sqrt{\pi p}\,e^{-\frac{1}{p}}\mathrm{I}_n\left(\frac{1}{p}\right) \doteqdot \frac{1}{\sqrt{x}}\mathrm{J}_{2n}(2\sqrt{2x}), \quad . \quad . \quad (39)$$

$$e^{-\frac{1}{p}}\mathrm{I}_n\left(\frac{1}{p}\right) \doteqdot \mathrm{J}_n^2(\sqrt{2x}), \quad . \quad . \quad . \quad . \quad (40)$$

which follow immediately from known integrals (see Watson, 'Bessel Functions,' pp. 394, 395).

Writing the identity,

$$e^{-\frac{1}{p}} I_n\left(\frac{1}{p}\right) = \frac{1}{p} \cdot \sqrt{p}\, e^{-\frac{1}{p}} I_n\left(\frac{1}{p}\right) \cdot \sqrt{p},$$

and applying the product theorem, we get the relation

$$J_n^2(\sqrt{2x}) = \int_0^x \frac{1}{\sqrt{\pi\xi}} J_{2n}(2\sqrt{2\xi}) \frac{1}{\sqrt{\pi(x-\xi)}} d\xi,$$

or by an obvious transformation,

$$J_n^2(\alpha) = \frac{2}{\pi} \int_0^{\frac{\pi}{2}} J_{2n}(2\alpha \sin\theta)\, d\theta. \quad . \quad . \quad . \quad (41)$$

Some of the formulæ in the foregoing groups, namely, (17), (18), (31), and (32), were already published elsewhere*.

(iii.) *Symbolic Evaluation of Integrals.*

In connexion herewith we mention that the ordinary equation (R 11) may already give a means to evaluate integrals: If the integral on the left- or on the right-hand side is known, we find the other, as was shown already in P.† But here we mean another symbolic method, which is best explained again with the aid of some examples.

Suppose we wish to prove the formulæ

$$\int_0^\infty \frac{\sin s}{s} ds = \frac{\pi}{2},$$

$$\int_0^\infty \frac{\cos s}{1+s^2} ds = \frac{\pi}{2} \frac{1}{e},$$

$$\int_0^\infty \frac{\cos s}{\sqrt{s}} ds = \sqrt{\frac{\pi}{2}}.$$

We can consider the integrals

$$\int_0^\infty \frac{\sin \alpha s}{s} ds, \qquad \int_0^\infty \frac{\cos \alpha s}{1+s^2} ds, \qquad \int_0^\infty \frac{\cos \alpha s}{\sqrt{s}} ds,$$

* Balth. van der Pol, *Handelingen XXIIIe Ned. Natuur- en Geneesk. Congres*, April 1931, Delft.

† P. pp. 872, 887.

where the introduced parameter α will be treated symbolically:

$$\alpha \doteqdot \frac{1}{p}.$$

Thus we get functions of p, which in the above cases allow immediate integration with respect to s, and the resulting functions of p can thereupon be interpreted backwards into functions of α, where, in order finally to obtain the required result, $\alpha=1$ is to be taken.

For illustration, we take

$$\int_0^\infty \frac{\cos \alpha s}{1+s^2} ds \doteqdot \int_0^\infty \frac{p^2}{p^2+s^2} \frac{ds}{1+s^2} = \frac{\pi}{2} \frac{p}{p+1} \doteqdot \frac{\pi}{2} e^{-\alpha};$$

hence

$$\int_0^\infty \frac{\cos s}{1+s^2} ds = \frac{\pi}{2} \frac{1}{e}.$$

Sometimes it is advisable to introduce two parameters, α and β, and to treat them both symbolically:

$$\alpha \doteqdot \frac{1}{p}; \quad \beta \doteqdot \frac{1}{q},$$

as is, *e. g.*, the case for the evaluation of

$$\int_0^\infty \frac{\sin^2 s}{s^2} ds \quad \text{by means of} \quad \int_0^\infty \frac{\sin \alpha s}{s} \cdot \frac{\sin \beta s}{s} ds,$$

or in the more complicated cases in the authors' paper on simultaneous symbolic calculus *.

However, here we study the symbolic evaluation by means of *one* parameter only.

Often the integral, whose value has to be determined, must be put in a form more suitable for the introduction of α and its interpretation. This occurs, *e. g.*, in the following integral:

$$S = \int_0^\infty \frac{J_n(s)\, ds}{s^{n-m+1}}.$$

Writing $s=2\sqrt{t}$, we get

$$2^{n-m+1} S = \int_0^\infty \frac{J_n(2\sqrt{t})\, dt}{t^{\frac{n-m+2}{2}}} = \int_0^\infty \frac{t^{\frac{n}{2}} J_n(2\sqrt{t})\, dt}{t^{\frac{2n-m+2}{2}}}.$$

* Balth. van der Pol and K. F. Niessen, Phil. Mag. xi. p. 368 (1931).

Introduce and treat, now, α in the following way:

$$2^{n-m+1}\mathrm{S}(\alpha) = \int_0^\infty \frac{(\alpha t)^{\frac{n}{2}}\mathrm{J}_n(2\sqrt{\alpha t})}{t^{\frac{2n-m+2}{2}}}\,dt,$$

$$\alpha \doteqdot \frac{1}{p},$$

$$2^{n-m+1}\mathrm{S}(\alpha) \doteqdot \int_0^\infty \left(\frac{p}{t}\right)^{-n} e^{-\frac{t}{p}} t^{-\frac{2n-m+2}{2}}\,dt = \frac{\Pi\left(\frac{m}{2}-1\right)}{p^{n-\frac{m}{2}}},$$

where we first used (F 5) with (R 1), and secondly Euler's formula for the Π-function. Hence

$$2^{n-m+1}\mathrm{S}(\alpha) = \frac{\Pi\left(\frac{m}{2}-1\right)}{\Pi\left(n-\frac{m}{2}\right)}\alpha^{n-\frac{m}{2}}.$$

With $\alpha=1$ and $2\sqrt{t}=s$, this gives

$$\int_0^\infty \frac{\mathrm{J}_n(s)\,ds}{s^{n-m+1}} = \frac{1}{2^{n-m+1}}\frac{\Pi\left(\frac{m}{2}-1\right)}{\Pi\left(n-\frac{m}{2}\right)}, \quad . \quad . \quad . \quad (42)$$

being Weber's integral (see Watson, 'Bessel Functions,' p. 391).

(iv. *a*.) *Transformation of the Original Relation into one with the Factor* $e^{-\frac{1}{p}}$.

In the following examples a predominant role is played by the relation (F 5):

$$\frac{1}{p^n}e^{-\frac{1}{p}} \doteqdot x^{\frac{n}{2}}\mathrm{J}_n(2\sqrt{x}).$$

1. We start with a known integral, *e. g.*, with

$$\int_0^\infty e^{-\alpha s}s^n\mathrm{J}_n(s)\,ds = \frac{2^n}{\sqrt{\pi}}\Pi(n-\tfrac{1}{2})\frac{1}{(\alpha^2+1)^{n+\frac{1}{2}}}. \quad . \quad (43)$$

Substitute

$$\alpha = \beta + \frac{1}{p},$$

thus

$$\int_0^\infty e^{-\beta s} e^{-\frac{s}{p}} s^n \mathrm{J}_n(s)\,ds = \frac{2^n}{\sqrt{\pi}} \frac{\Pi(n-\frac{1}{2})}{(\beta^2+1)^{n+\frac{1}{2}}} \frac{p^{2n+1}}{\left[\left(p+\frac{\beta}{\beta^2+1}\right)^2+\left(\frac{1}{\beta^2+1}\right)^2\right]^{n+\frac{1}{2}}}. \quad (44)$$

For a later purpose we prefer to write (44) first in the form

$$\int_0^\infty \frac{e^{-\beta s}}{s^n} \frac{s^{2n}}{p^{2n}} e^{-\frac{s}{p}} \mathrm{J}_n(s)\,ds = \frac{2^n}{\sqrt{\pi}} \frac{\Pi(n-\frac{1}{2})}{(\beta^2+1)^{n+\frac{1}{2}}} \frac{p}{\left[\left(p+\frac{\beta}{\beta^2+1}\right)^2+\left(\frac{1}{\beta^2+1}\right)^2\right]^{n+\frac{1}{2}}}. \quad (45)$$

So far, p was introduced and treated as an ordinary constant, but from here we will consider p as a symbolic parameter, used in a symbolic calculus, where $\frac{1}{p}$ is the image of some quantity x :

$$\frac{1}{p} \doteqdot x.$$

Thanks to the symbolic nature we ascribed to p, we can interpret backwards both members of (45) into functions of x. For the interpretation of the left-hand side we use

$$\frac{s^{2n}}{p^{2n}} e^{-\frac{s}{p}} \doteqdot (xs)^n \mathrm{J}_n(2\sqrt{xs}), \quad . \quad . \quad . \quad . \quad (46)$$

originating from (F 5) and (R 1), so that the integral belongs to the original :

$$x^n \int_0^\infty e^{-\beta s} \mathrm{J}_{2n}(2\sqrt{xs}) \mathrm{J}_n(s)\,ds.$$

To find the original $h(x)$ of the right-hand side of (45), we apply (R 4) and determine $h(x)$ by means of

$$e^{\frac{\beta}{\beta^2+1}x} h(x) \doteqdot \frac{2^n}{\sqrt{\pi}} \frac{\Pi(n-\frac{1}{2})}{(\beta^2+1)^{n+\frac{1}{2}}} \frac{p}{\left[p^2+\left(\frac{1}{\beta^2+1}\right)^2\right]^{n+\frac{1}{2}}},$$

hence,

$$h(x) = e^{-\frac{\beta}{\beta^2+1}x} (\beta^2+1)^{n+\frac{1}{2}} \left(\frac{x}{\beta^2+1}\right)^n \mathrm{J}_n\left(\frac{x}{\beta^2+1}\right).$$

The original functions belonging to both members of (45) being equal, we have the new relation,

$$\int_0^\infty e^{-\beta s} J_{2n}(2\sqrt{sx}) J_n(s)\, ds = \frac{1}{\sqrt{\beta^2+1}} e^{-\frac{\beta}{\beta^2+1}x} J_n\left(\frac{x}{\beta^2+1}\right), \quad . \quad . \quad . \quad (47)$$

yielding the value of an infinite integral in whose integrand appear two Bessel functions with arguments of a different kind with respect to the integration variable.

Substituting $\beta=0$ in (47), we have the special case

$$\int_0^\infty J_{2n}(2\sqrt{sx}) J_n(s)\, ds = J_n(x). \quad . \quad . \quad . \quad (48)$$

2. In another example we consider the known integral *,

$$\int_0^\infty e^{-\alpha\frac{s^2}{4}} s^{n+1} J_n(s)\, ds = \frac{2^{n+1}}{\alpha^{n+1}} e^{-\frac{1}{\alpha}}. \quad . \quad . \quad . \quad (49)$$

We substitute again

$$\alpha = \beta + \frac{1}{p},$$

thus,

$$\int_0^\infty e^{-\beta\frac{s^2}{4}} e^{-\frac{s^2}{4p}} s^{n+1} J_n(s)\, ds = \left(\frac{2}{\beta}\right)^{n+1} \frac{p^{n+1}}{\left(p+\frac{1}{\beta}\right)^{n+1}} e^{-\frac{1}{\beta}\frac{p}{p+\frac{1}{\beta}}}.$$

Divide both members by p^n in order to get easily interpretable functions of p,

$$\int_0^\infty e^{-\beta\frac{s^2}{4}} s^{n-1} \left(\frac{s^2}{4p}\right)^n e^{-\frac{s^2}{4p}} J_n(s)\, ds = \left(\frac{2}{\beta}\right)^{n+1} \frac{p}{\left(p+\frac{1}{\beta}\right)^{n+1}} e^{-\frac{1}{\beta}\frac{p}{p+\frac{1}{\beta}}}. \quad . \quad . \quad . \quad (50)$$

Ascribing now a symbolic nature to p,

$$\frac{1}{p} \doteqdot x,$$

we can interpret backwards both members of (50).

For the first one we use

$$\left(\frac{s^2}{4p}\right)^n e^{-\frac{s^2}{4p}} \doteqdot \left(\frac{xs^2}{4}\right)^n J_n\left(2\sqrt{\frac{xs^2}{4}}\right), \quad . \quad (51)$$

* Watson, 'Bessel Functions,' p. 394, (4).

originating from (F 5) and (R 1), whereupon the whole first member can be easily interpreted.

In order to find the original $h(x)$, corresponding to the second member in (50), we apply (R 4) and have to determine $h(x)$ from

$$e^{\frac{1}{\beta}x}\, h(x) \doteq 2^{n+1}\beta^{n-1}e^{-\frac{1}{\beta}}\frac{1}{(\beta^2 p)^n}e^{\frac{1}{\beta^2 p}}.$$

Now,

$$\frac{1}{p^n}e^{\frac{1}{p}} \doteq x^{\frac{n}{2}}\mathrm{I}_n(2\sqrt{x}),$$

where

$$\mathrm{I}_n(y) = \frac{1}{i^n}\mathrm{J}_n(iy).$$

Thus

$$e^{\frac{1}{\beta}x}h(x) = 2^{n+1}\beta^{n-1}e^{-\frac{1}{\beta}}\left(\frac{x}{\beta^2}\right)^{\frac{n}{2}}\mathrm{I}_n\left(2\sqrt{\frac{x}{\beta^2}}\right),$$

and thus $h(x)$ is known.

Equating the original functions we found to belong to the first and second member of (50), we obtain, with

$$\sqrt{x} = \alpha,$$

$$\int_0^\infty e^{-\beta\frac{s^2}{4}} s\mathrm{J}_n(s)\mathrm{J}_n(\alpha s)\,ds = \frac{2}{\beta}e^{-\frac{\alpha^2+1}{\beta}}\mathrm{I}_n\left(\frac{2\alpha}{\beta}\right), \quad . \quad (52)$$

thus deriving in a very simple way Weber's second exponential integral (*cf.* Watson, 'Bessel Functions,' p. 395, form (1)).

3. It is not advisable to take $\beta=0$ in this formula, for the right-hand member then would take the form $0\times\infty$. In connexion herewith two formulæ can easily be derived, again with symbolic methods :

a. The value of (52) for $\beta=0$.

b. A discontinuous integral of a different nature.

For their derivation it is better to go back to (49), where the substitution

$$\alpha = \frac{1}{p}$$

gives

$$\int_0^\infty e^{-\frac{s^2}{4p}} s^{n+1}\mathrm{J}_n(s)\,ds = 2^{n+1}p^{n+1}e^{-p}. \quad . \quad . \quad (53)$$

From this we can derive two results.

a. For the evaluation of (52) with $\beta=0$ we divide both members of (53) by p^n, just as in the case $\beta>0$,

$$\int_0^\infty \frac{1}{p^n} e^{-\frac{s^2}{4p}} s^{n+1} J_n(s)\,ds = 2^{n+1} p e^{-p}. \quad . \quad . \quad (54)$$

The right-hand member now containing the factor e^{-p} is of a form entirely different from that in the case $\beta>0$, since, according to (6), pe^{-p} is the image of an impulsive function with its maximum at $x=1$, which is indicated by the Dirac δ-function, $\delta(x-1)$.

The left-hand member of (54) can again be interpreted by means of (51). Thus we obtain for the integral (52) with $\beta=0$ (by substituting again $\sqrt{x}=\alpha$),

$$\int_0^\infty s J_n(\alpha s) J_n(s)\,ds = \frac{2}{\alpha^n}\delta(\alpha^2-1). \quad . \quad . \quad . \quad (55)$$

b. Returning to (53) we divide both members by p^{m+1}, where we suppose

$$m > n.$$

In the relation, thus obtained,

$$\int_0^\infty \frac{1}{p^{m+1}} e^{-\frac{s^2}{4p}} s^{n+1} J_n(s)\,ds = 2^{n+1}\frac{e^{-p}}{p^{m-n}}; \quad . \quad . \quad (56)$$

p is understood again to be a symbolic parameter. The first member then can be interpreted with the aid of

$$\left(\frac{s^2}{4p}\right)^{m+1} e^{-\frac{s^2}{4p}} \doteq \left(\frac{s^2 w}{4}\right)^{\frac{m+1}{2}} J_{m+1}\left(2\sqrt{\frac{s^2 w}{4}}\right).$$

The second member by means of

$$e^{-p}\frac{1}{p^{m-n}} \doteq \begin{cases} 0 & \text{for } x<1, \\ \dfrac{(x-1)^{m-n}}{\Pi(m-n)} & \text{for } x>1, \end{cases}$$

which is based upon (F 1) and (R 5).

Equating the original functions belonging to the first and second member of (56), we get (again with $x=\sqrt{\alpha}$)

$$\int_0^\infty \frac{J_{m+1}(\alpha s) J_n(s)\,ds}{s^{m-n}} = \begin{cases} 0 & \text{for } \alpha<1, \\ \dfrac{(\alpha^2-1)^{m-n}}{2^{m-n}\Pi(m-n)\alpha^{m+1}} & \text{for } \alpha>1, \end{cases} \quad . \quad . \quad . \quad (57)$$

in accordance with Watson, 'Bessel Functions,' p. 401, (2).

4. In another example of this group the term $e^{-\frac{1}{p}}$ originates from the substitution $\alpha = \frac{1}{p}$ in the known integral,

$$\int_0^\infty \frac{J_0(s)\, s\, ds}{\sqrt{s^2+\alpha^2}} = e^{-\alpha}$$

giving

$$\int_0^\infty J_0(s) \frac{ps}{\sqrt{p^2 s^2+1}}\, ds = e^{-\frac{1}{p}}.$$

Considering here, again, p as a symbolic parameter for which

$$\frac{1}{p} \doteqdot x,$$

we obtain by interpretation of both members,

$$\int_0^\infty J_0(s) J_0\left(\frac{x}{s}\right) ds = J_0(2\sqrt{x}), \quad (x>0). \quad (58)$$

a relation already known to Heaviside *.

5. One may also start from

$$\int_0^\infty e^{-\alpha s} s^n ds = \frac{\Pi(n)}{\alpha^{n+1}}.$$

Substitute

$$\alpha = 1+\frac{1}{p},$$

$$\int_0^\infty e^{-\left(1+\frac{1}{p}\right)s} s^n ds = \Pi(n)\left(1+\frac{1}{p}\right)^{-(n+1)}. \quad . \quad (59)$$

Now from (36) we know

$$e^{-x} L_n(x) \doteqdot \Pi(n)\left(1+\frac{1}{p}\right)^{-(n+1)}. \quad . \quad . \quad (36)$$

Interpretation of both members of (59) leads therefore to

$$L_n(x) = e^x \int_0^\infty e^{-s} s^n J_0(2\sqrt{s.x})\, ds. \quad . \quad (60a)\dagger$$

* O. Heaviside, *l. c.* iii. p. 281, form 295.

† In a recent paper by Sommerfeld (*Ann. d. Phys.* xi. p. 272, 1931) we found this equation ascribed to Epstein and Muskat (Proc. Nat. Acad. xv. p. 405, 1929).

In order to obtain a similar expression for Hermite's polynomials we transform the original function by means of our rules, so that the image contains a factor $\left(1+\frac{1}{p}\right)^{-n}$, and then replace this by means of (59) by an integral containing $e^{-\frac{s}{p}}$.

We use (21 *a*) for polynomials of odd order

$$\mathrm{He}_{2n+1}(\sqrt{x}) \doteqdot 2^{2n+1}\Pi(n+\tfrac{1}{2})\frac{1}{\sqrt{p}}\left(\frac{1-p}{p}\right)^{n} \quad . \quad (21\,a)$$

and by application of (R 4),

$$e^{-x}\mathrm{He}_{2n+1}(\sqrt{x}) \doteqdot 2^{2n+1}\Pi(n+\tfrac{1}{2})(-1)^{n}\frac{1}{\sqrt{p+1}}\left(\frac{p}{p+1}\right)^{n+1}$$

$$\text{,,} \qquad \doteqdot 2^{2n+1}\Pi(n+\tfrac{1}{2})(-1)^{n}\frac{1}{\sqrt{p}}\left(1+\frac{1}{p}\right)^{-(n+\frac{1}{2})}$$

$$\text{,,} \qquad \doteqdot 2^{2n+1}(-1)^{n}\frac{1}{\sqrt{p}}\int_{0}^{\infty} e^{-\left(1+\frac{1}{p}\right)s}\,s^{n+\frac{1}{2}}\,ds$$

$$\text{,,} \qquad \doteqdot 2^{2n+1}(-1)^{n}\int_{0}^{\infty} e^{-s}\,s^{n}\left(\frac{s}{p}\right)^{\frac{1}{2}}e^{-\frac{s}{p}}\,ds,$$

from which, by interpretation backwards,

$$\mathrm{He}_{2n+1}(\sqrt{x}) = (-1)^{n}2^{2n+1}x^{\frac{1}{4}}e^{x}\int_{0}^{\infty} e^{-s}\,s^{n+\frac{1}{4}}\mathrm{J}_{\frac{1}{2}}(2\sqrt{sx})\,ds, \quad (60\,b)$$

expressing Hermite polynomials of odd order as an integral containing a Bessel function.

Using

$$\mathrm{J}_{\frac{1}{2}}(x) = \sqrt{\frac{2}{\pi x}}\sin x$$

and introducing $\xi=\sqrt{x}$ and $t=\sqrt{s}$, we can write the expression (60 *b*) also in the form

$$\mathrm{He}_{2n+1}(\xi) = \frac{(-1)^{n}2^{2n+2}}{\sqrt{\pi}}e^{\xi^{2}}\int_{0}^{\infty} e^{-t^{2}}t^{2n+1}\sin(2\xi t)\,dt.$$

7. The images (36) and (21 *a*) lend themselves also very well to an application of the product theorem.

First combining two images of the type (36), we have

$$\frac{1}{p}\cdot n!\left(1+\frac{1}{p}\right)^{-(n+1)}\cdot m!\left(1+\frac{1}{p}\right)^{-(m+1)}$$

$$= n\,!\,m\,!\frac{1}{p}\left(1+\frac{1}{p}\right)^{-(n+m+2)}$$

$$= \frac{n\,!\,m\,!}{(n+m+1)\,!}\int_0^\infty e^{-s}s^{n+m}\frac{s}{p}\epsilon^{-\frac{s}{p}}\,ds.$$

By application of the product theorem we get

$$\int_0^x e^{-\xi}\mathrm{L}_n(\xi)e^{-(x-\xi)}\mathrm{L}_m(x-\xi)\,d\xi$$

$$= \frac{n\,!\,m\,!}{(n+m+1)\,!}\int_0^\infty e^{-s}s^{n+m}(sx)^{\frac{1}{2}}\mathrm{J}_1(2\sqrt{sx})\,ds,$$

or

$$\int_0^x \mathrm{L}_n(\xi)\mathrm{L}_m(x-\xi)\,d\xi$$

$$= \frac{n\,!\,m\,!}{(n+m+1)\,!}x^{\frac{1}{2}}e^x\int_0^\infty e^{-s}s^{n+m+\frac{1}{2}}\mathrm{J}_1(2\sqrt{sx})\,ds. \quad (60\,aa)$$

8. Now combining an image (36) with an image (21 *a*) we construct the identity,

$$\frac{1}{p}\cdot n\,!\left(1+\frac{1}{p}\right)^{-(n+1)}\cdot(-1)^m 2^{2m+1}\Pi(m+\tfrac{1}{2})\frac{1}{\sqrt{p}}\left(1+\frac{1}{p}\right)^{-(m+\frac{3}{2})}$$

$$= (-1)^m 2^{2m+1}\Pi(n)\Pi(m+\tfrac{1}{2})\frac{1}{p^{\frac{3}{2}}}\left(1+\frac{1}{p}\right)^{-(n+m+\frac{5}{2})}$$

$$= (-1)^m 2^{2m+1}\frac{\Pi(n)\Pi(m+\frac{1}{2})}{\Pi(n+m+\frac{3}{2})}\frac{1}{p^{\frac{3}{2}}}\int_0^\infty e^{-(1+\frac{1}{p})s}s^{n+m+\frac{3}{2}}\,ds.$$

Application of the product theorem gives

$$\int_0^x e^{-\xi}\mathrm{L}_n(\xi)e^{-(x-\xi)}\mathrm{He}_{2m+1}(\sqrt{x-\xi})\,d\xi$$

$$= (-1)^m 2^{2m+1}\frac{\Pi(n)\Pi(m+\frac{1}{2})}{\Pi(n+m+\frac{3}{2})}\int_0^\infty e^{-s}s^{n+m}(sx)^{\frac{1}{4}}\mathrm{J}_{\frac{1}{2}}(2\sqrt{sx})\,ds$$

or

$$\int_0^x \mathrm{L}_n(\xi)\mathrm{He}_{2m+1}(\sqrt{x-\xi})\,d\xi$$

$$= (-1)^m 2^{2m+1}\frac{\Pi(n)\Pi(m+\frac{1}{2})}{\Pi(n+m+\frac{3}{2})}x^{\frac{1}{4}}e^x\int_0^\infty e^{-s}s^{m+n+\frac{3}{4}}\mathrm{J}_{\frac{1}{2}}(2\sqrt{sx})\,ds.$$

$$\ldots \quad (60\,ab)$$

9. Finally, combining two images both of the type (21 *a*), we start with the identity :

$$\frac{1}{p}\cdot(-1)^n 2^{2n+1}\Pi(n+\tfrac{1}{2})\frac{1}{\sqrt{p}}\left(1+\frac{1}{p}\right)^{-(n+\frac{3}{2})}\times$$
$$(-1)^m 2^{2m+1}\Pi(m+\tfrac{1}{2})\frac{1}{\sqrt{p}}\left(1+\frac{1}{p}\right)^{-(m+\frac{3}{2})}$$
$$=(-1)^{m+n}2^{2(m+n+1)}\Pi(n+\tfrac{1}{2})\Pi(m+\tfrac{1}{2})\frac{1}{p^2}\left(1+\frac{1}{p}\right)^{-(m+n+3)}$$
$$=(-1)^{m+n}2^{2(m+n+1)}\frac{\Pi(n+\frac{1}{2})\Pi(m+\frac{1}{2})}{\Pi(m+n+2)}\frac{1}{p^2}$$
$$\int_0^\infty e^{-\left(1+\frac{1}{p}\right)s}s^{m+n+2}\,ds,$$

which, interpreted backwards, means

$$\int_0^x e^{-\xi}\mathrm{He}_{2n+1}(\sqrt{\xi})\,e^{-(x-\xi)}\mathrm{He}_{2m+1}(\sqrt{x-\xi})\,d\xi$$
$$=(-1)^{m+n}2^{2(m+n+1)}\frac{\Pi(n+\frac{1}{2})\Pi(m+\frac{1}{2})}{\Pi(m+n+2)}\times$$
$$\int_0^\infty e^{-s}s^{m+n}(sx)\mathrm{J}_2(2\sqrt{sx})\,ds,$$

or

$$\int_0^x \mathrm{He}_{2n+1}(\sqrt{\xi})\mathrm{He}_{2m+1}(\sqrt{x-\xi})\,d\xi$$
$$=(-1)^{m+n}2^{2(m+n+1)}\frac{\Pi(n+\frac{1}{2})\Pi(m+\frac{1}{2})}{\Pi(m+n+2)}xe^x\times$$
$$\int_0^\infty e^{-s}s^{m+n+1}\mathrm{J}_2(2\sqrt{sx})\,ds. \quad . \quad (60\,bb)$$

We further remark, that in (60 *aa*), (60 *ab*), and (60 *bb*) the factor containing the Π-functions can also be expressed as a Beta-function, for we have (see (29))

$$\mathrm{B}(n+1,\,m+1)=\frac{\Pi(m)\Pi(n)}{\Pi(m+n+1)}.$$

(iv.*b*.) *Transformation of the Original Relation into one containing the Factor* $\dfrac{p}{\sqrt{p^2+1}}e^{-\sqrt{p^2+1}\,\lambda}$.

In this group the following relation is used :

$$\frac{p}{\sqrt{p^2+1}}\,e^{-\sqrt{p^2+1}\,s} \doteq \begin{cases} J_0(\sqrt{x^2-s^2}) & \text{for } x>s \\ 0 & \text{for } x<s. \end{cases} \quad . \quad . \quad (61)$$

We will now give a few examples, arranged according to an increasing complication of the known integrals with which we start.

1. In the simplest case we begin with

$$\int_0^\infty e^{-\alpha s}\,ds = \frac{1}{\alpha};$$

wherein we substitute

$$\alpha = \sqrt{p^2+1},$$

whereupon we multiply both members with $\frac{p}{\sqrt{p^2+1}}$, so that

$$\int_0^\infty \frac{p}{\sqrt{p^2+1}}\,e^{-s\sqrt{p^2+1}}\,ds = \frac{p}{p^2+1}.$$

Considering now p again as a symbolic parameter for which

$$\frac{1}{p} \doteq x,$$

we get, by application of (61) for the interpreted members, the equation

$$\int_0^x J_0(\sqrt{x^2-s^2})\,ds = \sin x, \quad . \quad . \quad . \quad . \quad (62)$$

a well-known integral, where the upper limit became $s=x$ on account of the fact that the function on the right-hand side of (61) is zero for $s>x$.

2. In the same way we obtain, from the known integral

$$\int_0^\infty e^{-\alpha s}\cos s\,ds = \frac{\alpha}{\alpha^2+1}$$

by substitution of $\alpha = \sqrt{p^2+1}$ and multiplication with $\frac{p}{\sqrt{p^2+1}}$,

$$\int_0^\infty \frac{p}{\sqrt{p^2+1}}\,e^{-s\sqrt{p^2+1}}\cos s\,ds = \frac{p}{p^2+2},$$

which, interpreted backwards, in a calculus, where

$$\frac{1}{p} \doteqdot x,$$

leads, by means of (F 3), to

$$\int_0^x J_0(\sqrt{x^2-s^2}) \cos s\, ds = \frac{1}{\sqrt{2}} \sin(x\sqrt{2}), \quad . \quad (63)$$

being a special case of Sonine's formula (Watson, 'Bessel Functions,' p. 376, (1)).

3. New formulæ can be obtained, if we apply this method together with the product theorem.

E. g., the known integral,

$$\int_0^\infty e^{-as} \sin s\, ds = \frac{1}{a^2+1},$$

leads, after the above transformation, to

$$\int_0^\infty \frac{p}{\sqrt{p^2+1}} e^{-s\sqrt{p^2+1}} \sin s\, ds = \frac{1}{p} \cdot \frac{p}{\sqrt{p^2+1}} \cdot \frac{p}{p^2+2},$$

or by interpretation, if

$$\frac{1}{p} \doteqdot x$$

and application of (F 6), (F 3), and (R 15) to

$$\int_0^x J_0(\sqrt{x^2-s^2}) \sin s\, ds = \frac{1}{\sqrt{2}} \int_0^x J_0(x-\xi) \sin(\xi\sqrt{2})\, d\xi.$$

. . . (64)

4. Or we may start with the given integral,

$$\int_0^\infty e^{-as} J_0(s)\, ds = \frac{1}{\sqrt{a^2+1}},$$

which leads to

$$\int_0^\infty \frac{p}{\sqrt{p^2+1}} e^{-s\sqrt{p^2+1}} J_0(s)\, ds = \frac{p}{\sqrt{p^2+1}} \cdot \frac{p}{\sqrt{p^2+2}} \cdot \frac{1}{p}.$$

Hence,

$$\int_0^x J_0(\sqrt{x^2-s^2}) J_0(s)\, ds = \int_0^x J_0(x-\xi) J_0(\xi\sqrt{2})\, d\xi. \quad (65)$$

5. Take, for a last example, the known integral,

$$\int_c^{\infty} e^{-\alpha s}\,ds = \frac{e^{-c\alpha}}{\alpha}.$$

Replace $\alpha = \sqrt{p^2+1}$ and multiply with $\dfrac{p}{\sqrt{p^2+1}}$, then

$$\int_c^{\infty} \frac{p}{\sqrt{p^2+1}} e^{-\sqrt{p^2+1}\,s}\,ds = \frac{1}{p}\cdot\frac{p}{\sqrt{p^2+1}}\cdot\frac{p}{\sqrt{p^2+1}} e^{-c\sqrt{p^2+1}}. \quad . \quad . \quad . \quad (66)$$

Relating symbolically

$$\frac{1}{p} \doteq x,$$

and using (61), the original, belonging to the left-hand side of (66), will be

$$\int_c^{x} \mathrm{J}_0(\sqrt{x^2-s^2})\,ds \quad \text{for } x>c. \quad . \quad (67)$$

The last condition is necessary, since for $x<c$ we would have $x<$ all values of s, available in the left-hand side of (66), so that its image would disappear on account of (61). The original of the right-hand side will be of the form

$$\int_0^{x} h_1(x-\xi)h_2(\xi)\,d\xi,$$

where

$$h_1(\xi) = \mathrm{J}_0(\xi),$$

$$h_2(\xi) = \begin{cases} \mathrm{J}_0(\sqrt{\xi^2-c^2}) & \text{for } \xi>c, \\ 0 & \text{for } \xi<c. \end{cases}$$

The original thus becomes

$$\int_c^{x} \mathrm{J}_0(x-\xi)\mathrm{J}_0(\sqrt{\xi^2-c^2})\,d\xi. \quad . \quad . \quad . \quad (68)$$

Equating (67) and (68) we get

$$\int_c^{x} \mathrm{J}_0(\sqrt{x^2-s^2})\,ds = \int_c^{x} \mathrm{J}_0(x-\xi)\mathrm{J}_0(\sqrt{\xi^2-c^2})\,d\xi. \quad (69)$$

For $c=0$,

$$\int_0^{x} \mathrm{J}_0(\sqrt{x^2-s^2})\,ds = \int_0^{x} \mathrm{J}_0(x-\xi)\mathrm{J}_0(\xi)\,d\xi,$$

being in accordance with (62), since by P 883 we have

$$\int_0^{x} \mathrm{J}_0(x-\xi)\mathrm{J}_0(\xi)\,d\xi = \sin x.$$

(v.) *The Mixed Group.*

1. In the theory of propagation of radiowaves over the earth, an important role is played by the integral S :

$$S = \int_0^\infty \frac{J_0(\lambda r) e^{-\sqrt{\lambda^2-k^2}\, z} \lambda d\lambda}{\sqrt{\lambda^2-k^2}} = \frac{e^{ik\sqrt{r^2+z^2}}}{\sqrt{r^2+z^2}}, \quad . \quad (70)$$

where k is a complex quantity in the first quadrant. The root $\sqrt{\lambda^2-k^2}$ is to be taken with a positive real part. The symbolic calculus provides a proof of this formula in a very simple way.

We prefer here to use a symbolic calculus, where it is not r, but r^2, which is represented by $\frac{1}{p}$,

$$r^2 \doteqdot \frac{1}{p},$$

so that a function $h(r^2)$ of r^2 is represented by

$$h(r^2) \doteqdot p \int_0^\infty e^{-pr^2} h(r^2) d(r^2). \quad . \quad . \quad . \quad (71)$$

To evaluate the integral S by means of the symbolic calculus, we first write

$$J_0(\lambda r) = J_0\left(2\sqrt{\frac{\lambda^2}{4} r^2}\right) \doteqdot e^{-\frac{\lambda^2}{4p}}$$

on account of (F 5), where x is to be replaced by r^2. Therefore

$$S \doteqdot \int_0^\infty e^{-\frac{\lambda^2}{4p}} e^{-z\sqrt{\lambda^2-k^2}} \frac{\lambda\, d\lambda}{\sqrt{\lambda^2-k^2}}.$$

We transform this function of p by the substitution,

$$\lambda = 2p\sqrt{u},$$

giving

$$S \doteqdot p \int_0^\infty e^{-pu-2pz\sqrt{u-\left(\frac{k}{2p}\right)^2}} \frac{du}{\sqrt{u-\left(\frac{k}{2p}\right)^2}}.$$

Putting

$$u-\left(\frac{k}{2p}\right)^2 = v^2,$$

we get

$$S \doteqdot 2p \int_{-\frac{ik}{2p}}^\infty e^{-pv^2-\frac{k^2}{4p}-2pzv}\, dv.$$

Defining a new variable t by means of

$$v = -i\frac{k}{2p} + \sqrt{t^2 + z^2} - z,$$

we have

$$S \doteqdot p \int_0^\infty e^{-pt^2} \frac{e^{ik\sqrt{t^2+z^2}}}{\sqrt{t^2+z^2}} d(t^2),$$

and, therefore, by means of (71)

$$S = \frac{e^{ik\sqrt{r^2+z^2}}}{\sqrt{r^2+z^2}}.$$

2. The heuristic value of the symbolic calculus appears, *e.g.*, clearly from the following examples.

We can from the known relation

$$H^{(2)}_{n+\frac{1}{2}}(ix) = \sqrt{\frac{2}{\pi}}\, i^{n+\frac{1}{2}} x^{n+\frac{1}{2}} \left(\frac{1}{x}\frac{d}{dx}\right)^n \left(\frac{e^x}{x}\right), \quad . \quad (72)$$

derive another expression for the Hankel function $H^{(2)}_{n+\frac{1}{2}}(ix)$. From (F 8) we know, on the one hand, that the harmonic $P_n(1-x)$ in a symbolic calculus where

$$x \doteqdot \frac{1}{p},$$

is represented by

$$P_n(1-x) \doteqdot e^{-p} p^{n+1} \left(\frac{1}{p}\frac{d}{dp}\right)^n \left(\frac{e^p}{p}\right), \quad . \quad . \quad (F\,8)$$

where the image shows a remarkable similarity with the right member of (72).

On the other hand, Rodrigues's formula

$$P_n(y) = \frac{1}{2^n n!}\frac{d^n}{dy^n}(y^2-1)^n,$$

gives

$$P_n(1-x) = \frac{1}{n!}\frac{d^n}{dx^n}\left(x - \frac{x^2}{2}\right)^n, \quad . \quad . \quad . \quad (73)$$

being a polynomial in x with positive powers. For such a polynomial $h(x)$ we found already (see (7))

$$h(x) \doteqdot p\, h\left(-\frac{d}{dp}\right)\frac{1}{p}.$$

Hence

$$\left(x-\frac{x^2}{2}\right)^n \doteq p\left(-\frac{d}{dp}-\frac{1}{2}\frac{d^2}{dp^2}\right)^n \frac{1}{p}. \quad . \quad . \quad (74)$$

The function on the left-hand side, and also its first $(n-1)$ differential quotients disappear for $x=0$. Therefore, we may apply rule (R 2) n-times to (74), giving in connexion with (73),

$$P_n(1-x) \doteq \frac{1}{n!}p^n p\left(-\frac{d}{dp}-\frac{1}{2}\frac{d^2}{dp^2}\right)^n \frac{1}{p}$$

or

$$P_n(1-x) \doteq p^{n+1}\left(1+\frac{1}{2}\frac{d}{dp}\right)^n \frac{1}{p^{n+1}}, \quad . \quad . \quad (75)$$

which is a new symbolic representation of $P_n(1-x)$*. We thus have two images (F 8) and (75) for the same original $P_n(1-x)$, and these always being identical, we have

$$e^{-p}p^{n+1}\left(\frac{1}{p}\frac{d}{dp}\right)^n\left(\frac{e^p}{p}\right) = p^{n+1}\left(1+\frac{1}{2}\frac{d}{dp}\right)^n \frac{1}{p^{n+1}}.$$

This equation being an identity, we may replace here p by any arbitrary value $s>0$, so that we have in general the identity:

$$e^{-s}\left(\frac{1}{s}\frac{d}{ds}\right)^n\left(\frac{e^s}{s}\right) = \left(1+\frac{1}{2}\frac{d}{ds}\right)^n \frac{1}{s^{n+1}}\,\dagger \quad . \quad . \quad . \quad (76)$$

We now apply this result to (72) and obtain a new expression for $H^{(2)}_{n+\frac{1}{2}}(is)$:

$$H^{(2)}_{n+\frac{1}{2}}(is) = \sqrt{\frac{2}{\pi}}(is)^{n+\frac{1}{2}}e^s\left(1+\frac{1}{2}\frac{d}{ds}\right)^n \frac{1}{s^{n+1}}. \quad . \quad (77)$$

In an analogous way we derive from

$$H^{(1)}_{n+\frac{1}{2}}(is) = \sqrt{\frac{2}{\pi}}i^{n+\frac{1}{2}}s^{n+\frac{1}{2}}\left(\frac{1}{s}\frac{d}{ds}\right)^n\left(\frac{e^{-s}}{-s}\right), \quad . \quad (78)$$

* The image (75) could, contrary to Rodrigues's formula (73), be used for a definition of spherical harmonics with fractional index. One would only have to expand the binomial and to interpret backwards the individual terms on the right-hand side of (75). Thus a solution is obtained of the differential equation for $P_n(1-x)$ with fractional index. A similar remark can be made with respect to (72) and (77) below.

† It might be of interest to show how this identity, which was found easily in a symbolic way, can also be proved by using ordinary analysis. We have

$$\frac{1}{s}\frac{d}{ds}\left(\frac{e^s}{s}\right) = \frac{1}{s}\frac{d}{ds}\int_{-1}^{+\infty} e^{-s\xi}\,d\xi = \frac{1}{s}\int_{-1}^{+\infty} e^{-s\xi}(-\xi)d\xi$$

$$= \frac{1}{s}\int_{-1}^{+\infty} e^{-s\xi}\,d\left(\frac{1}{2}-\frac{\xi^2}{2}\right) = \int_{-1}^{+\infty}\left(\frac{1}{2}-\frac{\xi^2}{2}\right)e^{-s\xi}\,d\xi.$$

the new expression

$$H^{(1)}_{n+\frac{1}{2}}(is)=(-1)^{n+1}\sqrt{\frac{2}{\pi}}(is)^{n+\frac{1}{2}}e^{-s}\left(1-\frac{1}{2}\frac{d}{ds}\right)^n\frac{1}{s^{n+1}}. \quad (79)$$

3. The symbolic calculus may also very successfully be applied to prove theorems, in which in some direct or indirect way an impulsive function (or Dirac function) occurs. For instance, as an example of relations based upon orthogonal functions we can easily prove the relation

$$F(x)=\int_{s=0}^{s=\infty}F(s)\,s\int_{\lambda=0}^{\lambda=\infty}J_0(\lambda s)\,J_0(\lambda x)\,\lambda d\lambda\,ds\ . \quad (80)$$

in the following way.

It will be sufficient to show that

$$s\int_{\lambda=0}^{\lambda=\infty}J_0(\lambda s)\,J_0(\lambda x)\,\lambda d\lambda$$

is an impulsive function $\delta(x-s)$ being infinite at $s=x$. This can be done by using the symbolic calculus again, where

$$x\doteq\frac{1}{p}.$$

In this way we have

$$s\int_{\lambda=0}^{\lambda=\infty}J_0(\lambda s)\,J_0(\lambda x)\,\lambda d\lambda\doteq s\int_{\lambda=0}^{\lambda=\infty}J_0(\lambda s)\frac{p}{\sqrt{p^2+\lambda^2}}\lambda d\lambda=p\,e^{-sp}, \quad (81)$$

the last step being based upon a known integral.

By repeating this transformation n-times, one obtains

$$\left(1\ \frac{d}{s\ ds}\right)^n\left(\frac{e^s}{s}\right)=\frac{1}{n!}\int_{-1}^{\infty}\left(\frac{1}{2}-\frac{\xi^2}{2}\right)^n e^{-s\xi}\,d\xi,$$

and with

$$\xi=-1+x,$$

$$e^{-s}\left(1\ \frac{d}{s\ ds}\right)^n\left(\frac{e^s}{s}\right)=\frac{1}{n!}\int_0^{\infty}e^{-sx}\left(x-\frac{x^2}{2}\right)^n dx.$$

Now

$$\int_0^{\infty}e^{-sx}x^k\,dx=\frac{k!}{s^{k+1}}=\left(-\frac{d}{ds}\right)^k\frac{1}{s}.$$

Hence:

$$e^{-s}\left(1\ \frac{d}{s\ ds}\right)^n\left(\frac{e^s}{s}\right)=\frac{1}{n!}\left(-\frac{d}{ds}-\frac{1}{2}\frac{d^2}{ds^2}\right)^n\frac{1}{s}=\left(1+\frac{1}{2}\frac{d}{ds}\right)^n\frac{1}{s^{n+1}}.$$

Now from (6) we know that $p\,e^{-sp}$ corresponds to an impulsive function $\delta(x-s)$ with its maximum at $x=s$. This was just what we had to prove in order to establish the theorem(80).

It was perhaps instructive to speak here of impulsive functions, but this was not necessary. We need only to prove the symbolic relation (81), since substituted into (80), it leads to

$$F(x) \doteqdot p\int_0^\infty e^{-ps}F(s)\,ds,$$

which is the basic definition of the symbolic calculus, and hence (80) has been proved*.

4. In conclusion we give a few remarks concerning the examples in the groups IV. a and IV. b. There the positive constant α was replaced by $\alpha=\beta+\frac{1}{p}$ or by $\alpha=\sqrt{p^2+1}$. It will be obvious that the possibilities are not exhausted by this choice, since any substitution

$$\alpha=f(p)$$

may be used as long as $f(p)>0$ for $p>0$.

The practical question, however, is to use such transformations, that functions of p emerge, the original functions of which are known. Therefore the substitutions we used in IV. a and IV. b were successful.

Nevertheless, we shall now show that some other substitutions may also be of use sometimes.

In integrals of the type

$$\alpha\int_0^\infty e^{-\alpha s}h(s)\,ds = f(\alpha), \qquad \ldots \quad (82)$$

it can be useful to substitute for instance :

$$\alpha=\sqrt{p},$$

giving

$$\int_0^\infty \sqrt{p}\,e^{-s\sqrt{p}}\,h(s)\,ds = f(\sqrt{p}). \qquad \ldots \quad (83)$$

Considering now again p as a symbolic parameter,

$$\frac{1}{p}\doteqdot x,$$

* Compare also a similar consideration in Part I.

we use, for the terpretation of the left-hand side *,

$$\sqrt{p}\, e^{-s\sqrt{p}} \doteqdot \frac{1}{\sqrt{\pi x}} e^{-\frac{s^2}{4x}}. \quad . \quad . \quad . \quad . \quad . \quad (84)$$

The applied substitution, therefore, will be successful only if we happen to know also the interpretation $\mathrm{X}(x)$ of $f(\sqrt{p})$ in the right-hand side of (83),

$$f(\sqrt{p}) \doteqdot \mathrm{X}(x).$$

In that case we will have derived the relation

$$\int_0^\infty \frac{1}{\sqrt{\pi x}} e^{-\frac{s^2}{4x}} h(s)\, ds = \mathrm{X}(x). \quad . \quad . \quad . \quad (85)$$

There is a multitude of known integrals of the type (82), namely, those expressing the relation

$$h(x) \doteqdot f(p),$$

between an original $h(x)$ and its known image $f(p)$. We have, of course, to select those pairs $h(s)$ and $f(\alpha)$, where $f(\alpha)$ is of such a form that $f(\sqrt{p})$ can easily be interpreted too.

For example, take in (82)

$$h(s) = \cos s \quad \text{with} \quad f(\alpha) = \frac{\alpha^2}{\alpha^2 + 1}.$$

Now in this case

$$f(\sqrt{p}) = \frac{p}{p+1} \doteqdot e^{-x} = \mathrm{X}(x).$$

Thus we find by substitution into (85) at once the relation

$$\frac{1}{\sqrt{\pi x}} \int_0^\infty e^{-\frac{s^2}{4x}} \cos s\, ds = e^{-x}. \quad . \quad . \quad . \quad (86)$$

5. Another substitution which sometimes is useful for integrals of the type (82) is

$$\alpha = p + \frac{1}{p}$$

giving

$$\int_0^\infty e^{-ps - \frac{s}{p}} h(s)\, ds = \frac{f\left(p + \frac{1}{p}\right)}{p + \frac{1}{p}}, \quad . \quad . \quad . \quad (87)$$

* See, *e.g.*, J. R. Carson, 'Electric Circuit Theory and the Operational Calculus,' p. 39, formula (g).

which can be considered as an equation between two symbolic mages.

For the interpretation of the first one we use

$$\frac{1}{p} \doteq x,$$

$$e^{-\frac{s}{p}} \doteq J_0(2\sqrt{sx}),$$

and by (R 5)

$$e^{-ps}\, e^{-\frac{s}{p}} \doteq \begin{cases} 0 & \text{for } s > x, \\ J_0(2\sqrt{s(x-s)}) & \text{for } s < x, \end{cases} \quad . \quad . \quad (88)$$

so that the first member of (87) corresponds to the original:

$$\int_0^x J_0(2\sqrt{s(x-s)})\, h(s)\, ds,$$

where the upper limit $s = x$ follows from the fact that the original in (88) was zero for $s > x$.

Suppose, now, that we also know the original $Y(x)$ of the right-hand side of (87):

$$\frac{f\left(p + \frac{1}{p}\right)}{p + \frac{1}{p}} \doteq Y(x).$$

Then we find the new relation

$$\int_0^x J_0(2\sqrt{s(x-s)})\, h(s)\, ds = Y(x). \quad . \quad . \quad (89)$$

For instance, we may take in (82)

$$h(s) = 1, \text{ to which belongs } f(\alpha) = 1$$

for

$$1 \doteq 1.$$

In this case we have

$$\frac{f\left(p + \frac{1}{p}\right)}{p + \frac{1}{p}} = \frac{p}{p^2 + 1} \doteq \sin x = Y(x).$$

Thus we find by means of (89)

$$\int_0^x J_0(2\sqrt{s(x-s)})\, ds = \sin x. \quad . \quad . \quad . \quad (90)$$

The above examples clearly show the great variety of successful substitutions as well as the freedom in the choice of the original integrals, from which one can start to derive new ones. It is hoped that the many examples treated above may again show the great heuristic value of the symbolic calculus.

List of some Results obtained above.

$$\sum_{n=0}^{\infty} (-1)^n \frac{L_n(x)}{n!} = \tfrac{1}{2} e^{\frac{1}{2}x}. \quad . \quad . \quad . \quad . \quad . \quad (17)$$

$$\sum_{n=0}^{\infty} \frac{L_n(x)}{n!\, n!} = e\, J_0(2\sqrt{x}). \quad . \quad . \quad . \quad . \quad (18)$$

$$\sum_{n=0}^{\infty} \frac{(-1)^n L_{2n}(x)}{(2n)!} = \tfrac{1}{2} e^{\frac{x}{2}} \left(\cos \frac{x}{2} + \sin \frac{x}{2} \right). \quad . \quad . \quad (20)$$

$$\sum_{n=0}^{\infty} \frac{(-1)^n}{(2n+1)!} He_{2n+1}(x) = e \sin 2x, \quad . \quad . \quad (22)$$

$$\int_0^x L_{n-m}(\xi)\, L_m(x-\xi)\, d\xi = \frac{\Pi(n-m)\,\Pi(m)}{\Pi(n)} \int_0^x L_n(\xi)\, d\xi. \quad (31)$$

$$He_{2n+1}(x) = (-1)^n \frac{(2n+1)!}{n!\, n!} 2 \int_0^x L_n(x^2 - \xi^2)\, d\xi. \quad (32)$$

$$\int_0^x e^{\xi} \xi^{2n} L_n(x-\xi)\, d\xi = \sqrt{\pi}\, \Pi(2n)\, e^{\frac{x}{2}} x^{n+\frac{1}{2}} I_{n+\frac{1}{2}}\left(\frac{x}{2}\right). \quad (37)$$

$$J_n^2(\alpha) = \frac{2}{\pi} \int_0^{\frac{\pi}{2}} J_{2n}(2\alpha \sin\theta) d\theta. \quad . \quad . \quad . \quad (41)$$

$$\int_0^{\infty} e^{-\beta s} J_{2n}(2\sqrt{s\alpha})\, J_n(s)\, ds = \frac{1}{\sqrt{\beta^2+1}}\, e^{-\frac{\beta}{\beta^2+1}\alpha} J_n\left(\frac{\alpha}{\beta^2+1}\right).$$

$$. \quad . \quad . \quad (47)$$

$$\int_0^{\infty} J_{2n}(2\sqrt{sx})\, J_n(s)\, ds = J_n(\alpha). \quad . \quad . \quad . \quad (48)$$

$$\int_0^{\infty} e^{-\beta \frac{s^2}{4}} s\, J_n(s)\, J_n(\alpha s)\, ds = \frac{2}{\beta} e^{-\frac{\alpha^2+1}{\beta}} I_n\left(\frac{2\alpha}{\beta}\right) \text{ (Weber).} \quad (52)$$

$$\int_0^{\infty} s\, J_n(\alpha s)\, J_n(s)\, ds = \frac{2}{\alpha^n} \delta(\alpha^2 - 1). \quad . \quad . \quad (55)$$

$$\int_0^{\infty} \frac{J_{m+1}(\alpha s)\, J_n(s)}{s^{m-n}}\, ds = \frac{(\alpha^2-1)^{m-n}}{2^{m-n}\, \Pi(m-n)\, \alpha^{m+1}} \begin{pmatrix} \alpha > 1 \\ m > n \end{pmatrix}$$

(Sonine and Schafheitlin). . . (57)

$$\int^{\infty} \mathrm{J}_0(s)\,\mathrm{J}_0\left(\frac{\alpha}{s}\right) ds = \mathrm{J}_0(2\sqrt{\alpha}) \quad (\alpha > 0) \quad \text{(Heaviside)}.$$

. . . (58)

$$\mathrm{L}_n(x) = e^x \int_0^{\infty} e^{-s}\, s^n\, \mathrm{J}_0(2\sqrt{sx})\, ds. \quad . \quad . \quad . \quad (60\,a)$$

$$\mathrm{He}_{2n+1}(\sqrt{x}) = (-1)^n\, 2^{2n+1}\, x^{\frac{1}{4}}\, e^x \int_0^{\infty} e^{-s}\, s^{n+\frac{1}{4}}\, \mathrm{J}_{\frac{1}{2}}(2\sqrt{sx})\, ds.$$

. . . (60 *b*)

$$\int_0^x \mathrm{L}_n(\xi)\, \mathrm{L}_m(x-\xi)\, d\xi = \frac{\Pi(n)\,\Pi(m)}{\Pi(n+m+1)}\, x^{\frac{1}{2}}\, e^x \int_0^{\infty} e^{-s}\, s^{m+n+\frac{1}{2}}\, \mathrm{J}_1(2\sqrt{sx})\, ds. \quad (60\,aa)$$

$$\int_0^x \mathrm{L}_n(\xi)\, \mathrm{He}_{2m+1}(\sqrt{x-\xi})\, d\xi = (-1)^m\, 2^{2m+1}\, \frac{\Pi(n)\,\Pi(m+\frac{1}{2})}{\Pi(m+n+\frac{3}{2})}\, x^{\frac{3}{4}}\, e^x \times \int_0^{\infty} e^{-s}\, s^{m+n+\frac{3}{4}}\, \mathrm{J}_{\frac{3}{2}}(2\sqrt{sx})\, ds. \quad . \quad . \quad (60\,ab)$$

$$\int_0^x \mathrm{He}_{2n+1}(\sqrt{\xi})\, \mathrm{He}_{2m+1}(\sqrt{x-\xi})\, d\xi = (-1)^{m+n}\, 2^{2(m+n+1)}\, \frac{\Pi(n+\frac{1}{2})\,\Pi(m+\frac{1}{2})}{\Pi(m+n+2)}\, x\, e^x \times \int_0^{\sqrt{x}} e^{-s}\, s^{m+n+1}\, \mathrm{J}_2(2\sqrt{sx})\, ds. \quad . \quad . \quad (60\,bb)$$

$$\int_0^a \mathrm{J}_0(\sqrt{\alpha^2 - s^2})\, \cos s\, ds = \frac{1}{\sqrt{2}} \sin(\alpha\sqrt{2}) \quad \text{(Sonine)}. \quad (63)$$

$$\int_a^x \mathrm{J}_0(x-\xi)\, \mathrm{J}_0(\sqrt{\xi^2 - a^2})\, d\xi = \int_a^x \mathrm{J}_0(\sqrt{x^2 - s^2})\, ds. \quad (69)$$

$$\mathrm{H}^{(1)}_{n+\frac{1}{2}}(is) = (-1)^{n+1} \sqrt{\frac{2}{\pi}}\, (is)^{n+\frac{1}{2}}\, e^{-s} \left(1 - \frac{1}{2}\frac{d}{ds}\right)^n \frac{1}{s^{n+1}}, \quad (79)$$

$$\mathrm{H}^{(2)}_{n+\frac{1}{2}}(is) = \sqrt{\frac{2}{\pi}}\, (is)^{n+\frac{1}{2}}\, e^{s} \left(1 + \frac{1}{2}\frac{d}{ds}\right)^n \frac{1}{s^{n+1}}. \quad . \quad . \quad . \quad (77)$$

The following new images were found :—

$$\mathrm{He}_{2n+1}(\sqrt{x}) \doteqdot \frac{(2n+1)!}{n!}\, \frac{\sqrt{\pi}}{\sqrt{p}} \left(\frac{1}{p} - 1\right)^n, \quad . \quad . \quad . \quad (21)$$

$$P_n(1-x) \doteq \left\{ \begin{matrix} e^{-p} p^{n+1} \left(\frac{1}{p}\frac{d}{dp}\right)^n \left(\frac{e^p}{p}\right), \\ p^{n+1} \left(1+\frac{1}{2}\frac{d}{dp}\right)^n \frac{1}{p^{n+1}}, \end{matrix} \right\} \text{identical.} \quad (75)$$

Note added in the Proof.—In order to prove formula (41) (for the special case of n being an integer) by means of ordinary analysis, one may start with Graf's generalization of Neumann's addition theorem, given in the form *

$$\sum_{m=-\infty}^{m=+\infty} J_{\nu+m}(Z) J_m(z) \begin{matrix} \cos \\ \sin \end{matrix} m\phi = J_\nu(\tau) \begin{matrix} \cos \\ \sin \end{matrix} \nu\psi, \quad . \quad . \quad (91)$$

where τ and ψ follow from Z, z, and ϕ in a geometrical way:

If Z and z represent the length of two sides of a triangle and ϕ the included angle, then τ is the length of the other side, and ψ the angle between Z and τ.

From (91) we obtain

$$\int_0^\pi J_\nu(\tau) \begin{matrix} \cos \nu\psi \cos m\phi \\ \sin \nu\psi \sin m\phi \end{matrix} d\phi = \frac{\pi}{2} J_{\nu+m}(Z) J_m(z).$$

For $Z=z=\alpha$, we have

$$\psi = \frac{\pi}{2} - \frac{\phi}{2}, \qquad \tau = 2\alpha \sin \frac{\phi}{2}.$$

Choosing further the case $m=-n$ and $\nu=2n$, where n is an integer, so that the relation

$$J_{-n}(\alpha) = (-1)^n J_n(\alpha)$$

can be used, we get with $\frac{\phi}{2} = \theta$

$$2\int_0^{\frac{\pi}{2}} J_{2n}(2\alpha \sin\theta) \begin{matrix} \cos^2(2n\theta) \\ \sin^2(2n\theta) \end{matrix} d\theta = \frac{\pi}{2} J_n^2(\alpha).$$

Adding these twe formulæ, we arrive at (41).

Eindhoven,
October 29, 1931.

*Watson, 'Bessel Functions,' p. 361.

XLVIII. *The Surface Tensions of Mixtures of Normal Propyl Alcohol and Benzene.* *By* R. C. Brown, *B.Sc., Lecturer in Physics, University College, London* *.

Introduction.

THE purpose of this paper is to describe an apparatus and technique for the accurate measurement of the surface tensions of mixtures of volatile liquids and to record the results obtained for mixtures of normal propyl alcohol and benzene. These two liquids were chosen in order to investigate whether there was any connexion between the surface tension-composition curve and viscosity-composition curve published by Dunstan †, which shows that, over the range from 0 to 10 per cent. of propyl alcohol, the viscosities of the mixtures are less than that of either of the pure

Fig. 1.

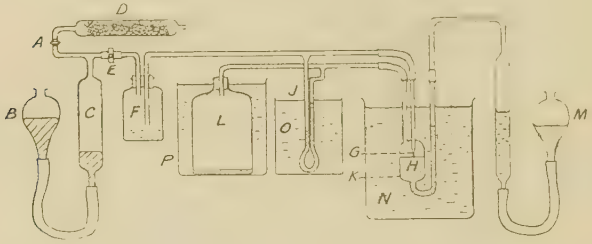

substances. The minimum occurs in Dunstan's curve at about 5 per cent.; the number of results which he determined in this neighbourhood was, however, small. The present measurements of surface tension cover the whole range from 0 to 100 per cent.

Method and Apparatus.

The method used for measuring the surface tensions was Jaeger's "maximum bubble-pressure" method, the principle of which needs no discussion here.

The apparatus was so designed that the liquid under test was not in direct communication with the atmosphere, so that changes of composition due to evaporation of the mixture and contamination were almost completely avoided.

Fig. 1 shows diagrammatically the arrangement employed.

* Communicated by Prof. E. N. da C. Andrade, D.Sc., Ph.D.

† Journ. Chem. Soc. lxxxvii. p. 11 (1905).

The tap, A, was opened and the mercury reservoir, B, was first raised and then lowered so that the tube, C, was filled with air which had been drawn through calcium chloride and glass wool packed in D. A being then closed, the air in C could be made to flow into the rest of the apparatus through a piece of pressure tubing constricted by a screw-clip, E, at a rate which could be controlled by alterations in the height of B. The air thus flowing passed over anhydrous phosphorus pentoxide in F, and reached the jet, G, where it formed bubbles in the usual way in the liquid under test, H, contained in a special glass apparatus, K. The space above H communicated with one arm of a manometer, J, and a large bottle, L. The other arm of J was connected to the tube leading to the jet. Thus the difference of level in the two arms of J gave the excess pressure inside the bubble above that in the space above H, and was independent of the actual pressure inside the apparatus. The function of L was merely to increase the volume of the space into which the bubbles escaped. Evaporation from the surface of H into this space was reduced by introducing a small quantity of the test liquid into L.

The jet was set with its plane actually coincident with the free surface of H, adjustment of the level of H being made by raising or lowering the reservoir, M, which was provided with a slow-motion movement. After a little practice and with convenient lighting of the jet and liquid this adjustment could be made quite easily and consistently repeated. The escape of a bubble caused the surface of H to be lowered slightly, so that it was necessary to bring it back to the plane of the jet before each reading of maximum pressure was taken.

The glass apparatus, K, was connected to the rest of the apparatus by pressure tubing at the three points shown in the diagram. The bulb in which the bubbles were formed was of about 4·5 cm. diameter. N was a large glass beaker containing water maintained at a temperature of $20{\cdot}00 \pm {\cdot}02°$ C., and O was a vessel with optical glass sides also containing water at the same temperature. Finally, the large bottle L was kept at approximately 20° C. by the water-bath P.

The liquid used in the manometer was butyl phthalate, and proved thoroughly satisfactory, having a very low vapour pressure at 20° C. The same liquid was also used in the reservoir M. The levels of liquid in the manometer arms were measured by means of a large Casella cathetometer supported in a 6 ft. iron frame and provided with a micrometer cross-wire, one graduation on the screw-head of which

corresponded to 0·0094 mm. This method was extremely convenient, since by means of the cross-wire the slow changes of level of the meniscus could be followed right up to the maximum pressure point.

The jet, G, was made by drawing down a piece of medium-walled glass tubing and cutting at the constricted part in the usual way. After a number of attempts a very satisfactory jet was produced and no grinding was necessary. The mean diameter of the jet was obtained from measurements made by means of a microscope fitted with an eye-piece scale and a stage micrometer, several different objectives (and therefore magnifications) being used. The glass apparatus, K, into which the jet was sealed, could be tilted so as to ensure that the plane of the jet was horizontal—a state of affairs which could be judged accurately by eye when the jet was just below the surface of the liquid.

Before each new mixture was introduced into K the latter was completely filled with chromic acid, allowed to stand, washed in running tap-water and conductivity water, and dried by passing dust-free air into each of the three inlets in turn whilst it was heated to well above 100° C.

Special features of the apparatus and method were therefore :—

1. Total enclosure of the liquid prevented
   - (*a*) evaporation and consequent changes in composition of mixture, and
   - (*b*) contamination from the atmosphere.
2. By setting the tip of the jet in the free surface of the liquid the measurement of its depth below the surface was obviated, and it was not necessary to know accurately the densities of the mixtures used, since in this circumstance the density occurs only in a small correcting term.
3. The mixtures were made up by weighing actually in the glass apparatus, K, before the latter was connected to the remainder of the apparatus.

Materials used.

The normal propyl alcohol was supplied by British Drug Houses, Ltd., and one bottle sufficed to complete all the measurements. The surface tension of the alcohol suffered no measurable change throughout the whole research.

Kahlbaum benzene was used, fresh quantities being redistilled and partially frozen (the liquid being rejected) for each mixture. The boiling-point of the benzene thus prepared was 79·9° C. at 76·0 cm. Hg and the freezing-point was 5·5° C.

Results.

The following equation was used in calculating the surface tensions :

$$T = \frac{rg}{2}(H\rho - \tfrac{2}{3}r\sigma),$$

where r = mean radius of the jet = ·0142(3) cm.

g = acceleration due to gravity = 981·2 cm./sec.^{2}

H = maximum bubble-pressure in cm. of butyl phthalate.

ρ = density of butyl phthalate at 20·0° C. = 1·0458 gm./c.c.

σ = density of test liquid.

Benzene.

The surface tension of each specimen of benzene used in making up the mixtures was determined. In this way seventeen values of the maximum bubble pressure for benzene were obtained. They ranged from 3·9623 to 3·9660 cm. of butyl phthalate, the mean value being 3·9642 ± ·0002 cm.

The density of benzene at 20° C. was taken as 0·88 gm./c.c.

Using these figures, and assuming a probable error of ± ·00002 cm. in the above value for the radius of the jet, we get :—

The surface tension of benzene at 20·00 ± ·02° C. against air saturated with vapour = 28·89 ± ·04 dyne/cm.

The "standard" value quoted in the International Critical Tables, and based upon the results of Richards and Coombs *, Richards and Carver †, and Harkins and Brown ‡, all of whom used the capillary rise method, is 28·88 ± ·03 dyne/cm.

Normal Propyl Alcohol.

Two determinations of the surface tension of the sample of propyl alcohol used in the research were made with an interval of one month between them. The results differed by only one part in 3000, the value being 23·78 dyne/cm. at 20° C. The density of the alcohol was assumed to be

* Journ. Amer. Chem. Soc. xxxvii. p. 1656 (1915).

† *Ibid.* xliii. p. 827 (1921).

‡ *Ibid.* xli. p. 499 (1919).

0·80 gm./c.c. The International Critical Tables give as the most probable result $23{\cdot}8 \pm {\cdot}2$ dyne/cm., based on the work of Morgan and Owen *, Ramsay and Shields †, Renard and Guye ‡, Richards and Mathews §, and Schiff ‖.

Mixtures of Benzene and Normal Propyl Alcohol.

The densities of the various mixtures were not known, but it was estimated that a change of density from, say, 0·90 to 0·75 gm./c.c. (within which range all the densities certainly lie) makes a difference of only one part in 3000 to the surface tension as calculated from the formula already given, since

Fig. 2

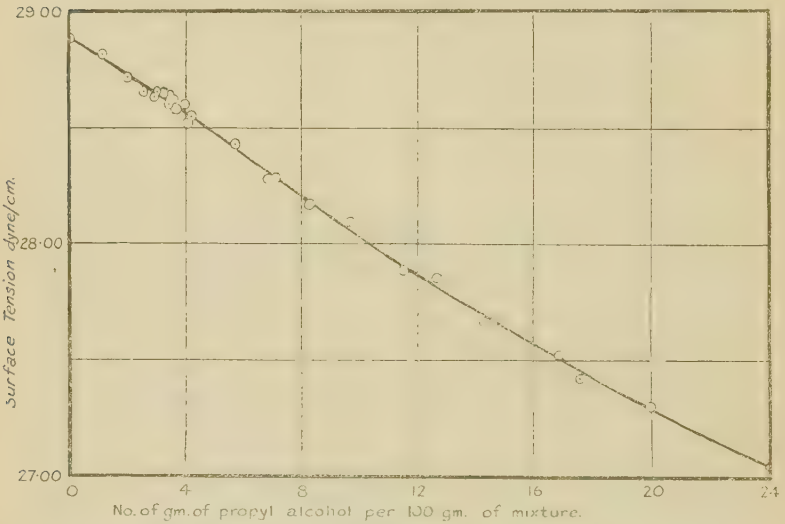

the term $\frac{2}{3}r\sigma$ is of the order of 0·008, whilst the magnitude of $H\rho$ is 4·0.

1. *For low concentrations of alcohol* :

As explained before, it was intended to investigate as carefully as possible the surface tension-concentration curve for low concentrations of alcohol. Fig. 2 shows the results obtained up to 24 per cent. of alcohol. A considerable number of these were determined in the neighbourhood

* *Ibid.* xxxiii. p. 1713 (1911).
† Journ. Chem. Soc. lxiii. p. 1089 (1893).
‡ *Journ. de Chim. Phys.* v. p. 81 (1907).
§ Journ. Amer. Chem. Soc. xxx. p. 8 (1908).
‖ *Ann. der Chem.* (Justus Leibig) ccxxiii. p. 47 (1884).

between 2 and 5 per cent., and a sufficient number throughout the rest of the region to fix the general trend of the curve. A definite reversal of curvature is shown by the graph at about 7 per cent., the portion between the pure benzene point and the point of inflexion being convex upwards. The centre of this region therefore lies at about 3·5 per cen

2. *For all concentrations of alcohol*:

Fig. 3 shows the surface tension-concentration curve over the whole range 0 to 100 per cent. of alcohol. The curve closely resembles that found by Morgan and Scarlett * for mixtures of ethyl alcohol and benzene, and presents no unexpected features.

Fig. 3.

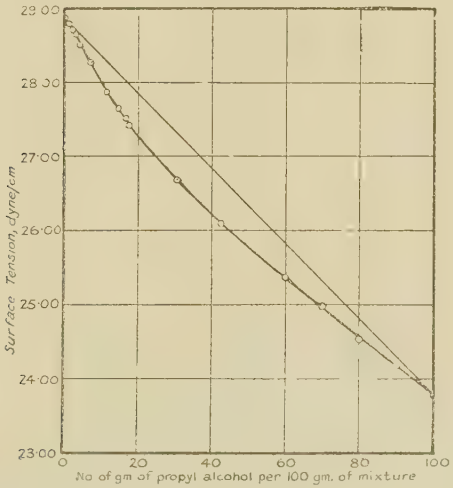

Discussion of Results.

Fig. 2 establishes definitely that the curvature of the graph undergoes a reversal at 7 per cent. of alcohol, the effect being outside the limit of experimental error. This region corresponds to the range over which Dunstan found that the viscosities of mixtures are below those of the pure substances †.

It has been suggested by Denison ‡ that the deviation from a straight line of a property-composition curve can be

* Journ. Amer. Chem. Soc. xxxix. p. 2275 (1917).
† *Loc. cit.*
‡ Trans. Farad. Soc. viii. pp. 20 & 35 (1912).

accounted for by postulating a combination of some nature between the molecules of the two substances concerned. The degree of combination is a maximum when the percentage composition of the mixture is such that the ratio of the total numbers of molecules of the two substances is equal to the ratio of their numbers in the compound molecule. At this percentage composition the maximum deviation from the straight line law will take place. Denison showed that a maximum deviation often does occur at a percentage which represents some simple numerical ratio between the numbers of the molecules of the two simple substances present. Morgan and Scarlett * have determined the surface tension-concentration curves for various mixtures together with their deviations from the corresponding straight lines,

Fig. 4.

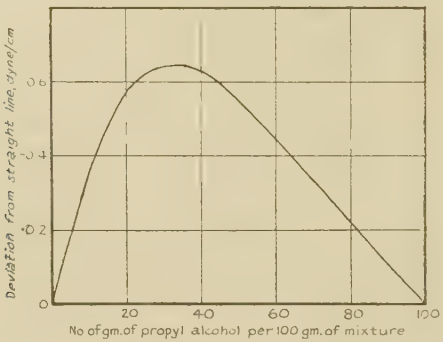

and each mixture shows a maximum deviation at a percentage composition giving a simple ratio.

Fig. 4 shows the deviation-composition curve for mixtures of propyl alcohol and benzene obtained from the present measurements by reading deviations directly from the surface tension-concentration curve (fig. 3). The maximum deviation occurs at 34 per cent. (to the nearest whole number). A proportion of three molecules of benzene to two molecules of propyl alcohol would correspond to 33·9 per cent., so that, assuming Denison's theory, the present research provides evidence that molecular groups having a composition $3C_6H_6.2C_3H_8O$ are formed in the mixture.

It gives me great pleasure to thank Professor E. N. da C. Andrade, D.Sc., for the helpful interest with which he has followed the course of this research.

* *Loc. cit.*

XLIX. *Note on the Slow Motion of Fluid.*

By W. R. Dean, *M.A.*, *Trinity College, Cambridge* *.

1. In a recent paper † Prof. A. E. H. Love has developed a method of biharmonic analysis and applied it to the solution of some important problems of the theory of elasticity. The analytical method is a general one, and its employment appears to make possible the solution of a wide class of problems not only of elasticity but also of the theory of the slow motion of viscous fluids, of special interest among the latter being some cases of two-dimensional motion past various types of obstacle. There are, for instance, some

Fig. 1.

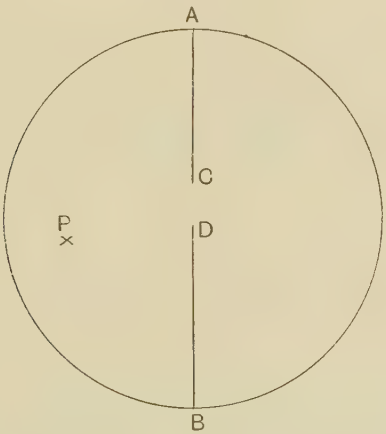

examples of fluid motion considered in general terms by Rayleigh ‡, who concludes from them that "the formation of eddies observed in practice is not wholly due to the influence of the terms involving the squares of the velocities, but would persist in certain cases even though the motion were made infinitely slow."

Rayleigh considers an elastic plate (shown as circular in fig. 1) clamped along its circumference and along barriers AC, DB which nearly divide it into two independent parts. Suppose that pressure normal to the plane of the plate is applied at some isolated point P. The part of the plate near

* Communicated by the Author.

† Proc. London Math. Soc. (2) xxix. pp. 189–242 (1929).

‡ 'Scientific Papers,' iv. pp. 78–93.

P will move in the direction (say downwards) of the applied force, but Rayleigh points out that the plate will, as it were, pivot about the supports C and D, with the result that parts of the plate on the right of the barriers will move upwards. There will be two sets of closed contours. In the corresponding fluid motion there will be an eddy on the right of the barriers. As another example * Rayleigh concludes that an eddy will be formed by fluid moving along a barrier into which a channel at right angles to the barrier opens.

Love's work should make it possible to examine such problems in detail. However, it seemed to be a desirable preliminary to apply the method, which makes use of somewhat heavy analysis, to a problem of a simpler character

Fig. 2.

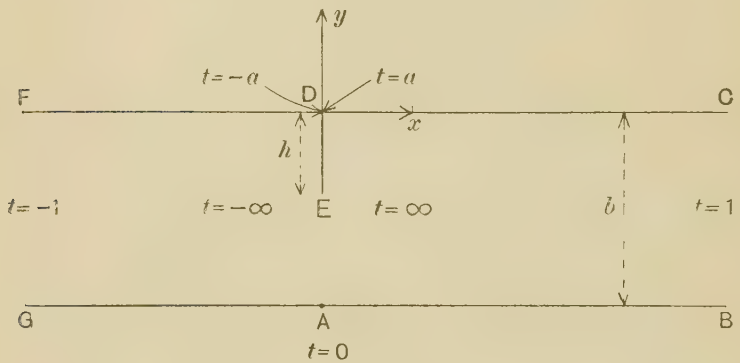

than, for instance, the second of those cited above, which is certain to present difficulty. In this paper is therefore considered the two-dimensional motion of fluid in a channel in which there is (as shown in fig. 2) a projection, although there is clearly no possibility of an eddy in this example. The analysis shows that, although it would be exceedingly difficult to reach results of great numerical accuracy, the work involved in ascertaining the general character of the motion is not specially heavy. In the more important problems, like that mentioned above, no more than the general character of the motion is required, for the question is whether in given conditions an eddy does or does not exist, and we can conclude that the solution of some problems of this type is practicable by Love's method of analysis.

* *Loc. cit.* p. 89.

2. The simplest type of fluid motion is obtained in the channel represented in fig. 2 if it is supposed that the boundary GAB is moved in its own line with constant velocity (and therefore imparts the same velocity to the fluid in contact with it) while the boundary CDEF is held fixed. Let D be the origin of Cartesian coordinates (x, y), let DC be the x axis, and let GB be the line $y=-b$, $b>0$. The stream-function ψ must then satisfy the differential equation

$$\left(\frac{\partial^2}{\partial x^2}+\frac{\partial^2}{\partial y^2}\right)^2\psi\equiv\nabla_1^4\psi=0 \quad . \quad . \quad . \quad . \quad (1)$$

at all points of the channel, the boundary conditions

$$\psi=\frac{\partial\psi}{\partial\nu}=0 \quad . \quad . \quad . \quad . \quad . \quad . \quad . \quad (2)$$

on CDEF, $\frac{\partial}{\partial\nu}$ denoting as usual differentiation with respect to distance measured normal to the boundary; and the boundary conditions

$$\psi=k, \qquad \frac{\partial\psi}{\partial\nu}=k', \qquad y=-b, \quad . \quad . \quad . \quad (3)$$

k and k' being constants whose values depend on the velocity of GB.

3. Love's analysis starts from the fact that if $u+iv$ is a function of $z\,(=x+iy)$ then $xv-yu$ is a biharmonic function of the variables x, y. It is clear that

$$xv-yu=\mathrm{I}[(x-iy)(u+iv)]=-\mathrm{I}[(x+iy)(u-iv)], \quad (4)$$

where $\mathrm{I}[f]$ denotes the imaginary part of f. The problem of finding a suitable biharmonic function is therefore reduced to that of finding a suitable function of z, and the first step in this process is, according to Love's work, the conformal representation of the interior of the region concerned on the interior of a circle of unit radius.

The region ABCDEFG in the plane of z can be represented conformally on a half-plane (t) by the transformation of Schwarz and Christoffel. Let the new variable t be such that at B and C $t=1$; at F and G $t=-1$; at D $t=\pm a$, where a is real and greater than unity and the positive or negative sign is appropriate, according as D is approached

from C or F; at E $t=\pm\infty$, with the same sign convention. The required relation between z and t is then such that

$$\frac{dz}{dt}=\frac{C}{(1-t^2)(a^2-t^2)^{1/2}}, \quad . \quad . \quad . \quad . \quad (5)$$

where C is a positive real constant.

The upper half of the plane of t can be represented conformally on the interior of the circle $|\zeta|=1$ by the relation

$$\zeta=\frac{i-t}{i+t}. \quad . \quad . \quad . \quad . \quad . \quad . \quad (6)$$

The relation between z and ζ necessary to transform ABCDEFG into the interior of the circle is consequently such that

$$\frac{dz}{d\zeta}=-\frac{iC}{\sqrt{a^2+1}}\frac{1+\zeta}{(1+\zeta^2)\left(1+\zeta^2+\frac{a^2-1}{a^2+1}2\zeta\right)^{1/2}}, \quad (7)$$

and can be expressed in finite terms if necessary. If an acute angle α determined by

$$\cos\alpha=\frac{a^2-1}{a^2+1}, \qquad \sin\alpha=\frac{2a}{a^2+1} \quad . \quad . \quad . \quad (8)$$

is introduced, equation (7) can be written

$$\frac{dz}{d\zeta}=-\frac{iC}{\sqrt{a^2+1}}\frac{1+\zeta}{(1+\zeta^2)(1+\zeta e^{i\alpha})^{1/2}(1+\zeta e^{-i\alpha})^{1/2}}. \quad (9)$$

The correspondence between the walls of the channel and the circumference of the circle is shown in fig. 3.

If $\zeta=r(\cos\theta+i\sin\theta)$ one side of the projection DE corresponds to the circumference of the circle between $\theta=\pi-\alpha$ and $\theta=\pi$, and it can be seen from equation (9) that the y coordinates of points of the projection are given in terms of θ by

$$y=\frac{C}{2\sqrt{a^2+1}}\int_{\pi-\alpha}^{\theta}\frac{\cos\frac{\theta}{2}d\theta}{\cos\theta\sqrt{-\cos\frac{\theta-\alpha}{2}\cos\frac{\theta+\alpha}{2}}}$$

$$=-\frac{C}{2\sqrt{a^2+1}}\int_{\pi-\theta}^{\alpha}\frac{\sin\frac{\theta}{2}d\theta}{\cos\theta\sqrt{\sin\frac{\alpha+\theta}{2}\sin\frac{\alpha-\theta}{2}}}; \quad (10)$$

the integral can, if required, be expressed in finite terms. For h, the height of the projection, and b, the breadth of the channel, we have

$$h = \frac{C}{2\sqrt{a^2+1}} \int_0^\alpha \frac{\sin\frac{\theta}{2}\,d\theta}{\cos\theta\sqrt{\sin\frac{\alpha+\theta}{2}\sin\frac{\alpha-\theta}{2}}}, \qquad (11)$$

and

$$b = \frac{C\pi}{2\sqrt{a^2-1}}.$$

Fig. 3.

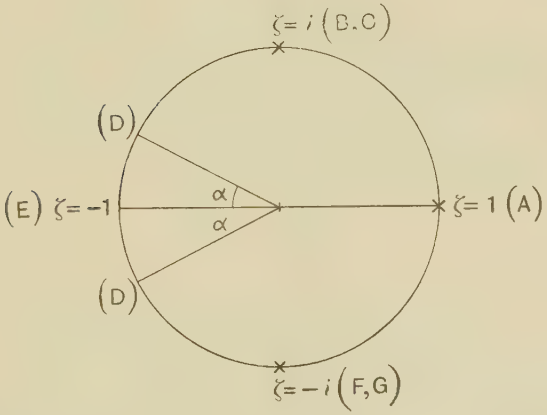

4. Love * takes as a typical biharmonic function

$$-\mathrm{I}[(x-iy)\zeta^n],$$

where n is a positive integer. Since ζ^n is a function of z, this expression is of the form (4) ; moreover, since any function of z of the kind required can be expanded as a power series in ζ, convergent when $|\zeta|<1$, any biharmonic function of the kind required can be expanded as a series of these typical solutions. An expression alternative to that above is, since $\zeta = re^{i\theta}$,

$$\mathrm{I}[(x+iy)r^n e^{-ni\theta}].$$

From equation (7) z is given in terms of ζ by a series of the form

$$z = i(c_0 + c_1\zeta + c_2\zeta^2 + \ldots),$$

* *Loc. cit.* § 1.51.

the coefficients c being real, and the solution can accordingly be expressed as

$$\mathrm{I}\left[i\left(\sum_{m=0}^{\infty} c_m r^m e^{mi\theta}\right) r^n e^{-ni\theta}\right]$$

$$= \sum_{m=0}^{n} c_m r^{n+m} \cos(n-m)\theta + \sum_{m=n+1}^{\infty} c_m r^{m+n} \cos(m-n)\theta. \quad (12)$$

A harmonic function may clearly be added, and Love accordingly uses solutions such as

$$\sum_{m=0}^{n} c_m (r^{n+m} - r^{n-m}) \cos(n-m)\theta + \sum_{m=n+1}^{\infty} c_m (r^{m+n} - r^{m-n}) \cos(m-n)\theta,$$

which vanish at the boundary $r=1$. The use of solutions of this type in the problem of the present paper led to some difficulty, which arose from the circumstance that the region we are concerned with is unbounded ; the typical solution, say ψ_n, will therefore be left in the form

$$\psi_n = \sum_{m=0}^{n} (c_m r^{n+m} + d_m r^{n-m}) \cos(n-m)\theta + \sum_{m=n+1}^{\infty} (c_m r^{m+n} + d_m r^{m-n}) \cos(m-n)\theta, \quad (13)$$

the coefficients d being arbitrary.

5. When the boundary GAB is moved in its own line with constant velocity the fluid is set into uniform shearing motion, somewhat modified by the projection. It is therefore convenient to write

$$\psi = -y^2 + \phi \quad . \quad . \quad . \quad . \quad . \quad (14)$$

for the stream-function. The first term which corresponds to the motion of uniform shear does not vanish on the projection DE, but otherwise, since DE is in the direction of the y axis, satisfies all the conditions of § 2.

The function ϕ must therefore satisfy the differential equation

$$\nabla_1^4 \phi = 0, \quad . \quad . \quad . \quad . \quad . \quad . \quad (15)$$

and the condition

$$\frac{\partial \phi}{\partial \nu} = 0,$$

or the equivalent * condition

$$\frac{\partial \phi}{\partial r} = 0, \quad . \quad . \quad . \quad . \quad . \quad . \quad (16)$$

at all points of the boundary; lastly, ϕ must equal y^2 on DE and must vanish elsewhere on the boundary, so that when $r=1$

$$\left.\begin{aligned} \phi = y^2, \quad & \pi - \alpha \leq \theta \leq \pi + \alpha, \\ = 0, \quad & \begin{cases} 0 \leq \theta < \pi - \alpha, \\ \pi + \alpha < \theta \leq 2\pi. \end{cases} \end{aligned}\right\} \quad . \quad . \quad . \quad (17)$$

The required function ϕ is the sum of a series of the functions ψ_n of the preceding paragraph. Let the constants d of expression (13) be chosen so that the differential coefficients with respect to r of the coefficients of the cosines vanish when $r=1$; accordingly, in the first sum

$$d_m = -\frac{n+m}{n-m} c_m, \quad . \quad . \quad . \quad . \quad . \quad (18)$$

and in the second

$$d_m = -\frac{m+n}{m-n} c_m. \quad . \quad . \quad . \quad . \quad . \quad (19)$$

When $m=n$, d_m is not defined by (18), and we take $d_n=0$. The reason for this is that the last term ($m=n$) of the first sum in (12) is $c_n r^{2n}$; the corresponding harmonic function is therefore a constant and cannot be used to nullify the boundary value of the derivative. After the above step we consequently have only a biharmonic function whose normal derivative is constant at the boundary, not one with a zero derivative. These constants are eliminated below (§ 7) by combining the functions ψ_n in pairs. We then have a series of functions which satisfy (15) and (16) and which can be combined to satisfy the last condition (17) after the boundary values of ϕ have been expanded as a cosine series.

6. It is now assumed that the height h of the projection is small in comparison with b, the breadth of the channel. The assumption is, at least in theory, unnecessary, for it would certainly be possible to continue at the expense of some heavy algebra without it; but it introduces a very considerable simplification into the subsequent arithmetical work without interfering in any way with the main object

* See § 9.

of this paper, which is to assess the practical difficulty or applying Love's method of analysis to problems of the kind mentioned in § 1.

The assumption that h/b is small implies that the angle α of § 3 is small, and hence from (8) that $1/a$ is small. To expand the boundary values of ϕ as a cosine series the values of y^2 at all points of the projection must be expressed in terms of θ. Since α is small and θ varies between $\pi-\alpha$ and π on one side of the projection, the variable in integral (10) is small throughout the range of integration; equation (10) can therefore be replaced by

$$y = -\frac{C}{2a}\int_{\pi-\theta}^{\alpha}\frac{\theta\,d\theta}{(\alpha^2-\theta^2)^{1/2}}$$

$$= -\frac{C}{2a}\left[\alpha^2-(\pi-\theta)^2\right]^{1/2};$$

replacing α by $\sin\alpha$ and $\pi-\theta$ by $\sin\theta$, we can write

$$y^2 = \frac{C^2}{4a^2}\left[\sin^2\alpha-\sin^2\theta\right]. \quad . \quad . \quad . \quad . \quad (20)$$

We have now to expand as a Fourier series, say

$$\sum_0^\infty f_n\cos n\theta,$$

the function which is equal to y^2 when $\pi-\alpha<\theta<\pi+\alpha$, and which vanishes for all other values of θ; from equation (17) ϕ must be equal to this function when $r=1$. Consequently we must have

$$\phi = f_0+f_1\cos\theta+\ldots+f_n\cos n\theta+\ldots,\ r=1, \quad . \quad (21)$$

where

$$f_0 = \frac{C^2}{8\pi a^2}\left[\frac{1}{2}\sin 2\alpha-\alpha\cos 2\alpha\right],$$

and generally

$$f_n = \frac{(-1)^n}{n}\frac{C^2}{4\pi a^2}\left[\frac{\sin(n-2)\alpha}{n-2}-\frac{\sin(n+2)\alpha}{n+2}\right],\ n=1, 2, 3, \ldots,$$

$$. \quad . \quad . \quad (22)$$

the first term in the bracket being α when $n=2$.

It is still easier to calculate the coefficients c of § 4. When $r=1$,

$$y = c_0+c_1\cos\theta+c_2\cos 2\theta+\ldots,$$

and to a first approximation (in which the values of y on the

projection can be assumed zero) the boundary values of y are given by

$$y = -\frac{C\pi}{2a}, \quad -\frac{\pi}{2} < \theta < \frac{\pi}{2}, \quad \ldots \quad (23)$$

$$= 0, \quad \frac{\pi}{2} < \theta < \frac{3\pi}{2}. \quad \ldots \quad (24)$$

All that is needed is the expansion of this function as a cosine series. Approximately then the coefficients c with even suffixes vanish and

$$c_{2n+1} = \frac{(-1)^{n+1}}{2n+1}\frac{C}{a}. \quad \ldots \quad (25)$$

The effect of these approximations is that terms of the second and higher powers of α are ignored.

7. Inserting the values of the coefficients c and d given by equations (18), (19), and (25) in expression (13), we arrive at a series of functions ϕ_1, ϕ_3, ... given by

$$\frac{a\phi_1}{C} = r^2 - \frac{\cos 2\theta}{3}(r^4 - 2r^2) + \frac{\cos 4\theta}{5}\left(r^6 - \frac{3r^4}{2}\right) - \frac{\cos 6\theta}{7}\left(r^8 - \frac{4r^6}{3}\right) + \ldots,$$

$$\frac{a\phi_3}{C} = \cos 2\theta(r^4 - 2r^2) - \frac{r^6}{3} + \frac{\cos 2\theta}{5}(r^8 - 4r^2) - \frac{\cos 4\theta}{7}\left(r^{10} - \frac{5r^4}{2}\right) + \ldots,$$

$$\frac{a\phi_5}{C} = \cos 4\theta\left(r^6 - \frac{3r^4}{2}\right) - \frac{\cos 2\theta}{3}(r^8 - 4r^2) + \frac{r^{10}}{5} - \frac{\cos 2\theta}{7}(r^{12} - 6r^2) + \ldots,$$

and similar equations. These functions are biharmonic, but do not satisfy the boundary condition (16), nor can they be made to do so by the addition of harmonic functions. However, it is clear that the functions $(\phi_1 + \phi_3)$, $(\phi_3 + \phi_5)$, $(\phi_5 + \phi_7)$, ... do satisfy the condition. The difficulty does not arise with the functions ϕ_2, ϕ_4, ϕ_6, ... which are given by

$$\frac{a\phi_2}{C} = \cos\theta(r^3 - 3r) - \frac{\cos\theta}{3}(r^5 - 5r) + \frac{\cos 3\theta}{5}\left(r^7 - \frac{7r^3}{3}\right) - \frac{\cos 5\theta}{7}\left(r^9 - \frac{9r^5}{5}\right) + \ldots,$$

$$\frac{a\phi_4}{C} = \cos 3\theta\left(r^5 - \frac{5r^3}{3}\right) - \frac{\cos\theta}{3}(r^7 - 7r) + \frac{\cos\theta}{5}(r^9 - 9r) - \frac{\cos 3\theta}{7}\left(r^{11} - \frac{11r^3}{3}\right) + \ldots,$$

$$\frac{a\phi_6}{C} = \cos 5\theta\left(r^7 - \frac{7r^5}{5}\right) - \frac{\cos 3\theta}{3}\left(r^9 - \frac{9r^3}{3}\right) + \frac{\cos\theta}{5}(r^{11} - 11r) - \frac{\cos\theta}{7}(r^{13} - 13r) + \ldots$$

and similar equations; these functions are biharmonic and satisfy condition (16).

If then we assume for ϕ an expression of the form

$$\phi = A_1\phi_2 + A_2(\phi_1 + \phi_3) + A_3(\phi_2 + \phi_4) + A_4(\phi_3 + \phi_5) + \ldots,$$

where the coefficients A are constant, the problem is reduced to finding the values of A_1, A_2, A_3, ..., so that

$$(\phi)_{r=1} = \sum_{n=0}^{\infty} f_n \cos n\theta. \quad . \quad . \quad . \quad . \quad (26)$$

It is easily seen that when $r = 1$

$$\frac{a\phi_2}{2C} = \left[-1 + \left(1 - \frac{1}{3}\right)\right]\cos\theta - \left(\frac{1}{3} - \frac{1}{5}\right)\cos 3\theta + \left(\frac{1}{5} - \frac{1}{7}\right)\cos 5\theta - \ldots,$$

$$\frac{a(\phi_2 + \phi_4)}{2C} = -\left(\frac{1}{3} - \frac{1}{5}\right)\cos\theta + \left[-\frac{1}{3} + \left(\frac{1}{5} - \frac{1}{7}\right)\right]\cos 3\theta - \left(\frac{1}{7} - \frac{1}{9}\right)\cos 5\theta + \ldots,$$

$$\frac{a(\phi_1 + \phi_3)}{2C} = \frac{1}{1.3} - \left[\frac{1}{2} + \left(\frac{1}{3} - \frac{1}{5}\right)\right]\cos 2\theta + \left(\frac{1}{5} - \frac{1}{7}\right)\cos 4\theta - \left(\frac{1}{7} - \frac{1}{9}\right)\cos 6\theta + \ldots,$$

$$\frac{a(\phi_3 + \phi_5)}{2C} = -\frac{1}{3.5} + \left(\frac{1}{5} - \frac{1}{7}\right)\cos 2\theta - \left[\frac{1}{4} + \left(\frac{1}{7} - \frac{1}{9}\right)\right]\cos 4\theta + \left(\frac{1}{9} - \frac{1}{11}\right)\cos 6\theta - \ldots,$$

Consequently the problem is formally solved if coefficients A_1, A_3, A_5, ... are found such that

$$\left[-1+\left(1-\frac{1}{3}\right)\right]A_1-\left(\frac{1}{3}-\frac{1}{5}\right)A_3+\left(\frac{1}{5}-\frac{1}{7}\right)A_5-\ldots=\frac{af_1}{2C},$$

$$-\left(\frac{1}{3}-\frac{1}{5}\right)A_1+\left[-\frac{1}{3}+\left(\frac{1}{5}-\frac{1}{7}\right)\right]A_3-\left(\frac{1}{7}-\frac{1}{9}\right)A_5+\ldots=\frac{af_3}{2C},$$

and coefficients A_2, A_4, A_6, ... such that

$$-\left[\frac{1}{2}+\left(\frac{1}{3}-\frac{1}{5}\right)\right]A_2+\left(\frac{1}{5}-\frac{1}{7}\right)A_4-\left(\frac{1}{7}-\frac{1}{9}\right)A_6+\ldots=\frac{af_2}{2C},$$

$$\left(\frac{1}{5}-\frac{1}{7}\right)A_2-\left[\frac{1}{4}+\left(\frac{1}{7}-\frac{1}{9}\right)\right]A_4+\left(\frac{1}{9}-\frac{1}{11}\right)A_6-\ldots=\frac{af_4}{2C},$$

and so on. The constant term on each side of equation (26) is ignored.

8. Before it can be concluded that the formal solution as obtained above does in fact satisfy the conditions of the problem some difficult questions of convergence must first be settled. But in practice there is no difficulty, for only a finite number of terms of the ϕ-series can be handled numerically, and it is a straightforward matter to estimate the extent to which such an expression for ϕ fails to satisfy the imposed conditions. A good deal of preliminary work showed that a reasonable approximation could be expected from the first fourteen terms of the series. We therefore write

$$\phi=A_1\phi_2+\sum_{m=2}^{14}A_m(\phi_{m-1}+\phi_{m+1}), \quad . \quad . \quad (27)$$

and choose A_1, A_2, ... so that the first fourteen of the equations of §7 are satisfied.

The problem has been completed numerically only in the case in which the angle α is 20°, the height of the projection being then rather more than one-tenth (0·113) of the breadth of the channel. To ensure that the projection exerts a pronounced influence on the fluid motion a value has been assigned to α that is somewhat large in view of the approximation of §6.

The values of the coefficients f_1, f_2, ... of equation (26) are given for $\alpha=20°$ in the following table, in which

$$f_r'=\frac{4\pi a^2 f_r}{C^2}.$$

TABLE I.

f_1'.....	$-\cdot0533$	f_6'	$\cdot0339$	f_{11}'.....	$-\cdot0069$
f_2'.....	$\cdot0514$	f_7'	$-\cdot0281$	f_{12}'.....	$\cdot0030$
f_3'.....	$-\cdot0483$	f_8'	$\cdot0223$	f_{13}'.....	$\cdot0001$
f_4'.....	$\cdot0443$	f_9'	$-\cdot0167$	f_{14}'.....	$-\cdot0023$
f_5'.....	$-\cdot0394$	f_{10}' ...	$\cdot0115$		

Solution of the equations of §7 then gives the values for A_1, A_2, ... shown in Table II., wherein

$$A_r' = \frac{8\pi a A_r}{C}.$$

TABLE II.

A_1'.....	$\cdot1835$	A_6'	$-\cdot1997$	A_{11}'.....	$\cdot0285$
A_2'.....	$-\cdot0920$	A_7'	$\cdot1362$	A_{12}'.....	$-\cdot0373$
A_3'.....	$\cdot0552$	A_8'	$-\cdot1810$	A_{13}'.....	$\cdot0421$
A_4'.....	$-\cdot1834$	A_9'	$\cdot2036$	A_{14}'.....	$\cdot0322$
A_5'.....	$\cdot2689$	A_{10}'.....	$-\cdot1135$		

9. The detailed working out of the stream-lines would be a difficult matter, and one which is in the present problem scarcely necessary, since the general pattern of the flow is obvious. The only detailed work that has been undertaken is consequently the evaluation of the stream-function ψ at points of the line EA, the continuation of the projection.

The functions $\phi_1, \phi_2, \ldots$ are most easily evaluated in terms of the coordinates r, θ of the ζ-plane. The line of the projection corresponds to the real axis of the ζ-plane, and there is the following relation, derived from integration of equation (7), between the ordinates of points of EA and the corresponding values of r,

$$y = -\frac{C}{\sqrt{a^2-1}} \tan^{-1}\left(\frac{1+a^2t^2}{a^2-1}\right)^{1/2},$$

where

$$t = \frac{1+r}{1-r},$$

and negative values of r are assigned to points of the line $\theta = \pi$.

Setting $\alpha = 20^\circ$ in equation (8), we have $a^2 = 32\cdot17$, whence the relation between y and r shown in Table III.

TABLE III.

r...	−1·00	−·95	−·90	−·80	−·50	0
$-\sqrt{a^2-1}y/C$...	·1773	·1791	·1848	·2086	·3658	·8009

r...	·50	·80	·90	·95	1·00
$-\sqrt{a^2-1}y/C$...	1·2543	1·4619	1·5190	1·5456	1·5708

Table IV. shows the values of the functions ϕ for several values of r, θ being equal to π. To obtain the corresponding values when $\theta=0$, such functions as $\phi_2+\phi_4$ should be reversed in sign and such functions as $\phi_1+\phi_3$ left unchanged. When $r=0$ all the functions vanish.

TABLE IV.

	$r=1·00$.	$r=·95$.	$r=·90$.	$r=·80$.	$r=·50$.
$a\phi_2/C$	·8584	·8556	·8472	·8144	·6022
$a(\phi_1+\phi_3)/C$	−·5251	−·5206	−·5080	−·4626	−·2404
$a(\phi_2+\phi_4)/C$	·8584	·8513	·8315	·7633	·4571
$a(\phi_3+\phi_5)/C$	−·5584	−·5492	−·5248	−·4472	−·1754
$a(\phi_4+\phi_6)/C$	·3251	·3141	·2864	·2061	−·0009
$a(\phi_5+\phi_7)/C$	−·3156	−·3028	−·2719	−·1892	−·0179
$a(\phi_6+\phi_8)/C$	·3251	·3105	·2770	·1936	·0475
$a(\phi_7+\phi_9)/C$	−·2576	−·2416	−·2062	−·1254	−·0124
$a(\phi_8+\phi_{10})/C$	·1981	·1807	·1440	·0671	−·0162
$a(\phi_9+\phi_{11})/C$.....	−·1961	−·1773	−·1396	−·0664	·0008
$a(\phi_{10}+\phi_{12})/C$	·1981	·1781	·1396	·0705	·0141
$a(\phi_{11}+\phi_{13})/C$	−·1690	−·1478	−·1091	−·0448	−·0019
$a(\phi_{12}+\phi_{14})/C$	·1421	·1200	·0812	·0220	−·0093
$a(\phi_{13}+\phi_{15})/C$	−·1414	−·1183	−·0796	−·0248	·0008

The corresponding values of ψ are tabulated below. A constant has been added to the values of ϕ given directly by equation (27) so that ψ may vanish when $r=-1$, that is, at the end of the projection.

TABLE V.

r...	−1·00	−·95	−·90	−·80	−·50	0
$-8\pi a^2\psi/C^2$...	0	·0371	·1387	·5031	3·1307	16·499

r...	·50	·80	·90	·95	1·00
$-8\pi a^2\psi/C^2$...	40·749	55·393	59·816	61·924	63·965

In fig. 4 is shown the relation between ψ and y, and, as a comparison, the relation between y and the stream-function, $-y^2$, of the undisturbed flow at great distance from the projection. About a quarter of the breadth b of the channel is covered by the figure; elsewhere on the section considered the influence of the projection is small, and the curves representing the two stream-functions are nearly coincident.

Fig. 4.

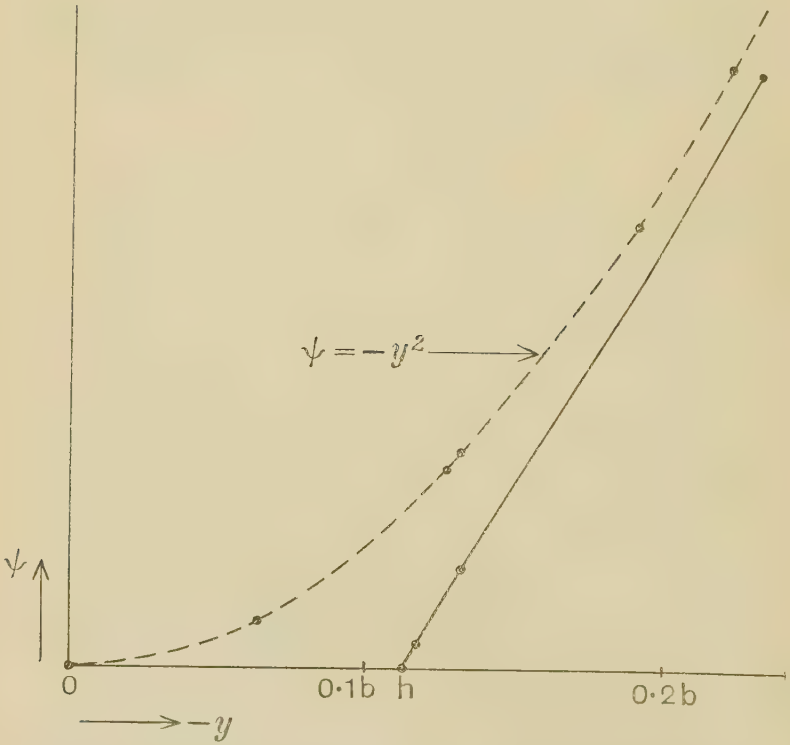

The point of most interest in the figure is the fact that $\partial\psi/\partial y$ does not vanish when $y=-h$, which implies that there is a finite velocity of slip at the end of the projection; but there is no reason to suppose that this is merely a consequence of the approximations that have been made, for when $r=1$ of the two conditions

$$\frac{\partial\psi}{\partial r}=0, \quad \frac{\partial\psi}{\partial\nu}=0,$$

the first implies the second at all points except those at which the modulus of the transformation $\left|\frac{d\zeta}{dz}\right|$ is infinite. The end E of the projection is from (7) one of these exceptional points, and this is the mathematical reason for the existence of the velocity of slip.

From a more general point of view it may be observed that such a velocity is not precluded by the generally accepted boundary condition governing the motion of viscous fluids; nor, in the problem of elasticity which corresponds to that of this paper, is the fact that a thin plane plate ABCFG, clamped on the edge CDEF, is actually inclined at E contrary to the usual definition of a clamped edge; for the ideas of velocity of slip and of clamping alike presuppose a boundary with finite curvature and a definite normal, while at E the boundary has no definite normal. These remarks evidently apply only to a sharp internal corner; with an external corner no difficulty of this kind arises.

10. It is not necessary to examine in the general case the convergence of the process of §7; for consider the function

$$\psi = -y^2 + \phi, \qquad \ldots\ldots \quad (28)$$

where ϕ is given by (27) and is therefore the sum of a finite number of the functions $\phi_1, \phi_2, \ldots$ The expression is biharmonic, and its derivative satisfies the boundary condition, but it does not itself exactly attain the required values on the boundary. It is convenient to write (28) in the equivalent form

$$\psi = [-y^2 + f(\theta)] + [\phi - f(\theta)],$$

where

$$f(\theta) = \sum_0^\infty f_n \cos n\theta.$$

The term in the first bracket attains the correct boundary values, so that the boundary values of the term in the second bracket represent the error in the expression for ψ. The function ϕ has been chosen so that there are no terms in $\cos\theta$, $\cos 2\theta$, ... or $\cos 14\theta$ in $\phi - f(\theta)$, which therefore consists first of the difference between $f(\theta)$ and the first 15 terms of its expansion as a Fourier series, and then of the terms in $\cos 15\theta$, $\cos 16\theta$, ... in ϕ. But these last terms are very small: the coefficient of $\cos 15\theta$ in ϕ is

$$-\frac{C^2}{8\pi a^2}(\cdot 005),$$

the coefficient of $\cos 16\theta$ still smaller, while the successive coefficients are on the whole decreasing. We can conclude that the error arises almost entirely from the replacement of $f(\theta)$ by the first 15 terms of the series, and is quite small.

The errors introduced by the assumption that h/b is small are ignored in the preceding remarks; these are more difficult to assess, since it is one of the consequences of this assumption that the functions ϕ_1, ϕ_2, ... are not exactly biharmonic. But the magnitudes of these errors depend merely on the value assigned to α, the whole assumption being, moreover, avoidable. This matter has therefore no bearing on the general question of the practical difficulty of applying this analysis to such problems as those mentioned in §1. In those problems the important thing is to decide whether eddies do or do not exist—to determine, that is to say, the general character of the fluid motion; no great accuracy is demanded. The work of this paper is enough to show that questions of this kind can be answered by Love's method of analysis without special difficulty.

L. *An X-ray Investigation of the Crystals of o-Azotoluene.* *By* Mata Prasad, *D.Sc.*, *and* K. V. Desai, *M.Sc.**

THE crystals of azo-benzene

have been studied by Prasad (Phil. Mag. x. p. 306 (1930)), who found that they belong to the space group C_{2h}^5 and that the unit cell contains four molecules, contrary to the results of Becker and Jancke (*Zeit. Phys. Chem.* xcix. p. 242 (1921)). He further found that there exists nearly complete symmetry about the $(20\bar{1})$ plane both in respect to the geometrical relation and to the intensities of reflexions by corresponding planes.

o-Azotoluene,

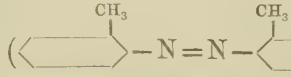

is similar to azobenzene except for the two methyl groups attached to the benzene rings in an ortho-position to the nitrogen atoms. Also the crystals of azobenzene and *o*-azotoluene belong to the monoclinic prismatic class of

* Communicated by Sir W. H. Bragg, O.M., K.B.E., M.A., F.R.S.

crystals. An X-ray examination of the crystals of *o*-azotoluene was, therefore, undertaken to determine if they bear any structural identity with the crystals of azobenzene.

The crystals of *o*-azotoluene were prepared by the slow evaporation of its solution in alcohol. The $c(001)$ face is a prominent face; other faces found to develop are $r(40\bar{1})$, $p(111)$ and $o(11\bar{1})$. The axial ratios found by crystallographers are

$$a:b:c \;::\; 2{\cdot}2254:1:1{\cdot}7077$$
$$\text{and } \angle\beta = 101^\circ 4'$$

(*cf.* Groth, *Chemische Krystallographie*, v. p. 65).

The crystals were examined by the rotating crystal method. With a Shearer tube fitted with a copper anti-cathode and a Universal Photogoniometer, designed by J. D. Bernal and manufactured by W. G. Pye & Co., Cambridge, the rotation photographs about the a and b axes were taken, and the lengths of these axes were calculated. Assuming $\angle\beta$ to be $101^\circ 4'$ (Groth's value), the length of the c axis was determined from (002) and (004) planes, which appeared as very strong spots on both the a and b rotation photographs.

The dimensions of the unit cell were thus found to be

$$a = 13{\cdot}93 \text{ Å.U.}, \quad b = 6{\cdot}604 \text{ Å.U.}, \quad c = 14{\cdot}55 \text{ Å.U.}$$

The axial ratios are

$$a:b:c \;::\; 2{\cdot}109:1:2{\cdot}204.$$

The various reflecting planes were identified from the oscillation photographs taken about a and b axes at intervals of 15 degrees. The indices of the planes, corresponding to the spots which appeared on the oscillation photographs, were worked out by Bernal's method of analysis (Proc. Roy. Soc. A, cxiii. p. 117 (1926)). Tables I. and II. give the indices of the planes observed together with a rough idea of their relative intensities. The intensities of the spots were evaluated by eye-estimation in the same way as described by Prasad (*loc. cit.*) and the same symbols have been used.

Table I. shows that the planes (hol) are halved when h is odd and (okl) are halved when k is odd. Also (010) is halved. These halvings correspond to the space group C_{2h}^5 and Γm lattice.

The number of the molecules in the unit cell required by the space group is four; the number of the molecules calculated from the dimensions of the unit cell and the

density of the crystal being also four, the molecules in the unit cell are asymmetric. The elements of symmetry of the unit cell are, in accordance with the space group, a glide

Table I.

Axial planes.	(*hol*) planes.	(*okl*) planes.	(*hko*) planes
020 m.s.	201 v.w.	021 m.s.	110 m.s.
002 v.s.	203 m.s.	022 w.	130 w.
004 v.s.	$20\bar{2}$ v.s.	023 w.	220 s.
005 w.	$20\bar{3}$ s.	024 m.s.	310 m.s.
007 w.	$20\bar{4}$ s.	025 m.s.	330 m.s.
200 v.s.	$20\bar{5}$ m.s.	026 w.	420 w.
400 v.w.	$20\bar{6}$ w.		510 w.
600 w.	401 m.s.		710 w.
	403 m.s.		
	$40\bar{2}$ s.		
	$40\bar{5}$ w.		
	$40\bar{6}$ w.		
	$60\bar{4}$ m.s.		

Table II.

111 w.	215 w.	311 w.	411 m.s.	511 w.
112 v.s.	$21\bar{4}$ v.s.	312 w.	$41\bar{2}$ v.w.	512 m.s.
113 v.s.	221 m.s.	313 w.	$41\bar{4}$ v.w.	513 w.
114 m.s.	222 w.	314 m.s.	$41\bar{5}$ m.s.	514 m.s.
115 w.	223 m.s.	$31\bar{1}$ w.	$41\bar{6}$ m.s.	$51\bar{1}$ w.
116 w.	224 w.	$31\bar{2}$ m.s.	421 v.w.	$51\bar{2}$ w.
$11\bar{1}$ m.s.	225 w.	$31\bar{3}$ m.s.	422 w.	$51\bar{4}$ w.
$11\bar{2}$ s.	226 v.w.	$31\bar{4}$ m.s.	423 w.	$51\bar{7}$ w.
$11\bar{3}$ v.s.	$22\bar{1}$ s.	$32\bar{4}$ w.	424 w.	$52\bar{3}$ v.w.
$11\bar{4}$ v.s.	$22\bar{2}$ m.s.	$32\bar{5}$ w.	$42\bar{1}$ w.	$62\bar{3}$ v.w.
$11\bar{5}$ s.	$22\bar{3}$ w.	$32\bar{6}$ w.	$42\bar{2}$ w.	$71\bar{4}$ v.w.
$11\bar{6}$ w.	$22\bar{4}$ w.	331 w.	$42\bar{3}$ w.	
$11\bar{7}$ v.w.	$22\bar{5}$ w.	332 w.	$42\bar{5}$ m.s.	
$12\bar{3}$ m.s.	$22\bar{6}$ w.	333 w.	$42\bar{6}$ m.s.	
$12\bar{4}$ m.s.	$22\bar{7}$ w.		$43\bar{3}$ v.w.	
133 w.				
$13\bar{1}$ w.				

plane of symmetry parallel to the (*ac*) face and a screw axis parallel to *b* axis (*cf.* Astbury and Yardley, Phil. Trans. A, ccxxiv. pp. 221–257).

These results show that the crystals of azobenzene and *o*-azotoluene are identical in the following respects: (1) the

crystals belong to the space group C_{2h}^5 ; (2) the planes (*hol*) are halved if h is odd and (010) is also halved ; (3) the molecules in the unit cell are four and they are asymmetric ; and (4) the value of $c \sin \beta$, *i. e.* the spacing of (001) planes is 14·29 Å. The same value of $c \sin \beta$ in the two crystals may indicate that the molecules in the unit cell lie with their length along the direction $c \sin \beta$; as the lengths of the molecules of the two substances, represented according to their chemical formula, are identical.

The crystals of *o*-azotoluene show no geometrical symmetry about the direction of $(20\bar{1})$ plane in (010) face. Table III. gives the strongly reflected planes referred to this direction as one of the coordinate axes and shows that the intensities of reflexion of the corresponding planes, *i. e.* of the $(h'k'l')$ and

TABLE III.

202 v.s.	$20\bar{2}$ v.s.	1113 w.	$11\bar{1}\bar{3}$ w.
204 v.w.	$20\bar{4}$ m.s.	222 s.	$22\bar{2}$ m.s.
208 m.s.	$20\bar{8}$ m.s.	224 m.s.	$22\bar{4}$ m.s.
406 m.s.	$40\bar{6}$ w.	226 w.	$22\bar{6}$ w.
111 m.s.	$11\bar{1}$ m.s.	228 m.s.	$22\bar{8}$ w.
113 w.	$11\bar{3}$ s.	2210 w.	$22\bar{1}\bar{0}$ w.
115 v.s.	$11\bar{5}$ v.s.	2212 w.	$22\bar{1}\bar{2}$ w.
117 v.s.	$11\bar{7}$ v.s.	311 w.	$31\bar{1}$ m.s.
119 m.s.	$11\bar{9}$ s.	313 m.s.	$31\bar{3}$ m.s.
1111 w.	$11\bar{1}\bar{1}$ w.	315 w.	$31\bar{5}$ m.s.

$(h'k'\bar{l}')$ in the crystal of *o*-azotoluene, are not so completely identical as in that of azobenzene.

Summary.

The structure of crystals of *o*-azotoluene has been examined by the rotating crystal method. The dimensions of the unit cell are found to be

$$a = 13{\cdot}93 \text{ Å.U.}, \quad b = 6{\cdot}604 \text{ Å.U.}, \quad c = 14{\cdot}55 \text{ Å.U.}$$
$$\angle\beta = 101^\circ 4'.$$

The cell contains four molecules. The crystal belongs to space group C_{2h}^5 and Γm lattice. No complete symmetry about $(20\bar{1})$ has been observed as in the case of azobenzene, but the value of $c \sin \beta$ in this crystal is the same as in that of azobenzene.

Chemistry Laboratory,
The Royal Institute of Science,
Bombay.

LI.—*On the Theory of Equations of State.* *By* T. S. Wheeler, *Ph.D., F.R.C.Sc.I., F.I.C., Principal, Royal Institute of Science, Bombay* *.

Summary.

A general expression for the work of dilution of a system of charged particles in thermal equilibrium is deduced from thermodynamic and dimensional considerations. Some special applications of this expression are considered.

Notation.

a = van der Waals's pressure constant.

a', a_1', etc. = constants for a given system of particles.

B_{s+1} = the virial coefficient corresponding to V^{-s}.

$\overline{B_L}$ = the value of B_2, $(s=1)$, calculated on the Leiden system, multiplied by 10^4.

$\overline{B_y}$ = a constant for a given system of ions.

b', b_1' = constants.

c = concentration of a salt in gram-mols. per litre.

C', C, C_1, C_2 = constants occurring in the expressions for virial coefficients.

D = a function of a temperature-variable property of the medium separating the particles. (Dielectric constant.)

e = a function of an intrinsic property (charge) of each of the particles which is independent of temperature.

E = electrical internal energy change associated with W.

$\overline{E}$ = value of E when D is independent of temperature.

f, F = functions.

G_{yz} = a constant for a given system of ions.

g = osmotic coefficient.

i = van't Hoff factor.

k = Boltzmann's constant.

k_2 = constant.

$\overline{m}$ = number of ions in a molecule.

* Communicated by the Author.

m = index expressing the variation of a force with inverse distance.

n = index expressing the variation of a force with inverse distance.

N = total number of particles in volume V.

N_y = number of particles of the yth kind in volume V.

$\mathfrak{N}$ = number of molecules in 1 gram-mol.

p = pressure.

q = constant $(= 3\gamma)$.

r = distance between two particles.

s = index of V.

T = absolute temperature.

$\bar{U}$ = mutual potential of the particles.

V = volume containing N particles.

W = electrical work of dilution.

w = Debye and Hückel's valency factor.

w_y = valency of the yth kind of ion.

x refers to one of the forces between a particle of the yth and a particle of the zth kind.

$\alpha, \beta, \gamma, \delta$ = constants.

θ = deviation of osmotic coefficient $= (1-g)$.

λ, μ = force coefficients.

σ = diameter of a particle.

ϕ = function equivalent to W.

Introduction.

In a recent paper[1] the author has shown that for a dilute solution of a salt yielding small ions the electrical work done by the interionic forces can be expressed as the product of a potential energy corresponding to the law of force specified, multiplied by a sum of a series, each term of which consists of a power of the ratio of the potential energy to a thermal kinetic energy.

In this paper an attempt is made to generalize somewhat this result and to consider some particular applications of it.

The System of Particles Considered.

We consider a volume V containing at temperature T and pressure p N small spherically symmetrical gaseous

particles. There are i kinds of these particles present, and N is given by

$$N = N_1 + N_2 + N_3 + \ldots N_y \ldots N_z \ldots N_i. \quad . \quad . \quad (1)$$

Each particle is present in sufficient numbers to permit of statistical treatment.

We assume that the xth of the separate forces between a particle of the yth kind and a particle of the zth kind at a distance r from each other can be expressed by

$$f_{yz,x}(r) = \lambda_{yz,x}/r^{n_{yz,x}} = e_{yz,x}/(D \cdot r^{n_{yz,x}}), \quad . \quad . \quad (2)$$

where e is a function of an intrinsic property of each of the particles which is independent of temperature and D is a function of a temperature-variable property of the medium separating the particles.

The Electrical Work of Expansion.

We define the "electrical" work of expansion W as the work done by the forces between the particles when the gaseous system is reversibly and isothermally expanded to infinity *.

If $W_{yz,xr}$ is the electrical work done by the xth force between a particle of the yth kind and a particle of the zth kind at an initial distance r from each other, then the total work done by the xth forces between all the yz pairs is given by

$$W_{yz,x} = \sum_r W_{yz,xr}. \quad . \quad . \quad . \quad . \quad . \quad (3)$$

The work done by the total forces between all the yz pairs is given by

$$W_{yz} = \sum_x W_{yz,x}. \quad . \quad . \quad . \quad . \quad . \quad . \quad (4)$$

The total electrical work is given by

$$W = \sum_y \sum_z W_{yz} = \sum_y \sum_z \sum_x \sum_r W_{yz,xr}, \quad . \quad . \quad . \quad (5)$$

the summation being taken over all pairs in the usual manner. It is convenient in what follows to replace the suffix yz, x by a dash, for example, $W_{yz,x}$ is written W'.

The General Form of the Work Function.

We *assume* that we can put

$$W' = \phi(\bar{e}', D, T, V) = \phi', \quad . \quad . \quad . \quad . \quad (6)$$

* It is assumed that it is unnecessary formally to distinguish between expansion at constant volume and at constant pressure [2].

where $\bar{e}'$ is a function of all the e properties (charges) and involves e' in some special manner.

W will be the sum of a number of ϕ functions ; we have, in fact, ((4), (5)),

$$W = \sum_y \sum_z \sum_x \phi' = \bar{\Sigma}\phi',$$

where $\bar{\Sigma}$ is equivalent to

$$\sum_y \sum_z \sum_x . \quad . \quad . \quad . \quad . \quad . \quad . \quad . \quad . \quad (7)$$

We can apply to ϕ' considerations similar to those applied to the work function in the simpler case previously discussed [1].

We have :—

1. ϕ' must vanish when V is indefinitely increased.

2. ϕ' must vanish when D is indefinitely increased.

3. ϕ' must vanish when e' vanishes.

4. The general charging and discharging process described by Debye [3] enables us to write

$$pV = NkT - V(\delta W/\delta V)_{T, D} \quad . \quad . \quad . \quad . \quad (8)$$

$$= NkT - V\bar{\Sigma}(\delta\phi'/\delta V)_{T, D}, \quad . \quad . \quad . \quad (9)$$

and to deduce that $V(\delta\phi'/\delta V)_{T, D}$ has the dimensions of energy.

5. Writing

$$-E/T^2 = (\delta(W/T)\delta T)_V = \bar{\Sigma}(\delta(\phi'/T)/\delta T)_V, \quad . \quad (10)$$

we can deduce that $T(\delta\phi'/\delta T)_{V, D}$ must have the dimensions of energy, since the expansion of (10) gives

$$E = \bar{\Sigma}\left[[\phi' - T(\delta\phi'/\delta T)_{V, D}]\left[1 - \frac{T(\delta\phi'/\delta D)_{V, T}(\delta D/\delta T)_V}{\phi' - T(\delta\phi'/\delta T)_{V, D}}\right]\right].$$

$$. \quad . \quad . \quad (11)$$

6. Employing the general method which Bjerrum [4] applied to two particles attracting according to the inverse square law, it can readily be shown that

$$[1 + (T/D)(\delta D/\delta T)_V]$$

must be a factor of E and E′.

Hence from (11)

$$D(\delta\phi'/\delta D)_{V, T} = -\phi' + T(\delta\phi'/\delta T)_{V, D}. \quad . \quad . \quad (12)$$

Consequently $D(\delta\phi'/\delta D)_{V, T}$ must have the dimensions of energy.

We can satisfy the six conditions set out above if we put

$$\phi' = a_1' T^{\alpha_1'} D^{\beta_1'} V^{\gamma_1'} e'^{\delta_1'} + a_2' T^{\alpha_2'} D^{\beta_2'} V^{\gamma_2'} e'^{\delta_2'} + \ldots \quad (13)$$

$$= \Sigma a_1' T^{\alpha_1'} D^{\beta_1'} V^{\gamma_1'} e'^{\delta_1'}, \quad \ldots \quad (14)$$

where a_1', a_2', etc. are such functions of all the "charges" that they do not become infinite when e' vanishes, and α_1', β_1', γ_1' δ_1', etc. are constants of which the β' and γ' constants are negative and the δ' constants are positive.

The Relations between the Indices occurring in ϕ'.—The relations between the α', β', γ', and δ' constants can be deduced in a manner similar to that previously described for the simpler case then considered[1]; the treatment is modified in that the Clausius virial equation is here directly applied.

From (12) it follows that

$$\beta_1' = \alpha_1' - 1\ ;\ \beta_2' = \alpha_2' - 1\ ;\ \text{etc.} \quad \ldots \quad (15)$$

The Clausius virial equation, assumed to be valid for the system considered, is

$$pV = NkT + (1/3)\Sigma\Sigma\Sigma rf'(r). \quad \ldots \quad (16)$$

From (2)

$$\Sigma\Sigma rf'(r) = (e'/D)\Sigma\Sigma(1/r^{n'-1}). \quad \ldots \quad (17)$$

The mutual potential of the particles at a given instant as regards the xth force between the yth and the zth particles is given by

$$U' = -(e'/D)\Sigma\Sigma\int_{\infty}^{r}(1/r^{n'})dr \quad \ldots \quad (18)$$

$$= (e'/D)(1/(n'-1))\Sigma\Sigma(1/r^{n'-1}). \quad \ldots \quad (19)$$

When D is independent of temperature this mutual potential is equal to the internal energy of the solution corresponding to the force under consideration (E′), so that from (11), (14), (19), and (17) we have

$$E' = \phi'\Sigma(1-\alpha_1') = \bar{U}' = (1/(n'-1))\Sigma\Sigma rf'(r), \quad (20)$$

and (16) becomes

$$pV = NkT + (1/3)\Sigma(n'-1)\phi'\Sigma(1-\alpha_1'). \quad \ldots \quad (21)$$

From (9) and (14)

$$pV = NkT - \bar{\Sigma}\phi'\Sigma\gamma_1'. \quad \ldots \quad (22)$$

From (15), (21), and (22) we can deduce relations between α', β', and γ', which enable us to write

$$\phi' = \Sigma a_1' T^{1+3\gamma_1'/(n'-1)} D^{3\gamma_1'/(n'-1)} V^{\gamma_1'} e'^{\delta_1'}. \quad \ldots \quad (23)$$

If now we put

$$\delta_1' = -3\gamma_1'/(n'-1), \quad . \quad . \quad . \quad . \quad (24)$$

we can write (23)

$$\phi' = \frac{e'}{D\overline{V}^{(n'-1)/3}} \sum b_1' \left(\frac{e'}{D\overline{V}^{(n'-1)/3}(kT)} \right)^{-1-(3\gamma_1'/(n'-1))} \quad (25)$$

by a suitable choice of the b' constants.

The right-hand side of (25) is of the form of a static potential energy corresponding to the law of force under consideration, multiplied by a series, each term of which consists of a power of the ratio of the static potential energy to a kinetic energy. Since this expression is of the correct energy dimensions, the b' constants will be of zero dimensions in energy, and will contain expressions involving only the particle charges, the numbers of the various kinds of particles, and pure numerical constants, *e.g.*, π.

If we put $q_1' = 3\gamma_1'$, $q_2' = 3\gamma_2'$, etc. where the q constants are always negative, we can write (23)

$$\phi' = \Sigma a_1' (e'/D)^{-q_1'/(n'-1)} T^{1+(q_1'/(n'-1))} V^{q_1'/3} \quad . \quad (26)$$

$$= \Sigma a_1' \lambda'^{-q_1'/(n'-1)} T^{1+(q_1'/(n-1)} V^{q_1'/3}, \quad . \quad . \quad (27)$$

and

$$W = \bar{\Sigma} \Sigma a_1' \lambda'^{-q_1'/(n'-1)} T^{1+(q_1'/(n'-1))} V^{q_1'/3}. \quad . \quad (28)$$

We may now consider some applications of the general expression given in (28).

Solutions of Strong Electrolytes with Small Ions.

Putting $n' = 2$ and $\lambda' = w_y w_z e^2/D$, where w_y is the valency of the yth kind of ion, and assuming that ϕ' is a one-termed function, we have, if q_1' is put arbitrarily equal to $-3/2$,

$$\phi' = a' (w_y w_z e^2/D)^{3/2} T^{-1/2} V^{-1/2}. \quad . \quad . \quad . \quad (29)$$

And if ϕ'' is the dilution work evolved by the electrical forces between the yth kind of ions and all the ions in the solution we can write

$$\phi'' = B_y (e^2/D)^{3/2} T^{-1/2} V^{-1/2} (G_{y1} + G_{y2} + \ldots + G_{yz} + \ldots + G_{yi}),$$

$$. \quad . \quad . \quad (30)$$

where B, G_{y1}, etc. are functions of numerical constants such as π, of the valencies of the various ions and the number of ions present. B_y will contain $k^{-1/2}$ as a factor

(see (25)), and the various functions will also be related by equations of the type

$$B_y G_{yz} = a'(w_y w_z)^{3/2}. \quad . \quad . \quad . \quad . \quad . \quad (31)$$

Debye's[5] actual expression for ϕ'' is given by

$$\phi'' = \frac{-2\pi^{1/2} w_y^2 N_y}{3k^{1/2}} \left(\frac{e^2}{D}\right)^{3/2} T^{-1/2} V^{-1/2} (\Sigma N_1 w_1^2)^{1/2}, \quad (32)$$

to which ϕ'' is equivalent if we put

$$B_y = (-2\pi^{1/2}/3)(w_y^2 N_y / k^{1/2}), \quad . \quad . \quad . \quad (33)$$

and

$$\Sigma G_{y1} = (\Sigma N_1 w_1^2)^{1/2}. \quad . \quad . \quad . \quad . \quad . \quad . \quad (34)$$

It will be seen that ΣG_{y1} is independent of y. It was by their brilliant use of the Poisson equation that Debye and Hückel were able to express the work function for one kind of ion as a function of the properties and numbers of that kind of ion, and a separate function of the properties of the solution as a whole, which did not involve the properties of the one kind of ion in any special fashion.

We will return later to the case of ions with a definite radius.

Potential of Crystal Lattices.

To obtain the work function for a uniform system in which the ions have no thermal motion we make the index of T in (28) equal to zero wherever it occurs.

The expressions for the work function corresponding to each force then reduce each to one term, since there is only one possible value for each q index. For example, in (26)

$$q_1' = q_2' = q_3' = \ldots = -(n'-1), \quad . \quad . \quad (35)$$

so that (26) becomes

$$\phi' = a'(e'/D) V^{-(n'-1)/3}, \quad . \quad . \quad . \quad . \quad (36)$$

and (28) may be written

$$W = \overline{\Sigma}\, a'(e'/D) V^{-(n'-1)/3}, \quad . \quad . \quad . \quad . \quad (37)$$

which is the general expression for the work function, and in this case for the potential function (*cf.* (20), d_1' etc. $= 0$), of a crystal lattice.

The Gaseous Equation of State.

From (8) and (28) we have

$$pV = NkT - \Sigma\Sigma (q_1'/3) a_1' \lambda'^{-q_1'/(n'-1)} T^{1+(q_1'/(n'-1))} V^{q_1'/3}, \quad (38)$$

which is the general form of the equation of state.

We can derive from this equation expressions for the related functions g, i, etc. in the manner described in the previous paper [1].

We can also deduce expressions for the various virial coefficients [6]; these we will now consider.

We have

$$pV = NkT(1 + B_2/V + \ldots + B_{s+1}/V^s + \ldots, \quad . \quad (39)$$

where B_{s+1} is the virial coefficient corresponding to V^{-s}.

Putting $q_1'/3 = -s$, we have from (38)

$$B_{s+1} = \overline{\Sigma}\, C'(e'/D)^{3s/(n'-1)} T^{-3s/(n'-1)} \quad . \quad . \quad (40)$$

$$= \overline{\Sigma}\, C'(\lambda'/T)^{3s/(n'-1)}, \quad . \quad . \quad . \quad . \quad . \quad (41)$$

C' will contain expressions involving the particle charges, and the numbers of the various kinds of particles.

Debye's result for W with small ions (see (32)) corresponds to $s + 1 = 3/2$.

From (41), if the particles are all of one kind, with a force given by λ/r^n between each pair, the second virial coefficient B_2 is given by

$$B_2 = C\left(\frac{\lambda}{T}\right)^{3/(n-1)} \quad . \quad . \quad . \quad . \quad . \quad . \quad (42)$$

Jeans' expression for the second virial coefficient (repulsive force) in this case can be written [7]

$$B_2 = (2\pi/3)N(\lambda/(n-1)\,kT)^{3/(n-1)}\,\Gamma((n-4)/(n-1)) \,. \quad (43)$$

so that

$$C = (2\pi/3)N(1/(n-1)\,k)^{3/(n-1)}\,\Gamma((n-4)/(n-1)). \quad (43')$$

If the particles are all of one kind, with forces given by λ/r^n and μ/r^m between them, (41) gives

$$B_2 = C_1(\lambda/T)^{3/(n-1)} + C_2(\mu/T)^{3/(m-1)}. \quad . \quad . \quad (44)$$

No assumption is made as regards the signs of λ and μ, which will depend on the direction of the forces.

The expression developed by Lennard-Jones [7] for B_2 in the case under consideration is of the form

$$B_2 = K_2((\lambda/T)(T/\mu))^{3/(n-m)}\,F[(\mu/T)(T/\lambda)^{(m-1)/(n-1)}], \quad (45)$$

where the function F consists of the sum of a series of powers of the expression involved. λ here corresponds to a repulsive, and μ to an attractive force. In this expression the effect of each force is not separated: whether it will ever be possible to develop a method of analysis which

will give an expression of the type of (44) with definite values for C_1 and C_2 remains to be seen.

As an example of the utilization of (44) Table I. shows the application of the equation

$$B_L = 78{\cdot}2/T^{3/(21-1)} - 11{,}200/T^{3/(4-1)}, \quad . \quad . \quad (46)$$

that is,

$$B_L = 78{\cdot}2/T^{\cdot 15} - 11{,}200/T, \quad . \quad . \quad . \quad . \quad . \quad (47)$$

to the calculation of the second virial coefficient of argon. ($\overline{B}_L$ is the value of B_2 calculated on the Leiden system [8] multiplied by 10^4.)

Table I.

Second Virial Coefficient of Argon [9].

Temperature ° C.	Log $\overline{B}_L$ observed.	Log $\overline{B}_L$ calculated (47).
−121·21	1·57 (*n*) *	1·57 (*n*)
−120·24	1·56 (*n*)	1·56 (*n*)
−119·2	1·56 (*n*)	1·56 (*n*)
−115·86	1·55 (*n*)	1·54 (*n*)
−113·8	1·53 (*n*)	1·53 (*n*)
−109·88	1·51 (*n*)	1·51 (*n*)
−102·51	1·46 (*n*)	1·47 (*n*)
−87·05	1·38 (*n*)	1·39 (*n*)
−57·72	1·22 (*n*)	1·23 (*n*)
0	·87 (*n*)	·86 (*n*)
20·39	·75 (*n*)	·68 (*n*)

* (*n*) indicates that $\overline{B}_L$ is negative and that the log $-\overline{B}_L$ is given.

As will be clear from (46), the value of n, the index for the repulsive force, is 21, and of m, the index for the attractive force, is 4 (*cf.* (51)).

Lennard-Jones[10] found that values for $(n;m)$ of (14·3; 5), (21; 5), and (25; 5) gave satisfactory results with (45). (44) appears to be more sensitive than (45) to variations in the values of n and m. An expression of this form may therefore be of use in the determination of the values of these indices.

The van der Waals Equation.

If in (44) we take λ/r^n as a repulsive force, and observe that a rigid spherical particle corresponds to the repulsive force λ/r^n when $n \to \infty$, the diameter being given by

$$\underset{n \to \infty}{\text{Lt.}} \quad \lambda^{1/(n-1)} = \sigma^{(11)}, \quad . \quad . \quad . \quad . \quad . \quad (48)$$

we obtain

$$B_2 = C_1\sigma^3 + C_2(\mu/T)^{3(m-1)}*. \quad . \quad . \quad . \quad (49)$$

Now van der Waals's equation can be written, ignoring virial coefficients higher than the second,

$$pV = NkT\left[1 + \frac{(2/3)\pi\sigma^3 N}{V} - \frac{a}{VNkT}\right]. \quad . \quad (50)$$

Hence B_2 from (50) is given by

$$B_2 = (2/3)\pi\sigma^3 N - a/(NkT), \quad . \quad . \quad . \quad (51)$$

which is equivalent in form to (49) if $m = 4$.

Van der Waals's cohesive force can thus be regarded as varying as the inverse fourth power of the distance [12].

Solutions of Strong Electrolytes with Ions of Finite Size.

If in (28) we assume that all the particles have the diameter σ, and if we represent this condition by making one of the n indices infinite as in (48), we can write (28)

$$W = \bar{\Sigma}\Sigma a_1'\lambda'^{-q_1'/(n'-1)}T^{1+(q_1'/(n'-1))}V^{q_1'/3} + \Sigma a_1\sigma^{-q_1}TV^{q_1/3}; \quad . \quad . \quad . \quad (52)$$

(38) then becomes

$$pV = NkT - \bar{\Sigma}\Sigma(q_1'/3)a_1'\lambda'^{-q_1'/(n'-1)}T^{1+(q_1'/(n'-1))}V^{q_1'/3} - \Sigma(a_1q_1/3)\sigma^{-q_1}TV^{q_1/3}. \quad . \quad . \quad . \quad . \quad . \quad (53)$$

If we put $q_1 = -3$, $a_1 = (2/3)\pi N^2 k$, and suppress the Σ sign, the correction for the size of the ions in (53) becomes similar to the van der Waals correction given in (50).

Inserting as a first approximation Debye and Hückel's value for the electrical work of dilution and the van der Waals values for a_1 and q_1, (53) becomes (*cf.* (32))

$$pV = NkT - \sum\left(\frac{\pi^{1/2}w_y^2 N_y}{3k^{1/2}}\left(\frac{e^2}{D}\right)^{3/2}T^{-1/2}V^{-1/2}\right)\left(\Sigma N_1 w_1^2\right)^{1/2} + (2/3)\pi N^2 k\sigma^3 TV^{-1}. \quad . \quad . \quad . \quad . \quad . \quad (54)$$

We assume now that we are dealing with 1 gram-mol. of a salt which yields $\bar{m}$ ions per molecule, so that we can put

$$N = \bar{m}\bar{N}, \quad . \quad . \quad . \quad . \quad . \quad . \quad (55)$$

where $\bar{N}$ is the number of molecules in 1 gram-mol.

If now

$$pV = g\bar{m}NkT, \quad . \quad . \quad . \quad . \quad . \quad (56)$$

* Keesom's [13] value for B_2 in this case is related to (45).

comparing (54) and (56) we can write (for $T = 273{\cdot}1^\circ$)

$$\theta = 1-g = [{\cdot}263w\sqrt{mc}] - (2/3)\pi m\bar{N}\sigma^3 c\,10^{-3}, \quad (57)$$

where c is the concentration of the salts in gram-mols. per litre, and w is Debye and Hückel's valency factor. (For the calculation of the term in square brackets see Debye and Hückel[14].)

From (57)

$$\sigma = \left[\frac{{\cdot}263w\sqrt{mc}-\theta}{(2/3)\pi mc\bar{N}\,10^{-3}}\right]^{1/3} \quad . \quad . \quad . \quad . \quad . \quad (58)$$

$$= \left[\frac{7{\cdot}876\times10^{-22}}{\sqrt{mc}}\left({\cdot}263w - \frac{\theta}{\sqrt{mc}}\right)\right]^{1/3} . \quad . \quad (59)$$

As an example of the application of (59) we take values for potassium sulphate given by Debye and Hückel[14].

TABLE II.

w for potassium sulphate $= 2\sqrt{2}$.

$\sqrt{mc}$.	θ observed.	$\sigma\times10^8$ (cm.) calculated from (59).
·0906	·0647	6·3
·110	·0729	8·3
·136	·0776	9·9
·176	·101	9·1
·229	·128	8·6
·280	·147	8·5
·369	·178	8·2
·516	·220	7·9
·600	·238	7·7

The values of σ obtained are larger than the value calculated by Debye and Hückel ($2{\cdot}7\times10^{-8}$ cm.), but they are of the right order and show the approximate validity of (54). No great accuracy can be expected, since the values inserted for the second and third terms in the general equation (53) can only be regarded as first approximations to the correct values.

References.

(1) Wheeler, *Phys. Zeit.* xxxii. p. 674 (1931).
(2) Gatty, Phil. Mag. (7) xi. p. 1082 (1931); Scatchard, J. Amer. Chem. Soc. liii. p. 2037 (1931).
(3) Debye, *Phys. Zeit.* xxv. p. 98 (1924); Fowler, Trans. Faraday Soc. xxiii. p. 440 (1927); 'Statistical Mechanics,' pp. 197, 319 (1929).

(4) Bjerrum, *Zeit. Phys. Chem.* cxix. p. 150 (1926).
(5) Debye, *loc. cit.* p. 99.
(6) Kamerlingh-Onnes, Proc. Sect. Sciences, Amsterdam, iv. p. 125 (1902).
(7) See Lennard-Jones, Proc. Roy. Soc. cvi. A, p. 466 (1924).
(8) Lennard-Jones, 'Statistical Mechanics' (Fowler), p. 220 (1929).
(9) Kamerlingh-Onnes and Crommelin, Com. Phys. Lab. Leiden, no. 118 B, p. 24 (1910): Lennard-Jones, Proc. Roy Soc. cvi. A, p. 470 (1924).
(10) Lennard-Jones, *loc. cit.* p. 469.
(11) Lennard-Jones, *loc. cit.* p. 452.
(12) *Cf.* Keesom, Com. Phys. Lab. Leiden, Supp. no. 26, p. 4 (1912).
(13) Keesom, *loc. cit.*, Supp. no. 24 B, p. 32 (1912); Lennard-Jones, *loc. cit.* p. 467.
(14) Debye and Hückel, *Phys. Zeit.* xxiv. p. 200 (1923); Fowler, 'Statistical Mechanics,' p. 321 (1929).

LII. *The Equations of Motion of a Viscous Fluid.* *By* J. Prescott, *M.A.*, *D.Sc.**

AFTER searching in several places for a simple and at the same time satisfying proof of the equations of viscous flow, I felt that there was room for another one. In some books the writers borrow all the fundamental equations of elasticity, and then deduce those of viscous flow by an analogy which they do not prove to exist. Other writers, and these the best, produce very good proofs with rather a greater call on mathematics than is necessary. Still others use more doubtful methods than the analogy with elasticity. Even Stokes's proof, which has the great merit of starting from one physical assumption, has the drawback that few people would be willing to grant the truth of this physical assumption.

My object in this paper is to derive the equations of viscous flow by easy logical steps from the simplest physical assumption that we know about the subject, and one that can be tested quite easily. This assumption is the law of viscosity in the simplest case of all—that of laminar flow.

In the general case of flow of a fluid the particle which is at the point (x, y, z) at time t has component velocities u, v, w, which may be functions of x, y, z, and t. We get the simplest case of laminar flow if we take

$$u = f(z), \quad v = 0, \quad w = 0.$$

This means that all the particles which are in a plane perpendicular to the z-axis move with the same velocity parallel to

* Communicated by the Author.

the x-axis. This velocity u is, of course, different in different planes, or there would be no relative motion and no viscous flow.

Our one physical assumption, apart from the laws of mechanics, is that the friction per unit area between two planes of particles separated by the geometrical plane at z is proportional to the velocity gradient $\frac{\partial u}{\partial z}$—that is, the frictional drag, in the direction δx, of the upper plane on the lower plane across an element of area δA perpendicular to the z-axis at the point (x, y, z), is

$$\delta F = \mu \frac{\partial u}{\partial z} \delta A,$$

where μ is a constant, called the coefficient of viscosity. The friction per unit area is therefore

$$f = \mu \frac{\partial u}{\partial z}. \quad . \quad . \quad . \quad . \quad . \quad . \quad . \quad (1)$$

Now let us consider what is happening to a rectangular element $\delta x \times \delta y \times \delta z$, at the point (x, y, z), due to the motion we are considering, on the assumption that $f(z)$ is a function increasing as z increases. (This last assumption leads to the same equations as the contrary assumption.)

In consequence of the difference of velocities at z and $(z+\delta z)$ the rectangle $\delta x \times \delta z$ is changing into a parallelogram. Suppose the line of particles which was along δz at time t has turned through a small angle $d\theta$ in a further interval dt; then, since the relative velocity of the two opposite faces at z and $(z+\delta z)$ is $\frac{\partial u}{\partial z} \delta z$, it follows that the relative displacement in time dt is

$$\left(\frac{\partial u}{\partial z} \delta z\right) dt = \delta z \times d\theta,$$

from which

$$\frac{\partial u}{\partial z} = \frac{\partial \theta}{\partial t}.$$

If we write ϕ for the angle inside the parallelogram (fig. 1) we see that

$$\frac{\partial \theta}{\partial t} = -\frac{\partial \phi}{\partial t},$$

and so

$$\frac{\partial u}{\partial z} = -\frac{\partial \phi}{\partial t}.$$

Consequently the frictional drag per unit area is

$$f = -\mu \frac{\partial \phi}{\partial t}. \quad . \quad . \quad . \quad . \quad . \quad (2)$$

We shall now turn to the general case where u, v, w, are all functions of x, y, z, t, and shall find the equations of motion which are consistent with (2).

Fig. 1.

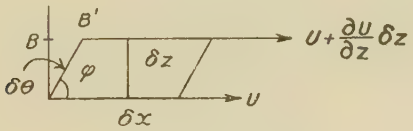

We have a further assumption to make, but one about the truth of which there is no doubt : it is that the viscous drag depends on the relative motion of the parts of the liquid, and not at all on any uniform translation or bodily rotation, in which there is no relative motion.

When neither u nor w is zero we must still suppose that the relative *slip* of the two planes of particles at z is $-\frac{\partial \phi}{\partial t}$, ϕ being the angle inside the parallelogram in fig. 1. Actually

Fig. 2.

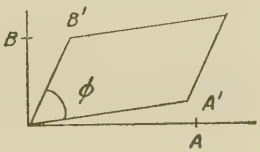

the true displacement is now shown in fig. 2, since all the sides of the parallelogram rotate.

It is easy to show in this case that

$$-\frac{\partial \phi}{\partial t} = \frac{\partial u}{\partial z} + \frac{\partial w}{\partial x}.$$

If the component velocity v exists at the same time it will be granted that this will have no effect on the component drag in any plane perpendicular to v. Therefore we conclude that

the frictional drag per unit area, in the x-direction, on a plane perpendicular to the z-axis, is

$$f_{zx} = -\mu \frac{\partial \phi}{\partial t}$$

$$= \mu\left(\frac{\partial u}{\partial z} + \frac{\partial w}{\partial x}\right). \quad . \quad . \quad . \quad . \quad . \quad . \quad (3)$$

This equation is the natural and logical extension of (1) to the general case of flow.

If we interchange z and x in (3), and consequently w and u, we get, for the frictional drag in the z-direction per unit of area perpendicular to the x-axis,

$$f_{xz} = \mu\left(\frac{\partial w}{\partial x} + \frac{\partial u}{\partial z}\right)$$

$$= f_{zx}. \quad . \quad . \quad . \quad . \quad . \quad . \quad . \quad . \quad . \quad (4)$$

Fig. 3.

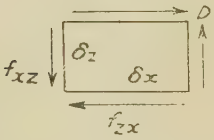

The result $f_{xz} = f_{zx}$ is the same relation as for shear stresses in elasticity, and could be proved by statics, as is usual in the subject of elasticity. The statical proof consists in taking moments about the point D for the equilibrium of the element shown in fig. 3. The normal forces are left out of the figure ; when these are taken into account it will be found that their contribution to the moment equation is a quantity of smaller order than the contribution of the frictions. The moment equation is therefore

$$(f_{xz}\delta z\, \delta y)\delta x = (f_{zx}\delta x\, \delta y) \times \delta z,$$

from which

$$f_{xz} = f_{zx}. \quad . \quad . \quad . \quad . \quad . \quad . \quad . \quad . \quad (5)$$

This last result, deduced from statics, affords a verification of (3) ; for from (1) we may surely assume that, when w is not zero,

$$f_{xx} = \mu \frac{\partial u}{\partial x} + s_1, \quad . \quad . \quad . \quad . \quad . \quad . \quad (6)$$

where s_1 is something depending on w. From this last equation we get, by interchanging the axes of x and z,

$$f_{xz} = \mu \frac{\partial w}{\partial x} + s_2, \quad . \quad . \quad . \quad . \quad . \quad . \quad (7)$$

where s_2 similarly depends on u.

Since $f_{zx} = f_{xz}$ by (5), the simplest, though not perhaps the only, conclusion from (6) and (7), is that

$$f_{xx} = \mu\left(\frac{\partial u}{\partial z} + \frac{\partial w}{\partial x}\right).$$

All our assumptions, taken together, are completely expressed in the typical equation

$$f_{xy} = f_{yx} = \mu\left(\frac{\partial u}{\partial y} + \frac{\partial v}{\partial x}\right), \quad . \quad . \quad . \quad . \quad (8)$$

where μ is a constant called the coefficient of viscosity.

Fig. 4.

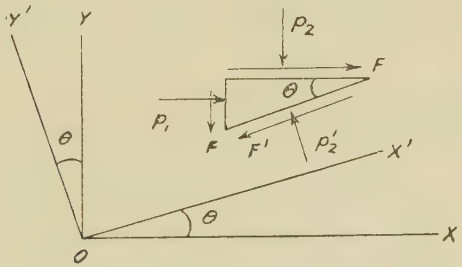

So far we have found no connexion between the normal pressures on the faces and the viscosity. We shall next show that (8) and the two corresponding equations will give us all we seek.

Let p_1, p_2, p_3, be the normal pressures in the liquid at the point x, y, z, in the direction OX, OY, OZ. We shall find that these are, as a rule, unequal in a viscous fluid. It is only in a frictionless fluid that the pressure at a point is the same in every direction.

Let us consider the stresses on faces which are perpendicular to a set of rectangular axes OX', OY', OZ, the axes OX' and OY' making an angle θ with the old axes OX and OY respectively, while OZ is the same in both sets of axes. We shall write F for f_{xy}.

Let p_1', p_2', and $f_{x'y'}$ (for which we shall write F′) be the stresses relative to the new axes which correspond to p_1, p_2, and F relative to the old axes. The pressure p_3 is, of course, the same for both sets of axes. Also let u' and v' be the component velocities relative to the new axes corresponding to u and v relative to the old. For shortness we shall write l and m for $\cos\theta$ and $\sin\theta$.

Now since

$$\frac{\mathrm{F}}{\mu}=\frac{\partial u}{\partial y}+\frac{\partial v}{\partial x},$$

it follows that

$$\frac{\mathrm{F}'}{\mu}=\frac{\partial u'}{\partial y'}+\frac{\partial v'}{\partial x'};$$

but

$$u'=lu+mv, \qquad v'=lv-mu,$$
$$x=lx'-my', \qquad y=ly'+mx',$$

from which

$$\delta u'=\frac{\partial u'}{\partial x}\delta x+\frac{\partial u'}{\partial y}\delta y$$
$$=\frac{\partial u'}{\partial x}(l\delta x'-m\delta y')+\frac{\partial u'}{\partial y}(l\delta y'+m\delta x').$$

Therefore

$$\frac{\partial u'}{\partial y'}=-m\frac{\partial u'}{\partial x}+l\frac{\partial u'}{\partial y}$$
$$=-m\left(l\frac{\partial u}{\partial x}+m\frac{\partial v}{\partial x}\right)+l\left(l\frac{\partial u}{\partial y}+m\frac{\partial v}{\partial y}\right)$$
$$=l^2\frac{\partial u}{\partial y}-m^2\frac{\partial v}{\partial x}+lm\left(\frac{\partial v}{\partial y}-\frac{\partial u}{\partial x}\right). \quad . \quad . \quad . \quad (9)$$

Similarly

$$\frac{\partial v'}{\partial x'}=l^2\frac{\partial v}{\partial x}-m^2\frac{\partial u}{\partial y}+lm\left(\frac{\partial v}{\partial y}-\frac{\partial u}{\partial x}\right). \quad . \quad . \quad (10)$$

Consequently

$$\frac{\mathrm{F}'}{\mu}=(l^2-m^2)\left(\frac{\partial u}{\partial y}+\frac{\partial v}{\partial x}\right)+2lm\left(\frac{\partial v}{\partial y}-\frac{\partial u}{\partial x}\right)$$
$$=(l^2-m^2)\frac{\mathrm{F}}{\mu}+2lm\left(\frac{\partial v}{\partial y}-\frac{\partial u}{\partial x}\right). \quad . \quad . \quad . \quad (11)$$

Again, if A denotes the area of that face of the triangular prism in fig. 4 on which F′ acts, then the areas of the other faces are lA and mA. Consequently, by resolving the forces

which act on the prism in the direction of F′ we get, after division by A,

$$\begin{aligned} F' &= (lF + mp_1)\cos\theta - (mF + lp_2)\sin\theta \\ &= (l^2 - m^2)F + lm(p_1 - p_2). \quad . \quad . \quad . \quad . \quad . \quad (12) \end{aligned}$$

In equations (11) and (12) we have got two expressions for F′ which must be identical for all values of θ, and therefore for all possible values of lm. By equating the coefficients of lm in the two values of F′ we find *

$$p_1 - p_2 = 2\mu\left(\frac{\partial v}{\partial y} - \frac{\partial u}{\partial x}\right), \quad . \quad . \quad . \quad . \quad (13)$$

whence

$$p_1 + 2\mu\frac{\partial u}{\partial x} = p_2 + 2\mu\frac{\partial v}{\partial y}.$$

By rotating the axes about OY instead of about OZ we should have found

$$p_1 + 2\mu\frac{\partial u}{\partial x} = p_3 + 2\mu\frac{\partial w}{\partial z}.$$

Let Q be written for each of the quantities such as $p_1 + 2\mu\frac{\partial u}{\partial x}$, that is,

$$Q = p_1 + 2\mu\frac{\partial u}{\partial x} = p_2 + 2\mu\frac{\partial v}{\partial y} = p_3 + 2\mu\frac{\partial w}{\partial z}; \quad . \quad (14)$$

then

$$3Q = p_1 + p_2 + p_3 + 2\mu\Delta, \quad . \quad . \quad . \quad . \quad (15)$$

where

$$\Delta = \frac{\partial u}{\partial x} + \frac{\partial v}{\partial y} + \frac{\partial w}{\partial z}, \quad . \quad . \quad . \quad . \quad . \quad (16)$$

which can be proved to be the rate at which the density of the fluid at (x, y, z) is decreasing divided by the density at that point—that is, if ρ is the density,

$$\Delta = -\frac{1}{\rho}\frac{d\rho}{dt}. \quad . \quad . \quad . \quad . \quad . \quad . \quad . \quad (17)$$

Next, by resolving the forces on the triangular prism in the direction of p_2', we find

$$\begin{aligned} p_2' &= (lF + mp_1)\sin\theta + (mF + lp_2)\cos\theta \\ &= l^2p_2 + m^2p_1 + 2lmF. \quad . \quad . \quad . \quad . \quad . \quad . \quad (18) \end{aligned}$$

In like manner we could prove that

$$p_1' = l^2p_1 + m^2p_2 - 2lmF \quad . \quad . \quad . \quad . \quad (19)$$

* Or merely by puttin $\theta = 45°$, so that $l = m$, we get the same result.

Therefore

$$p_1' + p_2' = (l^2 + m^2)(p_1 + p_2)$$
$$= p_1 + p_2. \quad . \quad . \quad . \quad . \quad . \quad . \quad . \quad . \quad (20)$$

Consequently, since p_3' is the same as p_3,

$$p_1' + p_2' + p_3' = p_1 + p_2 + p_3. \quad . \quad . \quad . \quad . \quad (21)$$

Now, as we can bring the axes into any possible directions by three successive rotations about three lines, say about OZ, then about OX′, and next about the new axis OY″, and as the relation (21) would persist after each rotation, it is clear that this relation is true for all rectangular axes.

Let us now put

$$3p = p_1 + p_2 + p_3, \quad . \quad . \quad . \quad . \quad . \quad . \quad (22)$$

so that p denotes the arithmetic mean of the normal pressures in three perpendicular directions at the point (x, y, z). Then equation (15) gives

$$Q = p + \tfrac{2}{3}\mu\Delta, \quad . \quad . \quad . \quad . \quad . \quad . \quad . \quad (23)$$

and therefore

$$p_1 = Q - 2\mu\frac{\partial u}{\partial x}$$
$$= p + \tfrac{2}{3}\mu\Delta - 2\mu\frac{\partial u}{\partial x}, \quad . \quad . \quad . \quad . \quad . \quad (24)$$

with similar expressions for the other two component pressures.

Since Δ and p have the same values for all sets of rectangular axes, it should be observed that the same is true also for Q.

The completion of the problem from this point—that is, the derivation of the dynamical equations—is much the same in all books. Since the rest is quite short, we may as well complete the proof here.

Let α_x denote the x-component acceleration of the particle of fluid which is at (x, y, z) at time t. This same particle will be at the point $x + u\delta t$, $y + v\delta t$, $z + w\delta t$, at time $t + \delta t$. If, then,

$$u = F(x, y, z, t), \quad . \quad . \quad . \quad . \quad . \quad . \quad (25)$$

and if Δu is the increase of the velocity of this particular particle in the interval δt, then

$$u + \Delta u = F(x + u\delta t, y + v\delta t, z + w\delta t, t + \delta t)$$
$$= F(x, y, z, t) + u\delta t\frac{\partial u}{\partial x} + v\delta t\frac{\partial u}{\partial y} + w\delta t\frac{\partial u}{\partial z} + \delta t\frac{\partial u}{\partial t}.$$

Consequently

$$\alpha_x = \lim \frac{\Delta u}{\delta t}$$

$$= u\frac{\partial u}{\partial x} + v\frac{\partial u}{\partial y} + w\frac{\partial u}{\partial z} + \frac{\partial u}{\partial t} \quad . \quad . \quad . \quad . \quad (26)$$

Now let us consider the motion of an element of fluid of dimensions $\delta x . \delta y . \delta z$ of density ρ under the action of a force which has components X, Y, Z, per unit mass. Fig. 5 shows all the stresses in the x-direction except the frictions of the type f_{xy}, and these can be inferred from the other pair of frictions shown in the figure.

Fig. 5.

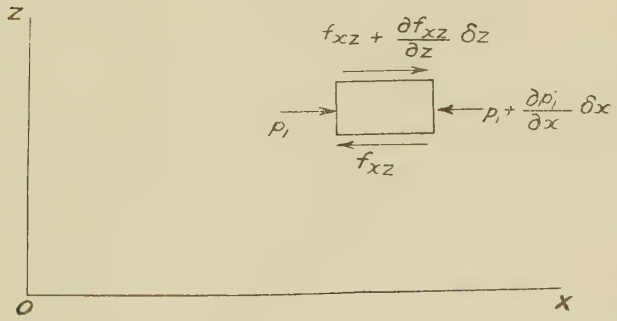

Resolving in the direction OX, we get

$$(\rho\,\delta x\,\delta y\,\delta z)\alpha_x = (\rho\,\delta x\,\delta y\,\delta z)\mathrm{X} + \delta x\,\delta y\left(\frac{\partial f_{xz}}{\partial z}\delta z\right)$$

$$+ \delta x\,\delta z\left(\frac{\partial f_{xy}}{\partial y}\delta y\right) - \delta y\,\delta z\left(\frac{\partial p_1}{\partial x}\delta x\right),$$

from which

$$\rho(\alpha_x - \mathrm{X}) = \frac{\partial f_{zx}}{\partial z} + \frac{\partial f_{xy}}{\partial y} - \frac{\partial p_1}{\partial x} \quad . \quad . \quad . \quad . \quad (27)$$

The substitution of the values of the stresses from equations (8) and (24) in this last equation gives

$$\frac{\partial p_1}{\partial x} - \mu\left(\nabla^2 u + \frac{1}{3}\frac{\partial \Delta}{\partial x}\right) = -\rho(\alpha_x - \mathrm{X}). \quad . \quad . \quad (28)$$

Two similar equations are got by resolving in the directions of the other two axes. These three are the equations of viscous flow of a fluid.

College of Technology,
Manchester.

LIII. *The Effect of Surface Changes on the Photoelectric Emission of Silver and Gold.* *By* T. E. Clarke, *B.Sc., University College, Nottingham* *.

A GREAT deal of work has been done on the effect of "outgassing" on the photoelectric properties of various metals ; something has also been done on the effect on the photoelectric emission caused by alterations in the physical state of the metal. Yet no attention appears to have been paid to the possibility that the observed effects may be due to the two causes acting jointly.

The present work was undertaken to investigate the changes in photoelectric emission, produced by alternately straining and annealing a metal ; and to determine how far the observed changes were due to physical change of the metal itself and how far to changes in the adsorbed gas layer on the metal surface. We use the word strain to indicate the state of the metal surface after being mechanically polished by rubbing with a polished steel surface.

Beilby † has shown that a thin ($50\,\mu$–$500\,\mu$) modified layer (vitreous layer) can be produced on the surface of an annealed metal by polishing, and that this layer returns to the original state on heating to a certain temperature. This fact has been used ‡ to explain an increase in photoelectric sensitivity observed on polishing a metal in air at a pressure of 10^{-3} mm. Hg.

The Photoelectric Cell.

This consists of a cylindrical glass vessel, A, about a foot long, closed at one end by a glass disk having an optically worked quartz window, C, at its centre, and at the other end by a glass-stopper-like arrangement, B, which is made to fit into A by means of a large vacuum-tight ground-joint. The glass disk and window C are attached by means of hard wax seals. The part B carries two stout copper leads which pass out through two copper-glass joints H, O, and support across their inner extremities (*i. e.*, the ends projecting into the main part A) the thin metal strip P constituting the cathode. This strip is screwed down to the ends of the two leads by means of small screws tapped axially into them, and is held taut by a spring, J, fixed

* Communicated by Prof. P. E. Shaw, M.A., D.Sc.

† 'Aggregation and Flow of Solids'

‡ R. F. Hanstock, Phil. Mag. x. p. 937 (Nov. 1930).

between the two leads and insulated from one of them by a glass sleeve. The anode consists of a shallow copper cylinder, G, supported rigidly in the centre of the cell on a stout copper rod which passes out of the cell through a copper-glass joint on the side-tube, D. A large copper cylinder, F, completely screens the anode G except near the cathode P, where a circular aperture in the screen admits the electrons from the cathode. The lead from the screen F passes through the side-tube and copper-glass joint E. Parallel slits cut in the ends of the two cylinders F and G serve to define a narrow beam of the ultra-violet light which enters through the quartz window. A constant beam is incident on the cathode strip, since constant parallelism of the slits is ensured by fixing the outer cylinder F firmly by means of phosphor-bronze spring-clips. The firmness of the inner cylinder G is maintained by its stout supporting rod. The leakage path from the cathode to the anode is very large, and is further increased by the glass sleeve K projecting into the cell from the ground-joint. The dotted circle round the cathode strip in fig. 1 *a* indicates another side-tube M of wider diameter which enters the main tube perpendicular to the plane of fig. 1 *a*, carrying the polishing lever N. This section of the cell is shown in plan in fig. 1 *b*.

By means of a large copper-glass joint a flexible metal tube, I, of the type used for "vacuum levers"* is fitted as an extension to the side-tube as shown in fig. 1 *b*. A thick steel rod N (4 mm. diam.) passes through into the cell, the outer end being soldered to the outer end of the flexible tube and the inner end, which is highly polished, resting on the cathode strip. Thus, by up and down movements of the flexible tube the polished steel end can be moved to and fro over the strip, at the same time sufficient pressure being exerted to produce a polish. In this manner the metal is polished *in vacuo* without any scratching or tearing of the surface and without introducing any complicated and troublesome mechanism.

Experimental Arrangement.

The tube L is connected to the pumping system and vapour-trap, and to a McLeod gauge. The pump used is a Gaede two-stage steel diffusion-pump backed by a "Hyvac," and the pumping speed is 2500 c.c. per sec. with a backing pressure of only 2 mm. : thus it may be expected to deal

* Brose and Keyston, Journ. Sci. Instr. i. p. 19 (1930).

effectively with any vapours given off within the system. The outer half of the ground-joint is greased with Leybold's stiff "Ramsayfett."

The anode lead is carried directly through a short, wide, brass tube, which is earthed, to a quadrant electrometer situated close to the cell. The capacity of the system is thus kept at a small value, so that the rate of deflexion for a given current is as large as possible. The "time of

Fig. 1 *a*.

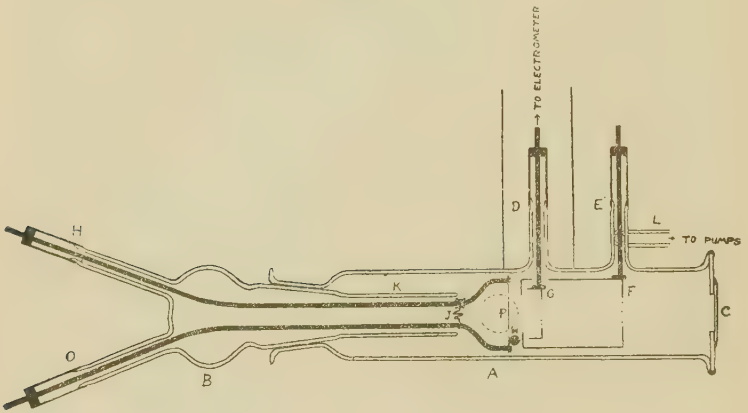

Fig. 1 *b*.

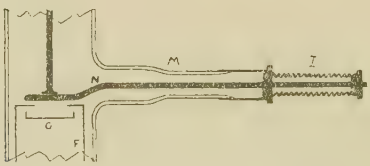

deflexion" method was used in measuring the photoelectric current, the cathode P being maintained at a negative potential, and the screen F at a smaller negative potential, so that the emitted electrons are collected on G and so charge up the electrometer.

A quartz mercury-vapour-lamp in an earthed metal housing is used as the source of U.V. radiation, the full radiation being used. It is found necessary to connect a variable resistance in series with the lamp, so that slight changes occurring in the electricity supply can be compensated for. The ends of the cathode strip are

connected by way of the copper-glass joints to a battery of large storage cells which provide the 25 amps. or so necessary to raise the strips of silver and gold to red heat.

Procedure and Results.

Since the specimen had of necessity to be illuminated for a short time at intervals during the course of an

Fig. 2.

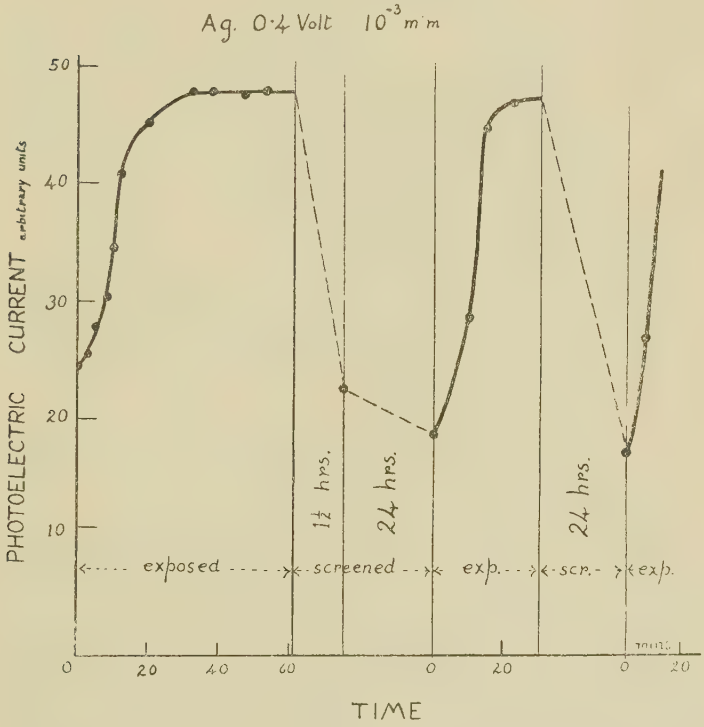

experiment, for the purpose of measuring the emission, the possibility of the occurrence of so-called "fatigue" effects was not overlooked. Accordingly a preliminary series of experiments was undertaken to investigate how the photoelectric emission for silver and gold was influenced by continued exposure to ultra-violet light.

The variation of current with time of exposure was observed (1) when the current was saturated (−30 volts on cathode), and (2) when there was practically no accelerating potential (−0·4 volts on cathode). In the second

case, *i. e.*, for unaccelerated emission, at a pressure of 10^{-3} mm., the current increased rapidly at first, and reached a maximum, which was twice the initial value, in about 40 minutes. On screening the source of light the emission gradually resumed its original value in about 90 minutes. At a pressure of 10^{-6} mm. Hg. no such increase occurred, and at both pressures the saturated current showed no appreciable change on continued exposure of the metal to ultra-violet light.

At this point it is worthy of note that, in the case of unaccelerated emission at a pressure of 10^{-3} mm., the first "recovery" value of the current was appreciably lower than the initial value, and after a second exposure and rest the second "recovery" value was lower than the first but to a less marked degree : this is seen from fig. 2. It thus appears that, although there is a negative "fatigue" while the metal is exposed, there is also a small resultant positive "fatigue."

It was concluded that the "fatigue" observed at relatively high pressure was due in some way to the presence of adsorbed gas, and that the adsorbed gas still present at 10^{-6} mm. was inoperative in producing "fatigue." This eliminates one possible cause of change in sensitivity in the next series of observations.

We now go on to the investigation of the effect of heat treatment and subsequent polishing, and to the separation of the effect due to physical change in the metal from secondary effects due to adsorbed gas.

The metal strip cathode was highly polished by means of fine emery cloth, pumice powder, and opticians' rouge, thoroughly washed in benzene, and then placed in the apparatus. The latter was quickly exhausted and heated, together with connecting tubing etc., until the pump maintained a constant pressure of the order of 10^{-6} mm. Hg. Now the work of Werner* shows that when the pressure is maintained at a low value there is an increase in emission up to a constant value, consistent with the assumption that the adsorbed gas layer is gradually diminished in thickness to a limiting value. Accordingly the pumps were allowed to run for several hours under constant conditions before any readings were taken. Current measurements taken at intervals during this time of standing confirmed Werner's results, showing a regular increase with time up to a constant value. It was thus reasonable to assume that,

* J. Werner, *Zeit. für. Phys.* lxvii. p. 211 (1931).

after a sufficient time of standing under the same vacuum conditions, a residual gas layer existed in a state of equilibrium at the surface of the metal. Having reached a stable state in which the photoelectric emission remained constant, the problem then was to investigate the effect of annealing the metal, assuming it to be originally in the polished or strained state. The cathode was heated to the point of redness for four minutes, after which the heating current was slowly decreased to zero. During this heating a positive restraining potential of 30 volts was applied to the strip to prevent any thermionic emission. Measurements of the photoelectric current were taken at intervals from the time at which the heating current was switched off, and the time at which each measurement was taken was noted. When the variation with time became small the apparatus was left for a period of 20 hours, the pressure being 10^{-3} mm., after which the pressure was again reduced to 10^{-6} mm. and the same conditions as at the beginning were maintained for an hour. After this time the readings had become constant. The annealed strip was then polished *in vacuo*, the emission being measured at intervals during the process, and was finally allowed to stand under exactly the same conditions as before. The emission again assumed a constant value.

Explanation of Curves.

Fig. 3 is a graphical representation of the complete cycle for silver. The part AB represents the constant emission for the polished metal under equilibrium conditions (stable adsorbed gas layer at 10^{-6} mm.). Heating the strip produces a sudden increase in emission to the value at C. This may be the resultant effect due to a change in the metal and also in the adsorbed gas layer. The effect of standing with the pressure at 10^{-6} mm. is shown by the fall from C to D, which is attributed to a return of gas to the surface of the silver. After 20 hours standing at 10^{-3} mm. and subsequent evacuation at 10^{-6} mm. for an hour a constant value, represented by DE, is attained. Now, since the vacuum conditions leading up to the point A have been repeated before the point D of the cycle, it is reasonable to assume that the stable adsorbed gas layer is the same at both points: this assumption is justified by subsequent results. Then the difference between the ordinates of AB and DE must be entirely due to a change in the primary emission, *i. e.*, to a change in

the metal itself due to annealing. The ordinate of AB represents the emission for the polished metal and that of DE the emission for the annealed metal.

The part EF of the curve shows the effect of re-polishing *in vacuo* and indicates a roughly linear increase in emission with time of polishing, up to a maximum at F. Now, after standing to allow complete re-formation of the disturbed gas layer, a constant value is again reached at G, and the fact that the value of emission at G is approximately the

Fig. 3.

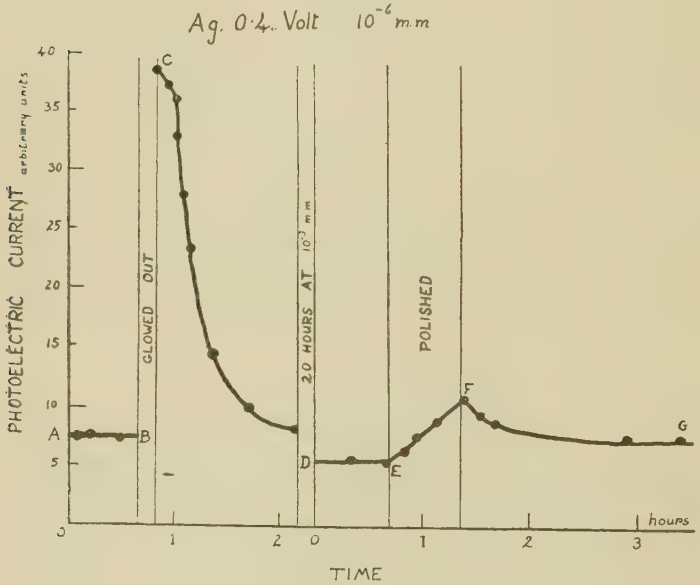

same as that for the polished metal at A shows that the conditions prevailing at A have been repeated at G. This strengthens our assumption that the surface gas always returns to the same extent, under the same pressure conditions, provided that sufficient time is allowed for a state of equilibrium to be established.

The second peak, F, in the curve, brought about by re-polishing, is also explained in the same way as that due to heating, *i.e.*, it is due both to a change in state of the metal itself and to a removal of gas from the surface by the polishing process. In standing this gas ultimately returns to its former stable condition.

Fig. 4 represents a similar cycle for gold. This shows the same characteristics as the curve for silver, although in this case the re-polishing has not quite brought the emission up to the initial value for polished gold. There is, however, quite a definite change in the emission accompanying the change from the annealed to the polished state. The slight discrepancy is probably due to the fact that the same degree of polish as that existing initially, was not quite obtained by means of the polished steel cylinder. This is borne out by the fact that subsequent annealing and polishing *in vacuo* produced repetition of the lower value.

Fig. 4.

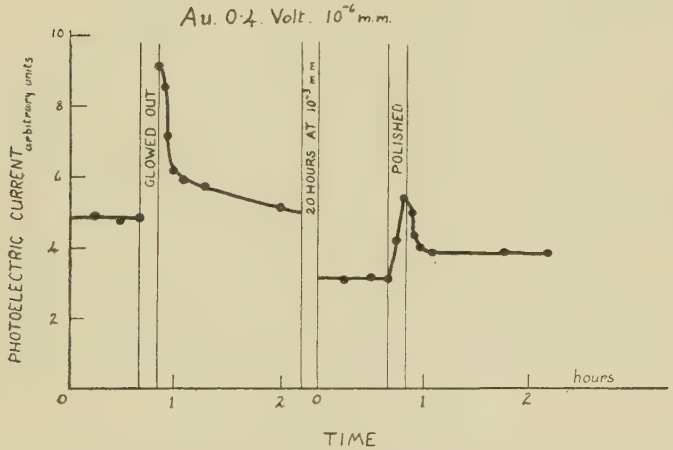

Saturation Current Experiments.

Observations have also been made on the saturation current, the procedure being the same as for the unaccelerated emission. The results show no effects similar to those described above, which may be attributed to changes in the adsorbed gas layer, but there is a marked increase in sensitivity on polishing and a decrease of the same magnitude on annealing.

Conclusion.

It is apparent from this work that the photoelectric emission of a metal, in the absence of a strong accelerating field, can be used as an indicator of changes occurring in the adsorbed gas layer on the surface of the metal.

The probable explanation is that, since under these conditions the emitted electrons will have energies ranging from a very small value up to a maximum, a change in depth of the adsorbed gas layer will produce a corresponding change in the proportion of slower electrons restrained by the layer. Such a change will have very little effect on the saturated emission, owing to the higher energy of the electrons. The saturation current is, in fact, only affected by an alteration in the true contact potential (and therefore in the long wave limit) : since no "gas" effects occur in the saturation current experiments, it is apparent that the removal of adsorbed gas in the manner described has no effect on the contact potential, while the polishing and annealing processes alter it to a definite extent which can be repeated.

An investigation of the behaviour of the long wave limit under the above conditions is desirable, and it is intended to carry on the work in this direction for a series of metals.

In conclusion, I wish to express my thanks to Professor P. E. Shaw for facilities provided for this work and for valuable advice during the course of the experiments.

LIV. *Some Properties of Porous Building Materials.*—Part III. *A Theory of the Absorption and Transmission of Water by Porous Bodies.* *By* E. Madgwick, *M.C., M.Sc., Ph.D.**

Introduction.

THIS section is concerned with an elucidation of the laws governing the flow of water in porous bodies under certain conditions, and the expression of those laws in terms of definite physical constants which can be determined experimentally. The flow is always considered to take place from a plane surface of the material, initially dry, and to proceed in a direction normal to the surface. It may occur under the action of capillary or applied forces, or both. Capillary forces are always operative when absorption is proceeding ; transmission is due solely to applied forces. Three cases of practical importance will be considered :—

(*a*) Entering surface horizontal, the direction of flow being vertically downwards. Absorption is assisted

* Communicated by Sir F. E. Smith, K.C.B , C.B.E., Sec.R.S.

by a head of water equal to the depth of penetration added to the pressure (if any) which is applied at the surface; when the water flows through the material the capillary forces are no longer effective.

(*b*) Absorption from a horizontal surface, the flow being vertically upwards. The absorption is retarded by a head of water equal to the height of penetration, and proceeds until the opposing forces are equal.

(*c*) Absorption from a vertical surface, the flow being horizontal. If the surface in question is that of a wall the absorption is generally due to capillarity only, but may be assisted to some slight extent by wind pressure; if it forms the side of a tank filled with water the pressure arising from the head of water will also be of consequence.

The porosity has been defined as the volume of water which is absorbed by unit volume of the material under the experimental conditions to be described. Although experiments on some specimens are completed within the short space of an hour, it has been found that very little further absorption takes place over a much longer period; and it is probable that the amount of water which is absorbed under these conditions approximates closely to that which is absorbed in the course of the slow immersion test of Hirschwald or the four days' immersion test of Kreüger.

The Fundamental Equation.

In deriving the fundamental equation we shall take the case of vertically downward flow. Let the pressure at the surface of the material be gh, i. e., that due to a head of h centimetres of water, and consider the conditions for equilibrium at the moment the depth of penetration is x. The applied pressure is then $gh+gx$. For unit area of cross-section of the material let α be the total area of cross-section of the pores normal to the direction of flow, and β the sum of their perimeters. Then the force due to the applied pressure is $(gh+gx)\alpha$ per unit area, and that due to capillarity is $\beta \mathrm{T}\cos\theta$, where T is the surface tension and θ the angle of contact. Thus the force assisting the motion is

$$(gh+gx)\alpha+\beta \mathrm{T}\cos\theta \text{ per unit area.}$$

Assume that the resistance to flow is proportional to the

average velocity—which is proportional to the rate of penetration $\frac{dx}{dt}$. It will be proportional also to the average length of the path of the water within the material, and this is proportional to the depth of penetration x. The force resisting the motion is then $C'x\frac{dx}{dt}$, where C' is a constant for the material, and the total force per unit area is

$$(gh+gx)\alpha+\beta T\cos\theta-C'.x\frac{dx}{dt}.$$

This is equal to the rate of change of momentum of the water contained within a prism of the material of unit cross-section and height x. Let the porosity be B. The mass of this water is Bx and its average velocity is $k\frac{dx}{dt}$, where k is a constant; hence the rate of change of momentum is

$$\frac{d}{dt}\left(Bkx\frac{dx}{dt}\right).$$

Thus

$$gh+gx+\frac{\beta T\cos\theta}{\alpha}-\frac{C'}{\alpha}.x\frac{dx}{dt}=\frac{Bk}{\alpha}.\frac{d}{dt}\left(x\frac{dx}{dt}\right).$$

$\frac{\beta T\cos\theta}{\alpha}$ can be written gh', i. e., capillarity is in effect equivalent to a head h' of water. Hence, writing also $\frac{C'}{\alpha}=C$,

$$gh+gx+gh'-cx\frac{dx}{dt}=\frac{Bk}{\alpha}.\frac{d}{dt}\left(x\frac{dx}{dt}\right).$$

The term on the right-hand side of this equation can be neglected if it is small in comparison with $gh+gx+gh'$. To get some idea of the order of magnitude of h' the arrangement shown in the accompanying figure was used. The specimen was fixed to a brass cap of the type which is employed for the air permeability and water absorption tests, and the space enclosed by the specimen and the cap, together with the tube A B C, was filled with water. After the lapse of a few minutes the end C of the tube was allowed to dip into mercury, so that as water was absorbed by the specimen mercury was drawn up the tube to a height which remained steady for some time. It was found that the absorption of water was then accompanied by the withdrawal of air, a result which is to be

anticipated from the following considerations. In consequence of the rise of mercury in the vertical tube there is applied to the stone a definite negative pressure which opposes the flow. If all the pores were similar this pressure would increase until it just balanced the capillary forces, and would give a direct measure of h'. But since the pores vary in size and shape, a state of affairs is reached such that the capillary forces in the finer pores are sufficient, but those in the larger pores insufficient, to overcome the opposing pressure. Thus the value of the pressure which is measured in this way is a property of the largest pores and is less than the average value gh' as defined above. Expressed in centimetres of water it is always large compared with unity and

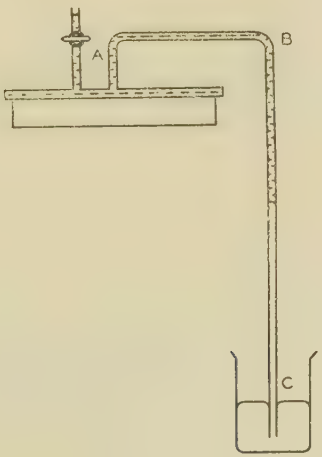

often equal to several hundreds. Thus gh' is great compared with 1000. Now $\frac{B}{\alpha}$ and k are greater than unity, but of that order of magnitude ; they each, in fact, represent the ratio of the length of the average tortuous path followed by the water to that of the shortest possible path. It only remains to show that $\frac{d}{dt}\left(x\frac{dx}{dt}\right)$ is small. This is estimated roughly as follows. In the absorption experiments to be described the total quantity of water absorbed at any time may readily be obtained from the curves; then, from a knowledge of the porosity, the distance penetrated at that time may be calculated. It is found that the results are well

represented by the equation $t = mx^n$, where m and n are constants, m of the order some hundreds and n in the region of 2. This equation gives, by successive differentiation,

$$\frac{d}{dt}\left(x\frac{dx}{dt}\right) = (2-n)\Big/ n^2 m^{\frac{2}{n}} t^{2-\frac{2}{n}}, \text{ or } (2-n)/n^2 m^2 x,$$

which is seen to be extremely minute compared with 1000 for any appreciable value of t or x and for permissible values of m and n. Leaving out the term in question, the equation of motion becomes simply

$$gh + gx + gh' = cx\frac{dx}{dt}. \quad . \quad . \quad . \quad . \quad (10)$$

The Capillary Pressure.

h' will be termed the *capillary head* and gh' the *capillary pressure*. The term $gh + gx + gh'$ represents the total pressure, capillary plus applied. Calling this p, we may write equation (10)

$$p = cx\frac{dx}{dt}. \quad . \quad . \quad . \quad . \quad . \quad . \quad (11)$$

Regarding the factor $\frac{dx}{dt}$ generally as the rate of movement of the water normally to the entering surface, which may vary, as in the case of absorption, or be constant, as in the case of transmission, it is clear that equation (11) applies equally to the three cases of downward, upward, and horizontal flow for both absorption and transmission. Whenever absorption is proceeding the value of the capillary pressure is included in the term p; for all cases of transmission gh' is zero.

The Permeability.

Let q be the rate of absorption or transmission in cubic centimetres per second per square centimetre of material. Then

$$q = \mathrm{B}\frac{dx}{dt}, \quad \text{or} \quad \frac{dx}{dt} = \frac{q}{\mathrm{B}},$$

and substituting in equation (11),

$$q = \underset{c\ x}{\mathrm{B}\,p} = \underset{x}{\mathrm{P}\,p}. \quad . \quad . \quad . \quad . \quad . \quad (12)$$

writing $P = \frac{B}{\rho}$; or, if Q is the rate of absorption or transmission over an area A,

$$Q = A.P.\frac{p}{x} \quad . \quad . \quad . \quad . \quad . \quad . \quad . \quad (13)$$

The constant P represents the rate of flow through unit area of the material of unit thickness under the action of unit pressure, and is termed the *permeability*. (In these definitions a definite temperature is implied, since the surface tension and viscosity vary with temperature.)

The Resistivity.

Equation (13) is similar to that representing the corresponding case of the steady flow of heat or electricity, and, by analogy, P might be called the conductivity. $\frac{1}{P} = \sigma$ will be referred to as the *resistivity*. Equation (13) may thus be written

$$Q = \frac{Ap}{\sigma x} \quad . \quad . \quad . \quad . \quad . \quad . \quad . \quad (14)$$

The Absorptivity.

A case of considerable practical importance is that in which absorption occurs under the action of capillarity only—that is, in which the value of p is gh'. Inserting this value in equation (13), we have

$$Q = A.P.\frac{gh'}{x},$$

and when $A = 1$ and $x = 1$,

$$q = Pgh',$$

which gives the rate of absorption per square centimetre of surface under the action of capillarity only at the moment when the depth of penetration is 1 centimetre. This will be termed the *absorptivity*, Z. Thus

$$Z = Pgh', \quad . \quad . \quad . \quad . \quad . \quad . \quad . \quad (15)$$

and the rate of absorption in the absence of any applied pressure is given simply by

$$Q = \frac{AZ}{x} \quad . \quad . \quad . \quad . \quad . \quad . \quad . \quad (16)$$

The Rate of Penetration.

The time which is taken for the water to penetrate to a given distance can be calculated from equation (11).

(a) *Vertically Downward Flow.*—In the case of vertically downward flow we have

$$p = gh + gx + gh' = g\mathrm{H} + gx,$$

writing $\mathrm{H} = h + h'$, the sum of the pressure in centimetres of water at the entering surface and the capillary head. Hence, remembering that $c = \mathrm{B}\sigma$,

$$\mathrm{H} + x = \frac{\mathrm{B}\sigma}{g} . x . \frac{dx}{dt}, \quad . \quad . \quad . \quad . \quad . \quad (17)$$

whence

$$t = \frac{\mathrm{B}\sigma}{g} \left\{ x - \mathrm{H} \log \left(1 + \frac{x}{\mathrm{H}} \right) \right\} . \quad . \quad . \quad (18)$$

By expanding the logarithmic term this is converted into the form

$$t = \frac{\mathrm{B}\sigma}{2g\mathrm{H}} . x^2 \left\{ 1 - \frac{2}{3} \frac{x}{\mathrm{H}} + \frac{2}{4} . \frac{x^2}{\mathrm{H}^2} \cdots \right\}$$

$$= \mathrm{D} . \frac{h'}{\mathrm{H}} . \frac{1}{x^2} \left\{ 1 - \frac{2}{3} \frac{x}{\mathrm{H}} + \frac{2}{4} . \frac{x^2}{\mathrm{H}^2} \cdots \right\}, \quad . \quad (19)$$

where $$\mathrm{D} = \frac{\mathrm{B}\sigma}{2gh'}.$$

When x is small compared with H equation (19) simplifies to

$$t = \mathrm{D} . \frac{h'}{\mathrm{H}} x^2. \quad . \quad . \quad . \quad . \quad . \quad . \quad . \quad (20)$$

and when $h = 0$ it further reduces to

$$t = \mathrm{D}x^2. \quad . \quad . \quad . \quad . \quad . \quad . \quad . \quad . \quad (21)$$

(*b*) *Vertically Upward Flow.*—Vertically upward flow is generally due solely to capillarity, i. e., $h = 0$ and $\mathrm{H} = h'$. Also, the head of water inside the material acts against the capillary forces and $p = gh' - gx$. Hence (*cf.* equation (17))

$$h' - x = \frac{\mathrm{B}\sigma}{g} . x . \frac{dx}{dt}$$

and

$$t = - \frac{\mathrm{B}\sigma}{g} \left\{ x + h' \log \left(1 - \frac{x}{h'} \right) \right\}, \quad . \quad . \quad (22)$$

or, by expanding the logarithmic term,

$$t = \mathrm{D}.x^2 \left\{ 1 + \frac{2}{3}\frac{x}{h'} + \frac{2}{4}\frac{x^2}{h'^2} \cdots \right\}, \quad . \quad . \quad . \quad (23)$$

which also simplifies to equation (21) when x is small in comparison with h'.

(c) *Horizontal Flow.*—For horizontal flow

$$p = gh + gh' = g\mathrm{H}$$

and (*cf.* equation (17))

$$\mathrm{H} = \frac{\mathrm{B}\sigma}{g} x \frac{dx}{dt};$$

whence

$$t = \frac{\mathrm{B}\sigma}{2g\mathrm{H}} x^2 = \mathrm{D}\frac{h'}{\mathrm{H}} x^2, \quad . \quad . \quad . \quad . \quad . \quad (24)$$

and when $h = 0$,

$$t = \mathrm{D}x^2. \quad . \quad . \quad . \quad . \quad . \quad . \quad . \quad . \quad . \quad . \quad (25)$$

D may be termed the *penetration constant*. It is equal to the time taken for the water to penetrate to unit distance under the action of capillarity only. Under these conditions, which are very common in practice, a simple expression emerges for the rate of absorption at any given time; for, from equations (25) and (16),

$$\mathrm{Q} = \mathrm{AZ}\sqrt{\frac{\mathrm{D}}{t}}. \quad . \quad . \quad . \quad . \quad (26)$$

Different Materials in Contact.

We now proceed to examine the flow of water into and through a series of slabs of different materials in intimate contact with one another.

(1) *Absorption and Transmission.*

Let p = the total pressure across the slabs,
$p_1, p_2 \ldots$ = the pressures across slabs 1, 2, ...,
$l_1, l_2 \ldots$ = their thicknesses,
$\sigma_1, \sigma_2 \ldots$ = their resistivities.

We have the conditions that the total pressure is the sum of the pressures across the separate slabs, and that q at any moment is constant throughout. Therefore

$$\begin{aligned} p &= p_1 + p_2 + \ldots \\ &= \sigma_1 l_1 q + \sigma_2 l_2 q \ldots \quad \text{by equation (14)} \\ &= q\Sigma\sigma l, \end{aligned}$$

and $$q = \frac{p}{\Sigma\sigma l},$$

or $$Q = A\frac{p}{\Sigma\sigma l}, \quad . \quad . \quad . \quad . \quad . \quad . \quad . \quad . \quad (27)$$

in further conformity with the thermal and electrical analogies. This equation applies equally to absorption or transmission in the same manner as equation (14). For absorption it is merely necessary to include in p the capillary pressure of the medium into which the water is penetrating.

(2) *Penetration.*

In investigating the rates of penetration into the successive slabs, we consider each separately and determine the time the water takes to penetrate to a given distance from the moment it enters.

(a) *Vertically Downward Flow.*—Let h' represent the capillary head in the nth medium. When the water has penetrated to a distance x in that medium,

$$q = \frac{p}{\sigma_1 l_1 + \sigma_2 l_2 + \ldots + \sigma_n x} \quad \text{by equation (27),}$$

and

$$p = g(h + l_1 + l_2 + \ldots + l_{n-1}) + gx + gh'$$
$$= g\mathrm{H} + gx,$$

writing H = the sum of the applied head at the surface of the medium under consideration and the capillary head of that medium. Then

$$q = \frac{g\mathrm{H} + gx}{\sum_1^{n-1} \sigma l + \sigma_n x};$$

also,

$$q = \mathrm{B}_n \cdot \frac{dx}{dt},$$

where B_n is the porosity of the nth medium. Thus

$$\mathrm{B}_n \frac{dx}{dt} = \frac{g\mathrm{H} + gx}{\sum_1^{n-1} \sigma l + \sigma_n x},$$

whence

$$t = \frac{\mathrm{B}_n\left(\sum_1^{n-1} \sigma l - \sigma_n \mathrm{H}\right)}{g} \log\left(1 + \frac{x}{\mathrm{H}}\right) + \frac{\mathrm{B}_n \sigma_n}{g} \cdot x. \quad (28)$$

(b) *Vertically Upward Flow.*—For upward flow we have, similarly,

$$B_n \cdot \frac{dx}{dt} = gh' - g(l_1 + l_2 + \ldots + l_{n-1}) - gx$$

$$= \frac{gH - gx}{\sum_1^{n-1} \sigma l + \sigma_n x},$$

whence

$$t = -\frac{B_n\left(\sum_1^{n-1} \sigma l + \sigma_n H\right)}{g} \log\left(1 - \frac{x}{H}\right) - \frac{B_n \sigma_n x}{g}. \quad (29)$$

(c) *Horizontal Flow.*—When the flow is horizontal we have simply

$$B_n \frac{dx}{dt} = \frac{gh + gh'}{\sum_1^{n-1} \sigma l + \sigma_n x} = \frac{gH}{\sum_1^{n-1} \sigma l + \sigma_n x},$$

which gives

$$t = \frac{B_n \sum_1^{n-1} \sigma l}{Hg} \cdot x \frac{B_n \sigma_n}{2Hg} \cdot x^2. \quad . \quad . \quad . \quad . \quad . \quad (30)$$

When x is small in comparison with H, equations (28) and (29) approximate to (30).

The constants h', p, σ, Z, D, and B will be referred to as the absorption constants. It will be observed that only three of them (h', σ, and D, for example) are independent; and, if the theory holds, these are sufficient to predict the circumstances of the flow of water under the conditions which have been described.

LV. *Some Properties of Porous Building Materials.*—Part IV. *The Determination of the Absorption Constants of a Homogeneous Specimen.* *By* E. Madgwick, *M.C., M.Sc., Ph.D.* *

The Experimental Method.

THE specimen which has been used in the air permeability test (Part II.) is already prepared for the water absorption test. The holders were designed primarily in this

* Communicated by Sir F. E. Smith, K.C.B., C.B.E., Sec.R.S.

connexion, and are shown in fig. 1. Before the specimen is placed between them they are heated to a temperature just above the melting-point of Faraday wax, a little of which is applied around the edges to render the joints air-

Fig. 1.

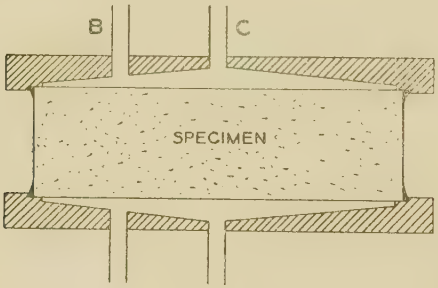

Fig. 2.

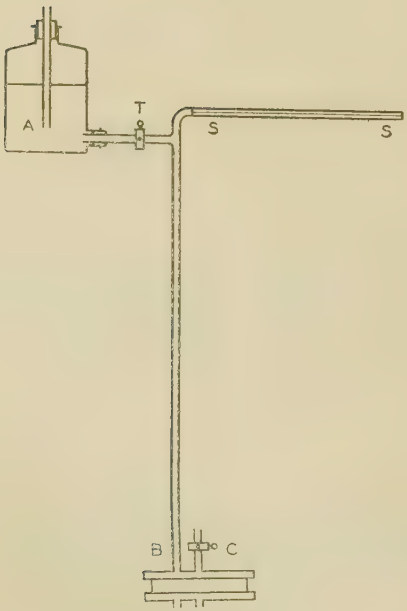

and water-tight. If the test is to be carried out at a pressure greater than about 50 cm. of water, the holders are clamped together while the wax is still soft.

The specimen so prepared is connected to the apparatus shown in fig. 2. A is an aspirator containing water, T a

glass tap, SS a capillary tube in front of a millimetre scale. To fill the space above the specimen the tap T is turned on while the tube C is left open, so that as water enters at B the air is driven out through C (see also fig. 1). When the space is completely filled with water C is closed, and the vertical tube and the capillary tube are also filled. The tap T is now closed, and the meniscus in the capillary tube moves along the scale as absorption proceeds. By observing the time taken to move through any distance the rate of absorption or transmission can be calculated from a knowledge of the bore of the capillary tube. The sensitivity of the apparatus can be altered by using capillary tubes of different bores. These are carefully selected so as to show no appreciable variation in cross-section throughout their lengths. At the beginning of an experiment it is usual to work with a movement of 50 cm., which may be reduced to as little as 2 cm. towards the end. The vertical glass tube is readily detachable in order that the head of water may be adjusted.

The time is noted the moment the specimen is wetted, and the rate of absorption is measured as soon as possible afterwards. Immediately one reading is finished another is commenced, the process being repeated until the rate of flow attains a constant value. The rate q at which water enters each square centimetre of the specimen, or the rate Q at which it enters the whole specimen of area A, is plotted against the time t.

The Theoretical Absorption Curve.

While absorption is proceeding the value of the pressure p is $g(h'+h+x)$, where h' is the capillary head, h the head of water at the entering surface, and x the depth of penetration. A convenient value of h is 50 cm.; h' is rarely less than 100 cm., and is sometimes greater than 1000 cm. The thickness of the specimen is generally between 1 and 4 cm. Thus p is nearly constant and approximately equal to $g\mathrm{H}$ where $\mathrm{H}=h'+h$. Then we have from equation (14)

$$x=\frac{\mathrm{A}g\mathrm{H}}{\sigma\mathrm{Q}},$$

and from equation (20)

$$t=\frac{\mathrm{B}\sigma}{2g\mathrm{H}}.x^2.$$

These give for the equation to the absorption curve in the case of a thin specimen

$$t = \frac{K_1}{Q_2}, \quad . \quad . \quad . \quad . \quad . \quad . \quad . \quad (31)$$

where

$$K_1 = \frac{BA^2 g H}{2\sigma} . \quad . \quad . \quad . \quad . \quad . \quad (32)$$

Assuming the water front to be perfectly uniform, absorption should proceed according to equation (31) until the under face of the specimen is reached and transmission commences. At that moment the capillary forces cease to operate and the value of the pressure p falls from $g(h'+h+l)$ to $g(h+l)$.

By equation (13) this results in a drop in the rate of flow from

$$Q_0 = \frac{APg(h'+h+l)}{l}, \quad . \quad . \quad . \quad . \quad (33)$$

representing the rate of absorption for a depth of penetration equal to the thickness of the specimen, to

$$Q_1 = \frac{APg(h+l)}{l}, \quad . \quad . \quad . \quad . \quad (34)$$

representing the steady rate of transmission. Further, this occurs at time

$$t_0 = D \cdot \frac{h'}{H} \cdot \left(1 - \frac{2}{3} \cdot \frac{l}{H} \cdots\right) l^2 \quad . \quad . \quad . \quad (35)$$

by equation (19).

The Experimental Absorption Curve.

Many tests have been carried out on natural stones, bricks, and plasters. A set of typical results for a specimen of Box Ground stone are plotted in fig. 3, which depicts the three characteristic features of absorption, the transition between absorption and transmission and steady transmission.

Box Ground is a stone of unusual homogeneity, in which absorption takes place in excellent agreement with equation (31). Generally there are between the theoretical and experimental absorption curves slight divergences which may either be random in character or, in the cases of certain materials, tend to conform to type. A number of causes may contribute to such divergences. All the materials with which we are concerned are unhomogeneous to some extent. Specimens have been examined in this connexion by allowing

them to absorb a staining solution of potassium permanganate and breaking them across after a suitable penetration had taken place. The advancing surface of the liquid is always characterized by irregularities, which in most cases are fairly uniform with regard to magnitude and distribution, but occasionally are so marked as to indicate definite discontinuities in the rates of penetration. Progressive

Fig. 3.

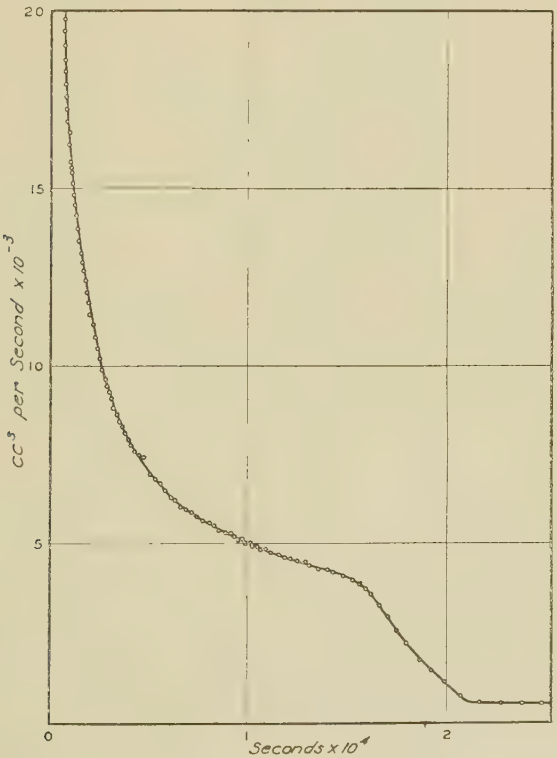

variations in the properties of such artificial test pieces as plasters are to be anticipated from the manner of their preparation. An edge effect is also present, the absorption being retarded somewhat in the vicinity of the waxed sides of the specimen. This, however, can be reduced to negligible proportions by using specimens sufficiently wide in proportion to their thickness. Corresponding to thicknesses of 1 and 2 inches, widths of 8 and 12 inches

respectively are adequate. In consequence of the drying out of a specimen there may be present at the surface a "skin" of appreciable resistance, which is not necessarily constant throughout the course of a test. To isolate any such effect would require sufficient experimental data for each material to eliminate the random consequences of unhomogeneity. Moreover, tests on different specimens of the same material reveal such variations in properties as to render a refinement of this sort unnecessary within the scope of our present investigation. In other connexions the skin effect is of considerable importance and will be examined in the next section.

The average depth of penetration may be defined as the depth to which the absorbed water would have reached had the penetration been uniform. Also, the total amount of water which has been absorbed at any stage is represented by the area under the curve up to the appropriate time.

The transition between absorption and transmission is gradual, due to the irregularity in the water front which has been remarked. The portion of the curve corresponding to this phase is shown in fig. 4. Transmission commences at b and absorption ends at c, the flow at any intermediate point comprising absorption and transmission together. In a thicker specimen absorption would continue according to equation (31), and be represented by the prolongation of the curve ab. Thus, if ab be extrapolated to a point d at which the area under the curve represents the quantity of water which is actually absorbed by the specimen throughout the whole course of the test, the point d will indicate the rate of absorption Q_0 (equation (33)) corresponding to an average depth of penetration equal to the thickness of the specimen and the time t_0 (equation (35)) taken to penetrate to that depth. The steady rate of transmission Q_1 (equation (34)) is given by the rate of flow beyond c.

To separate the contributions which absorption and transmission make to the rates of flow between b and c, consider a point f on bc, and let g be the point corresponding to the same time on the prolongation of ab. Suppose X to be the area over which transmission takes place ; then the rate of transmission is $Q_1 \frac{X}{A}$, where Q_1 is the rate of transmission over the whole specimen of area A, and the rate of absorption is $Q_2 . \frac{A-X}{A}$, where Q_2 represents what would be the rate of absorption over the whole area of the specimen corre-

sponding to the momentary average depth of the water front. Thus, if Q′ is the total rate of flow at *f*,

$$Q' = Q_1 \cdot \frac{X}{A} + Q_2 \cdot \frac{A-X}{A},$$

Fig. 4.

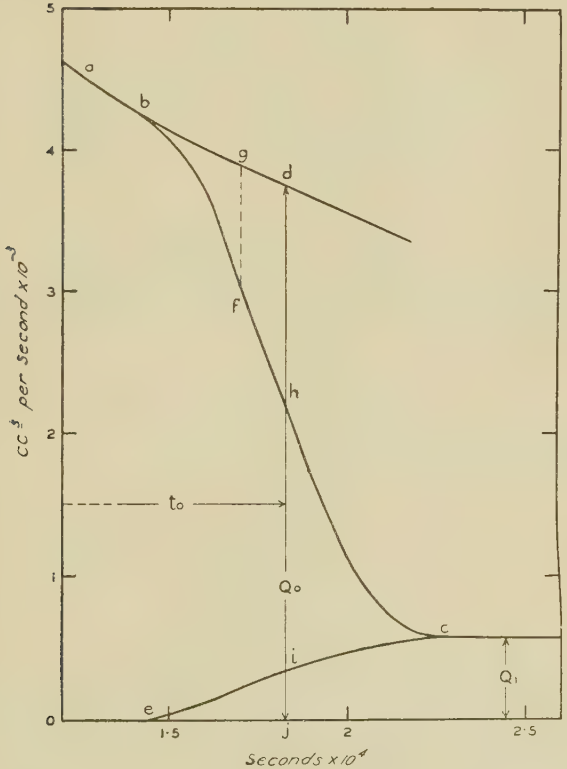

whence

$$X = \frac{A(Q_2-Q')}{Q_2-Q_1},$$

and the rate of transmission

$$\frac{Q_1 X}{A} = \frac{Q_1(Q_2-Q')}{Q_2-Q_1}.$$

Provided the irregularities in the water front are not too great the rate at which the average depth of penetration

increases during the period of combined absorption and transmission is approximately half that at which it would increase were absorption to proceed uninterrupted. Q_2 decreases from the value of Q at b to that at d, and at any moment approximates to the mean of the values at b and g. The rates of transmission as calculated in this way are shown by the line *ec*.

The total amount of water absorbed by the specimen is represented by the area under the experimental curve which is bounded by the line *ce*, and also by that under the extrapolated curve up to d. Thus, if the perpendicular dj to the time axis cut bc in h and ce in i, we see that the area hic is equal to the sum of the areas hbd and eij. The point d is determined by this condition.

Calculation of the Constants.

The values of Q_0, t_0, and Q_1 having been determined, the absorption constants may be calculated from equations (33), (34), and (35). From equations (33) and (34) the capillary head

$$h' = \frac{(Q_0 - Q_1)(h+l)}{Q_1}. \quad . \quad . \quad . \quad . \quad (36)$$

From equation (34) the permeability

$$P = \frac{Q_1 l}{A(h+l)g}. \quad . \quad . \quad . \quad . \quad . \quad (37)$$

The resistivity

$$\sigma = \frac{1}{P} = \frac{A(h+l)g}{Q_1 l}. \quad . \quad . \quad . \quad . \quad (38)$$

The absorptivity

$$Z = Ph'g = \frac{l(Q_0 - Q_1)}{A}. \quad . \quad . \quad . \quad . \quad (39)$$

From equation (35) the penetration constant

$$D = \frac{t_0}{l^2} \cdot \frac{H}{\left(1 - \frac{2}{3}\frac{l}{H} \cdots\right)h'}$$

$$= \frac{t_0}{l^2} \cdot \frac{\left(1 + \frac{2}{3} \cdot \frac{l}{H}\right)H}{h'},$$

since l is small in comparison with H,

$$= \frac{t_0}{l^2} \cdot \frac{(h+l)+h'}{h'}$$

writing $(H+l)$ for $(H+\frac{2}{3}l)$

$$= \frac{t_0 Q_0}{l^2(Q_0 - Q_1)} \quad . \quad . \quad . \quad . \quad . \quad (40)$$

by equation (36).
Also, from our definition of D_1 the porosity

$$B = \frac{2gh'D}{\sigma} = \frac{2t_0 Q_0}{Al}. \quad . \quad . \quad . \quad . \quad (41)$$

When the ordinates of the absorption curve represent the rates of flow q per sq. cm., equations (36)–(41) are modified by substituting $q_0 \,.\, A$ for Q_0 and $q_1 \,.\, A$ for Q_1.

The expression (41) is susceptible to inaccuracy from the causes which, as mentioned above, may affect equation (31). In practice a more precise value of the porosity, which is required in connexion with the determination of the saturation coefficient (Part I.), is obtained by estimating, from the area under the curve, the total amount of water absorbed by the specimen. After the specimen has been wetted two or three minutes elapse before observations are taken. The quantity of water absorbed during this period is determined as follows:—For purposes of extrapolation portions of the curve conform accurately enough to the equation $Q^n \,.\, t = \text{constant}$, where n is in the region of the theoretical value 2. n is evaluated for the first part of the curve by plotting $\log Q$ against $\log t$. Then the amount of water absorbed at time t is

$$\int_0^t Q dt = \frac{n}{n-1} Q_t \,.\, t,$$

where Q_t is the rate of absorption at time t. The area under the curve beyond t is measured by means of a planimeter.

The results of some tests are set out below. The series of values for Whitbed are selected to illustrate the extent to which the absorptive properties of a stone may vary. Of the six specimens the last two were cut from the same block, the remainder collected at random.

The method here described has been extensively applied to the routine testing of various kinds of building materials. The calculations are based on the assumptions that the specimen is homogeneous and that absorption is unaccompanied by chemical changes. An examination of the absorption curve readily reveals whether these conditions are approached sufficiently closely to justify the expressions of the absorptive properties of the material in terms of the

constants which have been defined. Even when such is not the case the curve invariably yields information of value.

Application to the Weathering Problem.

It has been remarked that the weathering of stone is intimately associated with the flow of water in it. Observations on structures built with the same stone have shown discrepancies in their weathering qualities, and from

Specimen.	Capillary head h'. cm. of water.	Resistivity. C.G.S. units $\times 10^8$.	Penetration Constant D. C.G.S. units.	Porosity.
Portland Whitbed .	276	10·7	365	·175
	135	4·01	189	·118
	167	4·25	153	·114
	275	20·7	523	·131
	249	11·1	350	·142
	264	10·5	320	·148
Portland Roach ...	196	49·3	1290	·101
Beerstone	556	4·46	871	·208
Monks Park.....	906	36·4	391	·195
Box Ground	1355	100·0	671	·178
Darley Dale	228	69·9	1170	·078
Longridge	514	48·7	3530	·073
Bath Stone	1078	43·3	446	·225
Wire-cut brick	201	5·46	277	·198
Sand-faced brick ...	95	0·336	24	·130
Gypsum plaster ...	684	20·8	374	·228

the table we see that the absorptive properties of the same material show considerable variations. The possible co-ordination of there two facts suggests a new avenue of investigation. Specimens for weathering tests may be selected to differ in their absorption constants but in other respects to be as nearly as possible similar.

LVI. *On the Effective Capacity of the Quadrant Electrometer.* By J. J. McHenry, *M.A., D.Sc.**

THE theory of the effective capacity of the quadrant electrometer has been treated theoretically by Sir J. J. Thomson, O.M.†, who showed that the motion of the

* Communicated by the Author.

† Phil. Mag. vol. xlvi. p. 536 (Dec. 1898).

needle, when at a high potential, caused an apparent increase in the effective capacity of the instrument. The effective capacity may be defined as the quantity of electricity necessary to increase by unity the potential of the insulated quadrants, the other pair of quadrants being earthed and the needle maintained at a given potential. In what follows the earthed pair of quadrants, together with the case of the instrument and screening tubes for connexions, will be called the first conductor ; the other pair of quadrants, with wires leading to them, will be called the second conductor ; and the needle will be called the third conductor.

Thomson's treatment is given here, with a slight change of notation.

If Q_2 is the charge on the second conductor,

$$Q_2 = q_{12}V_1 + q_{22}V_2 + q_{32}V_3,$$

where q_{22} is a coefficient of capacity and q_{12}, q_{32} coefficients of induction of the conductors. They depend on the position of the needle, and are therefore functions of the angle θ, which is the deflexion of the needle from the zero position in which it rests when $V_1 = V_2 = 0$ for all values of V_3.

When $V_1 = V_2 = 0$, $\quad (Q_2)_0 = (q_{32})_0 V_3$.

When $V_1 = 0$, and $V_2 \neq 0$, $\quad Q_2 = q_{22}V_2 + q_{32}V_3$.

The effective capacity

$$= \frac{Q_2 - (Q_2)_0}{V_2} = q_{22} + \frac{V_3}{V_2}\{q_{32} - (q_{32})_0\}.$$

Now $\quad \dfrac{d}{d\theta}(q_{12} + q_{22} + q_{32}) = 0$

when the needle is originally in the symmetrical position, and also, when θ is small, $\dfrac{d}{d\theta}(q_{12}) = 0$; so that

$$\frac{d}{d\theta}(q_{22}) = -\frac{d}{d\theta}(q_{23}).$$

Thus, neglecting powers of θ higher than the first,

$$q_{22} = (q_{22})_0 - b_1\theta \; ; \; q_{32} = (q_{32})_0 + b_1\theta,$$

and the effective capacity is

$$(q_{22})_0 - b_1\theta + b_1\theta\left(\frac{V_3}{V_2}\right),$$

or

$$(q_{22})_0 + b_1\theta\left(\frac{V_3}{V_2} - 1\right).$$

Now $\theta = kV_2V_3$, and the effective capacity is therefore

$$(q_{22})_0 + b_1k(V_3^2 - V_2V_3).$$

If $\frac{V_2}{V_3}$ is small, as is usual when the instrument is used heterostatically, the effective capacity is $(q_{22})_0 + b_1kV_3^2$.

The object of the present paper is to investigate the importance of the term $b_1k(V_3)^2$ in ordinary use, and to find out how far it explains the behaviour of the instrument in measuring currents or quantities of electricity. Now it is well known that the coefficient k in the above treatment is not a constant, but depends itself on the value of V_3, and this alters the form of the expression for the effective capacity. This alteration is due to the necessity of expanding the coefficient of capacity q_{33} to a higher power of θ than the first *.

When $\frac{V_2}{V_3}$ is small,

$$\theta = \frac{b_1V_2\left(V_3 - \frac{V_2}{2}\right)}{F + b_2V_3^2},$$

where b_1, as before, is $-\frac{d}{d\theta}(q_{22})$, or $+\frac{d}{d\theta}(q_{32})$; and b_2 is $\frac{d^2}{d\theta^2}(q_{23})$, or $-\frac{1}{2}\frac{d^2}{d\theta^2}(q_{33})$. F is the modulus of torsion of the suspending fibre. If we use the above expression for θ in finding the effective capacity we get, as before,

$$(q_{22})_0 + b_1\theta\left(\frac{V_3}{V_2} - 1\right),$$

or

$$(q_{22})_0 + \frac{b_1^2(V_3 - V_2)\left(V_3 - \frac{V_2}{2}\right)}{F + b_2V_3^2}.$$

Thus the effective capacity becomes, when V_2 is neglected,

$$m + \frac{b_1^2V_3^2}{F + b_2V_3^2}.$$

Here m is written instead of $(q_{22})_0$.

* Walker, Phil. Mag. (6) vi. p. 238 (Aug. 1903); Anderson, Phil. Mag. p. 380 (March 1912).

When the instrument is used idiostatically and $V_3 = V_1 = 0$,

$$\theta = \frac{-b_1 V_2^2}{2(F - a_2 V_2^2)},$$

where a_2 is $\frac{1}{2}\frac{d^2}{d\theta^2}(q_{11})$, or $\frac{1}{2}\frac{d^2}{d\theta^2}(q_{22})$. The charge on the insulated quadrants is Q_2, where

$$Q_2 = (q_{22})V_2 = (m - b_1\theta)V_2.$$

The effective capacity

$$= \frac{Q_2}{V_2} = m - b_1\theta = m + \frac{b_1^2 V_2^2}{2(F - a_2 V_2^2)}.$$

Here, in practice, the term $\frac{b_1^2 V_2^2}{2(F - a_2 V_2^2)}$ is small and may be neglected. It amounts in the electrometer studied here to about ·06 cm. when $V_2 = 5$ volts and θ about 50 divisions. The capacity m was 52·2 cm. The coefficients b_1 and b_2 may be easily compared with F, the modulus of torsion of the fibre suspending the needle, by finding in radians the values of θ for different values of V_2, V_3, and substituting in the formula $\theta = \frac{b_1 V_2 V_3}{F + b_2 V_3^2}$. Here V_2 must be small compared with V_3, and both must be expressed in electrostatic units. If $(V_3)_m$ is that potential of the needle which makes the angle θ a maximum for a given value of V_2,

$$\frac{b_2}{F} = \frac{1}{(V_3)_m^2}.$$

With the needle at a potential $(V_3)_m$,

$$\theta = \frac{b_1 V_2 (V_3)_m}{2F},$$

and by substitution of experimentally found values for θ and V_2, $\frac{b_1}{F}$ may be found. The effective capacity may then be expressed in terms of V_3 and F, and is equal to

$$m + \left\{ \frac{\left(\frac{b_1}{F}\right)^2}{\frac{1}{(V_3)^2} + \left(\frac{b_2}{F}\right)} \right\} F, \text{ or } m + xF,$$

where x can be calculated for different values of V_3. The expression for the increase in the effective capacity due to the motion of the needle may therefore be tested by plotting the values of x for given values of V_3 against the corresponding increases in the effective capacity of the electrometer as measured by experiment. It will be seen below that the graph so obtained is a straight line passing through the origin. In addition, F may be obtained by dividing the factor x into the observed value of the increase in the effective capacity for a given value of V_3.

The Experiments.

The effective capacity of the electrometer, called hereafter c, was found by comparison with a fixed condenser,

Fig. 1.

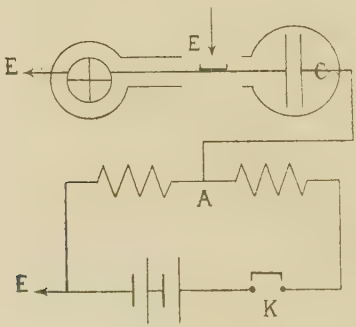

which will be denoted by C, and whose capacity was known to be approximately ·0000466 microfarads, or 41·94 e.s.u. The exact value of C is of no great importance in the experiments described here, as all the values of the quantity c are measured in terms of it. The value obtained for F depends on the value of C, and therefore also the values of b_1 and b_2. The experimental arrangements are shown in fig. 1. The condenser C is placed in series with the electrometer, one plate being joined to the insulated quadrants through the usual earthing key. The other plate of C is connected to the point A of a potentiometer. To begin with, both quadrants were earthed and the key K was open, so that A was also at zero potential. The needle was raised to the required potential and the earthing key raised so as to leave the working quadrants insulated, the

needle being in the zero position. When the key K was closed the point A and one plate of C was raised to a potential V and the other plate of the condenser and the insulated quadrants assumed a potential v. Since the quadrants and that plate of C connected to them were insulated, it is clear that

$$cv + C(v - V) = 0, \quad \text{or} \quad cv = C(V - v),$$

so that

$$\frac{c}{C} = \frac{V - v}{v}.$$

When the electrometer is used idiostatically

$$V_1 = v_3 = 0, \quad \text{and} \quad \frac{c}{C} = \frac{\sqrt{\theta_1} - \sqrt{\theta_2}}{\sqrt{\theta_2}},$$

where θ_1 and θ_2 are the deflexions caused by the potentials V and v respectively. When used heterostatically and when V_3 is large compared with V or v

$$\frac{c}{C} = \frac{\theta_1 - \theta_2}{\theta_2}.$$

It must be noted that to make $V_3 = 0$ it is not in general sufficient to join the needle to earth, on account of the contact difference of potential between the material of the needle and that of the quadrants. To make $V_3 = 0$, or, in other words, to make sure that the potential at a point in air just outside the needle is the same as that at a point in air just outside the earthed quadrants, a small potential must be applied to the needle, until with $V_1 = 0$ a reversal of the sign of V_2 causes no change in the deflexion observed. The electrometer used in these experiments had a needle made of silvered paper which was ·076 volts electronegative to the brass quadrants. Another electrometer had an aluminium needle which was ·263 volts electropositive to the quadrants.

In the above method the potential V is fixed and the deflexion θ_1 may be read at leisure, but the deflexion θ_2, which depends on v and which takes a minute or two to read, will be affected by any defect in the insulation of the electrometer or of the condenser. A leak in the electrometer makes θ_2 too small and a leak in the condenser makes it too big. When the readings given below were being taken the insulation was satisfactory, the deflexion θ_2 being steady. A variation of the method in which, with the electrometer system insulated and at zero potential, the potential of the point A is changed from V to zero, could also be used. In this case the insulated system has an original

charge $=-CV$, the charge due to the potential of the needle being, of course, left out of account. When V is changed to zero by opening the key K, the potential of the insulated system changes to v where v and V have now opposite signs. The charge on the insulated system remaining constant, we have

$$-CV = Cv + cv,$$

or

$$\frac{c}{C} = \frac{V+v}{-v}.$$

When the potential of the needle, V_3, is zero, the sign of v makes no change in θ_2, and we have, as before,

$$\frac{c}{C} = \frac{\sqrt{\theta_1} - \sqrt{\theta_2}}{\sqrt{\theta_2}}.$$

When $V_3 \neq o$ and $\frac{V_2}{V_3}$ is small we have

$$\frac{c}{C} = \frac{\theta_1 + \theta_2}{-\theta_2},$$

where θ_2 is the deflexion due to the potential v and is of opposite sign to θ_1. If we disregard the sign of θ_2 and deal in absolute values of the deflexions we get, as before,

$$\frac{c}{C} = \frac{\theta_1 - \theta_2}{\theta_2}.$$

In this second method when the insulated system has attained the potential v it may leak to earth either across the electrometer system or the condenser, so that the defective insulation of both c and C conspire to make the absolute value of v too small, and therefore the absolute deflexion θ_2 too small.

In our case the insulation of c and C was good, and the first method described gave steady values of θ_2, so that it alone was used. In cases where the condenser insulation is worse than that of the electrometer both methods should be used and means taken.

Table I. shows the values of V_3, θ_1, θ_2, and $\frac{c}{C}$. The values of V_3 go from zero to 250 volts. The deflexions given were not those read directly from the straight scale of the electrometer, but were reduced to readings on a circular scale having the mirror as centre. The deflexions

θ_1 and θ_2 are proportional to the angles of deflexion of the needle.

The values of V_3 and $\frac{c}{C}$ are shown in the graph of fig. 2.

The last reading given in the table, in which $\frac{c}{C} = 2{\cdot}74$, was

TABLE I.

V_3 (volts).	θ_1.	θ_2.	$\frac{c}{C}$.
0	191·5	38	1·244
40·5	143	58	1·47
81	118·4	41	1·86
119	137·5	40·5	2·40
161	142	37·2	2·82
200	137	33	3·15
250	126·3	28·3	3·46
157 (by sharing charges).....			2·74

Fig. 2.

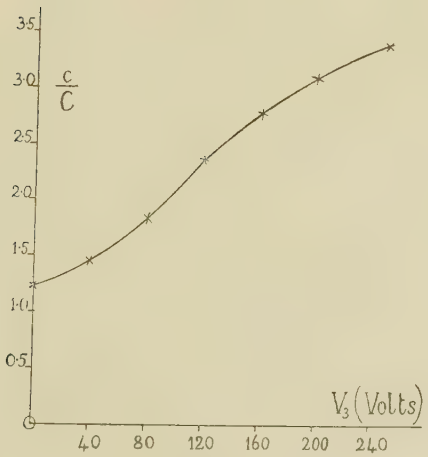

obtained by the method of "sharing the charges." The electrometer was charged to a given potential which was read from the value of the deflexion, and then was connected to the condenser, so that the charge was shared between c and C. The value 2·74 differs from that of the corresponding point on the graph (2·80) by about 2 per cent.

It will be observed that the effective capacity when V_3 is about 125 volts is double the capacity when $V_3 = 0$.

The increase in the effective capacity of the electrometer with V_3 is a very important factor in its behaviour when used to measure charges or currents. Let a quantity of electricity Q be given to the insulated quadrants, causing their potential to increase by V_2. Then $Q = cV_2$, where c is the effective capacity. Now $\frac{V_2}{V_3}$ being small,

$$V_2 = \frac{(F + b_2 V_3^2)\theta}{b_1 V_3}$$

or

$$V_2 = \frac{\theta}{\gamma},$$

where

$$\gamma = \frac{b_1 V_3}{F + b_2 V_3^2},$$

and may be called the sensitivity of the electrometer for measuring potentials. Q therefore is $\frac{c\theta}{\gamma}$, where $\frac{\gamma}{c}$ may be called the sensitivity for measuring charges. Table II. shows the deflexions (θ) observed for a value of $V_2 = \cdot 505$ volts, with different values of V_3. A graph of θ against V_3, V_2 being kept constant, shows how γ varies with V_3. This graph is shown in curve B of fig. 3. When these values of γ are divided by numbers proportional to c we obtain quantities proportional to the sensitivity of the electrometer in measuring charges, that is, to $\frac{\gamma}{c}$. These numbers are also shown in Table II. and plotted on curve A of fig. 3. The points obtained in this way are indicated by crosses. Curve B shows that the electrometer is most sensitive in measuring potentials when $V_3 = 157$ volts approximately. Curve A shows that the electrometer when used to measure charges is most sensitive when V_3 is in the neighbourhood of 80 volts, when no external loading condenser is added to increase the electrometer capacity. If this is done it is obvious that the value of V_3, which causes greatest sensitivity in measuring charges, will increase and approach the value of V_3, which causes the electrometer to be most sensitive in measuring potentials, the two values coinciding when the loading condenser is very big.

The variation with V_3 of the sensitivity of the electrometer in measuring charges was also studied by measuring

the time, T, necessary for a constant current, I, to produce a given deflexion, θ. Here

$$Q = I \times T = \frac{c\theta}{\gamma}, \quad \text{and} \quad \frac{\gamma}{c} = \frac{\theta}{IT};$$

TABLE II.

V_3 (volts).	$\gamma \times$ const.	$\frac{\gamma}{c} \times$ const.	T (secs.).	$\frac{1}{T} \times$ const.
40·5	70	111	94	106
58·5	—	—	70·2	143
81	116·4	146	68·3	146
101	—	—	70·5	142
119	137·3	133·2	—	—
121	—	—	73·4	136
141	140·4	—	—	—
161	141·6	117·3	80·4	124
182	140·8	—	88·5	113
200	138	102·2	—	—
243	—	—	105·5	95
250	128	86·3	—	—

Fig. 3.

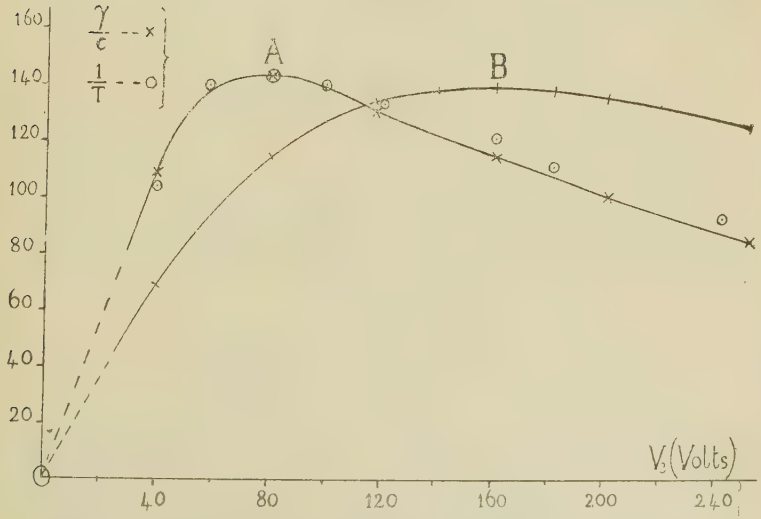

so that when I and θ are kept constant $\frac{\gamma}{c}$ is proportional to the reciprocal of T. A small quantity of uranium oxide

was placed on the lower of two plates inside an earthed box. The lower plate was joined to the electrometer, the upper being maintained at a constant potential of about 180 volts. T was the time taken, when the electrometer system was disconnected from earth, for the spot of light on the scale to move over seventy divisions. The values of $\frac{1}{T}$ are indicated by circles on fig. 3. The constants by which $\frac{\gamma}{c}$ and $\frac{1}{T}$ were multiplied were so chosen that their values, so multiplied, were made equal when $V_3 = 81$ volts. It will be seen that the values of $\frac{1}{T}$ lie near, but not quite on, curve A. In curve A, which shows the values of $\frac{\gamma}{c}$, c is the capacity of the electrometer and leads, but in measuring T this capacity is necessarily increased somewhat by the addition of the ionization chamber. This additional capacity was small, but not negligible. The addition of an external capacity to the effective capacity of the electrometer makes curve A alter in form towards that of curve B, with which it would coincide when the additional capacity is made very big. The small deviation of the values of $\frac{1}{T}$ from curve A may therefore be attributed to the addition of the extra capacity of the ionization chamber.

The experimental values of c therefore explain the variation with V_3 of the sensitivity of the instrument in measuring quantities of electricity. It remains now to find how these observed values agree with the theoretical expression for the effective capacity,

$$m + \frac{b_1^2 V_3^2}{F + b_2 V_3^2}, \quad \text{or} \quad m + \frac{b_1^2}{b_2 + \frac{F}{V_3^2}}.$$

Here m is, with sufficient accuracy, the value of the effective capacity when $V_3 = 0$, which may be seen from Table I. to be 1·244 C. Subtracting this from the full values of the effective capacity we obtain the increase in the latter values due to the motion of the needle or values of $c - m$. Now $c - m$, experimentally obtained, should be equal to

$$\frac{b_1^2}{b_2+\frac{\mathrm{F}}{\mathrm{V}_3^2}} \quad \text{or} \quad \left\{\frac{\left(\frac{b_1}{\mathrm{F}}\right)^2}{\frac{b_2}{\mathrm{F}}+\frac{1}{\mathrm{V}_3^2}}\right\}\mathrm{F}.$$

If V_3 be expressed in volts instead of electrostatic units we have

$$c-m=\left\{\frac{\left(\frac{b_1}{\mathrm{F}}\right)^2}{\frac{b_2}{\mathrm{F}}+\frac{300}{\mathrm{V}_3^2}}\right\}\times\mathrm{F}.$$

The ratios $\frac{b_2}{\mathrm{F}}$ and $\frac{b_1}{\mathrm{F}}$ were obtained from the following data :—

The electrometer is most sensitive in measuring potentials when $V_3 = 157$ volts ; therefore $b_2 \times \left(\frac{157}{300}\right)^4 = \mathrm{F}$; from which $\frac{b_2}{\mathrm{F}} = 3{\cdot}65$.

When $V_3 = 157$ volts and $V_2 = {\cdot}2526$ volts, $\theta = 70{\cdot}9$ divs. on a scale 1 metre from the mirror ; 800 divisions on the scale were equal to 795 mm. Substituting in the formula,

$$\theta = \frac{b_1 V_2 V_3}{2\mathrm{F}(300)^2} = \frac{70{\cdot}9 \times 795}{2000 \times 800} \text{ radians},$$

we get $\frac{b_1}{\mathrm{F}} = 160$.

Substituting these values in the formula given above, we have

$$c-m=\left\{\frac{(160)^2}{3{\cdot}65+\left(\frac{300}{\mathrm{V}_3}\right)^2}\right\}\times\mathrm{F}$$

$$= x\mathrm{F}.$$

The measured values of $c-m$ are given, in terms of the capacity C, in the second column of Table III. In the third column they are expressed in electrostatic units. The fourth column gives the corresponding values of the factor x. Fig. 4 shows $c-m$ plotted against x. The graph so obtained is a straight line passing through the origin, which shows that the theoretical expression for the effective capacity is verified by experiment.

Taking a point on the graph, $c-m = 73{\cdot}4$ cm.; $x = 4000$. Hence $F = \frac{73{\cdot}4}{4000} = {\cdot}0184$ dynes × cm. per radian. This

TABLE III.

V_3 (volts).	$\frac{c-m}{C}$.	$(c-m)$, in e.s.u.	x.
0	Negligible.	—	—
40·5	·226	9·48	437
81	·616	25·8	1474
119	1·156	48·5	2558
161	1·576	66·1	3595
200	1·906	80·0	4338
250	2·216	93·0	5029

Fig. 4.

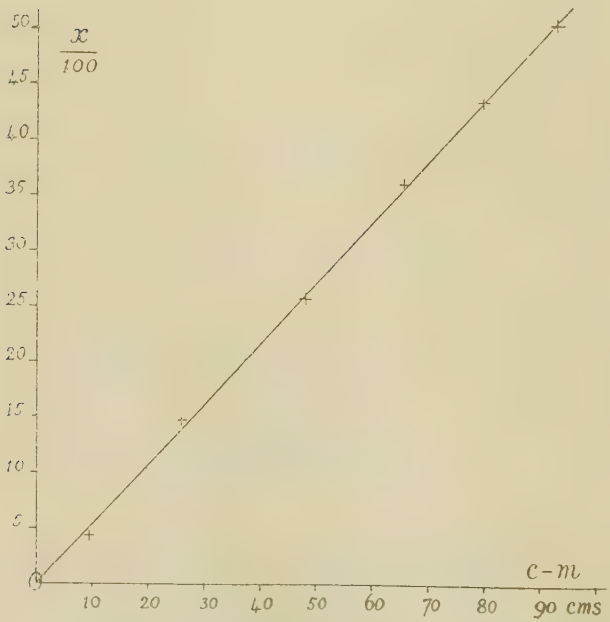

gives $b_1 = 2{\cdot}94$ cm./radian; $b_2 = {\cdot}0672$ cm./(radian)^2. The modulus of torsion of the suspension, F, was also found directly by hanging from it a small cylinder of aluminium and measuring the period of the torsional oscillations. The axis of rotation was perpendicular to the axis of the cylinder

and passed through its centre of gravity. The mass of the cylinder was 2·771 grm.; its length was 3·72 cm. and diameter ·594 cm. The period was 81·7 seconds. From these data F was found to be ·0193 c.g.s. units, which differs from the value determined above by about $4\frac{1}{2}$ per cent., which is not greater than the possible error in the assumed value of the capacity C.

The four constants of the electrometer, viz., b_1, b_2, m, and F, may therefore be found easily by electrical methods provided a suitable standard condenser is available. Here it will be remembered

$$b_1 = \frac{d}{d\theta}(q_{23}) = -\frac{d}{d\theta}(q_{13}),$$

$$b_2 = \frac{d^2}{d\theta^2}(q_{23}) = \frac{d^2}{d\theta^2}(q_{13}) = -\frac{1}{2}\frac{d^2}{d\theta^2}(q_{33}),$$

$$m = (q_{22})_0,$$

and F is the modulus of torsion of the fibre suspending the needle. These four constants determine to a reasonable degree of accuracy the whole behaviour of the instrument. We may, for example, find in terms of them the potential $(V_3)_\mu$ which makes the electrometer most sensitive in measuring charges, and an expression for this maximum sensitivity, as follows:—

$$\frac{\theta}{Q} = \frac{\theta}{cV_2} = \frac{b_1 V_3}{\left(m + \frac{b_1^2 V_3^2}{F + b_2 V_3^2}\right)(F + b_2 V_3^2)}$$

$$= \frac{1}{\frac{mF}{b_1 V_3} + \left(\frac{mb_2 + b_1^2}{b_1}\right) V_3}.$$

$\frac{\theta}{Q}$ is greatest when the denominator is least, V_3 alone being variable, or $\frac{\theta}{Q}$ is maximum when

$$V_3^2 = \frac{mF}{mb_2 + b_1^2} = \frac{F}{b_2 + \frac{b_1^2}{m}}$$

$$= (V_3)_\mu^2.$$

Thus, $$(V_3)_\mu = \sqrt{\frac{F}{b_2 + \frac{b_1^2}{m}}}.$$

The sensitivity for measuring potentials is

$$\frac{\theta}{V_2} = \frac{b_1 V_3}{F + b_2 V_3^2} = \frac{b_1}{\frac{F}{V_3} + b_2 V_3}.$$

$\frac{\theta}{V_2}$ is greatest when

$$V_3 = (V_3)_m = \sqrt{\frac{F}{b_2}}.$$

When m or $(q_{22})_0$ becomes very big $(V_3)_\mu = (V_3)_m$.

The maximum value of $\frac{\theta}{Q}$ is

$$2\sqrt{\frac{1}{m^2 F b_2 + m F b_1^2}} = \frac{b_1}{2\sqrt{mF(mb_2 + b_1^2)}}.$$

The fact that b_2, in electrometers of the usual pattern, is positive is shown by Walker (*loc. cit.*) to be due to the air gaps separating the quadrants. He thinks it probable that b_2 could be made to vanish by altering the angle of the needle, which is usually made in the form of a double sector of a circle. If this can be realized there is no theoretical limit to the sensitivity of the instrument in measuring potentials, but $\frac{\theta}{Q}$, the sensitivity for measuring charges, has still a maximum value $\frac{1}{2\sqrt{mF}}$ when $V_3 = \frac{\sqrt{mF}}{b_1}$.

University College, Galway.

LVII. *A Continuous Atomic Matrix.*

By W. R. Morgans, *M.Sc.* * †.

1. *Introduction.*

THE recent developments in the quantum theory enable us to calculate the intensity of the spectral lines which are emitted by the transition between two electronic states. For a theoretical treatment of many phenomena, however, such as rates of recombination, the intensity of continuous X-rays, and the photoelectric effect, further

* Communicated by the Author.
† Late Commonwealth Fellow.

knowledge of continuous matrices is required. Oppenheimer[3] gave a general treatment of hydrogen-like atoms, but his final results are not satisfactory in numerical computation. Epstein and Muskat[1] and Sugiura[2] have given the Schroedinger matrices for the affinity spectrum of hydrogen-like atoms in a more amenable form. The evaluation of the matrices for the capture of a cathode ray electron travelling in a definite direction, the z axis, by a bare nuclear charge Ze, has not yet been suitably determined. It appears that, from Temple's[4] work, it is convenient to use parabolical coordinates in such an investigation. The problem is essentially an analytical one, and it is proposed here to evaluate the matrices for such a collision problem, using parabolical coordinates. The method follows that given by Epstein[5].

2. *The Wave Functions.*

If we use the parabolical coordinates

$$x=\sqrt{\xi\eta}\cos\phi, \qquad y=\sqrt{\xi\eta}\sin\phi, \qquad z=\frac{\xi-\eta}{2},$$
$$0\leq\xi\leq\infty, \qquad 0\leq\eta\leq\infty, \qquad 0\leq\phi\leq 2\pi,$$

and assume the cathode ray electron and the nucleus as one system, then the Schroedinger wave equation for the electron travelling in the direction of the nuclear charge Ze is given by

$$\frac{\partial}{\partial\xi}\left(\xi\frac{\partial\psi}{\partial\xi}\right)+\frac{\partial}{\partial\eta}\left(\eta\frac{\partial\psi}{\partial\eta}\right)+\frac{1}{4}\left(\frac{1}{\xi}+\frac{1}{\eta}\right)\frac{\partial^2\psi}{\partial\phi^2}$$
$$+\frac{2\pi^2\mu\mathrm{E}}{h^2}(\xi+\eta)\psi+4\pi^2\frac{\mu e^2\mathrm{Z}}{h^2}\psi=0$$

where ψ is the amplitude function, μ and e the mass and charge of the electron, E the energy of the atomic system, and h is Planck's constant.

In order to obtain the wave function corresponding to the electron moving in the direction of the z axis with energy $\mathrm{E}>0$, Temple solved the above wave equation by omitting the angular term, and obtained a solution corresponding to the initial state of the electron, in which the wave associated has symmetry about the z axis. If we make the substitutions

$$\frac{k^2}{4}=\frac{2\pi^2\mu\mathrm{E}}{h^2}, \qquad a=\frac{h^2}{4\pi^2\mu e^2\mathrm{Z}}, \qquad n=\frac{1}{ak},$$

the solution found for the initial state becomes

$$\psi(n) = \mathrm{A}(n) e^{\frac{ik}{2}(\xi-\eta)} \mathrm{F}(in, 1, ik\eta),$$

where

$$\mathrm{F}(\alpha, j, x) = \sum_{p=0}^{\infty} \frac{\alpha(\alpha+1)\ldots(\alpha+p-1)}{j(j+1)\ldots(j+p-1)} \frac{x^p}{p!},$$

and n is a parameter characterizing the continuous state. $\mathrm{A}(n)$, the normalization factor, can be determined by Fues'[6] method of normalization, and has been shown by Oppenheimer to have the value

$$|\mathrm{A}(n)|^2 = \frac{2\pi\mu a}{h} \cdot e^{\pi n} n\Gamma(1-in)\Gamma(1+in).$$

The wave function for the final state of the electron, in which the energy $\mathrm{E}_1 < 0$, is more complex, and is given by the general solution of the wave equation above. If we make the substitution

$$-\frac{(k')^2}{4} = \frac{2\pi^2\mu \mathrm{E}_1}{h^2},$$

we find the solution to be

$$\psi(n_1 n_2 m) = \mathrm{A}(n_1 n_2 m)(\xi\eta)^{\frac{|m|}{2}} e^{-\frac{k'}{2}(\xi+\eta)} \mathrm{F}(-n_1, |m|+1, k'\xi)\mathrm{F}(-n_2, |m|+1, k'\eta) \begin{matrix}\cos \\ \sin\end{matrix} m\phi,$$

where $|m| = 0, 1, 2, \ldots, \infty$, and $k'(|m|+1+n_1+n_2) = \frac{1}{a}$, and $\mathrm{A}(n_1, n_2, m)$ is the normalization factor for the final state.

3. *The Matrices.*

We proceed with the evaluation of the Heisenberg matrices for transitions from the initial continuous state to the final state. It has been shown by Schroedinger that the components of the matrices are given by the expressions

$$q_x(n\ ;\ n_1 n_2 m) = \iiint x\psi(n)\psi^*(n_1 n_2 m)\,dx\,dy\,dz$$

(with analogous expressions for z and y), where $\psi^*(n_1 n_2 m)$ denotes the conjugate value of $\psi(n_1 n_2 m)$ and the integration is extended over the whole of space. If we introduce the coordinates ξ, η, ϕ, we obtain

$$q_{x,y}(n\,;\,n_1n_2m)=\frac{1}{4}\,\mathrm{A}(n)\mathrm{A}(n_1n_2m)\iiint\sqrt{\xi\eta(\xi+\eta)(\xi\eta)}^{\,|m|}$$
$$e^{-\frac{k'}{2}(\xi+\eta)}\,\mathrm{F}(-n_1,|m|+1,k'\xi)\mathrm{F}(-n_2,|m|+1,k'\eta)$$
$$e^{-\frac{ik}{2}(\xi-\eta)}\,\mathrm{F}(-in,\,1,\,-ik\eta)\begin{matrix}\cos\\ \sin\end{matrix}m\phi\begin{matrix}\cos\\ \sin\end{matrix}\phi\,d\xi\,d\eta\,d\phi.$$

The integration with respect to ϕ can be carried out immediately, giving a finite value $\pm\frac{\pi}{2}$ only when $m=\mp1$. Hence

$$|q_{x,y}(n\,;\,n_1n_2\pm1)|=\frac{\pi}{8}\,\mathrm{A}(n)\mathrm{A}(n_1n_2\pm1)\iint(\xi+\eta)\xi\eta$$
$$\mathrm{F}(-n_1,2,k'\xi)\mathrm{F}(-n_2,2,k'\eta)e^{-\frac{k'}{2}(\xi+\eta)}e^{-\frac{ik}{2}(\xi-\eta)}$$
$$\mathrm{F}(-in,1,-ik\eta)d\xi\,d\eta.$$

Also q_z is finite only when $m=0$, so that

$$|q_z(n\,;\,n_1n_20)|=\frac{\pi}{8}\,\mathrm{A}(n)\mathrm{A}(n_1n_20)\iint(\xi^2-\eta^2)e^{-\frac{k'}{2}(\xi+\eta)}$$
$$\mathrm{F}(-n_1,1,k'\xi)\mathrm{F}(-n_2,1,k'\eta)e^{-\frac{ik}{2}(\xi-\eta)}\mathrm{F}(-in,1,-ik\eta)d\xi\,d\eta.$$

For aid in the evaluation of these matrix integrals we introduce the function $\mathrm{H}^{\delta}_{\beta\gamma}(nn'\alpha\alpha')$, defined such that

$$\mathrm{H}^{\delta}_{\beta\gamma}(nn'\alpha\alpha')=\int_0^{\infty}e^{-\frac{(\alpha+\alpha')}{2}\xi}\,\xi^{\delta+\beta}\,\mathrm{F}(-n,\delta+1,\alpha\xi)$$
$$\mathrm{F}(-n',\delta+1-\gamma,\alpha'\xi)d\xi. \quad (1)$$

With this definition the expressions for the matrix elements become

$$|q_{xy}(n\,;\,n_1n_2\pm1)|=\frac{\pi}{8}\,\mathrm{A}(n)\mathrm{A}(n_1)[\mathrm{H}^1_{11}(n_1ok'ik)\mathrm{H}^1_{01}(n_2ink'-ik)$$
$$+\mathrm{H}^1_{11}(n_2ink'-ik)\mathrm{H}^1_{01}(n_1ok'ik)], \quad . \quad . \quad (2)$$

$$|q_z(n\,;\,n_1n_20)|=\frac{\pi}{8}\,\mathrm{A}(n)\mathrm{A}(n_1)[\mathrm{H}^0_{20}(n_1ok'ik)\mathrm{H}^0_{00}(n_2ink'-ik)$$
$$-\mathrm{H}^0_{20}(n_2ink'-ik)\mathrm{H}^0_{00}(n_1ok'ik)]. \quad . \quad . \quad (3)$$

4. *Evaluation of the Integrals.*

The integrals occurring in the matrix components come under the general form

$$\mathrm{H}^{\delta}_{\beta\gamma}(nn'\alpha\alpha'),$$

where $\gamma=1$; $\delta=0,1$; $\beta=0,1,2$.

By a number of reduction formulæ the above forms can be reduced to one suitable for evaluation. If we use the relation

$$F(\alpha, \gamma, x) = \frac{(\gamma-1)}{x}\left[F(\alpha, \gamma-1, x) - F(\alpha-1, \gamma-1, x)\right],$$

then

$$H^{\delta}_{\beta 1}(nn'\alpha\alpha') = \frac{\delta}{\alpha}\left[H^{\delta-1}_{\beta 0}(nn'\alpha\alpha') - H^{\delta-1}_{\beta 0}(n+1, n', \alpha, \alpha')\right]. \quad (4)$$

Again, the integral $H^{\delta}_{\beta 0}(nn'\alpha\alpha')$ may be written as

$$H^{\delta}_{\beta 0}(nn'\alpha\alpha') = \int_0^{\infty} y(n)y'(n')d\xi,$$

where

$$y(n) = e^{-\frac{\alpha}{2}\xi}\xi^{\frac{\delta+\beta}{2}}F(-n, \delta+1, \alpha\xi),$$

$$y'(n') = e^{-\frac{\alpha'}{2}\xi}\xi^{\frac{\delta+\beta}{2}}F(-n', \delta+1, \alpha'\xi).$$

It can be shown that $y(n)$ and $y'(n')$ are solutions of the following differential equations:

$$\xi\frac{d^2y}{d\xi^2} + (1-\beta)\frac{dy}{d\xi} + \left[-\frac{\alpha^2}{4}\xi - \frac{(\delta^2-\beta^2)}{4\xi} + \alpha\left(\frac{\delta+1}{2}+n\right)\right]y = 0, \quad (5)$$

$$\xi\frac{d^2y'}{d\xi^2} + (1-\beta)\frac{dy'}{d\xi} + \left[-\frac{\alpha'^2}{4}\xi - \frac{(\delta^2-\beta^2)}{4\xi} + \alpha'\left(\frac{\delta+1}{2}+n'\right)\right]y' = 0. \quad (6)$$

Multiply (5) by $y'(n')$ and (6) by $y(n)$ and subtract; then

$$y'\frac{d}{d\xi}\left(\xi\frac{dy}{d\xi}\right) - y\frac{d}{d\xi}\left(\xi\frac{dy'}{d\xi}\right) - \beta\left(y'\frac{dy}{d\xi} - y\frac{dy'}{d\xi}\right) + \frac{(\alpha'^2-\alpha^2)}{4}\xi yy' + \left[\alpha\left(\frac{\delta+1}{2}+n\right) - \alpha'\left(\frac{\delta+1}{2}+n'\right)\right]yy' = 0.$$

Integrating the expression between zero and infinity, and omitting terms that vanish at these limits, we find, after a little rearrangement, that

$$-2\beta\int_0^{\infty} y'\frac{dy}{d\xi}d\xi + \frac{(\alpha'^2-\alpha^2)}{4}H^{\delta}_{\beta+1,0}(nn'\alpha\alpha') + \left[\alpha\left(\frac{\delta+1}{2}+n\right) - \alpha'\left(\frac{\delta+1}{2}+n'\right)\right]H^{\delta}_{\beta 0}(nn'\alpha\alpha') = 0. \quad (7)$$

Again,

$$\frac{d}{d\xi}y(n)=-\frac{\alpha}{2}y(n)+\frac{(\delta+\beta)}{2\xi}y(n)$$
$$+e^{-\frac{\alpha}{2}\xi}\xi^{\frac{\delta+\beta}{2}}\frac{d}{d\xi}\mathrm{F}(-n,\delta+1,\alpha\xi).$$

If we use the relation

$$\frac{d}{d\xi}\mathrm{F}(-n,\delta+1,\alpha\xi)=-\frac{n}{\xi}[\mathrm{F}(-n+1,\delta+1,\alpha\xi)$$
$$-\mathrm{F}(-n,\delta+1,\alpha\xi)],$$

we may write

$$\int_0^\infty y'(n)\frac{dy}{d\xi}d\xi=-\frac{\alpha}{2}\mathrm{H}^{\delta}_{\beta 0}(nn'\alpha\alpha')+\frac{(\delta+\beta)}{2}\mathrm{H}^{\delta}_{\beta-1,0}(nn'\alpha\alpha')$$
$$+n\mathrm{H}^{\delta}_{\beta-1,0}(nn'\alpha\alpha')-n\mathrm{H}^{\delta}_{\beta-1,0}(n-1,n'\alpha\alpha').$$

Substituting this value in (7), we have

$$\mathrm{H}^{\delta}_{\beta+1,0}(nn'\alpha\alpha')=\frac{4}{(\alpha^2-\alpha'^2)}\left[\left\{\alpha\left(\frac{\delta+1}{2}+n\right)-\alpha'\left(\frac{\delta+1}{2}+n'\right)\right\}\right.$$
$$\mathrm{H}^{\delta}_{\beta 0}(nn'\alpha\alpha')-\beta(\delta+\beta+2n)\mathrm{H}^{\delta}_{\beta-1,0}(nn'\alpha\alpha')$$
$$\left.+2n\beta\mathrm{H}^{\delta}_{\beta-1,0}(n-1,n'\alpha\alpha')\right].$$

In particular

$$\mathrm{H}^{\delta}_{10}(nn'\alpha\alpha')=\frac{4}{(\alpha^2-\alpha'^2)}\left[\alpha\left(\frac{\delta+1}{2}+n\right)\right.$$
$$\left.-\alpha'\left(\frac{\delta+1}{2}+n'\right)\right]\mathrm{H}^{\delta}_{00}(nn'\alpha\alpha'),\quad(8)$$

$$\mathrm{H}^{\delta}_{20}(nn'\alpha\alpha')=\frac{4}{(\alpha^2-\alpha'^2)}\left[\frac{4}{(\alpha^2-\alpha'^2)}\left\{\alpha\left(\frac{\delta+1}{2}+n\right)\right.\right.$$
$$\left.-\alpha'\left(\frac{\delta+1}{2}+n'\right)+\alpha\right\}\left\{\alpha\left(\frac{\delta+1}{2}+n\right)\right.$$
$$\left.\left.-\alpha'\left(\frac{\delta+1}{2}+n'\right)\right\}\times\mathrm{H}^{\delta}_{00}(nn'\alpha\alpha')-(\delta+1+2n)\right.$$
$$\left.\mathrm{H}^{\delta}_{00}(nn'\alpha\alpha')+2n\mathrm{H}^{\delta}_{00}(n-1,n'\alpha\alpha')\right].\quad\ldots\quad(9)$$

If we use the relations (4), (8), (9) in the expressions

(2), (3), the x, y matrix components, for which $k'(2+n_1+n_2)=\frac{1}{a}=kn$, can be reduced to the form

$$|q_{x,y}(n;\, n_1 n_2 \pm 1)| = \frac{\pi A(n) A(n_1)}{2k'(k^2+k'^2)}\Big[H^0_{00}(n_1+1,\, ok'ik)$$
$$H^0_{00}(n_2+1,\, in\,k'-ik) - H^0_{00}(n_1\, ok'ik)$$
$$H^0_{00}(n_2\, in\,k'-ik)\Big].$$

Likewise the z matrix component, for which $k'(1+n_1+n_2)=\frac{1}{a}=kn$, reduces to

$$q_z(n\,;\, n_1 n_2\, 0)| = \frac{\pi A(n) A(n_1)}{(k'^2+k^2)}\Big[\Big\{(n_1-n_2)\frac{(k'^2-k^2)}{(k'^2+k^2)}$$
$$-\frac{2ikk'}{(k'^2+k^2)}(1+in)\Big\} H^0_{00}(n_1 ok'ik) H^0_{00}(n_2 in\,k'-ik)$$
$$+n_1 H^0_{00}(n_1-1,\, 0,\, k'\,ik) H^0_{00}(n_2\, in\,k'-ik)$$
$$-n_2 H^0_{00}(n_1\, ok'ik)\, H^0_{00}(n_2-1, in\,k'-ik)\Big].$$

The computation of the matrix components will be determined if the integral

$$H^\delta_{00}(nn'\alpha\alpha') = \int_0^\infty e^{-\frac{(\alpha+\alpha')}{2}\xi}\,\xi^\delta\, F(-n,\, \delta+1,\, \alpha\xi)$$
$$F(-n',\, \delta+1,\, \alpha'\xi)\,d\xi \quad . \quad . \quad . \quad . \quad (10)$$

can be evaluated, where n', α' are imaginary and n, α are real. We can represent the function

$$y(n) = \xi^{\delta/2} e^{-\frac{\alpha}{2}} F(-n,\, \delta+1,\, \alpha\xi)$$

in the following form:

$$y(n) = \frac{e^{\left(-\frac{\alpha}{2}\xi - i\pi n\right)}\,\Gamma(\delta+1)\,\Gamma(n+1)}{2\pi i(-\alpha)^{\delta/2}\, y^{\frac{\delta+2n}{2}}}$$
$$\int_\odot J_\delta(2\sqrt{-\alpha y\xi}\,t)\, t^{-\frac{(\delta+2n+2)}{2}} e^{-yt}\,dt, \quad (11)$$

where the path of integration is a loop around the pole $t=0$.

Likewise

$$y'(n') = \xi^{\frac{\delta}{2}} e^{-\frac{\alpha'}{2}} \mathrm{F}(-n', \delta+1, \alpha'\xi)$$

$$= \frac{e^{\left(-\frac{\alpha'}{2}\xi - i\pi n'\right)}\Gamma(\delta+1)\Gamma(n'+1)}{2\pi i(-\alpha')^{\frac{\delta}{2}} y^{\frac{\delta+2n'}{2}}} \int_c \mathrm{J}_\delta(2\sqrt{-\alpha' y \xi t})\, t^{-\frac{(\delta+2n'+2)}{2}} e^{-yt} dt, \quad (12)$$

where the path of integration is a complex loop coming from $+\infty$ along the real axis, making a positive circuit around the point $t=0$ and going back to $+\infty$. If we substitute (11), (12) in the integrand (10), and use the following relation from the theory of Bessel Functions,

$$\int_0^\infty \mathrm{J}_\delta(2\sqrt{a\xi})\mathrm{J}_\delta(2\sqrt{b\xi}) e^{-c\xi} d\xi = \frac{1}{c} e^{-\frac{(a+b)}{c} - i\frac{\delta\pi}{2}} \mathrm{J}_\delta\left(\frac{2i\sqrt{ab}}{c}\right), \quad (7)$$

the integrations can be carried out to give the result

$$\mathrm{H}^\delta_{00}(nn'\alpha\alpha') = (-1)^n \left(\frac{2}{\alpha+\alpha'}\right)^{\delta+1} \Gamma(\delta+1) u^{n+n'} \mathrm{F}\left(-n, -n', \delta+1, 1-\frac{1}{u^2}\right),$$

where $u = \dfrac{\alpha-\alpha'}{\alpha+\alpha'}$ and $\mathrm{F}\left(-n, -n', \delta+1, 1-\dfrac{1}{u^2}\right)$ is a hypergeometric function.

With this determination the matrix components become, after slight reductions and the use of the relation,

$$\mathrm{F}(a+1, b, c, z) - \mathrm{F}(a, b, c, z) = \frac{bz}{c} \mathrm{F}(a+1, b+1, c+1, z),$$

$$|q_{x,y}(n; n_1 n_2 \pm 1)| = 2\pi \mathrm{A}(n)\mathrm{A}(n_1) \frac{(-1)^{n_1+n_2}}{k'(k^2+k'^2)^2} v^{n_1-n_2-in} in(1-v^2)\mathrm{F}(-n_2, 1-in, 2, 1-v^2),$$

$$|q_z(n; n_1 n_2 0)| = 4\pi \mathrm{A}(n)\mathrm{A}(n_1) \frac{(-1)^{n_1+n_2}}{(k^2+k'^2)^2} v^{n_1-n_2-in} [\{(n_1+n_2+1)+v(n_1+1)\}\mathrm{F}(-n_2, -in, 1, 1-v^2) + n_2 v \mathrm{F}(-n_2+1, -in, 1, 1-v^2)],$$

where $$v = \frac{k'-ik}{k'+ik}.$$

5. *The Normalization factor* $A(n_1n_2m)$.

The factor $A(n_1n_2m)$ for the discrete Eigenfunction is defined by the relation

$$\frac{1}{4}\iiint(\xi+\eta)\psi^2(n_1n_2m)d\xi d\eta d\phi=1,$$

where the integration is extended throughout space. If we integrate with respect to ϕ, and make use of relation (1), we find

$$\frac{\pi}{4}A^2(n_1n_2m)[H^{|m|}_{10}(n_1n_1k'k')H^{|m|}_{00}(n_2n_2k'k') + H^{|m|}_{10}(n_2n_2k'k')H^{|m|}_{00}(n_1n_1k'k']=1. \quad . \quad (13)$$

But

$$H^{|m|}_{10}(nn'\alpha\alpha')=\frac{4}{(\alpha^2-\alpha'^2)}\left[\alpha\left(\frac{|m|+1}{2}+n\right) -\alpha'\left(\frac{|m|+1}{2}+n'\right)\right]H^{|m|}_{00}(nn'\alpha\alpha'),$$

which gives in the limit

$$\underset{\substack{\alpha\to\alpha'\\ n\to n'}}{\mathrm{Lt}}\ H^{|m|}_{10}(nn'\alpha\alpha')=\frac{2}{\alpha'}\left(\frac{|m|+1}{2}+n'\right)H^{|m|}_{00}(n'n'\alpha'\alpha').$$

The equation (13) becomes therefore

$$\frac{\pi}{4}A^2(n_1n_2m)\frac{2}{k'}(|m|+n_1+n_2+1) H^{|m|}_{00}(n_1n_1k'k')H^{|m|}_{00}(n_2n_2k'k')=1.$$

Furthermore, as

$$H^{|m|}_{00}(nn'\alpha\alpha')=(-1)^n\left(\frac{2}{\alpha+\alpha'}\right)^{|m|+1}\Gamma(|m|+1)u^{n+n'} F\left(-n',-n,|m|+1,1-\frac{1}{u^2}\right),$$

where

$$u=\frac{\alpha-\alpha'}{\alpha+\alpha'}$$

and

$$F(a,b,c,z)=\frac{\Gamma(c)\Gamma(c-a-b)}{\Gamma(c-a)\Gamma(c-b)}F(a,b,a+b+1-c,1-z),$$

when a, b are discrete numbers, then

$$\mathrm{H}_{00}^{|m|}(n_1 n_1 k' k') = \frac{(-1)^{n_1}}{(k')^{|m|+1}} \frac{\Gamma(|m|+1)^2 \Gamma(|m|+2n_1+1)}{\Gamma(|m|+1+n_1)^2} \operatorname*{Lt}_{u\to 0} u^{2n_1} \mathrm{F}\left(-n_1, -n_1, -2n_1-|m|, \frac{1}{u^2}\right),$$

$$= \frac{(-1)^{n_1}}{(k')^{|m|+1}} \frac{\Gamma(|m|+1)^2 \Gamma(|m|+2n_1+1)}{\Gamma(|m|+1+n_1)^2} \operatorname*{Lt}_{u\to 0} \sum_{p=0}^{n_1} \frac{n_1^2 (n_1-1)^2 \ldots (n_1-p+1)^2 u^{2(n_1-p)}}{(-1)^p p\,!\,(2n_1+|m|)\ldots(2n_1+|m|-p+1)}$$

$$= \frac{1}{(k')^{|m|+1}} \frac{\Gamma(|m|+1)^2 \Gamma(n_1+1)}{\Gamma(|m|+n_1+1)}.$$

Using this result in equation (13) we find that

$$\mathrm{A}(n_1 n_2 m) = \sqrt{\frac{2a}{\pi}} \frac{(k')^{|m|+2}}{\Gamma(|m|+1)^2} \sqrt{\frac{\Gamma(|m|+n_1+1)\Gamma(|m|+n_2+1)}{\Gamma(n_1+1)\Gamma(n_2+1)}}.$$

For the particular cases $m = \pm 1$ and $m = 0$ we find

$$\mathrm{A}(n_1 n_2 \pm 1) = (k')^3 \sqrt{\frac{2a}{\pi}(n_1+1)(n_2+1)},$$

$$\mathrm{A}(n_1 n_2 0) = (k')^2 \sqrt{\frac{2a}{\pi}}.$$

The matrices are now completely determined.

In conclusion, I wish to express my thanks to Prof. P. S. Epstein for suggesting this and related problems, and for his advice while the work was in progress.

References.

(1) Epstein and Muskat, Proc. Nat. Acad. Sciences, vol. xv. no. 5 (1929).
(2) Y. Sugiura, Phys. Rev. vol. xxxiv. no. 6 (1929).
(3) J. R. Oppenheimer, *Zeits. f. Phys.* xli. p. 268 (1927).
(4) G. Temple, Proc. Roy. Soc. A, cxxi. (1928).
(5) P. S. Epstein, Phys. Rev. vol. xxviii. no. 4 (1926).
(6) E. Fues, *Ann. Phys.* p. 80 (1926).
(7) N. Nielsen, 'Cylinderfunktionen,' p. 184.

LVIII. *Current Flow in a Circular Disk.* By J. H. Awbery, *B.A., B.Sc., F.Inst.P., Physics Department, National Physical Laboratory, Teddington, Middlesex* *.

Introduction.

IT is proposed in this paper to determine the electrical resistance of a circular disk when current is led in at two points, A and E (see fig. 1), the potential difference being observed at two other points, P, Q, on the same diameter as A, E. The current terminals and also the potential terminals are to be disposed symmetrically with respect to the centre O of the disk. (In fig. 1, A and E are shown further from the centre than P and Q, but the results obtained will still apply if they are nearer.) The electrodes project through the whole thickness of the disk.

Fig. 1.

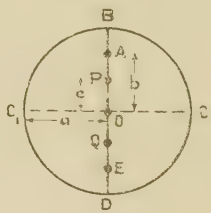

In the theory the potentials at A and E will be infinity, but this does not affect the application of the theory to cases where the potential electrodes do not coincide with the current electrodes ; the former will lie on an equipotential curve which is unaffected by any change occurring within the curve marked out by any equipotential which completely surrounds the current terminal. In theory, as in practice, we may take the diameter OC to be at zero potential, where OC is perpendicular to OB.

Calculation of Potential at any Point of Disk.

To solve the problem just enunciated we shall use the method of conformal representation, and to simplify the calculations we restrict ourselves to the hemisphere BCDEOPB. The resistance of the whole disk will be one-half of that found for the hemisphere.

* Communicated by Dr. G. W. C. Kaye, O.B.E.

Let OB = OC = a, OA = OE = b, OP = OQ = c, and let the potentials at B, D be $\pm V_0$.

It is clear that AE is one flow-line and that ABCDE is another. We use a flow function U such that U = 0 along ABCDE and U = U_0 along AE. Then writing $w = U + iV$, the electrical diagram is that of fig. 2, where potential V is measured vertically and U is measured horizontally.

To convert this figure into the hemisphere of fig. 1 we transform each into a straight line as an intermediary, as shown in fig. 3, which is lettered to correspond to figs. 1 and 2.

Fig. 2.

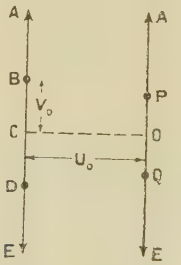

Fig. 3.

Consider first the transformation

$$t = (z+ia)^2/(z-ia)^2, \quad . \quad . \quad . \quad . \quad . \quad . \quad (1)$$

where t is the variable, say $(r+is)$, in fig. 3, and $z = (x+iy)$ is that in fig. 1.

Then

$$r+is = [x+i(y+a)]^2/[x+i(y-a)]^2$$
$$= [(x^2+y^2-a^2)+ix(2a)]^2/[x^2+(y-a)^2]^2,$$

or, equating the real and the imaginary parts,

$$r = [(x^2+y^2-a^2)^2-4a^2x^2]/[x^2+(y-a)^2]^2,$$
$$s = 4ax(x^2+y^2-a^2)/[x^2+(y-a)^2]^2.$$

It follows at once that s is zero or t is a real quantity if either $x=0$ or $x^2+y^2=a^2$, *i.e.* the figure in the t plane is the real axis (fig. 3) when the z figure is the semicircle $x^2+y^2=a^2$, with the diameter $x=0$ (BD in fig. 1). The corresponding values of t and z for the points with which we are concerned are found (by substitution in equation 1) to be :—

At B. $z=ia$ and $t=\pm\infty$.

A. $z=ib$ „ $t=(b+a)^2/(b-a)^2$.

P. $z=ic$ „ $t=(c+a)^2/(c-a)^2$.

O. $z=0$ „ $t=1$.

Q. $z=-ic$ „ $t=(a-c)^2/(a+c)^2$.

E. $z=-ib$ „ $t=(a-b)^2/(a+b)^2$, which is $1/t_A$.

D. $z=-ia$ „ $t=0$.

C. $z=a$ „ $t=(1+i)^2/(1-i)^2=-1$.

Thus it appears that equation (1) transforms fig. 1 to fig. 3. To establish a correspondence between figs. 1 and 2 we must transform the latter also to the straight line fig. 3.

To effect this we have the theorem of Schwarz and Christoffel (see Jeans, 'Electricity and Magnetism,' 3rd edition, p. 271), which gives the differential relation between w and t for the present case in the form

$$dw/dt = A(t-t_A)^{-1}(t-t_E)^{-1} = At_A/(t-t_A)(tt_A-1),$$

using t_A to represent the quantity $(b+a)^2/(b-a)^2$, the value of t at the point A.

From this equation

$$w = B + At_A \int \frac{dt}{(t-t_A)(tt_A-1)},$$

where A and B are constants to be subsequently determined.

Now

$$\int \frac{dt}{(t-t_A)(tt_A-1)} = \frac{1}{(t_A^2-1)} \log_e\left(\frac{t-t_A}{tt_A-1}\right),$$

so that, taking a new constant C, we find

$$w = B + C \log_e\left(\frac{t-t_A}{tt_A-1}\right). \quad . \quad . \quad . \quad . \quad . \quad (2)$$

We require the diagrams to correspond as follows :—

Point.	Value of w.	Value of t.
A	i	t_A
B	i	∞
C	0	-1
D	$-i$	0
E	$-i$	$1/t_A$
O	U_0	1

and it will be found that all these are satisfied if $C=-iU_0/\pi$ and $B=0$, together with the condition

$$\pi V_0 = U_0 \log t_A. \quad . \quad . \quad . \quad . \quad . \quad (2\,a)$$

Eliminating t from the equations (1) and (2), we find the relation between w and z in the form

$$e^{iw\pi/U_0} = \frac{(z+ia)^2 - t_A(z-ia)^2}{(z+ia)^2 t_A - (z-ia)^2}. \quad . \quad . \quad . \quad (3)$$

Writing $w = u+iv$, the real part of the left-hand side is

$$e^{-\pi V/U_0} \cos \pi U/U_0,$$

and the imaginary part is

$$ie^{-\pi V/U_0} \sin \pi U/U_0.$$

Similarly, substituting $(x+iy)$ for z, and rationalizing the denominator, the right-hand side of equation (3) reduces to the form $F(x, y)+iG(x, y)$, where

$$\begin{aligned}\Delta \,.\, F(x, y) = &[\{x^2(1-t_A)-(y+a)^2+t_A(y-a)^2\} \times \\ &\{x^2(t_A-1)-(y+a)^2 t_A+(y-a)^2\} \\ &+4x^2\{a^2(1+t_A)^2-y^2(1-t_A)^2\}],\end{aligned}$$

and

$$\begin{aligned}\frac{\Delta}{2x} \,.\, G(x, y) = &[\{y(1-t_A)+a(1+t_A)\}\{x^2(t_A-1) \\ &-(y+a)^2 t_A+(y-a)^2\} \\ &-\{x^2(1-t_A)-(y+a)^2+t_A(y-a)^2\}\{a(1+t_A)-y(1-t_A)\}].\end{aligned}$$

Here Δ has been written as an abbreviation for

$$\begin{aligned}&[x^2(t_A-1)+(y-a)^2 t_A+(y+a)^2]^2 \\ &\quad +4x^2[a(t_A+1)-y(1-t_A)]^2.\end{aligned}$$

By equating the real and imaginary parts of equation (3), and then squaring and adding the resulting equations, we obtain an expression for the potential V at any point of the disk,

viz., $$e^{-2\pi\overline{V}/U_0} = \{F(x, y)\}^2 + \{G(x, y)\}^2.$$

Resistance of Disk when all Electrodes lie on one Diameter.

At present, however, we are interested only in the potential along the diameter BD, so that, setting $x = 0$, the equation simplifies to

$$\Delta_0^2 e^{-2\pi\overline{V}/U_0} = [\{t_A(y-a)^2 - (y+a)^2\}\{(y-a)^2 + (y+a)^2 t_A\}]^2,$$

or

$$\Delta_0 e^{-\pi\overline{V}/U_0} = \pm[t_A(y-a)^2 - (y+a)^2][(y-a)^2 - (y+a)^2 t_A],$$

where Δ_0 is the value of Δ when $x = 0$, so that

$$\Delta_0 = [(y-a)^2 - t_A(y+a)^2]^2.$$

Thus

$$e^{-\pi\overline{V}/U_0} = \pm[t_A(y-a)^2 - (y+a)^2]/[(y-a)^2 - (y+a)^2 t_A], \quad . \quad . \quad . \quad (4)$$

where the ambiguous sign is to be interpreted so that the right-hand side is positive, since the exponential of a real number cannot be negative. In fact, the negative sign must be taken if $y < b$ and the positive if $y > b$. The limiting point is the point A, fig. 1, where

$$\overline{V} = \infty \quad \text{or} \quad e^{-\pi\overline{V}/U_0}$$

vanishes; on passing this point we move from one flow-line to another.

Taking logarithms of equation (4) we find finally that

$$\overline{V} = \frac{U_0}{\pi}\log_e \pm\left[\frac{(y-a)^2 - (y+a)^2 t_A}{t_A(y-a)^2 + (y+a)^2}\right], \quad . \quad . \quad (5)$$

an explicit expression for the potential $\overline{V}$ at any point y on the diameter BD.

U_0 is, of course, the total current flowing in the hemisphere between the two points A and E, whilst $\overline{V}$ is the potential of any point P in the diameter. The potential difference between P and Q, fig. 1, is twice this, so that inserting the resistivity ρ and thickness l of the material, the resistance of the hemisphere is $2\rho\overline{V}/lU_0$, or substituting

the value of t_A, writing c for y, and halving the value so as to obtain the resistance R of the whole circle, we find

$$R = \frac{\rho}{\pi l} \log \pm \left[\frac{(c-a)^2(b-a)^2-(c+a)^2(b+a)^2}{(b+a)^2(c-a)^2-(c+a)^2(b-a)^2}\right],$$

where a, b, c are the dimensions, as marked in fig. 1.

It is of interest to notice that this result gives an example of a reciprocal theorem ; the resistance is unaltered if the current is led in at the points which were originally potential terminals, and the potential measured at the original current terminals. A second point of interest is to note that for a constant thickness the resistance is independent of the size of the disk, provided that geometrical similarity is maintained.

Particular Cases: *Solution by "Point Charges."*

Among particular cases we notice that if $c = 0$ the resistance reduces to zero, as it should do since the potential difference vanishes.

If $c = b$ it becomes

$$\frac{\rho}{\pi l} \log \pm \left[\frac{(c-a)^4-(c+a)^4}{(c^2-a^2)^2-(c^2-a^2)^2}\right] = \infty .$$

This is to be expected, since now the potentials at the measuring points are infinitely great.

Finally, when $b = a$, the current terminals being now attached on the circumference of the circle,

$$R = \frac{\rho}{\pi l} \log \pm \frac{4a^2(a+c)^2}{4a^2(c-a)^2} = \frac{2\rho}{\pi l} \log \frac{a+c}{a-c}.$$

This result, as a matter of fact, may be very easily deduced by the method of "sources and sinks." Taking a point source of strength Q at B, and one of strength $-Q$ at D, the potential due to the former at the point (x, y) is

$$-\frac{Q}{2\pi} \log r = -\frac{Q}{4\pi} \log [x^2+(y-a)^2],$$

where r is the distance of (x, y) from B. Thus the potential due to the two together is

$$\frac{Q}{4\pi} \log \left[\frac{x^2+(y+a)^2}{x^2+(y-a)^2}\right],$$

which clearly makes the circumference a flow-line. On the diameter BD it reduces to

$$\frac{Q}{2\pi} \log \frac{y+a}{y-a},$$

or in the previous notation to

$$(Q/2\pi)\ \log\left(\frac{c+a}{c-a}\right).$$

Now the source Q at B emits quantity Q per unit time, of which only Q/2 flows within the circle, the remainder flowing outside. Thus the current in the whole circle is Q/2, and the potential difference between P and Q (fig. 1) is

$$\frac{Q}{\pi}\log\frac{c+a}{c-a}.$$

Consequently the resistance of the whole circle is

$$\frac{2\rho}{l\pi}\log\frac{c+a}{c-a},$$

as found by the other method.

Error due to slight Displacement of Electrodes.

Reverting to the general problem, we may pertinently enquire, with a view to practical application, what will be the effect on the resistance if any of the points is slightly displaced from its assumed position. These errors could of course be found by direct calculation, since the general expression for the potential is known, but such numerical calculation gives no clue as to the general effect of a displacement.

If the point P is slightly displaced laterally, so that its co-ordinates are $(\delta x, c)$, it will be seen that the real part of the right-hand side of equation (3) is not affected to the first order, whilst the imaginary part contains δx as a factor. Thus, on squaring and adding these, the potential difference is affected only to the second order of small quantities. Physically this is, of course, due to the fact that the equipotentials cut BD at right angles, so that any slight lateral variation moves a point along a single equipotential. Clearly the same applies to a lateral displacement of the point A.

If the displacement of P from the symmetrical position takes place along the diameter, so that y becomes $(c+\delta c)$, then expression (5) will hold for the potential at P, but with $(c+\delta c)$ written in place of y.

We thus find that $\pi V/U_0$ is approximately

$$\log \pm \begin{bmatrix} (c^2+a^2-2ac-2a\,\delta c-2c\,\delta c) & i\lambda(c^2+2c\,\delta c+a^2+2ac+2a\,\delta c) \\ i\lambda(c^2+2c\,\delta c+a^2-2ac-2a\,\delta c) & -(c^2+2c\,\delta c+a^2+2ac+2a\,\delta c) \end{bmatrix},$$

which reduces to

$$\log \pm \begin{bmatrix} (c^2+a^2)(1-t_A)-2ac(1+t_A) \\ (c^2+a^2)(t_A-1)-2ac(1+t_A) \end{bmatrix} \times \left[1+\frac{\delta c\,(2c-2a-2ct_A-2at_A)}{(c^2+a^2)(1-t_A)-2ac(1+t_A}-\frac{\delta c\,(2ct_A-2at_A-2c-2a)}{(c^2+a^2)(t_A-1)2ac(t_A+1)}\right],$$

or, expanding the logarithm of the second factor, $\pi\bar{V}/U_0$ is approximately

$$\log \pm \left[\frac{(c^2+a^2)(1-t_A)-2ac(1+t_A)}{(c^2+a^2)(t_A-1)-2ac(1+t_A)}\right] + \delta c\left[\frac{2(c-a)-2t_A(c+a)}{(c^2+a^2)(1-t_A)-2ac(1+t_A)} - \frac{2(c-a)t_A-1(c+a)}{(c^2+a^2)(t_A-1)-2ac(t_A+1)}\right].$$

Thus the potential difference between P and Q (since Q is unaltered) is increased * by

$$\frac{2U_0\,\delta c}{\pi}\left[\frac{(c-a)-t_A(c+a)}{(c^2+a^2)(1-t_A)-2ac(1+t_A)} - \frac{(c-a)t_A-(c+a)}{(c^2+a^2)(t_A-1)-2ac(1+t_A)}\right],$$

or the resistance is increased by

$$\frac{\rho\,\delta c}{l\pi}\left[\frac{(c-a)-t_A(c+a)}{(c^2+a^2)(1-t_A)-2ac(1+t_A)} - \frac{(c-a)t_A-(c+a)}{(c^2+a^2)(t_A-1)-2ac(1+t_A)}\right],$$

i. e., by

$$\frac{2a\rho\,\delta c(a^2-c^2)(1-t_A^2)}{\pi l\left[2t_A\{(a^2+c^2)^2+4a^2c^2\}-(1+t_A^2)(a^2-c^2)^2\right]}.$$

This vanishes if $a=c$ (it is impossible to make $t_A^2=1$ in practice), so that the best disposition of electrodes would seem to be reached by placing the potential terminals on the circumference of the circle, as their position will not then be sensitive to slight inaccuracies of construction.

* This result also follows by differentiating equation (5) with respect to y.

LIX. *Langmuir Probe Measurements in the Normal Copper Arc.* *By* Ervin H. Bramhall *.

Abstract.

Langmuir's theory of a collector in an ionized gas is applied to the normal arc in air, the collector being a fine platinum wire which is made to swing horizontally through a section of the arc. The volt-ampere probe characteristic is obtained by interposing between the cathode and probe a small alternating potential superimposed on a direct potential of suitable magnitude, and recording the current on an oscillograph used in conjunction with an amplifier. The complete characteristic is thus obtained on a single oscillogram. It is found that the density of the drift current is of the order of 100 timesthat of the random current, which leads to the conclusion that the temperature motion of the electrons is relatively unimportant. This complicates the interpretation of the probe characteristic according to the collector theory, so that, although satisfactory measurements of space potentials in the arc are secured, it is found possible to obtain only rough approximations to the electron density and energy. The results indicate a density of the order of 7×10^{11} cm.$^{-3}$ and an average energy of 2 volts.

The voltage gradient between the cathode fall space and the anode glow is found to be non-uniform, increasing greatly close to the electrodes. By extrapolation a cathode fall within the range, 11 to 13 volts, which is considerably below that generally accepted, is obtained.

Equations for the arc characteristics based on a uniform gradient, such as those of Steinmetz and Ayrton, are shown to be untenable at short lengths.

1. Introduction.

As long ago as 1888 Letcher † used a small electrode or probe, introduced into the arc discharge, to ascertain what was known as the back e.m.f. of the arc. Since then probe methods have been used by a series of investigators ‡ to determine space potential, arc gradient, cathode and

* Communicated by Lord Rutherford, O.M., D.Sc., F.R.S.

† *Centralb. f. Elekt.* x. p. 48 (1888).

‡ (*a*) Lügin, *Wien Sitz.* xcviii. p. 1192 (1889); (*b*) Duddell, Phil. Trans. Roy. Soc. cciii. A. p. 305 (1904); (*c*) Stark, *Ann. d. Phys.* xviii. p. 213 (1905); (*d*) Skinner, Phys. Rev. xii. p. 143 (1918); (*e*) Chrisler, Astrophys. Journ. liv. p. 273 (1921).

anode falls, and arc resistance ; employing, however, either a capacity or high resistance in series. Their results for the most part were rendered invalid by Langmuir and Mott-Smith *, who showed that under the condition of practically zero probe current the probe assumes a potential at which the number of positive ions absorbed is equal to the number of electrons, and that this potential differs considerably from the space potential.

It was shown that if the ions collected by a probe have a random or Maxwellian distribution the logarithm of the probe current is a linear function of the probe potential with respect to space, if this potential is such that arriving electrons are retarded, *i. e.*, negative. The slope of this line and the point where this slope changes provide information from which the space potential, the electron concentration, and the distribution temperature may be calculated.

The Langmuir probe (utilizing the above principle) is most readily adapted to the study of low-pressure discharges in which the temperature is not too high to permit the continuous immersion of the probe. It has been used thus by Emeléus†, Uyterhoeven ‡, and others in the low-pressure glow discharge, and by Compton, Van Voorhis §, and others in the mercury arc. Nottingham ‖ has recently extended its use to arcs between metal electrodes at normal pressure by swinging the probe at a known rate through the arc and measuring the total charge through the probe circuit at different voltages on a ballistic galvanometer.

The present investigation deals with the conditions existing in the arc between copper electrodes at atmospheric pressure. The principle of the Langmuir probe is utilized in so far as limitations imposed on it by the experimental conditions allow.

It is realized that the collector theory of Langmuir and Mott-Smith is not strictly applicable to the study of high-pressure discharges in which the electronic mean free path is so short that collisions in the ion sheath surrounding the collector can no longer be neglected. An application of the theory is, however, of importance if for no other reason than to indicate to what extent it may be relied upon to elucidate the complicated processes occurring in the normal

* Phys. Rev. xxviii. p. 727 (1926); Gen. Elect. Rev. xxvii. pp. 449, 538, 616, 762, 810 (1924).

† Camb. Phil. Soc. Proc. xxiii. p. 531 (1927).

‡ Nat. Acad. Sci. Proc. xv. p. 32 (1929).

§ *Ibid.* xiii. p. 336 (1927).

‖ Franklin Inst. Journ. ccvi. p. 43 (1928); ccvii. p. 299 (1929).

arc ; for it is indisputable that the probe method is the most powerful yet available for this purpose.

2. Theoretical Considerations.

The Collector Characteristic.

The complete current-voltage characteristic consists of three distinct parts :—

(*a*) When the probe is sufficiently negative to repel all electrons its current is small and consists entirely of positive ions which form a sheath around it of such a thickness that the probe exerts no influence beyond its boundaries.

(*b*) As the potential is made less negative, so that some electrons are able to pierce the sheath in spite of the retarding potential, the net positive ion current falls off and finally changes sign. This is the region where the Langmuir probe characteristic,

$$i = \mathrm{I}A\epsilon^{\left(\frac{eV}{KT}\right)}, \quad . \quad . \quad . \quad . \quad . \quad . \quad . \quad (1)$$

obtains. I is the random electron current density * in amps./cm.^{2} (*i. e.*, the random electron current at space potential divided by the area of contact, A, between the probe and the ionized gas), V is the probe potential with respect to that of space, e is the electronic charge, $1{\cdot}59 \times 10^{-19}$ coulombs, K is the Boltzmann constant, $1{\cdot}37 \times 10^{-16}$ ergs per degree, and T is the temperature corresponding to the Maxwellian distribution of electrons.

(*c*) When the space potential is reached the sheath, which has been decreasing in thickness, vanishes. The collector then receives the random, electron, and positive ion currents. The latter is so small as to be practically negligible compared with the former because of the relatively low speeds of the heavy positive ions ; and the total current is therefore negative.

The above considerations apply in their entirety only to the ideal case of ions having a purely thermal distribution. Actually this condition is never strictly fulfilled in any electric discharge, since there is always a drift of electrons

* The random current density is defined as the current in one direction due to the random motion of electrons through unit area of a plane perpendicular to that direction, and is given by the relation

$$\mathrm{I} = \frac{nev}{4},$$

n being the electron concentration, and $\bar{v}$ the mean velocity of thermal agitation.

and ions towards the electrodes, this constituting the current through the external circuit. In low-pressure discharges * the random and drift currents seem to be of about the same magnitude, but no previous determination of the relative magnitudes of these quantities has been made for the normal arc discharge between metal electrodes. It is therefore important to estimate the ratio of drift to random current densities, I_d/I, and to allow for its influence in the interpretation of results.

Fig. 1.

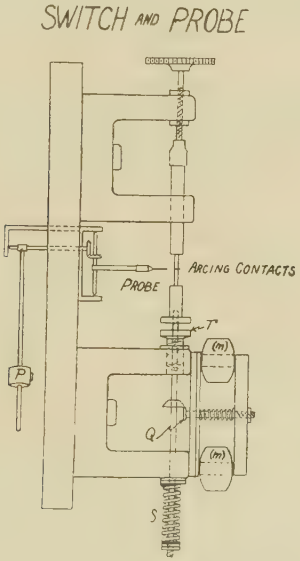

3. Experimental Procedure.

The arc is drawn between $\frac{1}{8}$-in. copper electrodes arranged in a vertical position as in fig. 1, the lower electrode being the cathode (negative). An insulated platinum probe, 0·012 in. diam., swings horizontally through the arc at the rate of 13 cm./sec., which remains practically constant for the short period it is in contact with the arc. The probe potential is adjusted by means of a battery interposed between the probe and cathode.

The entire sequence of operation necessary to draw the arc, record the transient phenomena, and break the circuit

* Emeléus, 'Conduction of Electricity through Gases,' p. 50

is performed automatically by a series of contacts operated by a falling weight. The total time elapsing between the make and break of the arc is thus made a small fraction of a second, thereby minimizing contact oxidation and other effects which tend toward non-uniformity of operation.

Methods of Measurement.

(a) *Using the Ballistic Galvanometer.*

To obtain the Langmuir probe characteristic, the method of Nottingham * was first tried. A ballistic galvanometer measures for different potentials the total charge, Q, picked up by the probe as it swings through the arc. Q is proportional to i_p, the current per unit length of the probe, in accordance with the relation

Fig 2.

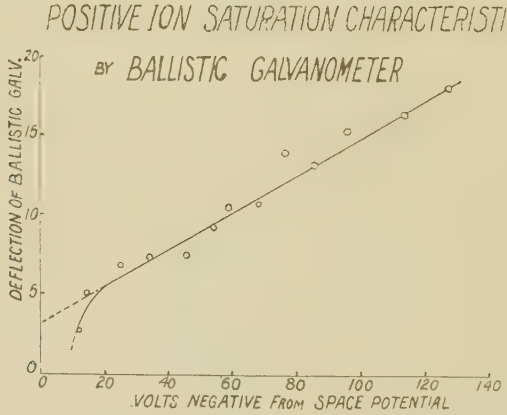

$$Q = \pi R_a^2 i_p / u,$$

where R_a is the arc radius and u is the probe velocity.

The positive ion saturation characteristic (fig. 2) could be obtained by this method, but in the region where equation 1) applies the results were too erratic to be satisfactory.

It is observed in connexion with this experiment that even with a probe potential 140 volts negative from space, that is, more negative by a value in excess of 100 volts than the cathode itself, the discharge is not interrupted. This

* *Loc. cit.*

illustrates the importance of a high cathode temperature in the low voltage arc, since the existence of such a temperature, producing an electron source in the cathode, is the only real distinction between it and the probe.

Fig. 3.

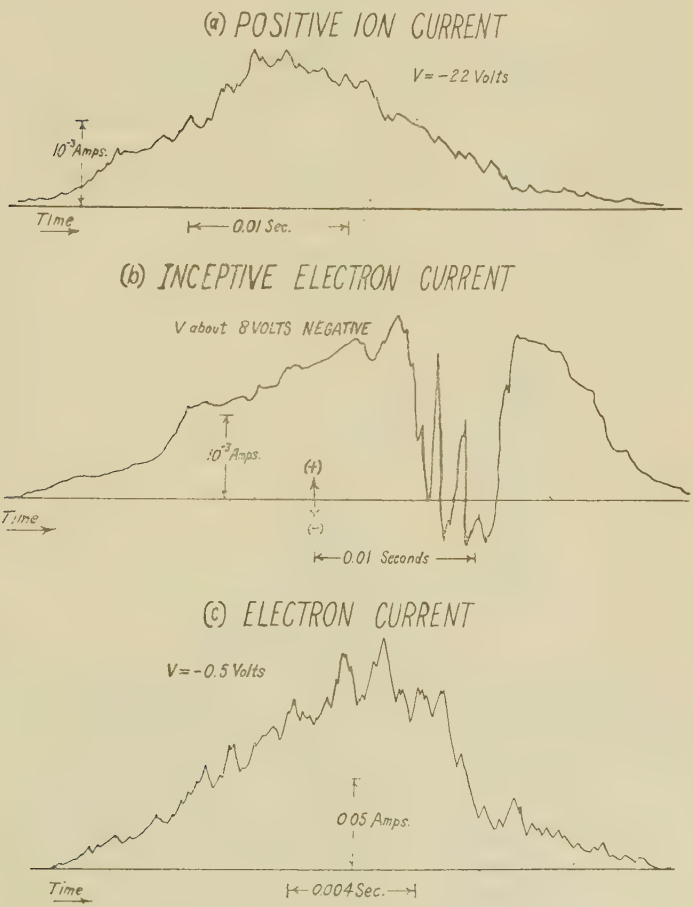

(b) *Using the Oscillograph with Amplifier.*

Alternatively the oscillograph was used in conjunction with a resistance coupled amplifier. Fig. 3 represents typical examples of records taken at different probe potentials. In (*a*) only positive ions are being collected—the probe potential is sufficiently negative to repel all electrons, so that

the current is small and positive. In (*c*) the current consists almost entirely of electrons, so that the current is large and negative.

As the probe voltage with respect to the cathode is raised in successive steps, approaching space potential, it is interesting to note the effect on the probe current. The maximum current (fig 3 (*a*)) decreases slightly, due to the decreasing thickness of the positive ion sheath and the consequent reduction in the contact area between the probe and arc; otherwise there is little disturbance until the potential is about 10 volts below that of space. Then indentations appear, due to the penetration of electrons into the sheath, particularly toward the centre of the arc, where the electron energy is maximum, as is evident in fig. 3 (*b*). Finally, the

Fig. 4.

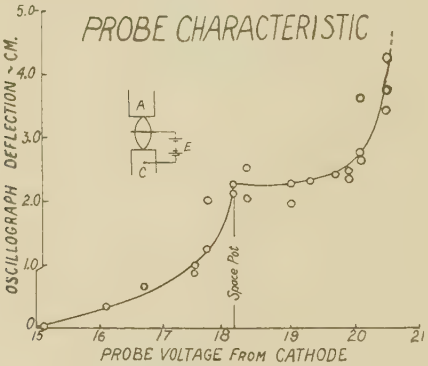

current completely reverses in direction and increases greatly in magnitude, its character being generally irregular (fig. 3 (*c*)). This explains the erratic behaviour of the ballistic galvanometer when used to measure the electron current.

By measuring the variation of probe current near the centre of the arc as the potential is raised it was found possible to obtain the characteristic (fig. 4) provided that a sufficient number of records were taken However, a more promising and less laborious method was devised, making use of an alternating probe potential.

When the peak of the alternating voltage is high enough to intersect the space potential the resulting current is represented in fig. 5. This oscillogram shows clearly the rapid variation of probe current as the space potential is approached, and suggests that the Langmuir probe characteristic might be obtained directly if, in the proximity of

space potential, the probe voltage were to vary more slowly.

This condition is fulfilled by the superposition of a small alternating potential on to a relatively high continuous voltage. Fig. 6 is an oscillogram thus obtained, the probe

Fig. 5.

PROBE CURRENT WITH ALTERNATING P. D.

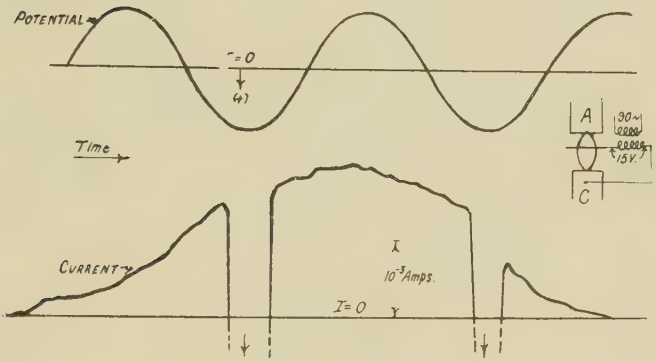

Fig. 6.

OSCILLOGRAM OF PROBE CURRENT AND VOLTAGE

24 Volts D.C. and 3 Volts A.C. on Probe

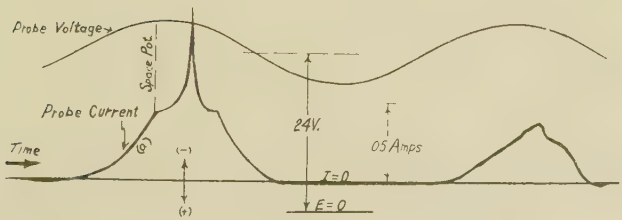

voltage being 3 volts, r.m.s., and 24 volts, d.c., with respect to the cathode. It was taken with the probe at a distance, *a*, 0·34 cm. from the cathode, with an overall arc length, *b*, of 0·39 cm., and an arc current of 7·5 amp. On this oscillogram the voltage vibrator measures the total probe voltage. Actually greater accuracy is attainable when this vibrator is connected only across the alternating potential.

4. Experimental Results.

The Ratio of Drift to Random Currents.

Fig. 7 shows that the semi-logarithmic plot of section (*a*) (fig. 6) is noticeably convex towards the voltage axis. According to the theory of Langmuir and Mott-Smith such a deviation from a straight line relationship signifies the existence of a ratio of drift to random currents high enough to influence the interpretation on the assumption of a purely thermal electron distribution of the probe characteristic. Consequently it is necessary to estimate this ratio.

Fig. 7.

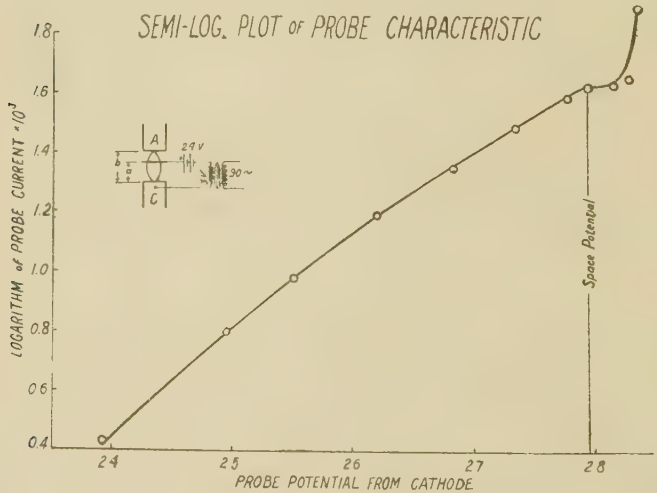

The drift current density,

$$I_d = \frac{I_a}{\pi R_a^2},$$

depends on the arc current, I_a, and the arc radius, R_a, at the section where the probe is introduced. The probe velocity being known, it is possible to estimate the arc diameter by noting the time on the oscillogram of probe current during which there is an observable deflexion. The result depends on the contribution of the region, consisting of ionized gases, surrounding the central nucleus towards the total current, the probe potential with respect to space, and the amplifier sensitivity. Therefore, since there is no evident manner of correlating the probe position with time on the oscillogram,

to obtain an unambiguous measure of R_a it is necessary to resort to a roundabout method.

As the probe enters the region surrounding the arc nucleus the current density to it should increase slowly at first, due to the increasing temperature and ion density. A greater increase should be noted as soon as the nucleus is reached, and thereafter the density of the probe current should remain more or less uniform. Consequently a study of the variation of probe current density, i, with the distance, X, between the centre-lines of probe and arc should afford a means of calculating R_a.

For a constant arc area the area of contact between the probe and arc depends on the effective probe radius which is the probe radius, c, plus a positive ion sheath of thickness, σ, which varies with the probe potential with respect to space. It is found that the experimental positive ion saturation characteristics correspond roughly to $\sigma = 0{\cdot}017\,c\mathrm{V}$ when $\mathrm{V} < -15$ volts, *i. e.*, sufficient to repel practically all electrons. The theory * for a plane collector gives

$$\sigma = \frac{k\mathrm{V}^{3/4}}{\sqrt{\mathrm{I}_p}},$$

where I_p is the positive ion current density and k is constant. The difference between the two relations may be attributed to high pressure effects, probe curvature, and sheath distortion due to the drift.

From the foregoing the quantity $(c+\sigma)$ is known for a specific example, and for convenience is made equal to unity. Then oscillograms such as fig. 3 (*a*) are readily convertible to curves giving the variation of positive ion current with X in units. Since, according to fig. 10, the increase of the area of contact, A, with X is almost linear until A is about 60 per cent. of the maximum, in this region the total current as a function of X should have the same form as that of the current density. In the example (fig. 8) the curve (*a*) is the total current. At P, the point where the slope changes, $\mathrm{X} = 11$ units and $i = 11$ per cent This latter represents the contribution of the region surrounding the arc nucleus, and must be subtracted from the total current to obtain that part which may properly be ascribed to the nucleus alone. Subtracting 11 per cent. from the ordinates of (*a*) and multiplying by 100/89 (to make the maximum current 100 per cent.) curve (*b*) is obtained, which is the true

* Emeléus, *ibid.* p. 43.

variation of i with X. The arc radius is in this case (11 − 1), or 10 units.

The calculation of R_a by the method of fig. 8 at different sections along the arc stream does not produce very consistent results, especially when a, the distance from the cathode, is large. The data for the conditions, $I_a = 8$ amp., $b = 1{\cdot}2$ cm., and a from 0·1 to 0·5 cm., conform roughly to the equation

$$B = 0{\cdot}005 + 0{\cdot}21\,a,$$

where B is the arc area and is πR_a^2. This gives a current density at the cathode, ($a = 0$), of 1600 amp./cm.², which, however, is unreliable because practical considerations impose

Fig. 8.

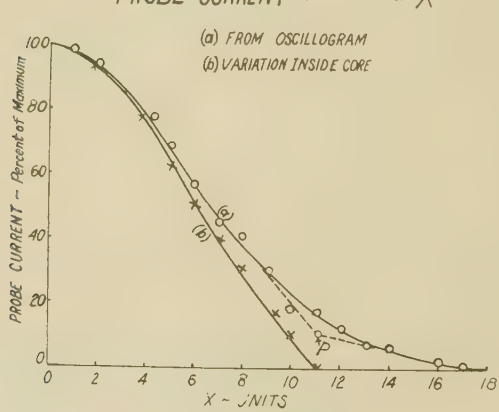

a lower limit of about 1 mm. on a, this being insufficiently close to justify extrapolation to the cathode. Otherwise the cathode current might be obtained directly. The drift current density calculated from (10) varies from 310 at $a = 0{\cdot}1$ cm. to 70 amp./cm.² at $a = 0{\cdot}5$ cm.

The literature on the subject is singularly lacking in directly comparable data, and the current density at the cathode is not known even approximately. It undoubtedly lies between 250 and 7000 amp./cm.², the values given by Compton * for carbon and iron, and is probably within the range given for tungsten, viz., 700 to 3200 amp./cm.². Compton's value for the current density in the middle of a *carbon* arc is 50 amp./cm.².

* Phys. Rev. xxi. p. 266 (1923); Journ. A. I. E. E. xlvi. p. 1192 (1927).

Since for short arcs any sectional area, and consequently the current density, varies with the total arc length, it is next to impossible to formulate a general law, and it becomes necessary to determine the area experimentally for each set of conditions. By the method described an accuracy not greater than 50 per cent. could be expected.

In the absence of a drift velocity, *i. e.*, for a purely thermal distribution, the electron current at space potential divided by the contact area would be the random current density, I. This amounts to between 1 and 5 amperes per square cm. in the present experiments, which, however, may differ considerably from the true random current because of the electron drift. In lieu of more accurate experimental data it can only be concluded that the ratio, (I_d/I), appears to be very high, and may exceed 100. This is much higher than in the low-pressure discharge, where the ratio seems to be about unity *.

Analysis of the Probe Characteristic.

The work of Langmuir and Mott-Smith † shows that, due to such a high ratio, the probe characteristic should approach one of two limiting forms corresponding to the case of ions having a large drift velocity on which is superimposed a relatively small temperature motion :

(1) When the retarding voltage, V, is small compared to V_0, the voltage equivalent of the drift velocity, in the limit as the temperature decreases,

$$i = 2cl\mathrm{I}\sqrt{1+\mathrm{V}/\mathrm{V}_0} \quad \text{for V greater than } -\mathrm{V}_0,$$
$$= 0 \quad \text{for V less than } -\mathrm{V}_0,$$

in which c and l are the radius and length of the cylindrical collector.

(2) When the retarding voltage is nearly equal to or greater than V_0, the temperature motion though, small, becomes important as $-V$ approaches V_0. For λ positive

$$\left(\lambda = \sqrt{\frac{e}{\mathrm{KT}}}\left(\sqrt{\mathrm{V}_0}-\sqrt{-\mathrm{V}}\right)\right),$$

the current is approximately a parabolic function of (V_0-V), while with λ negative the current decreases rapidly, $\log i$ becoming nearly a linear function of λ^2.

* Emeléus, 'Conduction of Electricity through Gases,' p. 50.

† Phys. Rev. xxviii. p. 727 (1926); Gen. Elect. Rev. xxvii. pp. 449, 538, 616, 762, 810 (1924).

From the form of the probe current-voltage curve (fig. 7), it is evident that the relative importance of the temperature and drift motions in the arc is such that (2) is the limiting form. This means that the temperature motion is great enough to become important when the retarding voltage, V, is small. The plot of

$$\sqrt{\log\left(\frac{1}{i}\right)} \text{ vs } \sqrt{-\mathrm{V}}$$

should be approximately linear when V is less than $-\mathrm{V}_0$. Fig. 7 is replotted, using these coordinates as in fig. 9. The curve is linear for $\sqrt{-\mathrm{V}} > 0{\cdot}8$, so that the theory gives

$$\mathrm{V}_0 = (0{\cdot}8)^2 = 0{\cdot}64.$$

Fig. 9.

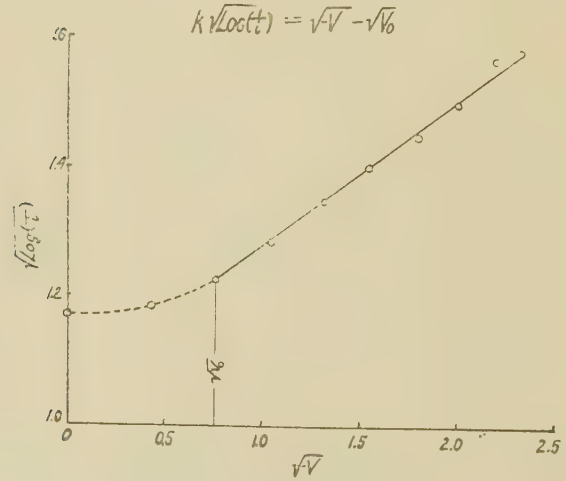

Electron Density and Energy.

If u_0 is the drift velocity and e is in e.s.u., it follows that

$$\mathrm{V}_0 = \frac{mu_0^2}{2e}.$$

Thus,

$$u_0 = \left(\frac{2e\mathrm{V}_0}{m}\right)^{1/2} = 0{\cdot}82 \times 10^9 \text{ cm./sec.}$$

Since the drift current density is

$$\mathrm{I}_d = \frac{neu_0}{3 \times 10^9},$$

the electron density is

$$n = \frac{3 \times 10^9}{eu_0} I_d.$$

Taking $I_d = 100$ amp./cm.^{2}, $n = 7{\cdot}7 \times 10^{11}$. This compares with $1{\cdot}8 \times 10^{10}$ and $11{\cdot}4 \times 10^{10}$ given by Emeléus † for low-pressure mercury discharges.

The approximate slope of the curve (fig. 7) near space potential is 0·55 ; so that the apparent electron distribution temperature, neglecting the influence of the drift velocity, is

$$T = \frac{e}{0{\cdot}55\,K} = 20{,}900° \text{ C.},$$

and the equivalent energy is 2·7 volts. These and other representative data similarly obtained for different conditions in the arc are incorporated in the following table.

				Column 1 (central).			Column 2 (side).	
I_a (amp.).	a (cm.).	b (cm.).	e_a (volts).	e_3 (volts).	T (° C.).	e_s*.	e_s.	T.
7·5	0·05	0·39	37·8	20·1				
	0·05	...	..	19·5	...	18·5		
	0·11	...	...	24·0	18,300	22·0	22·8	
	0·26	...	...	24·1				
	0·26	...	...	23·8	...	23·0		
	0·34	...	...	28·1	...	...	27·9	10,300
	0·34	...	...	27·2	16,700	26·5	27·7	8,850
	0·34	...	...	28·0	20,900			
4·1	0·18	0·32	46·0	25·5	7,900	23·5		
	0·26	0·49	58·0	30·5	...	29·4		
2·9	0·26	0·49	70·0	...	...	38·0	38·9	

* Indicated space potential corrected for voltage rise due to the introduction of the probe.

b is the arc length and a is the distance between the cathode and the plane section covered by the probe as it swings through the arc. The data of column 1 correspond to a probe position nearly central in the arc, while that of column 2 is for a lateral position.

The electron energy calculated from the temperatures of the table varies from 2·1 to 2·7 volts, but this is merely an

† 'Conduction of Electricity through Gases,' pp. 49, 51.

indication of its magnitude, since the error due to neglecting the drift velocity is indeterminate.

Effect of Variation of Contact Area.

Equation (1) shows that the total probe current depends on the contact area between probe and arc, so that the above analysis is valid only on the assumption of constant A. If the voltage variation is sufficiently rapid, or if the probe moves sufficiently slowly, the entire characteristic can be obtained in such a short time that the probe may be considered stationary in the arc for this period, in which case A is constant. However, the accuracy of measuring the current variation on the oscillogram decreases as the time is made shorter, and this factor limits the optimum rate of change of probe voltage. A lower limit for the probe velocity is fixed by its melting-point and the relative sizes of probe and arc. With a velocity of 13 cm./sec. and a 90-cycle voltage the complete characteristic is obtained within $\frac{1}{8}$ of a cycle or $\frac{1}{720}$ sec. The distance moved by the probe during this time is 0·018 cm., which is not more than $\frac{1}{6}$ of the arc radius extant in most of the experiments.

In order to estimate the change in contact area due to a motion of this magnitude the probe and arc are assumed to behave as cylinders, and the variation of surface contact area between them for different relative sizes is obtained graphically as a function of the distance between their centre-lines. It is convenient in fig. 10 to plot areas, A, as percentage of maximum, and distances, X, in units, one unit being the radius of the smaller cylinder.

Fig. 10 shows that if the probe position is near the centre of the arc A is practically constant over a period corresponding to $\frac{1}{6}$ of the arc radius. On the other hand, for a lateral position A may vary as much as 30 per cent. In the latter case it is necessary to allow for the variation of A in obtaining the true probe characteristic. This process entails considerable labour and is of doubtful accuracy, so that with few exceptions only the former case is considered when estimating the electron energy.

Potential Distribution.

From the tabulated data the potential distribution and the potential drops at the anode and cathode can be studied. First, however, the effect on the indicated space potential of the introduction of the cold, cylindrical probe should be

considered. The most obvious consequences are : (1) distortion or lengthening of the arc stream by impeding the natural motions of the ions ; (2) a high local cooling of the gases near the probe. The magnitude of the disturbance caused by both of these depends on the relative sizes of probe and arc, and is manifested by an increased overall voltage. Oscillograms of probe current, taken as the probe is traversing the arc, are generally symmetrical, and not unlike the curve of A as a function of X (fig. 10). This constitutes evidence that (1) is not important. The explanation probably lies in the high thermal motion of the electrons.

Fig. 10.

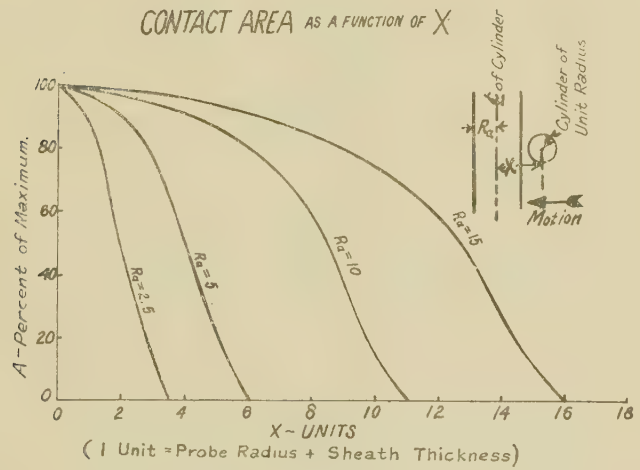

The actual rise in overall potential varies from 1 to 6 volts in the various experiments, depending on divers factors. It is necessary therefore to correct the indicated space potential for the voltage rise due to the introduction of the probe.

It seems unquestionable that the rise caused by (2) is entirely localized. In the steady state the loss of ions by diffusion and recombination at any section is exactly balanced by the number generated in that section by collisions of electrons with gas molecules. The introduction of the probe, by cooling the gas, increases the coefficient of recombination, which depends approximately on the third power of the temperature, and upsets the balance, necessitating an increased ion generation in its vicinity. This means that the

local gradient must be increased so that a higher percentage of the electrons acquire sufficient energy in the field to ionize on collision.

In accordance with this view, in obtaining the best values for space potential, half of the total voltage rise is assumed to occur between the probe and cathode, and is added to the indicated space potentials of the table.

The indicated space potential in the example (fig. 7) is 28 volts, and it is interesting to note that this is about 4 volts higher than would be obtained by the old method of measuring the potential assumed by a probe taking zero current.

Fig. 11.

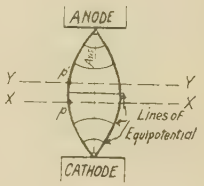

Fig. 12.

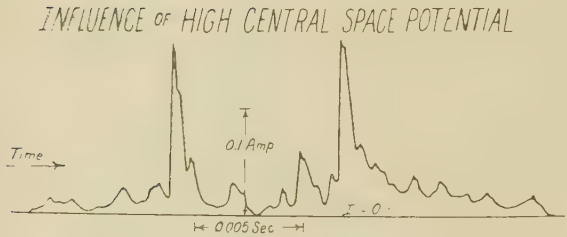

It is observed that e_s depends on the instantaneous probe position and may vary throughout the same section. There is definitely an increase or decrease in e_s when this position is towards the outer edge of the arc, according as the section considered is further from or closer to the cathode than the section bisecting the axis. The lines of equipotential in the arc are probably somewhat similar to those indicated in fig. 11. If the plane X–X is that covered by the probe it is evident that e_s is less at point p than at the axis, while the reverse is true in the plane Y–Y. This view is confirmed by an oscillogram (fig. 12) representing the former case. The arc current is 8 amperes, and the probe voltage with respect to the cathode remains constant at $+23{\cdot}5$ volts, which is slightly less than the space potential at the axis in

the section covered by the probe. The electron current is markedly higher towards the sides than at the centre, showing that the corresponding space potentials must be lower. At increased distances from the centre the current is naturally limited by the lower temperature and density of the electrons.

The potential distribution along the axis is plotted in fig. 13 for $I_a = 7{\cdot}5$ amp. and $b = 0{\cdot}39$ cm. The gradient U, which is the slope of this curve, evidently increases greatly towards the electrodes, though it becomes uniform a short distance away from them. This curve illustrates the fallacy

Fig. 13.

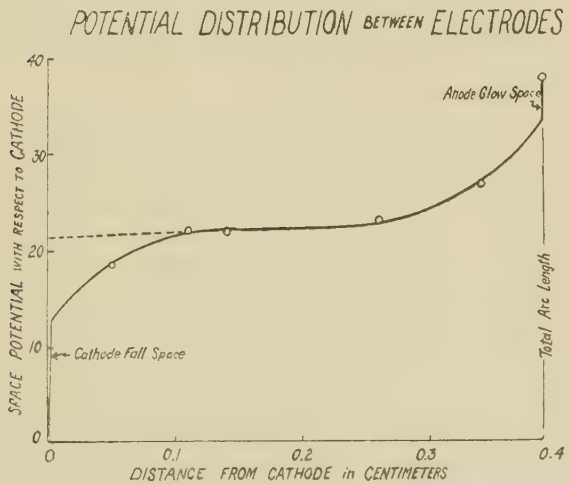

in the assumption of a uniform gradient which is commonly made *.

The increased gradient near the electrodes can be attributed to the cooling of the gas immediately adjacent, affecting the loss of ions and the gradient in the same way as did the introduction of the cold probe.

It is apparent from fig. 13 that large errors are likely to accrue if the cathode and anode falls are obtained by extrapolation to the electrodes on the basis of a uniform gradient. Particularly is this true if the gradient used is that obtaining midway between the electrodes. The closer to the cathode the potential is measured the less becomes the resulting

* Chrisler, Astrophys. Journ. liv. p. 273 (1921), also notes a non-uniform gradient.

error; but the proximity of the probe to the cathode is limited by practical considerations, so that accuracy is difficult to obtain.

If the central gradient be continued to the cathode (dotted lines, fig. 13) the present example gives 21 volts as the cathode fall. A facile experiment disproves such a high value, showing that it may be 50 per cent. or more in error. Fig. 14 reproduces an oscillogram of arc voltage taken as the contacts are separating. The minimum overall potential is only about 16 volts, and this remains practically the same for arc currents varying from 4 to 50 amperes, increasing at lower currents. The same is true for $\frac{1}{2}$-in. electrodes, so that size is not an important factor. The fact that the voltage is initially higher than this may be explained by the theory of collisions * when the arc length is less than the

Fig. 14.

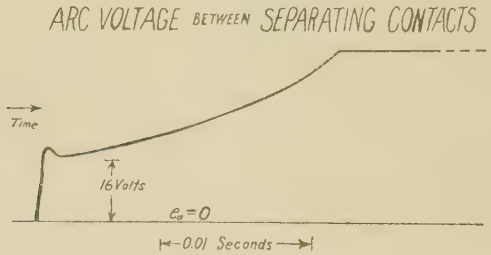

molecular mean free path. The minimum should occur when the length is equal to the thickness of the cathode fall space, in which case there is no positive column and the arc voltage is the sum of the anode and cathode falls †.

* J. J. Thomson, 'Conduction of Electricity through Gases,' p. 381; J. S. Townsend, 'Electricity in Gases,' chap. 8, 9.

† It has recently been stated (Bruce, Journ. I. E. E. lxix. p. 557 (1931)) that e_c, the contact voltage drop, which is the sum of anode and cathode falls, approaches 30 volts; and supporting experimental data are cited which give values of e_c ranging from 18 to 40 volts. However, in most of these cases the measurement was made on a low sensitivity scale—that is, the constants of the oscillograph circuit were not adjusted to give an accurate low voltage reading. The value, 16 volts, obtained above for *non-oxidized* contacts of pure copper, is probably more nearly correct, since the maximum oscillograph deflexion was made to correspond to a low voltage (about 20 volts) by limiting the arc length to a very small value. It must be remembered, however, that this value is not absolute, since the anode fall particularly is to some extent influenced by the experimental conditions.

The above fact and observations of the trend of the potential curves, similar to fig. 13, indicate a probable cathode fall within the range, 11 to 13 volts, and an anode fall from 3 to 5 volts. This latter value is applicable only for the particular experimental conditions.

As Compton * points out, the cathode fall is not necessarily the ionizing potential of the medium in which the arc is drawn, but it is interesting to note that Wahlin † gives 10·9 volts as the ionizing potential of copper vapour. In a copper arc in air at reduced pressure Hagenbach ‡ gives a cathode fall of 15·7 volts, which is nearly within the range determined. Nottingham § finds a value of 20·5 volts, but on the assumption of a uniform gradient between the probe and cathode. Chrisler ‖ gives a value of 16 volts.

Another instance occurs in the literature where the accepted cathode fall in a *tungsten* arc is greater than the overall voltage. Compton ¶ gives 16·2 volts for tungsten in hydrogen, while arcs have been obtained ** having an overall voltage less than 14 volts at 12 amperes and 17 volts at 2 amperes, the arc length being extremely short. Incidentally, if the cathode fall depends on the electron work function of the cathode material, as appears to be the case in the glow discharge ††, copper, which has a lower work function than tungsten, should also have a lower cathode fall.

Further evidence is forthcoming to show how the electrodes affect the gradient in their vicinity. After the source voltage, E, and the initial current, I_0, in a low-inductance circuit have been adjusted to the desired values, records of arc voltage similar to fig. 14 are taken as the contacts separate with an acceleration predetermined by adjustment of the spring, S, fig. 1. Then at any instant after the contacts start to separate the arc voltage and length are known. The corresponding arc current is obtained graphically or by the relation

$$I_a = I_0 (I - e_a/E).$$

The data from a number of such records taken at different initial currents, and voltages when necessary, give the characteristics at different arc lengths. For the present

* Phys. Rev. xxi, p. 266 (1923); Journ. A.I.E.E. xlvi. p. 1192 (1927).
† Phys. Rev. xxxii. p. 277 (1928).
‡ *Handb. d. Phys.* Springer, xiv. p. 335.
§ Franklin Inst. Journ. ccvi. p. 43 (1928); ccvli. p. 299 (1929).
‖ *Loc. cit.*
¶ *Loc. cit.*
** Anderson and Kretchmar, Phys. Rev. xxvi. p. 33 (1925).
†† 'International Critical Tables,' vi. (1929).

purpose it is convenient to plot e_a as a function of l for constant currents, as in fig. 15.

When l is large these curves are linear, indicating a uniform gradient, but as l decreases they become concave towards its axis. This curvature at short lengths means an increase in gradient which may undoubtedly be attributed to the proximity of the electrodes.

The average gradient, which is $(e_a - C)/l$, where C is the sum of anode and cathode falls, is obtained as a function of current with other parameters constant. The results, plotted on logarithmic paper, as in fig. 16, while not conforming exactly to the relation

$$U = kI_a^{-n},$$

Fig. 15.

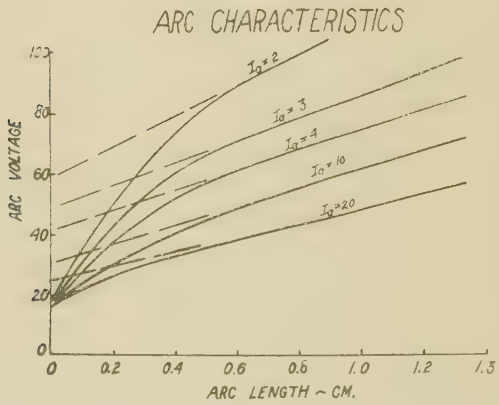

where U is the gradient and k and n are constants, do approximate to it in the range, 0·5 to 15·0 amperes. The best value of n is about 0·6. Then, since the arc area, B, varies as I_a, U varies as $B^{-0.6}$. Assuming that B varies as some power, p, of l within definite limits, $U = k_2 l^{-0.6p}$. Then

$$e_a = \int U dl = k_3 l^{(1-0.6p)}.$$

It follows that a straight line should connect $\log e_a$ and $\log l$, having a slope $(1-0.6p)$. Values of e_a and l from fig. 20 fulfil this condition very closely in the range 3 to 20 amperes, and l up to 0·25 cm. The slopes correspond to values of p from 0·92 to 0·99, decreasing with current. Therefore

within the specified limits the average arc area is approximately proportional to l, while the average gradient depends on the 0·6 power of this quantity.

For this reason equations such as those of Ayrton * and Steinmetz †, expressing the arc voltage in terms of current and length, which are based on a uniform gradient, are untenable when the arc length is short—that is, when the influence of the electrodes is important. Moreover, referring to fig. 13, the average gradient between the cathode fall space and any point in the arc depends in no simple manner on their distance apart, and has no physical significance.

Fig. 16.

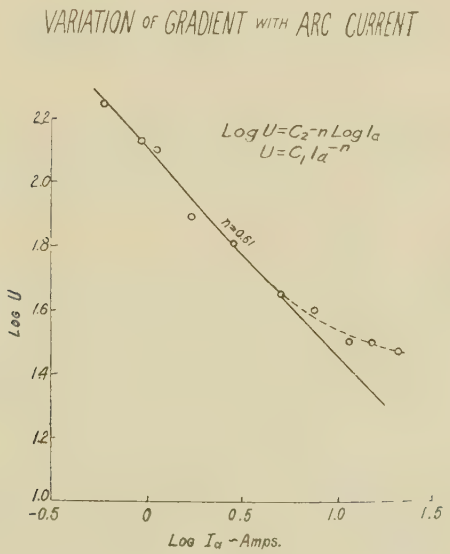

5. Summary of Results and Conclusions.

1. It may be concluded from the experimental results that the theory of the collector in an ionized gas may be applied to the case of the normal arc in air to obtain space potentials, but that extraneous factors prevent an accurate interpretation of the volt-ampere probe characteristic for the purpose of estimating the electron density and energy on the basis of this theory.

* H. Ayrton, 'The Electric Arc,' p. 186.
† C. P. Steinmetz, Trans. A. I. E. E. xxv. p. 802 (1906).

2. The probe characteristic is shown to approach a certain limiting form corresponding to a relatively small temperature motion of the electrons in the arc superimposed on a high drift velocity.

3. Measurements of sectional area in the arc stream by means of the probe give current densities from 70 to 310 amperes per square centimetre, increasing beyond this near the electrodes; and rough estimates of the actual ratio of drift to random currents show that this may exceed 100.

4. The electron density in the arc is found to be of the order of 7×10^{11} cm.$^{-3}$, and the average energy about 2 volts.

5. From measurements of space potential at various points in the arc it may be concluded that—

(*a*) The potential may not be the same throughout any sectional area. It may be higher or lower at the axis than towards the sides depending on the position of the area considered relative to the electrodes.

(*b*) The assumption of a uniform gradient between the cathode fall space and the anode glow is unjustified, the gradient increasing greatly near the electrodes.

(*c*) The cathode fall is probably within the range, 11 to 13 volts, which is comparable with the ionizing potential of copper vapour.

6. It is shown that equations similar to those of Ayrton and Steinmetz for the arc characteristics are untenable when the arc length is short, due to the variation of the average gradient with length.

Acknowledgment.

In conclusion, the author wishes to acknowledge his indebtedness to Dr. C. G. Lamb for his helpful interest, and to Professor C. E. Inglis, F.R.S., of the Staff of the Cambridge University Engineering Laboratory, where the present research was carried out.

LX. *Special Examples of the Elastic Ring acted upon by Equal and Equiangular Radial Forces.* *By* C. E. Larard, *M.Inst.C.E.* *

IN an investigation dealing with a circular elastic ring of uniform cross-section acted upon by any number of equal and equiangular forces the author obtained general equations for the two maximum flexural moments † on radial sections of the ring and also for the two maximum radial strains.

It is of some importance to calculate the particular values of the above quantities when N, the number of forces, is 2, 3, 4 . . . to 16.

The general equation given for the maximum negative flexural moment ‡ is

$$M_1 = \frac{PR}{2}\left(\cot\alpha - \frac{1}{\alpha}\right), \quad . \quad . \quad . \quad . \quad . \quad (1)$$

and for the maximum positive moment §

$$M_c = \frac{PR}{2}\left(\operatorname{cosec}\alpha - \frac{1}{\alpha}\right). \quad . \quad . \quad . \quad . \quad (2)$$

Reference to the illustrations in column 2 of Table I. will make clear the particular cases here considered.

The angle α in the above equations (1) and (2) is half the angle between any two adjacent forces, and is therefore equal to π/N. Thus α takes successively the values $\pi/2$, $\pi/3$, . . . $\pi/16$. Substituting these values in turn in equations (1) and (2) the results in columns 3 and 4 of Table I. are obtained. They are also plotted in the accompanying figure.

The numerical values of K_1 in column 3 give the maximum negative flexural moments per unit values of PR, and the values of K_2 in column 4 the maximum positive flexural moments per unit of PR.

The first of these maximum moments occurs at radial sections of the ring containing the line of action OP, and the second maxima at the radial sections midway between the lines of action of any two adjacent forces.

Comparing the values given in columns 3 and 4 of Table I. it will be noticed that the moments at the OP

* Communicated by the Author.

† Phil. Mag. xii. (July 1931), equations (6) and (8), p. 132.

‡ *Loc. cit.*

§ *Loc. cit.*

Table I.

1. Number of forces. N.	2. System of N equal forces. $\alpha = \frac{\pi}{N}$.	3. Maximum flexural moments. M_1 at section of each P $= \frac{PR}{2}\left(\cot\alpha - \frac{1}{\alpha}\right) = K_1 PR.$ Values of K_1.	4. Maximum flexural moments. M_c at mid-section between two adjacent P's $= \frac{PR}{2}\left(\operatorname{cosec}\alpha - \frac{1}{\alpha}\right) = K_2 PR.$ Values of K_2.
2.....		−0·31831	0·18169
3.....		−0·18879	0·09989
4.....		−0·13662	0·07049
5.....		−0·10758	0·05487
6.....		−0·08890	0·04507
8.....		−0·06613	0·03332
9.....		−0·05866	0·02951
10.....		−0·05271	0·02648
12.....		−0·04386	0·02199
15.....		−0·03501	0·01754
16.....		−0·03281	0·01644

sections of the ring do not differ much from twice the values of those for the mid-sections between the forces.

Consider next the two maximum radial strains.

Equation (24)* in the author's original paper gives the general expression for the alteration in the length of each radius joining the centre, O, of the ring to the point of application of each force P ; and this is the maximum radial strain.

This equation is written again with the three terms near the head of columns 2, 3, and 4 in Table II.

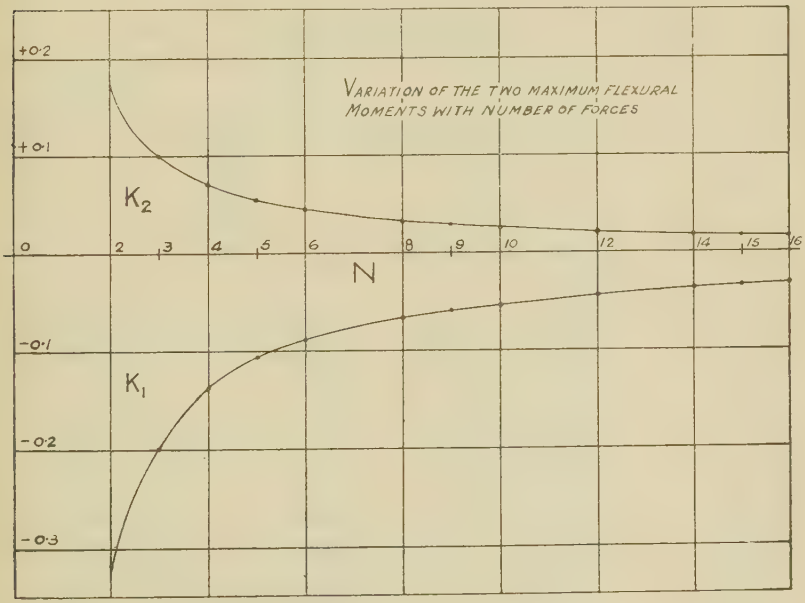

For the special cases here considered α takes successively the values $\pi/2$, $\pi/3$, . . . $\pi/16$, and therefore the equation for any one of these values takes the form

$$y_{OP} = K_3 \frac{PR^3}{EI} + K_4 \frac{PR}{EA} + K_5 \frac{CRP}{GA} . \quad . \quad . \quad (3)$$

The numerical values of K_3, K_4, and K_5 for the different values of $\alpha = \pi/N$ are given in columns 2, 3, and 4 of Table II.

* *Loc. cit.* p. 134.

Thus the numerical values of K_3 represent the alteration in the lengths of the radius OP for unit value of $\frac{PR^3}{EI}$, when bending alone is considered. K_4 gives the additional strain on OP due to hoop-stress per unit value of $\frac{PR}{EA}$, and K_5 the extra strain per unit of $\frac{CRP}{GA}$ when shear is also taken into account.

TABLE II.

1.	Total alteration in length of radius OP due to flexure, hoop-stress, and shear. 2. Strain due to bending	+	3. Strain due to hoop-stress	+	4. Strain due to shear-stress.
Number of forces. N.	$\frac{1}{4}\left(a\,\mathrm{cosec}^2\alpha+\cot\alpha-\frac{2}{a}\right)\frac{PR^3}{EI}$ or $K_3\frac{PR^3}{EI}$	+	$+\frac{1}{4}(a\,\mathrm{cosec}^2\alpha+\cot\alpha)\frac{PR}{EA}$ $K_4\frac{PR}{EA}$	+	$+\frac{1}{4}(a\,\mathrm{cosec}^2\alpha)\frac{CRP}{GA}$. $K_5\frac{CRP}{GA}$.

	Values of K_3.	Values of K_4.	Values of K_5.
2.....	0·07439	0·39270	0·39270
3.....	0·01594	0·49340	0·20473
4.....	0·00608	0·64270	0·14270
5.....	0·00298	0·79875	0·11056
6.....	0·00168	0·95661	0·09059
8.....	0·00069	1·27393	0·06683
9.....	0·00048	1·43287	0·05914
10.....	0·00035	1·59190	0·05306
12.....	0·00020	1·91006	0·04404
15.....	0·00010	2·38743	0·03511
16.....	0·00008	2·54657	0·03289

It may be stated that for most values of P, R, and A the second and third terms in equation (3) become numerically very small compared with the value of the first term, which considers flexure only.

The minimum radial strain occurs along a radius OC, where C is the mid-point on the arc between any two of the adjacent forces P, and the alteration in the length of OC is given by equation * $(45\,a)+(45\,b)+(45\,c)$ in the original

* *Loc. cit.* pp. 139, 140.

paper after Q has been written $=0$. Substituting $\alpha=\pi/N$, where N takes in turn the values 2, 3, . . . 16, the equation above simplifies to the terms given in columns 2, 3, and 4 of Table III., and these may be written

$$y_{OC} = K_6 \frac{PR^3}{EI} - K_7 \frac{PR}{EA} + K_8 \frac{CPR}{GA}.$$

The values of the three coefficients K_6, K_7, and K_8 are evaluated and given in the table.

TABLE III.

1.	Total alteration in length of radius OC due to flexure, hoop-stress, and shear.		
	2.	3.	4.
	Strain due to bending	+ Strain due to hoop-stress	+ Strain due to shear-stress.
Number of forces.	$\frac{1}{4}\left[\frac{2}{\alpha} - \operatorname{cosec}\alpha(\alpha\cot\alpha+1)\right]\frac{PR^3}{EI}$ or $K_6\frac{PR^3}{EI}$	$+\frac{1}{4}[-\operatorname{cosec}\alpha(1+\alpha\cot\alpha)]\frac{PR}{EA}$ $-K_7\frac{PR}{EA}$	$+\frac{1}{4}[\operatorname{cosec}\alpha(1-\alpha\cot\alpha)]\frac{CRP}{GA}$ $+K_8\frac{CRP}{GA}$.
	Values of K_6.	Values of K_7.	Values of K_8.
2.....	0·06831	0·25	0·25
3.....	0·01426	0·46321	0·11414
4.....	0·00539	0·63123	0·07587
5.....	0·00263	0·79315	0·05750
6.....	0·00148	0·95345	0·04655
8.....	0·00061	1·27263	0·03393
9.....	0·00042	1·43197	0·02993
10.....	0·00031	1·59124	0·02679
12.....	0·00017	1·90968	0·02217
15.....	0·00009	2·38725	0·01763
16.....	0·00007	2·54640	0·01651

In this case also it is the first term, due to flexure, which accounts for most of the strain, the other two terms, due to hoop-stress and shear-stress, being relatively small for most ordinary values of P, R, and A.

A comparison of the coefficients K_4 (Table II.) and K_7 (Table III.) show, on plotting with N as the other variable, that after the value $N=4$ a close and approximate linear relationship exists between the variables; thus strain along

OP due to hoop-stress is given closely by $0{\cdot}15915\,\mathrm{N}\,\frac{\mathrm{PR}}{\mathrm{EA}}$ and strain along OC due to hoop-stress is $-0{\cdot}15915\,\mathrm{N}\,\frac{\mathrm{PR}}{\mathrm{EA}}$.

Comparing the effects of the shear-stresses on the two strains along OP and OC it will be seen that the values of K_5 in column 4 Table II. are roughly twice the values of K_8 in column 4 Table III.

In conclusion, the author expresses his indebtedness to Dr. J. Ward and Mr. C. K. Larard for independently working out the numerical values given in the three tables.

Sept. 30, 1931.

LXI. *Periodic Orbits in a Field of Force defined by a certain Potential.* *By* M. A. Higab, *M.Sc., Ph.D., Lecturer in Mathematics in the Egyptian University, Cairo* *.

IN discussing the motion of an electron in the field of a non-neutral atom (Phil. Mag. vii. pp. 31–52, Jan. 1929, and vii. pp. 783–792, May 1929) the following problem arose :—

To find the condition for the existence of periodic orbits when a particle of unit mass moves in a field of force whose potential is

$$\mathrm{V}=\mu\int \mathrm{F}(r)dr+\frac{\lambda}{r^2}\int f(\theta)d\theta,$$

where r and θ are the usual polar coordinates and λ and μ are constants.

The object of the present paper is to establish that condition.

The equations of motion are

$$\ddot{r}-r\dot{\theta}^2=-\mu\mathrm{F}(r)+\frac{2\lambda\int f(\theta)\,d\theta}{r^3}, \quad . \quad . \quad . \quad (1)$$

$$\frac{1}{r}\frac{d}{dt}(r^2\dot{\theta})=-\frac{\lambda f(\theta)}{r^3} \quad . \quad . \quad . \quad . \quad . \quad . \quad . \quad . \quad (2)$$

* Communicated by the Author.

Equation (2) admits the integral

$$r^4\dot{\theta}^2 = A - 2\lambda\int f(\theta)d\theta, \quad . \quad . \quad . \quad . \quad . \quad (3)$$

where A is constant.

Since the left-hand side of equation (3) is positive, the right-hand side must also be positive.

Eliminating $\dot{\theta}$ between equations (1) and (3), we get

$$r = \frac{A}{r^3} - \mu F(r) \; ;$$

$$\therefore \quad \dot{r}^2 = -\frac{A}{r^2} - 2\mu\int F(r)dr + B, \quad . \quad . \quad . \quad (4)$$

where B is constant.

To obtain the significance of the constant B we have

$$\tfrac{1}{2}(\dot{r}^2 + r^2\dot{\theta}^2) + \mu\int F(r)dr + \frac{\lambda\int f(\theta)d\theta}{r^2} = \frac{B}{2},$$

i.e., B is twice the total energy.

The Differential Equation of the Path.

From equations (3) and (4) we get

$$\frac{1}{r^4}\left(\frac{dr}{d\theta}\right)^2 = \frac{-\frac{A}{r^2} - 2\mu\int F(r)dr + B}{A - 2\lambda\int f(\theta)d\theta}.$$

Putting $u = \frac{1}{r}$, and writing $\frac{du}{d\theta} = u_1$, we get

$$u_1^2 = \frac{-Au^2 + 2\mu\int F\left(\frac{1}{u}\right)\frac{du}{u^2} + B}{A - 2\lambda\int f(\theta)d\theta}$$

as the differential equation of the path.

Periodic Orbits.

Two types of periodic orbits are to be discussed separately :—

(*a*) Circular periodic orbits.

(*b*) Periodic orbits in general motion.

(a) *Circular Periodic Orbits.*

Let $r=a$, where a is constant, the equations (1) and (3) give

$$a^4\dot{\theta}^2=\mu a^3 \mathrm{F}(a)-2\lambda\int f(\theta)d\theta$$

and

$$a^4\dot{\theta}^2=\mathrm{A}-2\lambda\int f(\theta)d\theta$$

respectively.

These two equations are identical if $\mathrm{A}=\mu a^3\mathrm{F}(a)$.

Thus circular periodic orbits exist if

$$\mu a^3\mathrm{F}(a)-2\lambda\int f(\theta)d\theta$$

is positive.

The time is given by

$$t+\mathrm{E}=\sqrt{\frac{a}{\mu\mathrm{F}(a)}}\int\frac{d\theta}{\sqrt{1-\dfrac{2\lambda}{\mu a^3\mathrm{F}(a)}\int f(\theta)d\theta}},$$

where E is constant.

(b) *Periodic Orbits in General Motion.*

A necessary condition for periodic orbits is that u must be oscillatory. Putting $\dfrac{du}{d\theta}=0$, we get

$$\mathrm{B}-\mathrm{A}u^2+2u\phi(u)=0. \quad . \quad . \quad . \quad . \quad . \quad (5)$$

where

$$\phi(u)=\int \mathrm{F}\left(\frac{1}{u}\right)\frac{du}{u^2}.$$

Let α and β be two positive roots of equation (5), where $\alpha>\beta$;

$$\therefore\quad \mathrm{A}=2\mu\frac{\phi(\alpha)-\phi(\beta)}{\alpha^2-\beta^2}$$

and

$$\mathrm{B}=2\mu\frac{\beta^2\phi(\alpha)-\alpha^2\phi(\beta)}{\alpha^2-\beta^2}.$$

The motion in this case is included between two circles of radii α and β.

The equation of the path can be put in the form

$$\int_{u_0}^{u}\frac{du}{\sqrt{2\mu\dfrac{\beta^2\phi(\alpha)-\alpha^2\phi(\beta)}{\alpha^2-\beta^2}-2\mu\dfrac{\phi(\alpha)-\phi(\beta)}{\alpha^2-\beta^2}u^2+2\mu\phi(u)}}$$

$$=\sqrt{\frac{\alpha^2-\beta^2}{\phi(\alpha)-\phi(\beta)}}\int_{\theta_0}^{\theta}\frac{d\theta}{\sqrt{1-\dfrac{2\lambda(\alpha^2-\beta^2)}{\phi(\alpha)-\phi(\beta)}\chi(\theta)}},$$

where $\chi(\theta) = \int f(\theta)d\theta$, *i. e.*,

$$\Phi(u)-\Phi(u_0)=\sqrt{\frac{\alpha^2-\beta^2}{\phi(\alpha)-\phi(\beta)}}\int_{\theta_0}^{\theta}\sqrt{1-\frac{2\lambda(\alpha^2-\beta^2)}{\phi(\alpha)-\phi(\beta)}\chi(\theta)}\,d\theta.$$

The remaining conditions for periodic orbits are

$$\sqrt{\frac{\alpha^2-\beta^2}{\phi(\alpha)-\phi(\beta)}}\int_{\theta_0}^{k\pi+\theta_0}\frac{d\theta}{\sqrt{1-\frac{2\lambda(\alpha^2-\beta^2)}{\phi(\alpha)-\phi(\beta)}\chi(\theta)}}=2m\pi,$$

and $\Phi(u)$ must be an inverse function obeying the law

$$\Phi^{-1}[\Phi(u)+2m\pi]=\Phi^{-1}\Phi(u)=u,$$

where k and m are integers.

If these conditions are satisfied, then we have

$$\Phi(u)=\Phi(u_0)+2m\pi\ ;$$

$$\therefore\quad \Phi^{-1}\Phi(u)=\Phi^{-1}[\Phi(u_0)+2m\pi]$$

$$=\Phi^{-1}\Phi(u_0),$$

i. e., $$u=u_0.$$

This means that as θ increases from θ_0 to $\theta_0+k\pi$, then u returns to its original value and periodic orbits are formed.

As an example, take the case of an electron moving in the field of a non-neutral atom (Phil. Mag. vii. p. 786 (1929)). The equation of the path is

$$\cos^{-1}\frac{l/r-1}{e}-\cos^{-1}\frac{l/r_0-1}{e}=2\sqrt{\frac{A}{A+2\lambda}}\,F\left(\psi,\sqrt{\frac{4\lambda}{A+2\lambda}}\right).$$

Then, if

$$2\sqrt{\frac{A}{A+2\lambda}}\,F\left(k\pi,\sqrt{\frac{4\lambda}{A+2\lambda}}\right)=2m\pi,$$

then

$$\cos\cos^{-1}\frac{l/r-1}{e}=\cos\left[\cos^{-1}\frac{l/r_0-1}{e}+2m\pi\right],$$

i. e.,
$$\frac{l/r-1}{e}=\frac{l/r_0-1}{e},$$

i. e.,
$$r=r_0,$$

i. e., the electron returns to its point of projection and periodic orbits are formed.

LXII. *On the Stability of Laminar Motion of Viscous Fluids.* By Alfred Rosenblatt *.

THE problem of the stability of the laminar motion of incompressible viscous fluids has been treated by many eminent authors, especially by Lord Kelvin and Lord Rayleigh ; but, so far as I am aware, it is only Mr. F. Noether† who has made an attempt to investigate *finite* disturbances without giving rigorous proofs. I think therefore that it will not be without interest to examine rigorously the simpler case of *exponentially vanishing disturbance*. Having already treated the case of *initial rest*, I shall now investigate the case of fundamental motion of the form

$$u_0 = \frac{\mathrm{U}y}{\mathrm{H}}, \quad . \quad . \quad . \quad . \quad . \quad . \quad . \quad . \quad (1)$$

$y=0$, $y=\mathrm{H}$ being the equations of the walls, U the velocity of the latter.

1. I suppose the Stokes function to be of the form

$$\Psi = \Psi_0 + \sum_{k=1}^{\infty} \epsilon^k \Psi_k(x, y, t), \quad . \quad . \quad . \quad . \quad (2)$$

$$\Psi_k = e^{-k(\lambda x + \mu t)} f_k(y), \quad k = 1, 2, \ldots \quad . \quad . \quad (3)$$

In order to obtain dimensionless quantities we introduce, with Mr. Sommerfeld, the expressions

$$\xi = \frac{x}{\mathrm{H}}, \quad \eta = \frac{y}{\mathrm{H}}, \quad \tau = \frac{\mathrm{U}}{\mathrm{H}} t, \quad \gamma = \lambda \mathrm{H}, \quad \delta = \frac{\mu \mathrm{H}}{\mathrm{U}}, \quad \mathrm{R} = \frac{\mathrm{U}\mathrm{H}}{\nu}$$

$$. \quad . \quad . \quad (4)$$

(R number of Reynolds). We have now

$$\Psi_k = e^{-k(\gamma\xi + \delta\tau)} f_k(\eta).$$

Writing

$$\phi_k(\eta) = f_k''(\eta) + k^2\gamma^2 f_k(\eta),$$

* Communicated by Sir J. J. Thomson, O.M., F.R.S.

† "Zur Theorie der Turbulenz," *Jahr. d. Deutsch. Math. Ver.* T. 23 ; "Zur statistischen Deutung der Kármanschen Ähnlichkeitshypothese in der Turbulenztheorie," *Zeits. f. ang. Math. u. Mech.* 1931.

we obtain the following set of differential equations:

$$\left.\begin{aligned} \phi_k''(\eta) + [k^2\gamma^2 + k\mathrm{R}(\delta+\gamma\eta)]\phi_k(\eta) &= \frac{\gamma}{\nu} \sum_{\substack{l+m=k,\\ l,\ m=1,\ldots k-1}}, \\ [-l f_l \phi_m' + m f_l' \phi_m] &= \mathrm{D}_k(\eta), \\ k &= 1, 2, \ldots \end{aligned}\right\} \quad (5)$$

We replace now in the equations which determine $f_k(\eta)$, $\phi_k(\eta)$ the independent variable η by the variable z_k,

$$z_k = \frac{k^2\gamma^2 + k\mathrm{R}(\delta+\gamma\eta)}{(k\gamma\mathrm{R})^{\frac{2}{3}}} \quad . \quad . \quad . \quad . \quad . \quad (6)$$

The limits of η being 0 and 1, the limits z_k^0, z_k^1 of z_k are

$$z_k^0 = \frac{k^2\gamma^2 + k\mathrm{R}\delta}{(k\gamma\mathrm{R})^{\frac{2}{3}}}, \quad z_k^1 = \frac{k^2\gamma^2 + k\mathrm{R}(\delta+\gamma)}{(k\gamma\mathrm{R})^{\frac{2}{3}}}.$$

Writing

$$f_k(\eta) = \bar{f}_k(z_k), \qquad \phi_k(\eta) = \bar{\phi}_k(z_k),$$

$$\mathrm{D}_k(\eta) = \bar{\mathrm{D}}_k(z_k), \qquad g_k = -\frac{(k\gamma)^{\frac{2}{3}}}{\mathrm{R}^{\frac{1}{3}}},$$

we obtain the following two sets of equations:

$$\bar{f}_k''(z_k) + g_k^2 \bar{f}_k(z_k) = \frac{g_k^2}{k^2\gamma^2}\bar{\phi}_k(z_k), \quad . \quad . \quad . \quad . \quad (7)$$

$$\bar{\phi}_k''(z_k) + z_k\bar{\phi}_k(z_k) = \frac{g_k^2}{k^2\gamma^2}\bar{\mathrm{D}}_k(z_k) \quad . \quad . \quad . \quad . \quad . \quad (8)$$

2. The equations (7) are integrated by the formulæ

$$f_k(z_k) = \frac{g_k}{k^2\gamma^2}\int_{z_k^0}^{z_k} \sin g_k(z_k - u)\,\bar{\phi}_k(u)\,du, \quad . \quad . \quad (9)$$

and the equations (8) by the formulæ

$$\bar{\phi}_k(z_k) = \mathrm{A}_k\sigma_1(z_k) + \mathrm{B}_k\sigma_2(z_k) + \frac{g_k^2}{k^2\gamma^2} \int_{z_k^0}^{z_k} [\sigma_1(u)\sigma_2(z_k) - \sigma_2(u)\sigma_1(z_k)]\,.\,\bar{\mathrm{D}}_k(u)\,du. \quad (10)$$

$\sigma_1(z_k)$, $\sigma_2(z_k)$ are the following independent integrals of the *linear homogeneous equations* belonging to (8) :

$$\left.\begin{aligned}\sigma_1(z) &= (\tfrac{1}{3})^{\frac{1}{3}}\Gamma(\tfrac{2}{3})\sqrt{z}\,\mathrm{I}_{-\frac{1}{3}}(\tfrac{2}{3}z^{\frac{3}{2}}),\\ \sigma_2(z) &= (\tfrac{1}{3})^{-\frac{1}{3}}\Gamma(\tfrac{4}{3})\sqrt{z}\,\mathrm{I}_{\frac{1}{3}}(\tfrac{2}{3}z^{\frac{3}{2}}),\end{aligned}\right\} \quad . \quad . \quad (11)$$

I being the Bessel functions.

We have therefore

$$\overline{f_k}(z_k) = \frac{g_k}{k^2\gamma^2}\int_{z_k^0}^{z_k}\sin g_k(z_k-u)\left\{\mathrm{A}_k\sigma_1(u)+\mathrm{B}_k\sigma_2(u) + \frac{g_k^2}{k^2\gamma^2}\int_{z_k^0}^{u}[\sigma_1(\zeta)\sigma_2(u)-\sigma_2(\zeta)\sigma_1(u)]\,\overline{\mathrm{D}_k}(\zeta)\,d\zeta\right\}du. \quad . \quad . \quad . \quad (12)$$

The limit conditions are

$$\overline{f_k}(z_k^1) = 0, \qquad \overline{f_k}'(z_k^1) = 0.$$

3. We introduce the integrals

$$\mathrm{I}_i(a, b) = \int_a^b \sin g_k(b-u)\sigma_i(u)\,du, \quad i=1, 2, \quad (13)$$

$$\mathrm{J}_i(a, b) = \int_a^b \cos g_k(b-u)\sigma_i(u)\,du, \quad i=1, 2, \quad (14)$$

A_1, B_1 are determined by the equations

$$\left.\begin{aligned}\mathrm{A}_1\mathrm{I}_1(z_1^0, z_1^1)+\mathrm{B}_1\mathrm{I}_2(z_1^0, z_1^1) &= 0,\\ \mathrm{A}_1\mathrm{J}_1(z_1^0, z_1^1)+\mathrm{B}_1\mathrm{J}_2(z_1^0, z_1^1) &= 0,\end{aligned}\right\} \quad . \quad . \quad (15)$$

which give the *transcendental equation* determining γ, δ

$$\mathrm{D}_1(z_1^0, z_1^1) \equiv \mathrm{I}_1(z_1^0, z_1^1)\mathrm{J}_2(z_1^0, z_1^1)-\mathrm{I}_2(z_1^0, z_1^1)\mathrm{J}_1(z_1^0, z_1^1) = 0. \quad . \quad . \quad . \quad (16)$$

We have

$$\mathrm{A}_1 = -\mathrm{C}_1\mathrm{I}_2(z_1^0, z_1^1), \qquad \mathrm{B}_1 = \mathrm{C}_1\mathrm{I}_1(z_1^0, z_1^1), \quad . \quad (17)$$

C_1 being an arbitrary constant.

Inverting in (12) the order of integration, we obtain the following equations which determine A_k, B_k, $k \geq 2$:—

$$\left.\begin{aligned}&\mathrm{A}_k\mathrm{I}_1(z_k^0, z_k^1)+\mathrm{B}_k\mathrm{I}_2(z_k^0, z_k^1)\\ &\quad+\frac{g_k^2}{k^2\gamma^2}\int_{z_k^0}^{z_k^1}\overline{\mathrm{D}_k}(\zeta)[\sigma_1(\zeta)\mathrm{I}_2(\zeta, z_k^1)-\sigma_2(\zeta)\mathrm{I}_1(\zeta, z_k^1)]\,d\zeta = 0,\\ &\mathrm{A}_k\mathrm{J}_1(z_k^0, z_k^1)+\mathrm{B}_k\mathrm{J}_2(z_k^0, z_k^1)\\ &\quad+\frac{g_k^2}{k^2\gamma^2}\int_{z_k^0}^{z_k^1}\overline{\mathrm{D}_k}(\zeta)\,[\sigma_1(\zeta)\mathrm{J}_2(\zeta, z_k^1)-\sigma_2(\zeta)\mathrm{J}_1(\zeta, z_k^1)]\,d\zeta = 0.\end{aligned}\right\} \quad . \quad . \quad (18)$$

Writing

$$D_k(z_k^0, z_k^1) = I_1(z_k^0, z_k^1)\,J_2(z_k^0, z_k^1) - I_2(z_k^0, z_k^1), J_1(z_k^0, z_k^1), \quad \ldots \quad (19)$$

we have

$$\left.\begin{aligned} A_k = \frac{g_k^2}{D_k(z_k^0, z_k^1).k^2\gamma^2} \Big\{ & I_2(z_k^0, z_k^1) \\ & \int_{z_k^0}^{z_k^1} \overline{D_k}(\zeta)\,[\sigma_1(\zeta)J_2(\zeta\ z_k^1) - \sigma_2(\zeta)J_1(\zeta, z_k^1)]\,d\zeta - J_2(z_k^0, z_k^1) \\ & \int_{z_k^0}^{z_k^1} \overline{D_k}(\zeta)\,[\sigma_1(\zeta)I_2(\zeta, z_k^1) - \sigma_2(\zeta)I_1(\zeta, z_k^1)]\,d\zeta \Big\}, \\ B_k = \frac{g_k^2}{D_k(z_k^0, z_k^1).k^2\gamma^2} \Big\{ & J_1(z_k^0, z_k^1) \\ & \int_{z_k^0}^{z_k^1} D_k(\zeta)\,[\sigma_1(\zeta)I_2(\zeta, z_k^1) - \sigma_2(\zeta)I_1(\zeta, z_k^1)]\,d\zeta - I_1(z_k^0, z_k^1) \\ & \int_{z_k^0}^{z_k^1} D_k(\zeta)\,[\sigma_1(\zeta)J_2(\zeta, z_k^1) - \sigma_2(\zeta)J_1(\zeta, z_k^1)]\,d\zeta \Big\}. \end{aligned}\right\} \quad \ldots \quad (20)$$

We obtain therefore the following recurrent expressions for the $\overline{\phi_k}(z_k)$:—

$$\begin{aligned} & \overline{\phi_k}(z_k) \\ & = \frac{g_k^2}{D_k(z_k^0, z_k^1).k^2\gamma^2} \Big\{ \int_{z_k^0}^{z_k^1} D_k(\zeta)\,[\sigma_1(\zeta)\sigma_1(z_k)\{I_2(z_k^0, z_k^1)J_2(\zeta, z_k^1) \\ & - I_2(\zeta, z_k^1)J_2(z_k^0, z_k^1)\} - \sigma_2(\zeta)\sigma_2(z_k)\{I_1(\zeta, z_k^1)J_1(z_k^0, z_k^1) \\ & - I_1(z_k^0, z_k^1)J_1(\zeta, z_k^1)\} + \sigma_2(\zeta)\sigma_1(z_k)\{I_1(\zeta, z_k^1)J_2(z_k^0, z_k^1) \\ & - I_2(z_k^0, z_k^1)J_1(\zeta, z_k^1)\} - \sigma_1(\zeta)\sigma_2(z_k)\{I_1(z_k^0, z_k^1)J_2(\zeta, z_k^1) \\ & - I_2(\zeta, z_k^1)J_1(z_k^0, z_k^1)\}]\,d\zeta \\ & + D_k(z_k^0, z_k^1) \int_{z_k^0}^{z_k} D_k(\zeta)\,[\sigma_1(\zeta)\sigma_2(z_k) - \sigma_2(\zeta)\sigma_1(z_k)].\,d\zeta \Big\}. \end{aligned} \quad \ldots \quad (21)$$

4. In order that the expressions (21) may have a sense the expressions (19) for $k \geq 2$ must be different from zero We must therefore first of all calculate the *limit* of (19) for k tending to $+\infty$.

We have for large values of z the formulæ

$$\left.\begin{aligned}\sigma_1(z) &= \left(\frac{1}{3}\right)^{\frac{1}{3}}\Gamma\left(\frac{2}{3}\right)\cdot\frac{1}{z^{\frac{1}{4}}}\left\{\sqrt{\frac{3}{\pi}}\cos\left(\frac{2}{3}z^{\frac{3}{4}}-\frac{\pi}{12}\right)+\left(\frac{1}{z}\right)\right\},\\ \sigma_2(z) &= \left(\frac{1}{3}\right)^{-\frac{1}{3}}\Gamma\left(\frac{4}{3}\right)\cdot\frac{1}{z^{\frac{1}{4}}}\left\{\sqrt{\frac{3}{\pi}}\sin\left(\frac{2}{3}z^{\frac{3}{4}}-\frac{\pi}{12}\right)+\left(\frac{1}{z}\right)\right\}.\end{aligned}\right\} \quad . \quad . \quad . \quad (22)$$

Introducing the integrals

$$I_{1,2,3,4}=\int_{z_k^0}^{z_k^1}\begin{matrix}\sin\\ \cos\end{matrix}\Big\}\, g_k(z_k^1-u)\cdot\begin{matrix}\cos\\ \sin\end{matrix}\Big\}\left(\frac{2}{3}u^{\frac{3}{4}}-\frac{\pi}{12}\right)\frac{du}{u^{\frac{1}{4}}}, \quad (23)$$

we have for large values of k

$$D(z_k^0, z_k^1)=\frac{3}{\pi}\cdot\Gamma\left(\frac{2}{3}\right)\Gamma\left(\frac{4}{3}\right)(I_1I_4-I_2I_3)+\epsilon(k). \quad . \quad (24)$$

Writing

$$v=g_k(z_k-u)+\frac{2}{3}u^{\frac{3}{2}}-\frac{\pi}{12},$$

$$v'=g_k(z_k-u)-\frac{2}{3}u^{\frac{3}{2}}+\frac{\pi}{12},$$

$$\eta=\frac{k^2\gamma^2+k\mathrm{R}(\delta+\gamma\eta)}{(k\gamma\mathrm{R})^{\frac{2}{3}}},$$

we can replace the integrals $I_1 \ldots I_4$ by the integrals

$$I'_{1,4}=\frac{\sqrt{\mathrm{R}}}{2}\int_0^1(\sin v\pm\sin v')\,d\eta,$$

$$I'_{2,3}=\frac{\sqrt{\mathrm{R}}}{2}\int_0^1(\cos v'\pm\cos v)\,d\eta.$$

But we have

$$\frac{dv}{d\eta}=2k\gamma\left(1+\left(\frac{1}{k}\right)\right), \qquad \frac{dv'}{d\eta}=-\frac{\mathrm{R}(\delta+\gamma\eta)}{2\gamma}+\left(\frac{1}{k}\right);$$

we can therefore consider only the integrals containing v, and write

$$D_k(z_k^0, z_k^1)=-\frac{3\mathrm{R}}{4\pi}\Gamma\left(\frac{2}{3}\right)\Gamma\left(\frac{4}{3}\right)$$

$$\left\{\left(\int_0^1\sin v'\,d\eta\right)^2+\left(\int_0^1\cos v'\,d\eta\right)^2\right\}+\epsilon(k). \quad (25)$$

But we have

$$v' = g_k z_k + \frac{\pi}{12} + \frac{1}{3}\frac{(k\gamma)^2}{\mathrm{R}} - \frac{\mathrm{R}}{4}\frac{(\delta+\gamma\eta)^2}{\gamma^2} + \left(\frac{1}{k}\right)$$

$$= m - \frac{\mathrm{R}}{4}\left(\eta+\frac{\delta}{\gamma}\right)^2 + \left(\frac{1}{k}\right).$$

We have therefore

$$\left(\int_0^1 \sin v'\,d\eta\right)^2 + \left(\int_0^1 \cos v'\,d\eta\right)^2$$

$$= \left(\int_0^1 \sin\frac{\mathrm{R}}{4}\left(\frac{\delta}{\gamma}+\eta\right)^2 d\eta\right)^2 + \left(\int_0^1 \cos\frac{\mathrm{R}}{4}\left(\frac{\delta}{\gamma}+\eta\right)^2 d\eta\right)^2 + \epsilon(k),$$

and the limit D_∞ of $\mathrm{D}_k(z_k^0, z_k^1)$ is

$$\mathrm{D}_\infty = -\frac{3\mathrm{R}}{4\pi}\Gamma\left(\frac{2}{3}\right)\Gamma\left(\frac{4}{3}\right)$$

$$\left\{\left(\int_0^1 \sin\frac{\mathrm{R}}{4}\left(\frac{\delta}{\gamma}+\eta\right)^2 d\eta\right)^2 + \left(\int_0^1 \cos\frac{\mathrm{R}}{4}\left(\frac{\delta}{\gamma}+\eta\right)^2 d\eta\right)^2\right\}. \quad . \quad . \quad . \quad (26)$$

5. The integrals in the parenthesis are the well-known *Fresnel integrals.* Introducing the variable of integration,

$$\xi = \sqrt{\frac{2}{\pi}}\sqrt{\frac{\mathrm{R}}{4}}\left(\frac{\delta}{\gamma}+\eta\right),$$

we have

$$\int_0^1 \sin\frac{\mathrm{R}}{4}\left(\frac{\delta}{\gamma}+\eta\right)^2 d\eta = \sqrt{\frac{2\pi}{\mathrm{R}}}\,[\mathrm{S}(b)-\mathrm{S}(a)],$$

$$\int_0^1 \cos\frac{\mathrm{R}}{4}\left(\frac{\delta}{\gamma}+\eta\right)^2 d\eta = \sqrt{\frac{2\pi}{\mathrm{R}}}\,[\mathrm{C}(b)-\mathrm{C}(a)],$$

where $\mathrm{S}(\xi)$, $\mathrm{C}(\xi)$ are the Fresnel integrals

$$\mathrm{S}(\xi) = \int_0^\xi \sin\frac{\pi}{2}u^2\,du, \qquad \mathrm{C}(\xi) = \int_0^\xi \cos\frac{\pi}{2}u^2\,du, \quad (27)$$

and a, b are

$$a = \sqrt{\frac{\mathrm{R}}{2\pi}}\frac{\delta}{\gamma}, \qquad b = \sqrt{\frac{\mathrm{R}}{2\pi}}\left(1+\frac{\delta}{\gamma}\right). \quad . \quad (28)$$

We have, finally,

$$\mathrm{D}_\infty = -\sqrt{3}\,.\,\pi\{(\mathrm{S}(b)-\mathrm{S}(a))^2 + (\mathrm{C}(b)-\mathrm{C}(a))^2\}. \quad (29)$$

But it is well known that the *Cornu spiral,* whose equations are

$$x = C(\xi), \quad y = S(\xi), \quad . \quad . \quad . \quad . \quad (30)$$

has *no double point.* We obtain therefore our first result:

Theorem 1.—"The determinants (19), which appear in the denominators of the expressions (21) for the $\bar{\phi}_k(z_k)$, converge with $k \to +\infty$ to a number D_∞ given by (29), which is *always different from zero.*"

Writing

$$F(\xi) = C(\xi) + iS(\xi),$$

we have for large ξ

$$F(\xi) = \tfrac{1}{2}(1+i) + \frac{e^{i\frac{\pi}{2}\xi^2}}{i\pi\xi}(1+\epsilon(\xi')).$$

D_∞ tends therefore to zero if R or if $\frac{\delta}{\gamma}$ increases indefinitely.

If R and if $\frac{\delta}{\gamma}$ are contained in finite intervals D_∞ is absolutely superior to a positive number l and $D_k(z_k^0, z_k^1)$ tends *uniformly* to D_∞. Suppose now that R_0, δ_0, γ_0 satisfy the transcendental equation (16). We choose a number k_0, such that for the finite intervals containing R_0 and $\frac{\delta_0}{\gamma_0}$ and for any $k > k_0$ $D_k(z_k^0, z_k^1)$ is absolutely superior to $l > 0$ The roots R_0, δ_0, γ_0, common to two equations,

$$D_{k'}(z_{k'}^0, z_{k'}^1) = 0, \qquad D_{k''}(z_{k''}^0, z_{k''}^1) = 0, \quad . \quad . \quad (31)$$

form an *exceptional set,* and for a given R_0 there is only a *finite number* of roots, γ_0, δ_0, in limited intervals. In closed intervals not containing these exceptional values the $D_k(z_k^0, z_k^1)$ are *for all* k uniformly absolutely superior to a *fixed* positive number $m > 0$.

6. We shall now establish the *convergence* of the series

$$s_\varphi = \sum_{k=1}^{\infty} \epsilon^k e^{-k(\gamma\xi+\delta\tau)} \cdot \bar{\phi}_k(z_k), \quad . \quad . \quad . \quad . \quad (32)$$

and therefrom also the convergence of the series

$$s_f = \sum_{k=1}^{\infty} \epsilon^k e^{-k(\gamma\xi+\delta\tau)} \cdot f_k(\eta). \quad . \quad . \quad . \quad . \quad (33)$$

Consider the expressions (21). The integrals I, J are *uniformly* limited with respect to k. The interval of integration is of the order $k^{\frac{1}{3}}$ and the σ are of order $k^{-\frac{1}{3}}$. The formulæ (9) show that the $f_k(z_k)$ are of the order of the $\overline{\phi_k}(z_k)$ multiplied by k^{-1}, while the $f'_k(z_k)$ are of the order of $\overline{\phi_k}(z_k)$ multiplied by $k^{-\frac{1}{3}}$. The $\phi'(z_k)$ are of the order of the $\overline{\phi_k}(z_k)$ multiplied by $k^{\frac{2}{3}}$. Indeed, the $\sigma'(z_k)$ are of the order of $\sigma(z_k)$ multiplied by $k^{\frac{2}{3}}$, since we have

$$\sigma'(z) = \frac{1}{2z}\sigma(z) + \mathrm{A}z\mathrm{I}_n'\left(\frac{2}{3}z^{\frac{3}{2}}\right),$$

$$\mathrm{I}_n'\left(\frac{2}{3}z^{\frac{3}{2}}\right) = -\frac{3n}{2z^{\frac{3}{2}}}\mathrm{I}_n\left(\frac{2}{3}z^{\frac{3}{2}}\right) + \mathrm{I}_{n-1}\left(\frac{2}{3}z^{\frac{3}{2}}\right).$$

Let us now suppose that the functions

$$\overline{\phi_1}, \overline{\phi_2}, \ldots \overline{\phi_{k-1}}$$

have the majorant numbers

$$\Phi_1, \Phi_2, \ldots \Phi_{k-1},$$

and that the functions

$$\overline{\phi_i}', \overline{f_i}, \overline{f_i}', \quad i = 1, \ldots k-1$$

have respectively the majorant numbers

$$\Phi_i . i^{\frac{2}{3}}, \quad \Phi_i . \frac{1}{i}, \quad \Phi_i . i^{-\frac{1}{3}}.$$

Let us consider the expressions (21). It is easily seen that $\overline{\mathrm{D}_k}(\zeta)$ is a sum of terms whose majorant numbers are

$$\frac{\gamma}{\nu}(\gamma\mathrm{R})^{\frac{1}{3}} m \Phi_l \Phi_m.$$

It follows that there exists a positive number N *independent of k*, such that Φ_k, given by the formula *

$$\Phi_k = \mathrm{N}\sum_{i=1}^{k-1}\Phi_i\Phi_{k-i}, \quad . \quad . \quad . \quad . \quad . \quad (34)$$

is a majorant number of the function $\overline{\phi_k}(z_k)$, and that majorant numbers of the functions

$$\overline{\phi_k}'(z_k), \quad f_k(z\ ), \quad f_k'(z_k)$$

* *Cf.* the interesting papers of Mr. Odquist: "Die Randwertaufgaben der Hydromechanik zäher Flüssigkeiten," Dissertation, Stockholm, 1928; "Über die Randwertaufgaben der Hydromechanik zäher Flüssigkeiten," *Math. Zeits.* 1930, p. 32.

are respectively the numbers

$$k^{\frac{3}{2}}\Phi_k, \quad \frac{1}{k}\Phi_k, \quad k^{-\frac{1}{2}}\Phi_k.$$

The series

$$\left.\begin{aligned} S_\phi &= \sum_{k=1}^{\infty} \epsilon^k E_k \Phi_k, \\ E_k &= e^{-k(\gamma\xi+\delta\tau)}, \end{aligned}\right\} \quad . \quad . \quad . \quad . \quad . \quad (35)$$

is therefore a *majorant series* of s_ϕ. The radius ρ of convergence is found considering that S_ϕ satisfies the equation of second degree,

$$NS_\phi^2 - S_\phi + E_1 \epsilon \Phi_1 = 0. \quad . \quad . \quad . \quad . \quad (36)$$

We obtain

$$\rho = \frac{1}{4NE_1\Phi_1} \quad . \quad . \quad . \quad . \quad . \quad . \quad (37)$$

We have therefore the theorem:

Theorem 2.—"The series (2) for Ψ is absolutely and uniformly convergent with all derivatives for $|\epsilon| < \rho$, and satisfies the equation of 4th order for viscous fluids."

Cracow,
August 1931.

LXIII. *Relativistic Precession of Periodic Orbits in Central Force Fields. By* M. A. Omara, *Docteur ès Sciences (Grenoble), Lecturer in Applied Mathematics in the Egyptian University* *.

1. IT is a well-known fact that the path of a particle in a Newtonian field of force, when the relativistic variation of mass is taken into consideration, is no longer a Keplerian ellipse. It may be considered as an ellipse whose perihelion is advancing. The aim of this paper is to establish that this advance or precession of the perihelion is common to all periodic orbits described under central forces depending on the distance. The orbit is supposed nearly circular and the apsidal angles are compared, in Newtonian and in relativistic dynamics It is found that, for a given field of force, the relativistic apsidal angle

* Communicated by the Author.

exceeds slightly the corresponding Newtonian one. This slight excess depends, as well as in the case of the inverse square law of force, upon the inverse of the square of the velocity of light and may be interpreted in the same manner, and can be calculated to any degree of approximation.

2. A particle whose rest mass is m moves in a central force field derived from a potential $V(r)$. Let r and θ be the polar coordinates of the particle, referred to the centre of force as origin. The corresponding relativity Hamilton-Jacobi equation is :

$$\left(\frac{\partial S}{\partial r}\right) + \frac{1}{r^2}\left(\frac{\partial S}{\partial \theta}\right)^2 = 2m(E-V) + \frac{1}{c^2}(E-V)^2, \quad . \quad (1)$$

E being the constant of energy. The equation of the path is then

$$\beta = \frac{\theta}{2\sqrt{\alpha}} - \frac{1}{2}\int \frac{dr}{r\sqrt{\Phi(r)}},$$

where

$$\Phi(r) = 2mr^2(E-V) + \frac{r^2}{c^2}(E-V)^2 - \alpha,$$

α, β are arbitrary constants, α having the dimensions of the square of a moment of momentum.

Take a new variable $u = \frac{1}{r}$, and put $V(r) = W(u) = W$. The equation of the path becomes

$$\beta = \frac{\theta}{2\sqrt{\alpha}} + \frac{1}{2}\int \frac{du}{\sqrt{\Psi(u)}}, \quad . \quad . \quad . \quad . \quad (2)$$

where $\Psi(u) = 2m(E-W) + \frac{1}{c^2}(E-W)^2 - \alpha u^2$.

As the orbit is supposed periodic, r, and consequently u, must remain between two finite limits. Let the limits for u be u_1 and u_2 $(>u_1)$. The values u_1 and u_2 are consecutive roots of the equation

$$\Psi(u) = 0.$$

The apsidal angle is then

$$\Theta = \int_{u_1}^{u_2} \frac{\sqrt{\alpha}\,du}{\sqrt{\Psi(u)}} \quad . \quad . \quad . \quad . \quad . \quad . \quad (3)$$

A proposition of integral calculus, easy to prove, states that when u_1 and u_2 tend to a common limit a, such that $u_1 < a < u_2$, the limiting value of the integral $\int_{u_1}^{u_2} \frac{du}{\sqrt{\Psi(u)}}$ is

$$\pi\sqrt{\frac{-2}{\Psi''(a)}},$$

where $\Psi''(a)$ stands for $\frac{d^2\Psi}{du^2}$ for $u=a$.

Suppose the initial conditions so chosen that the orbit is nearly a circle of radius $\frac{1}{a}$, and take for approximate value of Θ the limiting value when u_1 and u_2 tend to a.

In order to calculate $\Psi''(a)$, we have

$$\frac{d\Psi}{du} = -2\left(m + \frac{E-W}{c^2}\right)\frac{dW}{du} - 2\alpha u,$$

and, for a circular motion,

$$\Psi'(a) = -2\left(m + \frac{E-W(a)}{c^2}\right)W'(a) - 2\alpha a = 0.$$

Also

$$\Psi''(a) = -2\left(m + \frac{E-W(a)}{c^2}\right)W''(a) + \frac{2}{c^2}W'^2(a) - 2\alpha.$$

Substituting for E from the preceding equation, we have

$$\Psi''(a) = -2\alpha\left(1 - a\frac{W''(a)}{W'(a)}\right) + \frac{2}{c^2}W'^2(a),$$

and then

$$\Theta = \frac{\pi}{\sqrt{1 - a\dfrac{W''}{W'} - \dfrac{W'^2}{\alpha c^2}}} = \frac{\pi}{\omega}\text{ (say)}. \quad . \quad . \quad . \quad (4)$$

W', W'' ... are written for $W'(a)$, $W''(a)$.

3. Another method of computing the apsidal angle is to pass by the differential equation of the path. This method has the advantage of showing the degree of approximation admitted.

From equation (2) we get

$$\alpha\left(\frac{du}{d\theta}\right)^2 = \Psi(u) = 2m(E-W) + \frac{1}{c^2}(E-W)^2 - \alpha u^2.$$

Differentiating again with respect to θ, dividing both sides by $\alpha\frac{du}{d\theta}$, and arranging, we get

$$\frac{d^2u}{d\theta^2}+u=-\frac{m}{\alpha}\left(1+\frac{\mathrm{E}-\mathrm{W}}{mc^2}\right)\frac{d\mathrm{W}}{du}.$$

Put $u=a$, then

$$a=-\frac{m}{\alpha}\left(1+\frac{\mathrm{E}-\mathrm{W}(a)}{mc^2}\right)\mathrm{W}'(a). \quad . \quad . \quad . \quad (5)$$

Eliminating E between these two equations, we have

$$\frac{d^2u}{d\theta^2}+u=\left[\frac{a}{\mathrm{W}'(a)}+\frac{\mathrm{W}(u)-\mathrm{W}(a)}{\alpha c^2}\right]\mathrm{W}'(u).$$

Put $u=a+x$, where x is a small quantity. Expanding by Taylor's theorem, and arranging, the equation becomes

$$\frac{d^2x}{d\theta^2}=-\omega^2x+\left(a\frac{\mathrm{W}'''}{\mathrm{W}'}+3\frac{\mathrm{W}'\mathrm{W}''}{\alpha c^2}\right)\frac{x^2}{2}$$
$$+\left(a\frac{\mathrm{W}^{\mathrm{IV}}}{\mathrm{W}'}+\frac{4\mathrm{W}'\mathrm{W}'''+3\mathrm{W}''^2}{\alpha c^2}\right)\frac{x^3}{6}+\ldots. \quad (6)$$

This equation can be integrated by successive approximations; but if we confine ourselves to the first order of small quantities, equation (6) may be written

$$\frac{d^2x}{d\theta^2}+\omega^2x=0,$$

and is satisfied by

$$x=\mathrm{A}\cos(\omega\theta-\epsilon),$$

where A and ϵ are arbitrary constants. The approximation to the path is given by

$$u=a+\mathrm{A}\cos(\omega\theta-\epsilon), \quad . \quad . \quad . \quad . \quad . \quad (7)$$

and the apsidal angle is again $\frac{\pi}{\omega}$.

4. When a particle of mass m describes a circle of radius $\frac{1}{a}$, with velocity v, the square of the moment of momentum,

$$\alpha=\frac{m^2v^2}{a^2},$$

also,

$$\frac{d\mathrm{W}}{du}=\frac{d\mathrm{V}}{dr}\frac{dr}{du}=\frac{\mathrm{F}}{u^2},$$

where F is the force acting on the particle. We have in this case

$$\mathrm{F}=mav^2,$$

and, therefore,

$$\mathrm{W}'(a)=\frac{mv^2}{a},$$

and then

$$\omega^2=1-a\frac{\mathrm{W}''}{\mathrm{W}'}-\frac{v^2}{c^2}.$$

Put

$$\lambda^2=1-a\frac{\mathrm{W}''}{\mathrm{W}'},\quad\text{and}\quad\gamma^2=1-\frac{v^2}{c^2\lambda^2};$$

then the apsidal angle may be written

$$\Theta=\frac{\pi}{\gamma\lambda}.$$

The ratio $\frac{v}{c}$ being in general very small, γ differs slightly from unity.

In Newtonian dynamics $\gamma=1$, and the apsidal angle is

$$\Theta_1=\frac{\pi}{\lambda}.$$

We have therefore the relation

$$\Theta\gamma^{-1}\Theta_1.$$

Let the angle θ be measured from a perihelion. During a radial vibration the angle θ increases in relativistic dynamics by an amount 2Θ, while in Newtonian dynamics the increment is $2\Theta_1$. We see that during this radial vibration the perihelion has a relative advance

$$2\Theta_1=(\gamma^{-1}-1).$$

Now suppose that the Newtonian orbit is a closed one, *i. e.*, there exists two integers, m and n, such that

$$m\Theta_1=n\pi.$$

Then, in relativistic dynamics, while the radius vector reverts to its original value θ increases by an amount

$2m\Theta$, and the perihelion from which θ is measured will have advanced by

$$2m\Theta_1(\gamma^{-1}-1).$$

It is evident that this advance or precession of the perihelion is uniform.

If we refer the motion of the particle to a system of coordinates which participates in the motion of the perihelion, *i. e.*, to the system

$$r=r, \qquad \phi=\gamma\theta,$$

we have again the same Newtonian orbit, as can be easily verified by substitution in equation (7).

5. As application consider (*a*) the case of the Keplerian ellipse: the potential is

$$V=-\frac{\mu}{r},$$

and then $\qquad W=-\mu u, \qquad W'=-\mu, \qquad W''=0.$

The correction factor γ has the meaning

$$\gamma^2=1-\frac{\mu^2}{ac^2},$$

and the advance of the perihelion during a radial vibration is approximately

$$\frac{\pi\mu^2}{ac^2}.$$

(*b*) The case of the central ellipse, *i. e.*, the one described under a force proportional to the distance. We have

$$V=\frac{\mu r^2}{2}, \quad \text{and therefore} \quad W=\frac{\mu}{2}u^{-2};$$

then $\qquad W'=-\mu a^{-3}, \qquad W''=3\mu a^{-4},$

and $\qquad \Theta_1=\frac{\pi}{2}.$

The correction factor γ is given by

$$\gamma^2=1-\frac{\mu^2}{4\pi a^6c^2}, \quad . \quad . \quad . \quad . \quad . \quad . \quad (8)$$

and the advance of the perihelion during a radial vibration is approximately

$$\frac{\pi\mu^2}{8\alpha a^3 c^2}.$$

6. The case of the central ellipse can be treated directly. The Hamilton-Jacobi equation is

$$\left(\frac{\partial S}{\partial r}\right)^2+\frac{1}{r^2}\left(\frac{\partial S}{\partial \theta}\right)^2=2m\left(\mathrm{E}-\frac{\mu r^2}{2}\right)+\frac{1}{c^2}\left(\mathrm{E}-\frac{\mu r^2}{2}\right)^2.$$

The equations of motion are

$$t-t_0=\int\left[m+\frac{\mathrm{E}}{c^2}-\frac{\mu r^2}{2c^2}\right]\frac{r\,dr}{\sqrt{\Phi(r)}},$$

$$\beta=\frac{\theta}{2\sqrt{\alpha}}-\int\frac{dr}{2r\sqrt{\Phi(r)}},$$

where

$$\Phi(r)=2m\left(\mathrm{E}-\frac{\mu r^2}{2}\right)r^2+\frac{r^2}{c^2}\left(\mathrm{E}-\frac{\mu r^2}{2}\right)^2-\alpha.$$

Put $r^2=z$, these equations become

$$t-t_0=\frac{1}{2}\left(m+\frac{\mathrm{E}}{c^2}\right)\int\frac{dr}{\sqrt{\Psi(z)}}-\frac{\mu}{4c^2}\int\frac{z\,dr}{\sqrt{\Phi(z)}}, \quad . \quad (9)$$

$$2\left(\frac{\theta}{\sqrt{\alpha}}-2\beta\right)=\int\frac{dr}{2\sqrt{\Psi(z)}}, \quad . \quad . \quad . \quad (10)$$

where

$$\Psi(z)=\frac{z}{c^2}\left(\mathrm{E}-\frac{\mu z}{2}\right)^2+2m\left(\mathrm{E}-\frac{\mu z}{2}\right)z-\alpha$$

$$=\frac{z}{c^2}\left(\mathrm{E}-\frac{\mu z}{2}\right)^2-m\mu\left(z-\frac{\mathrm{E}}{\mu}\right)^2+\frac{m\mathrm{E}^2}{\mu}-\alpha;$$

$\Psi(z)$ being a polynomial of the third degree the problem can be integrated in terms of elliptic functions. Take an auxiliary variable y defined by the equation

$$y=\int^z\frac{dr}{\sqrt{\Psi(z)}},$$

from which we have

$$\left(\frac{dz}{dy}\right)^2=\Psi(z). \quad . \quad . \quad . \quad . \quad . \quad (11)$$

The equation $\Psi(z)=0$ has three real and positive roots, as $\Psi(z)$ is negative for $z=-\infty$, 0, and $\frac{2\mathrm{E}}{\mu}$, and positive for

$z=\frac{E}{\mu}$ and $+\infty$. If the three roots be designated by z_1, z_2, z_3, we have

$$z_1 > \frac{2E}{\mu} > z_2 > \frac{E}{\mu} > z_3 > 0.$$

In the actual motion z lies between z_2 and z_3.

Define a new variable by the equation

$$z = Mx + N.$$

The constants M and N are to be so chosen that equation (11) takes the form

$$\left(\frac{dx}{dy}\right)^2 = \frac{\Psi(Mx+N)}{M^2} = 4(x-e_1)(x-e_2)(x-e_3),$$

with the condition that $e_1+e_2+e_3=0$.

e_1, e_2, e_3 are the roots corresponding to z_1, z_2, z_3 respectively. We find by identification

$$M = \frac{16\mu^2}{c^2}, \qquad N = \frac{\mu}{3}\left(m + \frac{E}{c^2}\right).$$

The inversion of the integral defining y gives

$$x = \wp(y+\gamma),$$

where γ is a constant and $\wp$ is the Weierstrassian elliptic function formed with the roots e_1, e_2, e_3. Since z lies between the roots z_2 and z_3, it follows that x lies between e_2 and e_3, and therefore the constant γ is of the form $\omega' + \gamma_0$, where ω' is the half period corresponding to the root e_3, *i.e.*, a purely imaginary quantity, and γ_0 is a real quantity depending on the lower limit of the integral defining y. If this limit be z_3, γ_0 is null.

The real half period ω will be given by

$$\omega = \int_{e_3}^{e_2} \frac{dx}{\sqrt{4(x-e_1)(x-e_2)(x-e_3)}}.$$

The equations of motion become

$$t - t_0 = \frac{1}{2}\left(m + \frac{E}{c^2}\right)\int dy - \frac{\mu}{4c^2}\int [M\wp(y+\omega') + N]\,dy, \quad (12)$$

$$2\left(\frac{\theta}{\sqrt{\alpha}} - 2\beta\right) = \int \frac{dy}{M\wp(y+\omega') + N} \quad (13)$$

Integrating (12) we have

$$t-t_0=\frac{1}{2}\left(m+\frac{\mathrm{E}}{c^2}\right)\left(1-\frac{\mu^2}{6c^2}\right)y+\frac{\mathrm{M}\mu}{4c^2}\zeta(y+\omega').$$

In order to integrate (13), take a constant k defined by

$$\wp(k)=-\frac{\mathrm{N}}{\mathrm{M}},$$

so that from equation (11) we have

$$\wp'(k)=\frac{i\sqrt{\alpha}}{\mathrm{M}}.$$

Equation (13) becomes

$$2\left(\frac{\theta}{\sqrt{\alpha}}-2\beta\right)=\frac{1}{i\sqrt{\alpha}}\int\frac{\wp'(k)}{\wp(y+\omega')-\wp(k)}\,dy.$$

Integrating, we get

$$2i(\theta-\theta_0)=\log\frac{\sigma(y+\omega'-k)}{\sigma(y+\omega'+k)}+2y\zeta(k),$$

where θ_0 is a new constant.

Or
$$e^{2i(\theta-\theta_0)}=e^{2y\zeta(k)}\frac{\sigma(y+\omega'-k)}{\sigma(y+\omega'+k)}. \quad . \quad . \quad . \quad (14)$$

We have also

$$\wp r^2=\mathrm{M}(y+\omega')+\mathrm{N}. \quad . \quad . \quad . \quad . \quad (15)$$

Equations (14) and (15) determine the path.

When y increases by 2ω, r reverts to its original value and θ increases by the quantity

$$2i[\eta\,.\,k-\omega\zeta(k)], \quad . \quad . \quad . \quad . \quad . \quad (16)$$

which evidently differs from π. The constant $\eta=\zeta(\omega)$.

We can obtain an approximate value for the increment (16) of the angle θ in the following manner. Equation (10) may be written

$$d\theta=\frac{\sqrt{\alpha}}{2}\frac{dz}{z\sqrt{\frac{\mu^2}{4c^2}(f-z)(z-g)(h-z)}}; \quad . \quad (17)$$

f and g are two finite quantities between which z lies, and h the third root of the cubic. Suppose the motion nearly circular

of radius $\frac{1}{a}$, and let b be the mean value of $z=r^2=\frac{1}{a^2}$. Let

$$f=b-e \quad \text{and} \quad g=b+e,$$

e being a small quantity.

From the equation

$$\Psi(z)=0$$

we have

$$f+g+h=\frac{4c^2}{\mu}\left(m+\frac{\mathrm{E}}{c^2}\right);$$

therefore

$$h=\frac{4c^2}{\mu}\left(m+\frac{\mathrm{E}}{c^2}\right)-2b.$$

Take another variable ϕ defined by

$$z=\frac{f+g}{2}+\frac{g-f}{2}\cos\phi=b+e\cos\phi.$$

Substituting in (17), we get

$$d\theta=\sqrt{\frac{\alpha}{2}}\frac{d\phi}{(b+e\cos\phi)\sqrt{\mathrm{H}^2-\frac{\mu^2 e}{4c^2}\cos\phi}}, \quad . \quad (18)$$

where

$$\mathrm{H}^2=\mu\left(m+\frac{\mathrm{E}}{c^2}\right)-\frac{3b\mu^2}{4c^2}$$

$$=\alpha a^4-\frac{\mu^2}{4a^2c^2},$$

as is easily verified on substituting for E from equation (5), where we put

$$\mathrm{W}(a)=\frac{\mu}{2a^2} \quad \text{and} \quad \mathrm{W}'(a)=-\frac{\mu}{a^2}.$$

Expanding the two expressions in the denominator of (18), neglecting squares and higher powers of e, and integrating between 0 and π, we get

$$\Theta=\frac{\pi}{2}\left(1-\frac{\mu^2}{4\alpha a^6c^2}\right)^{-\frac{1}{2}};$$

we have the same expression for γ as from (8).

7. Returning to equation (6), it will be easily seen that for a second approximation the apsidal angle is still $\frac{\pi}{\omega}$.

For a third approximation the coefficient of θ is no longer a multiple simply of ω. The differential equation may be written

$$\frac{d^2x}{d\theta^2} = -\omega^2 x + \mathrm{K}x^2 + \mathrm{L}x^3,$$

the meanings of K and L being evident.

This equation is satisfied by

$$x = \mathrm{A}\cos p(\theta-\epsilon) + \mathrm{A}^2[\mathrm{B} + \mathrm{C}\cos 2p(\theta-\epsilon)] + \mathrm{A}^3\mathrm{D}\cos 3p(\theta-\epsilon).$$

The constants B, C, D, and p are to be determined by substituting in the differential equation, neglecting powers of A higher than the third and equating coefficients on both sides. It will be found that

$$p^2 = \omega^2 - \frac{\mathrm{A}}{12}\left\{10\frac{\mathrm{K}^2}{\omega^2} + 9\mathrm{L}\right\} = \Gamma^2\Lambda^2,$$

where

$$\Lambda^2 = 1 - a\frac{\mathrm{W}''}{\mathrm{W}'} - \frac{\mathrm{A}^2 a}{24\mathrm{W}'}\left\{\frac{5a\mathrm{W}'''^2}{\mathrm{W}'(\mathrm{W}'-a\mathrm{W}'')} + 3\mathrm{W}''''\right\},$$

$$\Gamma^2 = 1 - \frac{1}{ac^2\Lambda^2}\left[\mathrm{W}''^2 + \frac{\mathrm{A}^2}{24}\left\{3(3\mathrm{W}''^2 + 4\mathrm{W}'\mathrm{W}''') + \frac{5\mathrm{W}'}{\mathrm{W}'-a\mathrm{W}''}\left(6a\mathrm{W}'''\mathrm{W}'''' + \frac{a^2\mathrm{W}''^2\mathrm{W}'''^2}{\mathrm{W}'(\mathrm{W}'-a\mathrm{W}'')}\right)\right\}\right] + \ldots,$$

and the apsidal angle is then

$$\Theta = \frac{\pi}{p} = \frac{\pi}{\Gamma\Lambda}.$$

In Newtonian dynamics the correction factor Γ, as well as γ, reduces to unity, and the apsidal angle is

$$\Theta_1 = \frac{\pi}{\Lambda}.$$

Summary.

It has been proved that a Newtonian periodic orbit described under central forces depending on the distance may be considered in relativistic dynamics as if it were revolving in its own plane about the centre of forces. The angular displacement for a radial libration has been calculated, and applications to fields proportional to the distance and to the inverse square of the distance have been given. The case of the first field has been treated fully, in terms of elliptic functions.

LXIV. *On the Electrical Oscillations of very short Wave-length.*

To the Editors of the Philosophical Magazine.

Gentlemen,—

In a note published in the Phil. Mag., October 1931, Mr. E. W. B. Gill gave an account of some observations made on a three-electrode valve, oscillating with positive grid. The valve, inserted in a Lecher circuit of fixed length, gave oscillations of several different periods, corresponding to the harmonics of the circuit, for different intervals of values in the grid tension (V) and in the emission current (i). Oscillations of greatest intensity for a given period were obtained by well determined couples of values of V and i; in four cases recorded by the author these conformed approximately to the relations

$$(\cdot)\quad \lambda^2 V = \text{const.},$$

$$(\cdot\cdot)\quad \frac{V^{3/2}}{i} = \text{const.}$$

If instead of varying V and i simultaneously V is kept constant and i is varied continuously, oscillations of different periods are also obtained. The values of i which, with given values of V, give rise to oscillations of the greatest strength having a wave-length λ, satisfy the relation

$$(\cdot\cdot\cdot)\quad \lambda^2 i = \text{const.}$$

The author remarked that none of the generally accepted theories were capable of explaining these results, and he therefore put forward an ingenious new model.

I think that all the facts observed by E. W. B. Gill can be also explained by the more extensive and precise scheme that I have developed in three notes in the *R. Acc. delle Scienze di Torino* during the year 1931 *.

In these I showed that the electrons contained between the plate and the grid of the valve, with positive grid, as a whole form an oscillating system whose frequency is a function of the total number N of the electrons. It follows therefore as a fundamental relation that

(a) $\lambda^2 N$ must be constant.

If N is calculated to a first approximation, by neglecting

* Vol. lxvi. pp. 123, 217, 383 (1st semester): Notes I., II., III.

space-charge effects, under the supplementary condition that V=const., then (*a*) clearly becomes

$$\lambda^2 i = \text{const.},$$

as I showed in Note I.

It is just this relation (···) that E. W. B. Gill found experimentally by V = constant.

A method of calculating N, taking into account the space-charge effects, is developed in Note III. I obtain an expression of the form

$$N = V/\left(\frac{V^{3/2}}{i}\right),$$

f being a numerically calculable function of $\frac{V^{3/2}}{i}$. It follows that, if $\frac{V^{3/2}}{i}$ remains constant, as in the experiments of E. W. B. Gill (··), then $\lambda^2 V = \text{const.}$ (·) is an immediate consequence of the relation (*a*) $\lambda^2 N = \text{const.}$

In a series of experiments (to be published shortly) which I have carried out with valves of many types the relation $\lambda^2 N = \text{const.}$, predicted by the theory, has proved itself valid in all cases as a satisfactory approximation. In special cases, when $\frac{V^{3/2}}{i}$ does remain constant, it is found that $\lambda^2 V$ is constant too.

Physical Institute,
University of Turin.
January 28th, 1932.

Yours faithfully,
Antonio Rostagni.

LXV. *On the Electrical Oscillations of very short Wave-length.*

To the Editors of the Philosophical Magazine.

Gentlemen,—

Professor Rostagni has most kindly sent me a copy of his note to you on short-wave oscillations, and I should like to make a few remarks thereon. I do not think Professor Rostagni and I are very far apart; his very interesting calculations, which I had not seen before, are the result of approaching the problem in a rather different manner. Where I am not in agreement with him is as to whether his theory affords a complete explanation of what is happening. He has proved that the space charges between the grid

and anode of a valve have natural periods of oscillation obeying observed laws, but that is a very different thing from proving that the electrons passing across the valve will maintain these oscillations. The theory I put forward tried to explain exactly how this regeneration occurred.

An analogy from sound illustrates the difference. The natural period of the air in an organ-pipe can be calculated ; this corresponds to Prof. Rostagni's work. The explanation of how a uniform stream of air blowing past the orifice can keep the pipe sounding corresponds to what I published.

Mr. Morrell has pointed out to me that my explanation of the valve's action corresponds exactly to the well-known explanation of the maintenance of sound in an organ-pipe, and it is therefore not surprising that Prof. Rostagni and I ultimately reach the same type of equation for the frequencies.

Yours faithfully,

Merton College, Oxford.
February 8, 1932.

E. W. B. Gill.

LXVI. *Transient Response of the Triode Valve Equivalent Network.*

To the Editors of the Philosophical Magazine.

Gentlemen,—

AN introductory remark in my paper on "The Transient Response of the Triode Valve Equivalent Network" in the January issue of your Journal, and its relation to the subsequent subject-matter of the paper, is liable to lead to difficulty and misinterpretation, and calls therefore for extension. It is stated that the distorting transient introduced by the elements of the triode network should be of short duration in comparison with the duration of the transient. This, however, is only a partial statement of the case. Taking the resistance capacity coupled amplifier example, in which the coupling condenser C_4 is given a value of 5×10^{-10} farads. the output voltage response to the unit input voltage consists of two components of time constants

$$T_1 = 1/3{\cdot}04\times10^6 \text{ sec.} \quad \text{and} \quad T_2 = 1/1968 \text{ sec.}$$

The output voltage is zero at time $t=0$, and then rises to a maximum at a rate governed mainly by T_1, after which it dies away at a rate determined by T_2. For an approach to perfect reproduction of the unit voltage pulse the duration of the transient rise must be as short as possible compared with

the duration of the applied pulse, so that T_1 must be small. On the other hand, the rate of output voltage decay after the maximum is attained must be as slow as possible, a consideration which calls for a large value of T_2 and therefore a large value of C_4, although a small value may appear to be indicated in the paper. This statement also relates in some measure to the C_4 value in the choke-coupled case considered. The effect on the nature of the response curves of decreasing T_1 and increasing T_2 is well demonstrated by C. W. Oatley in the 'Wireless Engineer,' viii. pp. 204 & 307 (1931). A comparison of the transformer-coupled amplifier with a resistance-capacity coupled circuit employing a value of $1\,\mu$f. for C_4 shows that not only is the voltage rise in the former case less rapid, but, further, that the voltage decays much more quickly. This emphasizes the superiority of a correctly adjusted resistance-capacity coupled amplifier—a point somewhat hidden by the value of C_4 chosen in the paper.

College of Technology,
Manchester.
22nd January, 1932.

Yours faithfully,
W. Jackson.

LXVII. *The Theory of the Electrification of Aerosols.*

To the Editors of the Philosophical Magazine.

Gentlemen,

I SHOULD like to point out that in a recent communication to the Philosophical Magazine (p. 1175, Dec. 1931) on the "Theory of the Electrification of Aerosols," equation (4), giving the relationship between the particulate volumes of the electrified and total particles in a coagulating system, was wrongly printed. The correct form of equation (4) is

$$\sigma_e = 1{\cdot}5\sigma + \left[\frac{e^{b^2(\sigma^2-\sigma_0^2)}}{\sigma_{e_0} - 1{\cdot}5\sigma_0} - \frac{b^2}{0{\cdot}75} e^{b^2\sigma^2} \left(\int_0^{\sigma} e^{-b^2\sigma^2}\, d\sigma - \int_0^{\sigma_0} e^{-b^2\sigma^2}\, d\sigma \right) \right]^{-1}. \qquad (4)$$

The numerical calculations quoted in the paper were, of course, made from the correct form of the equation as given above.

Yours faithfully,
H. S. Patterson.

Leeds University.
9th February, 1932.

LXVIII. *Notices respecting New Books.*

Die Quantenstatistik und ihre Anwendung auf die Elektronentheorie der Metalle. By L. Brillouin. Translated by E. Rabinowitsch. *Struktur der Materie*, XIII. [Pp. x + 530.] (Springer, Berlin, 1931. R.M. 42; bound 43.80.)

THE present book is a translation of 'Les statistiques quantiques' which has fitly been added to the 'Struktur der Materie' series. The author has taken advantage of the German edition to make a number of modifications and improvements in the treatment, and he has extended the account of the electron theory of metals, bringing it completely up-to-date.

The book opens with a lucid summary of the classical treatment of temperature radiation, involving the laws of Kirchhoff, Stefan, and Wien. The photon hypothesis is then introduced and the fundamental ideas of wave mechanics are outlined. After an account of classical statistical methods the quantum modifications, embodied in the Einstein-Bose and Fermi-Dirac statistics, are fully discussed, and applications are made to radiation and to emission and absorption processes. This first part of the book, clear and comprehensive without being unduly detailed, is admirably adapted to bridge the somewhat difficult gap between such a book as Rice's 'Introduction to Statistical Mechanics' and Fowler's large treatise.

The kernel of the book, for which the first part paves the way, is a detailed critical account, in two chapters occupying over two hundred pages, of the application of the Fermi-Dirac statistics to free electrons in metals by Sommerfeld, and of the later theoretical developments. An outstanding weakness of Sommerfeld's theory lay in the lack of precision as to the "mean free path of the electrons" which entered into the formulæ. Much of the later work may be regarded (though somewhat artificially) as being directed at a determination of this free path. Starting with free electrons, the problem is to determine the effect of the periodic field of the crystal lattice on the electron waves, and the effect of interchange of energy between them and the thermal motions of the crystal when electric (and magnetic) fields are applied. The discovery that there are allowed and disallowed energy bands has shed an entirely new light on the problem of conduction. In an alternative procedure the electrons, in the first approximation, are treated as bound to particular atoms. The work that has been carried out in this difficult field by Brillouin himself, Bloch, Peierls, and others is admirably discussed. The unified presentation, co-ordinating a multiplicity of original papers, will be invaluable, giving, as it does, a comprehensive account of developments which seem destined to be of fundamental significance for the understanding of the metallic and semi-metallic state.

In the last two chapters the distribution of electrons in atoms, and inside and near the surface of metals, and the distribution of atoms between different states under various conditions, are discussed. An appendix deals with formulæ for dispersive media, with the fundamentals of combinatory analysis, and with some very recent work by Nordheim and Peierls on the electron theory of metals.

The book will be of the greatest value to those who require either an introduction to recent developments in quantum statistics, or a full account of one of its most important applications.

Cours D'Electricité Théorique professé a l'école professionelle supérieure des postes et télégraphes. Par J. B. Pomey, Ingénieur en chef des postes et télégraphes. Tome III. [Pp. 315.] (Gauthier-Villars et Cie. Paper cover, fr. 90.)

This well-printed book gives a pretty complete account up to recent times of the mathematical theory of telegraphy and telephony.

After a short opening chapter on the equations of the electromagnetic field, the author plunges at once into his subject, and devotes a chapter to radiation from antennæ and wave propagation and reflection.

There follow several chapters on the Theory of Relativity with the necessary mathematical introductions.

This first half of the book is very largely mathematical, but the latter part is concerned in the main with the more technical task of giving an account of the theory of telephone transmission. Thus we have, in Chapter 8, an excellent treatment of the loaded line which gives particular attention to the questions of phase and frequency distortion. Other subjects dealt with in this section include the balancing of paired circuits, the localization of faults by impedance-frequency tests, and the theory of the repeater considered as a four-terminal network. The treatment of the subject as a whole may be said to be unusually comprehensive.

The following chapter develops the theory of artificial lines and frequency filters, the homographic transformation being also presented, while in the remaining sections we find the theory of the valve oscillator, the Gulstad relay, and a useful account of the latest work on operational circuit analysis. In this latter section the author makes frequent reference to the work of Carson in America, and manages to present, in a comparatively small space, a very clear statement of the theory as it stands at present.

Quartz Resonators and Oscillators. By P. Vigoureux, M.Sc., National Physical Laboratory. [Pp. 217+figs. 125.] (H.M. Stationery Office. Boards, 7*s.* 6*d.*)

This monograph has been produced under the auspices of the Radio Research Board, and will be found to be a most useful

and up-to-date account of Piezo-electricity in general and its applications.

The first of the five chapters is given up to a short general account of the physical properties of quartz, and here the first hint is given of the extraordinarily rapid war-time development of the subject initiated by the brothers Curie in 1880 by their discovery that some strained crystals exhibit electrical polarity.

This chapter is perhaps rather too condensed to permit the author to do justice to his subject. Terse dismissal of well-known properties is understandable under such self-imposed conditions of brevity, but many readers would have welcomed an extra line or two for a definition of such a term as "Permittivity" for example.

The section on the static Piezo electric effect is most useful, and the practical details for the preparation of quartz plates will be found specially useful to experimentalists.

The next section, on Piezo Electric Resonators, deals with a mass of interesting detail, both theoretical and experimental, and appears to be a very specially complete account of this most interesting subject.

Numerous circuits are given for oscillation maintenance, and a sub-section is devoted to quartz resonators as frequency standards and other applications.

The book closes with a chapter on the structure of quartz.

The book is sufficiently well printed and the numerous diagrams have been well and clearly prepared, while the references at the end of the book are very complete.

A most useful and welcome book, not only for the physicist, but for those on the look-out for the technical applications of Physics.

Die Maxwellsche Theorie. By H. A. Lorentz. Translated by Dr. H. Stücklen. [199 pp.] (Leipzic, Akademische Verlagsgesellschaft.)

This book (of which there is an English version, translated by Dr. L. Silberstein and A. P. H. Trivelli) is a continuation of the publication of the lectures on Theoretical Physics delivered by H. A. Lorentz at the University of Leiden.

The title "Maxwell's Theory" covers all the elements of electromagnetic theory. The first chapter proper (following an excellent summary of vector analysis) is devoted to a derivation of the equations of the electromagnetic field, and these are subsequently applied to the separate branches of electrostatics; current electricity, stationary and induced: the last two chapters being given to a short account of the energy of the electromagnetic field and the electromagnetic theory of light. The mathematics is treated vectorially, although where the condensed form of the vector notation is liable to render the assimilation of the equation difficult, the Cartesian form is given as well, so that even the amateur mathematician will find the book well within his powers.

The treatment is throughout logical, compact, and complete, howbeit the physical aspect of the fundamental equations is given rather scanty consideration; in particular, the account of the displacement current is so brief as to be almost breathless—but to one who wishes merely to appreciate the mathematical development this is no disadvantage.

Like all reprinted courses of lectures it is intended for serious study rather than for reference on particular problems; and for the purpose of acquiring a knowledge of electromagnetic theory it would be difficult to recommend a better treatise.

The Dipole Moment and Chemical Structure. Edited by P. Debye. Authorised translation by Winifred M. Deans. [Pp. x+134.] (London: Blackie & Son Ltd. Price 10*s*.)

The relation between molecular structure and the magnitude of the electric dipole moment was the subject of discussion at a recent conference at Leipzig, and the present volume is a collection of papers communicated by various workers in this particular field.

The theoretical considerations of Debye relative to the influence of permanent dipoles on the dielectric capacity of liquids and gases has given a marked impetus to the further investigation of dielectric properties, and the accuracy attainable in such measurements has been greatly increased in consequence. This, indeed, may be regarded as essential for the application of dipole moment data to various problems.

Results thus far obtained justify the view that dipole moments provide valuable information relative to the spacial configuration of molecules, and that such data afford a basis for the correlation of many physical and chemical properties of related compounds.

The collected papers describe recent advances in theory and experiment from both the physical and chemical standpoint. Particular interest attaches to those which deal with (1) the influence of temperature on the dielectric constants of gases and vapours, (2) the application of the molecular-beam method of observation, and (3) the connexion between dipole moment and reaction velocity.

To those physicists and chemists who are concerned with problems involving molecular polarization effects the book should be of value as a convenient source of information relative to the problems which are in course of investigation, although it does not in any way serve the purpose of a monograph on the subject. The translator's work has been thoroughly well done.

H. M. Dawson.

LXIX. *Proceedings of Learned Societies.*

GEOLOGICAL SOCIETY.

December 16th, 1931.—Prof. W. W. Watts, LL.D., Sc.D., F.R.S., Vice-President, in the Chair.

THE following communication was read :—

'The Tertiary Ring Complex of Slieve Gullion (Ireland).' By James Ernest Richey, M.C., B.A.I., F.G.S., with petrological notes by Herbert Henry Thomas, M.A., Sc.D., F.R.S.

The Tertiary intrusive complex of Slieve Gullion lies west of the Mourne Mountains and north-west of the Carlingford peninsula. Topographically, it consists of a ring of curving ridges and hills, 7 miles in diameter, which is bisected by a mountainous belt extending to the north-west. The ring and the North-West Belt mark the outcrops of a very simple ring-dyke complex and later Tertiary plutonics (not described in the present paper). The area was mapped by J. Nolan, F. W. Egan, and W. A. Traill of the Geological Survey over 60 years ago, and their work has now been extended by the Authors.

The Slieve Gullion Tertiary rocks are intruded around the western portion of the Newry Granite. This, in its composition and in its relations to Silurian country rocks, resembles the Lower Old Red Sandstone granites of the Southern Uplands of Scotland.

The Ring Complex forms a complete ring, except to the south-west, where it is broken through by the North-West Belt. It includes the following rocks, in order of age :— (1) Lavas of olivine-basalt, basalt with felspar phenocrysts, and trachyte, associated with (2) agglomerates, chiefly formed of fragments of Newry Granite and lying in vents along the south-western part of the ring. These, the Forkhill vents, are intruded by (3) an elongate vent-intrusion and an arcuate ring-dyke of porphyritic felsite. The remainder of the ring is constituted of (4) remarkable breccias, due largely to crushing and partly to explosion, associated with (5) an extensive ring-dyke of porphyritic granophyre, in part a double or triple intrusion. This ring-dyke is intruded to the north-west and south-east by masses belonging to the North-West Belt. The Ring Complex is perhaps entirely earlier than the North-West Belt.

The olivine-basalts are identical with the Hebridean plateau type, and predominate over the other lavas. All appear to be downslipped masses within the vents. The agglomerate-fragments consist of various other rocks in addition to granite, and are evidently well mixed together. They include locally all the Tertiary lava-types mentioned, as well as a glassy andesite. The felsite sometimes penetrates the agglomerates so intimately as to form a matrix for the fragments, as Nolan observed, and the vent-brecciation is ascribed to gases given off from the uprising felsite magma. Age-relations of the felsite and granophyre ring-dykes are proved at contacts. The crush-breccias include flinty crush-rock, and the crushing affects the granite-wall as well as the granophyre ring-dyke itself. The brecciation is most intense around the north and west sides of the ring-dyke. It suggests movement of the central block enclosed by the ring-fissure, but no marked subsidence can be proved.

The almost exact coincidence of the ring-fissure with the margin of the western portion of the Newry Granite is perhaps the most remarkable feature of the Ring Complex. A local magma-reservoir underlying the Tertiary complex would seem to owe its position to the Newry Granite. If so, the reservoir should perhaps be ascribed to crustal-subsidence rather than to crustal re-melting, since it was, mainly at least, filled with magma of normal Tertiary affinities.

January 13th, 1932.—Dr. H. H. Thomas, M.A., Sc.D., F.R.S., Vice-President, and afterwards

Prof. E. J. Garwood, M.A., Sc.D., F.R.S., President, in the Chair.

The following communication was read :—

'The Geological Structure of the Eastern Mendips.' By Francis Brian Awburn Welch, B.Sc., Ph.D., F.G.S.

The area here termed the Eastern Mendips comprises the Beacon Hill pericline, the most southerly situated of the four echeloned Mendip periclines and that bordering the Radstock Coalfield. As in the other three cases, the structure is anticlinal with a steeply folded north limb : the core is formed of Old Red Sandstone and Silurian, the Avonian outcropping on the flanks. The south limb is much concealed by Mesozoic strata, which also stretch across the eastern part of the area, so that the Avonian can only be seen in deep ravines.

The region can be divided into three parts—the eastern, the western, and the central. The western area is relatively

simple in structure and calls for little comment, except that on the north limb the D_3 Subzone has been detected. The eastern area is extensively faulted along the southern limb, the limestones being thrust along the line of the K-shales against the Old Red Sandstone. The central area forms a great thrust-block bordered by two north-and-south tear-faults which run through Downhead on the west and Chantry on the east. The beds on the north limb show little signs of faulting, whilst the limestones of the south limb were apparently thrust northward over the K-shales. The result was the production of a gigantic overfold on the north side (resembling in shape a breaking wave) under which the Coal Measures were thrust. All that remains of this overfold, which was shattered by minor thrusting, are the inliers of Vobster and Luckington, which lie in a due north line between the two tear-faults.

The whole sequence of events appears to have been the northward drive of the east-and-west pericline against the southern ' nose ' of the Coal Measure basin (with a north-and-south axis). Maximum resistance was offered to this movement along the line of this axis, and in this line lies the Central Fault Block. Consequently, the Coal Measures to the west are little disturbed, except for slight overfolding which gradually increases eastwards and reaches a maximum between the two tear-faults.

January 27th, 1932.—Prof. E. J. Garwood, M.A., Sc.D., F.R.S., President, in the Chair.

The following communication was read :—

' The Geology of the Ruhuhu Coalfields, Tanganyika Territory.' By Gordon Murray Stockley, A.R.C.S., D.I.C., F.G.S. ; with a report on some Fossil Plants from the Karroo Beds in the Ruhuhu River Depression, by Prof. John Walton, D.Sc., F.R.S.E., F.G.S. (Read by Mr. L. R. Cox, M.A., F.G.S., in the absence of the Author.)

The paper gives an outline of the geology of an area of some 1500 square miles situated east of Lake Nyasa, and drained by the Ruhuhu and its tributary rivers. The area, which is occupied by Karroo rocks, forms a depression between the mountains which lie to the north and south ; these are composed of gneisses and other rocks of the Primitive System, which are brought into juxtaposition with the Karroo rocks by faults of considerable magnitude—in one case at least 10,000 feet. The boundary of the gneiss is marked by steep

fault scarps. The whole area is also cut up into numerous fault blocks. The faults, which date from the period of rift faulting, mostly range in direction from north-east and south-west to north-north-west and south-south-east.

The rocks of the Primitive System fall into three groups : (a) highly altered felsitic and acid volcanic rocks ; (b) metamorphosed sedimentary rocks, consisting of quartzites, marbles, ophicalcites, phyllites, and mica-schists ; (c) gneisses and granulites.

The following classification of the Karroo rocks is proposed :—

		Feet.
(Lower Stormberg)	Manda Beds. Felspathic sandstones and marls with *Unio* and one bone bed ...	440
(Middle and Upper Beaufort ?)	Kingori Sandstones. Current-bedded grits and sandstones, conglomeratic in part	1200
(Lower Beaufort)	Lower Bone Bed. Mudstones with limestone nodules and sandstone beds, and containing reptilian bones and fossil wood	300
(Upper Ecca ? to Lower Beaufort)	Ruhuhu Beds. Fine-grained sandstones, shales, etc., with beds and nodules of magnesian limestone, and with occasional fossil wood (*Dadoxylon*) ; *Palæomutela* and *Glossopteris* present in the upper beds .....700 to	1000
(Ecca)	Upper Coal Measures. Clay-shales with coal seams, ironstones, and sandstone beds.....	335
(Do.)	Intermediate Marls and Sandstones.	450
(Do.)	Lower Coal Measures. Sandstones with coal seams, carbonaceous shales, and limestones	450
(Do. ?)	Basal Sandstones and Conglomerate.	1690
	Approximate total thickness.....	5865

The correlation of the Karroo Beds with the standard South African succession is based upon the evidence of the reptilian remains, mollusca, and plants described in the following papers. An account is given of the exposures of the two bone beds.

A report on the fossil plants from the Karroo rocks is added.

The Editors do not hold themselves responsible for the views expressed by their correspondents.